



Faculty of Science and Technology

Master's Thesis

Study program/Specialization: Master of Science in Petroleum Engineering/Drilling Engineering	Spring semester, 2012 Confidential
Author: Marcelo E. Guarani C.	
Faculty supervisor: Mesfin Belayneh External supervisor(s): Laetitia Lewis	
Title of thesis: Development of a method to assess the steerability of different PDC bit designs from field data, and correlation with theoretical bit model	
Credits (ECTS): 30	
Keywords: PDC Bit, Steerability, Rotary Steerable System, Dog Leg Severity (DLS), Bit Design, Drilling parameters, ROP, RPM	Pages: 140 Enclosure: 9 Stavanger, 14 th of June 2012

Acknowledgements

First of all I would like to show my gratitude to: Laetitia Lewis, my supervisor at Halliburton AS, her support, guidance and patience were essential for the development of the thesis, Mesfin Belayneh, my supervisor at the university who was always concern and open to help me.

This dissertation would not have been possible without the support and help of all the employees at HDBS (Halliburton Drill Bits and Services) and Sperry Drilling Services with whom I shared and learned a lot. I also own a sincere thankfulness to all the professors and staff at the University of Stavanger for the commitment and support that they provide to the students.

Finally I would like to thank my parents who are always there encouraging me and my friends in Norway who make this two years of study a pleasant and an enjoyable period of my life.

Abstract

The bit and directional tool are a part of the BHA system. This thesis work analyzes that part of the system. The objective of the thesis is to analyze the performance of different bit designs using a computer simulator and field data.

In the introduction part, background information about PDC bits steerability concepts is given, the main objectives are stated and the scope and limitations are explained from a variable by variable considered approach.

The literature review covers important concepts such as the geological setting for this engineering study, the directional tool selected description of PDC bits design, definition of steerability and a description of all the variables considered in the analysis is given.

In this thesis work, a methodology for the analysis of bit performance is developed. The proposed methodology consists of five main steps. These are: *Identification of Data Sources, Construction of the Main data Matrix, and Categorization and sorting of data, Simulation in DxD™ and Correlation of model.*

The applicability of the method is tested on wells drilled in the Oseberg field. The results are presented in six case studies that consider the 8 ½" and 12 ¼" section. During the development of these case studies, much meaningful insight was gathered, structured and presented here. In addition, the impact of different design features such as cutter structure, gage pad, sleeve gage length shape, among others was assessed and correlated with the simulator results.

The results from field case study and computer simulation shows that:

- The method developed was verified by the very different results that each steering behavior displayed. The walk tendency was disclosed when plotting the correlations for turning right and left.
- The positive impact of an active gage was verified, the importance of a flat profile was also seen in most of the cases as well as the improvement of reducing the number of blades of the sleeve to 4 and the addition of the MEG (modified Extended Gage) were also confirmed.
- The tilt length reduction also showed improvement in most bit designs.

Finally, since this is a very complex topic, it requires much more research to have a complete understanding of the behavior of the designed tools under subsurface conditions that encounters complex geological features. Some suggestions regarding the use of down-hole data available from special tools is presented and other possible approaches are listed in the suggestions part.

Table of Contents

1. Introduction.....	2
1.1 Background & Problem definition.....	2
1.2 Objectives	2
1.3 Scope and limitations	3
2 Literature Review.....	5
2.1 Rock strength.....	5
2.1.1 Geological setting.....	5
2.1.2 Laboratory tests	6
2.1.3 Estimation from field measurements ^[4]	7
2.2 Directional Drilling.....	8
2.2.1 Directional Tool.....	8
2.2.2 Main parts functionality:.....	9
2.2.3 Surveys.....	11
2.3 Fixed cutters bits	12
2.3.1 Range of applications	12
2.3.2 Bit Nomenclature.....	13
2.3.3 Material number and Serial number.....	13
2.3.4 Bit selection.....	13
2.3.5 Bit Features	14
2.4 Steerability.....	20
2.5 Description of variables.....	22
2.5.1 Side cutting.....	22
2.5.2 Bit Side Force.....	22
2.5.3 Dog Leg capability of BHA.....	22
2.5.4 Dog-Leg Severity (DLS)	23
2.5.4 Geo-Pilot™ deflection	23
3 Methodology	24
3.1 Structure of the Analysis.....	24
3.2 Identification of Data Sources.....	25
3.2.1 Use of DBS (Drilling Bits and Services) data base.....	26
3.2.2 EOW reports.....	27

3.2.3 Specifications Sheets	30
3.2.4 ADI files.....	31
3.2.5 Bit design files	32
3.3 Construction of the Main Data Matrix.....	34
3.3.1 Data from the definitive survey reports.....	34
3.3.2 Data from logging records.....	34
3.4 Categorization and sorting of data.....	35
3.4.1 Algorithm to identify the behavior	35
3.4.2 Statistical analysis to identify the relevant ranges of ROP and RPM.....	37
3.5 Simulation in Direction by Design DxD™.....	38
3.5.1 Introduction [21].....	38
3.5.2 Simulation Process	39
3.6 Validation of model	43
4 Data analysis & Interpretation	44
4.1 Oseberg Field	44
4.1.1 General Information	45
4.1.2 Formations drilled.....	46
4.2 Hypothesis.....	47
4.3 Case studies	47
4.3.1 Case A - 8 ½ section, FMF3651Z (487256) vs FMF3653Z (405148).....	48
4.3.2 Case B - 8 ½ section, Low ROP	72
4.3.3 Case C - 8 ½ section, Medium ROP.....	80
4.3.4 Case D - 8 ½ section, High ROP	96
4.3.5 Case E - 12 ¼" section.....	108
4.3.6 Case F - 12 ¼ section, with reamer to 13 ½"	120
5 Summary and major findings.....	135
5.1 Regarding the bit designs	136
5.2 Regarding the Directional tool.....	136
5.3 Regarding the methodology developed	136
6. Suggestions.....	138
7 References	139

List of Figures

Figure 1, Rock strength measurements from laboratory [3]	6
Figure 2, Stress strain plot [3].....	6
Figure 3, GP 5200 series [7]	9
Figure 4, GP 7600 series [7]	9
Figure 5, GP 9600 series [7]	9
Figure 6, Working principle of GP, point the bit [8]	10
Figure 7, GP with and without LHS	10
Figure 8, Non-rotating housing [7].....	11
Figure 9, L/MWD datasets example "Insite©" [9]	12
Figure 10, Standard PDC bit [10]	12
Figure 11, Impregnated Bit [10].....	12
Figure 12, Nomenclature example [7]	13
Figure 13, Bit profiles and Cone design.....	14
Figure 14, Back rake [14]	15
Figure 15, Small chamfer left (Higher depth of cut) [14].....	15
Figure 16, Cutters materials.....	16
Figure 17, Blades, symmetric and asymmetric designs.....	16
Figure 18, Spiraled (left) and Straight (right) blades	17
Figure 19, MEG (Modified Extended Gage).....	17
Figure 20, Gage pad and Gage sleeve design [12], [13].....	18
Figure 21, Standard matrix body (left) , Steel bullet body (right) [15].....	19
Figure 22, CFD Computational Fluid Dynamics [15]	19
Figure 23, Special designs [14]	20
Figure 24, Force Balancing	20
Figure 25, Side force Fs [20].....	22
Figure 26, Tilt angle.....	23
Figure 27, Field data tendencies flowchart.....	24
Figure 28, Model tendencies and Validation.....	25
Figure 29, Example of master report.....	26
Figure 30, Example of planned (red) and real trajectory followed (blue).....	28
Figure 31, Example of definitive survey report	28
Figure 32, Example of theoretical and actual Hook load and Torque.....	29
Figure 33, Example of Lithology Summary.....	30
Figure 34, Example of MWD run summary.....	30
Figure 35, Spec Sheet	31
Figure 36, Insite environment.....	32
Figure 37, SAP	33
Figure 38, iBits design files.....	33
Figure 39, Look up table	34
Figure 40, Behaviors algorithm	35
Figure 41, All data points in a run.....	36

Figure 42, Filtered only building behavior.....	37
Figure 43, Examples of ROP and RPM distribution.....	37
Figure 44, Capabilities of DxD ^[21]	38
Figure 45, iBits Software ^[21]	40
Figure 46, Gage design.....	40
Figure 47, Desing of Gage Pad and Sleeve.....	41
Figure 48, Input parameters.....	42
Figure 49, Simulation results.....	42
Figure 50, Oseberg field structural map ^[22]	44
Figure 51, Example of cross section in Oseberg field ^[22]	45
Figure 52, FMF3651Z (487256).....	48
Figure 53, FMF3653Z (405148).....	49
Figure 54, Example of well paths analyzed.....	49
Figure 55, FMF3651Z (487256) all data points.....	50
Figure 56, FMF3651Z-487256 building @ all ROP and RPM.....	52
Figure 57, FMF3651Z-487256 dropping @ all ROP and RPM.....	53
Figure 58, FMF3651Z-487256 turning @ all ROP and RPM.....	53
Figure 59, FMF3651Z-487256 T right @ all ROP and RPM.....	54
Figure 60, FMF3651Z-487256 T left @ all ROP and RPM.....	54
Figure 61, FMF3651Z-487256 holding @ all ROP and RPM.....	55
Figure 62, FMF3651Z-487256 all behaviors @ Range A.....	56
Figure 63, FMF3651Z-487256 building @ Range A.....	57
Figure 64, FMF3651Z-487256 dropping @ Range A.....	57
Figure 65, FMF3651Z-487256 turning @ Range A.....	58
Figure 66, FMF3651Z-487256.....	58
Figure 67, FMF3651Z-487256.....	59
Figure 68, FMF3653Z (405148) all data.....	60
Figure 69, FMF3653Z-405148 building @ all ROP and RPM.....	61
Figure 70, FMF3653Z-405148 dropping @ all ROP and RPM.....	61
Figure 71, FMF3653Z-405148 turning @ all ROP and RPM.....	62
Figure 72, FMF3653Z-405148 T right @ all ROP and RPM.....	62
Figure 73, FMF3653Z-405148 T left @ all ROP and RPM.....	63
Figure 74, FMF3653Z-405148 holding @ all ROP and RPM.....	63
Figure 75, FMF3653Z-405148 all behaviors @ Range A.....	64
Figure 76, FMF3653Z-405148 building @ Range A.....	65
Figure 77, FMF3653Z-405148 dropping @ Range A.....	65
Figure 78, FMF3653Z-405148 turning @ Range A.....	66
Figure 79, FMF3653Z-405148 T left @ Range A.....	66
Figure 80, FMF3653Z-405148 T right @ Range A.....	66
Figure 81, Design 487256 and 405148 field tendencies (turning).....	67
Figure 82, Bit parts.....	68
Figure 83, Input parameters.....	68

Figure 84, Designs 487256 and 405148 simulation (top) and field data (bottom) comparison	71
Figure 85, FMF3651Z (487256).....	73
Figure 86, FMF 3651Z (551396).....	74
Figure 87, Design (A) steering response all behaviors	74
Figure 88, Design (B) steering response all behaviors	75
Figure 89, Design 487256	75
Figure 90, Design 551396	75
Figure 91, Field tendencies Case B, 8 ½ section	76
Figure 92, 487256 vs 551396 simulation results	79
Figure 93 Model vs Field tendencies	79
Figure 94, FMF3653Z (405148).....	81
Figure 95, FMF3741Z (475040).....	82
Figure 96 Design (A) steering response all behaviors.....	82
Figure 97 Design (B) steering response all behaviors	83
Figure 98 Design (C) steering response all behaviors	83
Figure 99 Design (D) steering response all behaviors	84
Figure 100, Design (A) building.....	84
Figure 101, Design (D) building	84
Figure 102, Building field tendencies @ Medium ROP	85
Figure 103 Design (A) turning left	86
Figure 104 Design (B) turning left	86
Figure 105 Design (D) turning left	86
Figure 106, Turning left field tendencies @ Medium ROP	87
Figure 107 Design (C) turning right	87
Figure 108 Design (D) turning right.....	87
Figure 109, Turning right field tendencies @ Medium ROP	88
Figure 110, Building at Medium ROP	93
Figure 111, Turning left at Medium ROP	94
Figure 112, Turning right at Medium ROP	95
Figure 113, FMF3731 (384968).....	97
Figure 114, FMF3651Z (562259)	97
Figure 115 Design (A) steering response all behaviors all behaviors.....	98
Figure 116 Design (D) steering response all behaviors	98
Figure 117 Design (E) steering response all behaviors.....	99
Figure 118 Design (F) steering response all behaviors.....	99
Figure 119, Design (E) building.....	100
Figure 120, Design (F) building.....	100
Figure 121, Building field tendencies @ High ROP	100
Figure 122 Design (D) turning right.....	101
Figure 123 Design (E) turning right	101
Figure 124 Design (F) turning right.....	102
Figure 125, Turning right field tendencies @ High ROP	102

Figure 126, Building at high ROP	106
Figure 127, Turning right at High ROP	107
Figure 128, Design (375525) steering response all behaviors	108
Figure 129, Design 411639 steering response all behaviors	108
Figure 130, Design 438320 steering response all behaviors	109
Figure 131, Design 375525	110
Figure 132, Design 411639	111
Figure 133, Design 438320	111
Figure 134, 438320 Building ROP (left) and RPM (right) stats	112
Figure 135, 411639 Building stats ROP (left) and RPM (right) stats.....	112
Figure 136, 375525 Building stats ROP (left) and RPM (right) stats.....	113
Figure 137, Design (438320) @ Range E.....	114
Figure 138, Design (411639) @ Range E.....	114
Figure 139, Design (375525) @ Range E.....	114
Figure 140 Building field tendencies 12 ¼ Case E.....	115
Figure 141 Building @ range E	119
Figure 142, Design (605284) steering response all behaviors	120
Figure 143, Design (585609) steering response all behaviors	120
Figure 144, Design (478186) steering response all behaviors	121
Figure 145, Design (422785) steering response all behaviors	121
Figure 146, Design 605284	122
Figure 147, Design 585609	123
Figure 148, BHA type of design (605284).....	124
Figure 149, BHA type of design (585609).....	124
Figure 150, BHA type of design (478186).....	125
Figure 151, BHA type of design (422785).....	125
Figure 152, 605284 Building ROP (left) and RPM (right) stats	126
Figure 153, 585609 Building stats ROP (left) and RPM (right) stats.....	126
Figure 154, 478186 Building stats ROP (left) and RPM (right) stats.....	126
Figure 155, 422785 Building stats ROP (left) and RPM (right) stats.....	127
Figure 156, Design (605284) @ range F.....	127
Figure 157, Design (585609) @ range F.....	127
Figure 158, Design (478186) @ range F.....	128
Figure 159, Design (422785) @ range F.....	128
Figure 160 Field tendencies Case F M [130-170].....	128
Figure 161 Model (top) vs. field (bottom) tendencies	133

List of Tables

Table 1, Geo-Pilot™ System Specifications [7].....	8
Table 2, Summary design (487256) all data points	51
Table 3, Summary design (405148) all data-points.....	56
Table 4, Case A, Ranges for FMF3651Z vs FMF3653Z.....	56
Table 5, Summary design (405148) all data points	59
Table 6, Case B, Ranges @ Low ROP, 8 ½ section.....	72
Table 7, Low ROP, bit designs	73
Table 8, Case C, Ranges @ Medium ROP, 8 ½ section	80
Table 9, Medium ROP, bit designs for turning analysis	80
Table 10, Medium ROP , bit designs for building analysis.....	80
Table 11, Case D, Ranges @ High ROP, 8 ½ section	96
Table 12, High ROP, Bit designs for building analysis.....	96
Table 13, High ROP, bit designs for turning analysis.....	96
Table 14, Case E - 12 ¼ section	109
Table 15, Case E, Ranges.....	113
Table 16, Case F – 12 ¼ reamed to 13 ½ bit designs.....	122
Table 17, Case F, Ranges.....	127
Table 18, Summary table.....	135

Nomenclature

M/LWD: Measurements/Logging While Drilling

RSS : Rotary Steerable System

DLS : Dog Leg Severity

GP : GeoPilot™

CRS : Confined Rock Strength

CCS : Confined Compressive Strength

LHS : Lower Housing Stabilizer

PWD : Pressure While Drilling

GABI : Gamma Azimuthal at Bit Inclination

ECD : Equivalent Circulating Density

WOB : Weight on Bit

TQB : Torque on Bit

TMI : Thermal Mechanical Integrity

DxD : Direction by Design

ROP : Rate of Penetration

RPM : Revolutions per minute

SF : Side Force

JSA : Junk Slot Area

1. Introduction

1.1 Background & Problem definition

Within the drilling discipline there are many activities and scenarios that can be encountered. These involve fluids, casing design, drill string design, BHA design, bit selection, cementing, etc. All of these activities have a cycle behavior regarding the planning, operations and post well analysis. The following study will focus on the directional control activity during operations and emphasis will be set on post well analysis.

Directional control is one of the most important issues within the well construction process. The trajectory followed will allow the well to avoid problematic zones, to reach the target or targets within the uncertainty range and therefore achieve a successful exploration well or better well placement for production.

In order to achieve this trajectory the process begins with a planned well that is defined and modeled from geological interpretation and operational/logistic constrains. However, this planned trajectory is not always followed at a 100% match. This is explained mainly due to the geological and operational uncertainties.

In order to reduce these uncertainties and forecast the performance of a given system, many models have been developed. The study develops a method to assess field drilling data and compare representative measurements with model forecasted results.

Now, what are those representative field measurements? As it is well known from current drilling operations M/LWD (Measurements/Logging While Drilling) tools not only measure and send many parameters from down hole to surface, but also monitor and record surface drilling parameters. The study will define and use the most appropriate and available data in order to assess steerability from field.

The steerability concept is also a reference value that was measured and according to different authors and points of view can be represented by several values such as steer index^[1], dB/dt^[2], DLS, etc.

In addition, the study will focus only on the RSS (Rotary Steerable System) (point the bit). Where the long gage Geo-Pilot™ bits performance will be analyzed and discussed.

1.2 Objectives

The main objectives of the study are:

- Develop a method to compare theoretical model results with field data steerability parameters.
- Define the criteria by which the study is valid.

-
- Generate insight about the impact of the main operational, geological and design parameters on directional responsiveness.
 - Validate the model when comparing different bit designs under similar applications. Thus, being able to identify the most steerable design in different scenarios.
 - Analyze the historical data and model results, comparing DLS vs. GP deflection.
 - Quantify the impact of the features added/modified to new designs analyzing different tool runs.
 - Compile post run suggestions of improvement, from HDBS (Halliburton Drill Bits and Services) and Sperry Drilling points of view.

1.3 Scope and limitations

The study discusses the performance of long gage Geo-Pilot™ bits in the Oseberg field located in the central North Sea. What's more, it focuses on the 12 ¼ and 8 ½ sections, where directional control is of great importance to achieve the targets of the well construction process.

The conditions at which the data is taken are very different from well to well and from section to section. The following outline describes the variables considered and the way they were handled in the study.

ROP: For the analysis two approaches were taken. In one hand, for the 8 ½ section as the ROP was much more spread than in the 12 ¼ section, three ranges of ROP were identified and analyzed separately. In the other hand, in the 12 ¼ section more intervals with build data were available, and the approach was to directly identify the ranges of useful build data points by means of statistic of ROP and RPM.

RPM: the ranges of RPM for the 8 ½ section were mainly distributed in two categories low and high. For the 12 ¼ only one range was used as most data showed RPM values between 130 and 170 RPM.

WOB: Only surface WOB was available, and as the S-WOB in wells with high inclination angle is not accurate enough to model the directional behavior of the bit, it was not considered as a criterion. However, as ROP was reliable and according to drilling mechanics studies, both this parameter and RPM can be used to fully describe the bit dynamics.

Side force: the simulator computes a theoretical side force and the results of the study are assessed in terms of figures DLS vs SF (simulator) and DLS vs GP deflection (field). SF (field) is a variable that is not yet measured directly from the tools analyzed in the study. Therefore, the best approximations taken are only GP deflection [%] and DLS achieved.

Geology: as it is well known in the industry geological uncertainty is always present and every single well is different from others even in the same area or field. This is explained due to the horizontal and vertical heterogeneity. The geological features of the formations drilled are represented by the Confined Rock Strength profile (computed data from sonic, porosity and density logs) for each well. In order to normalize the data, an average benchmark of 7000 psi was taken for

the 8 ½ section, and for the 12 ¼ a value of 12000 psi. This is possible as all the well paths chosen are from the same platform and in nearby templates.

Fluids: No fluid dynamics considerations were taken into account in the study. The parameters analyzed were mainly operational, geometric, and mechanic. The formation erosion action of high flow can have a big impact in soft formations; however, as the formations considered have a CRS (Confined Rock Strength) of above 5000 psi, then that effect can be neglected. Another important impact is the hole cleaning conditions which might affect the drilling parameters and therefore the steerability tendencies. In order to deal with these the data considered is from runs that did not pointed out serious drilling problems and were drilled under normal drilling conditions.

Drill string conditions: the analysis focus mainly on the Geo-Pilot™ 5200, 7600 and 9600 series and long gage bits. It does not consider the whole BHA tendencies and additional stabilizers above the GP flex collar. However as defined and quantified from many previous studies on BHA design each design will have a different tendency.

2 Literature Review

The main topics to be covered in this chapter are:

- Rock strength
- Directional drilling with Point the bit RSS (Rotary Steerable Systems), MWD/LWD
- Bits design and characteristics
- Steerability (Side force, DLS)
- Drilling parameters

2.1 Rock strength

This mechanical property of rocks is what will mainly control how easy the drilling system will break through the formations.

2.1.1 Geological setting

The mechanical and physical properties of rocks are influenced by a large number of geological factors. Mineralogy and particle-contacts control strength on a small scale; tectonic deformation, igneous activity and metamorphism all result in substantial changes in the mechanical behavior of rocks through re-crystallization and fracturing.

Burial and erosion of sediments results in a series of consistent and predictable changes. The increase in sediment load during burial combined with cementation and filling pores results in:

- increased strength
- decreased porosity
- decreased permeability

Stripping away sediment by erosion and the consequent unloading and weathering results in the development of joints leading to:

- decreased strength
- increased porosity
- increased permeability

In general rocks become stronger and less porous and permeable as they get older. Recent sediments are normally weaker than ancient rocks with similar lithology and mineralogy.

Rocks and soils with a level of compaction corresponding to their present burial depth re said to be normally consolidated. Where erosion has occurred, rocks may be compacted much more than expected for their current depth of burial. These rocks and soils are said to be over consolidated. Rocks that have not compacted to the expected extent for their depth of burial, perhaps because fluids were not able to escape, are said to be under consolidated. Under consolidated rocks are often associated with high fluid pressures (overpressure). An overpressure is a pressure in excess of the pressure predicted from the normal hydrostatic gradient ^[3].

2.1.2 Laboratory tests

Rock strength is measured by laboratory testing. Strengths are very different depending on the stress field applied to the rock. All rocks and soils are very much stronger in compression than in tension.

The two common laboratory tests to determine the compressive strength of rock are:

- Uniaxial Unconfined Compression Test - A cylindrical rock core is loaded axially until it fails.
- Triaxial Confined Compression Test - A cylindrical rock core is placed in a cell, subjected to all around (confining) pressure by hydraulic oil acting through a thin impermeable membrane, and loaded axially to failure.

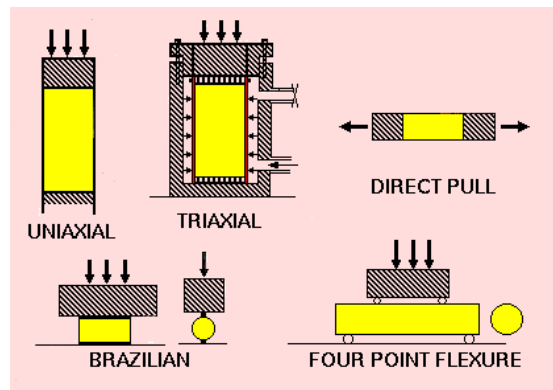


Figure 1, Rock strength measurements from laboratory [3]

Rocks fail in different ways depending on the temperature and pressure. At low temperatures and high strain rates rocks are brittle-elastic. They deform elastically at stresses up to about 70% of their strength then crack propagation becomes dominant and eventually the rock fails as cracks coalesce to form a large fracture or failure surface.

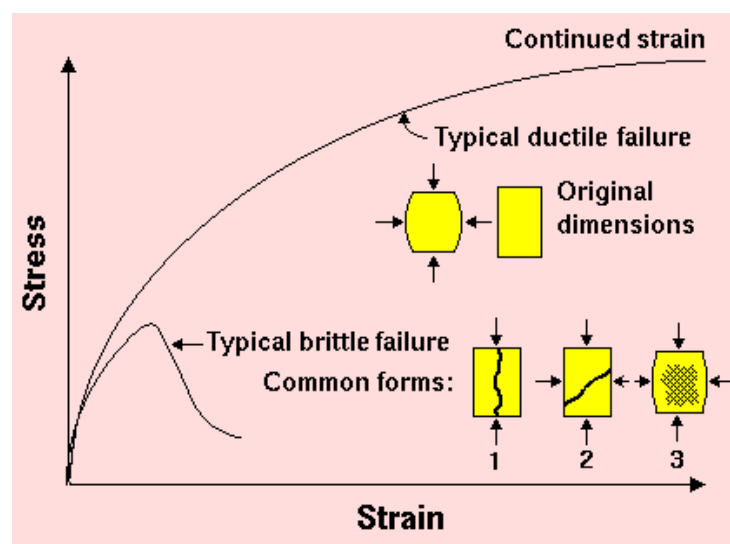


Figure 2, Stress strain plot [3]

At low confining pressures, shallow depths or near free surfaces, vertical splitting (1) is the usual failure mode. At higher confining pressures (deeper) a single shear plane develops (2). At even higher confining pressures, a network of inclined shears develops (3).

At low strain-rates, elevated temperatures and very high confining pressures the stress strain curve does not have a distinct maximum to indicate failure. Samples show the continuous deformation under load characteristic of ductile-plastic materials. Failed cores have a characteristic "barrel" shape. The transition from brittle-elastic behavior to ductile-plastic behavior is favored by:

- increasing pressure
- increasing temperature
- increasing fluid (pore) pressure

The change in behavior is called the brittle-to-ductile transition. For most rocks it occurs at temperatures and pressures outside the normal range of engineering. However, some shales, fine grained limestones (chalk) and most evaporates (rock salt, potash, gypsum etc) show ductile behavior in near-surface, low-temperature environments.

2.1.3 Estimation from field measurements [4]

Rock strength is usually estimated from core analysis and logs. The procedure is summarized in the following:

- Identify the complexity of lithofacies.
- Identify the logs available. If the formation is not so complex rock strength estimation can be done by GR and sonic logs only. If the formation is more complex and many lithologies are present the study will include, neutron porosity and density logs besides sonic information.
- The process begins by analyzing and cross checking the stratigraphic lithological information from logs and cutters SDL (Surface Data Logging) Mud logging plots.
- Then pinpointing and setting as benchmark the maximum and minimum values of GR and other properties for each lithology.
- Finally the software tool applies the algorithm to estimate the Unconfined Compressive Rock Strength and the Confined Compressive Rock Strength (considering the field of stress apply to the rock at different depths)

Due to the limited core information, other approach is to use log-core strength correlations; however these empirical correlations are developed for specific rock types, age, depth range, etc. [5]

An example of a correlation of Uni-axial compressive strength from sonic slowness (ms/ft) and p wave velocity from Horsrud.

$$C_o [\text{MPa}] = 0.77 \left(\frac{304.8}{\Delta t(\text{sonic})} \right)^{2.93} \quad C_o [\text{MPa}] = 0.77 V_p^{2.92} \quad [6]$$

2.2 Directional Drilling

2.2.1 Directional Tool

The directional tools analyzed are Geo-Pilot™ 5200, 7600, 9600

Geo-Pilot® System Specifications			
	5200 Series	7600 Series	9600 Series
Nominal Tool OD	5-1/4 in. / 133 mm	6-3/4 in. / 171 mm	9-5/8 in. / 244 mm
Hole Size	5-7/8 to 6-3/4 in. 149 to 171 mm	8-3/8 to 10-5/8 in. 213 to 270 mm	12 to 26 in. / 305 to 660 mm
Maximum Housing OD	5-1/4 in. / 133 mm	7-5/8 in. / 194 mm	10 in. / 254 mm
Length	16.2 ft / 4.9 m 27.7 ft / 8.4 m with flex sub	20.2 ft / 6.2 m 29.2 ft / 8.9 m with flex sub	21.7 ft / 6.6 m 30.9 ft / 9.4 m with flex sub
Nominal Tool Weight With Flex	1,250 lbm / 570 kgm	3,300 lbm / 1,500 kgm	4,850 lbm / 2,200 kgm
Connections			
Top	3-1/2 in. IF box	4-1/2 in. IF box	6-5/8 in. REG box
Bottom	3-1/2 in. IF pin	4-1/2 in. IF pin	6-5/8 in. REG pin
Minimum Steering Angle	5°	0°	0°
Design Performance (Build/Drop/Turn)	10°/100 ft / 10°/30 m	5°/100 ft / 5°/30 m	6°/100 ft / 6°/30 m
Maximum Dogleg Severity - Rotating	14°/100 ft / 14°/30 m	10°/100 ft / 10°/30 m	8°/100 ft / 8°/30 m
Maximum Dogleg Severity - Non-Rotating	25°/100 ft / 25°/30 m	21°/100 ft / 21°/30 m	14°/100 ft / 14°/30 m
Maximum Shaft Rotary Torque	8,000 lbf.ft / 1,085 daN.m	20,000 lbf.ft / 2,712 daN.m	30,000 lbf.ft / 4,067 daN.m
RPM Range	60 to 250	60 to 250	60 to 250
Maximum Mass Flow Rate - gpm x ppg - lpm x sg	5,000 lbm/min / 2,268 kgm/min	10,000 lbm/min / 4,536 kgm/min	20,000 lbm/min / 9,072 kgm/min
Maximum Weight On Bit	25,000 lbf / 11,121 daN	55,000 lbf / 24,465 daN	100,000 lbf / 44,482 daN
Vibration	As per Sperry's LWD vibration limits (available upon request)		
Mud Type	Compatible with all fluid systems including: WBM, OBM, SBM, and silicates; also with air, N2 and multiphase fluids like mist or foam.		
Maximum Sand Content	2%		
Pressure Loss Through Tool in Water (Calculated)	151 psi @ 200 gpm 1.04 MPa @ 577 lpm (water)	132 psi @ 500 gpm 0.91 MPa @ 1,893 lpm (water)	92 psi @ 1,000 gpm 0.63 MPa @ 3,785 lpm (water)
Maximum LCM limit*	120 lbm/bbl medium nut plug (well mixed) 342 kgm/m3	No Limit	No Limit
Maximum Operating Temp	302°F / 150°C	302°F / 150°C	302°F / 150°C
Maximum Pressure	Standard: 20,000 psi / 137.9 MPa Optional: 23,000 psi / 158.9 MPa	Standard: 18,000 psi / 124.1 MPa Optional: 21,000 psi / 144.8 MPa	Standard: 20,000 psi / 137.9 MPa Optional: 23,000 psi / 158.6 MPa
Maximum Overpull Operating	60,000 lbf / 26,689 daN	75,000 lbf / 33,362 daN	120,000 lbf / 53,379 daN
Ultimate Body Overpull Not Operating (No Continued Operation Replace Geo-Pilot Tool)	320,000 lbf / 142,343 daN	375,000 lbf / 166,808 daN	580,000 lbf / 222,411 daN
Geo-Span® Downlink Service	Surface pulser provides rapid communication and confirmation via InSite® control screen, independent manual control back-up system via pumps and rotary on/off signals rated 10,000 psi / 69 MPa operating H ₂ S service suitable for zones 1, IIA, T3		
Uplink	LWD system		
Surface Software	InSite® Rig Information Management System		
Inclinometer Accuracy and Span	+0.1° @ 2s, 0 to 160°		
For Directional, Gamma, Resistivity (For Typical MWD Tool Configurations) Survey Measure Point	35.0 ft / 10.7 m	25.0 ft / 7.7 m	26.5 ft / 8.1 m
Gamma Ray Measure Point	53.5 ft / 16.3 m	45.2 ft / 13.8 m	47.0 ft / 14.3 m
Vibration Measure Point	53.5 ft / 16.3 m	45.2 ft / 13.8 m	47.0 ft / 14.3 m
Resistivity Measure Point	46.2 ft / 14.1 m	38.3 ft / 11.7 m	40.1 ft / 12.2 m
At-bit Inclination Measure Point	10.2 ft / 3.1 m	3.2 ft / 1.0 m	3.3 ft / 1.0 m
At-bit Gamma Measure Point	20 ft / 6.1 m**	3.2 ft / 1.0 m	3.3 ft / 1.0 m
Power Supply	Lithium battery		
Maximum Run Duration	200 hours continuous orientation no power draw when deflection equals zero		

Table 1, Geo-Pilot™ System Specifications [7]

* LCM tolerance is limited by the MWD transmission system

** Distance quoted assumes the use of a PCG directional/gamma sonde

The table above shows the specifications of the different Geo-Pilot™ models considered in the study. There are other designs used in more specific applications such as the Geo-Pilot™ GXT that includes a power unit or the Geo-Pilot™ EDL with a design that enable the string to achieve very high DLS. Those designs will not be covered in the present study.

An advantage of considering only the designs 5200, 7600 and 9600 is that all of them present similar characteristics and is possible to categorize them as the standard group of directional tools for the sections 13 3/8, 12 1/4, and 8 1/2.

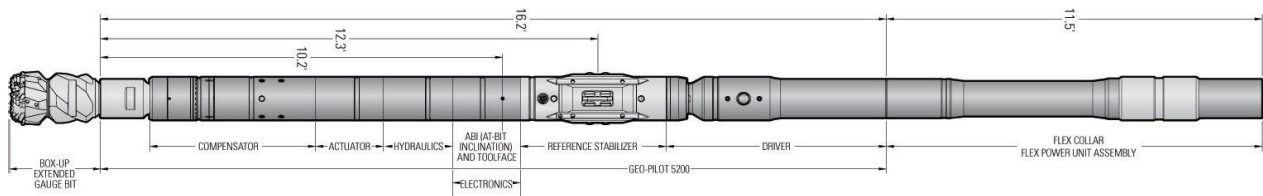


Figure 3, GP 5200 series [7]

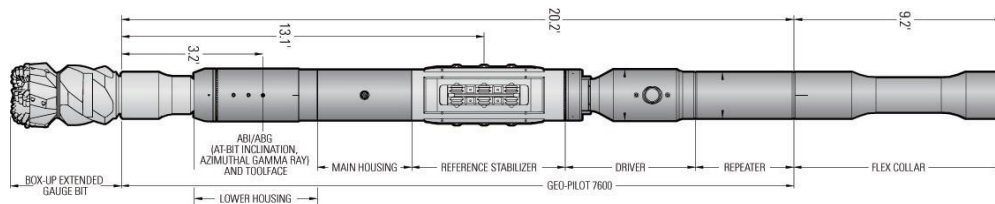


Figure 4, GP 7600 series [7]

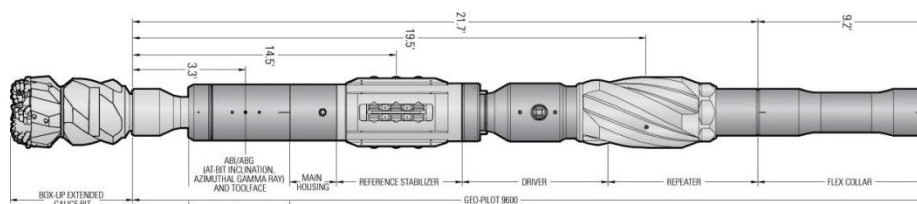


Figure 5, GP 9600 series [7]

2.2.2 Main parts functionality:

Main housing mechanism, the tool is deflected by means of an eccentric disc that bends the shaft. The result of that action is an angle of deflection between the hole axis and the angle of the lower end of the string. The combination of deflection and tool face achieve by the many positions of the eccentric allow the tool con gain directional control and drill in cruise mode or manual mode.

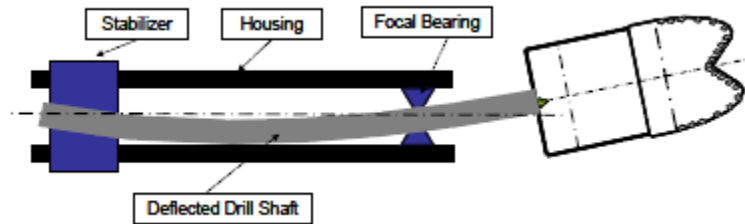


Figure 6, Working principle of GP, point the bit [8]

Lower Housing, inside the LH the GABI is installed around 1 m from the bit face in order to get accurate inclination and Azimuth measurements. The outer shape of the LH can be modified in order to increase the tilt length of the system and therefore achieve higher and more stable DLS. This is achieved and still in study to define the best shape in order to improve fluid dynamics and avoid problems such as balling.

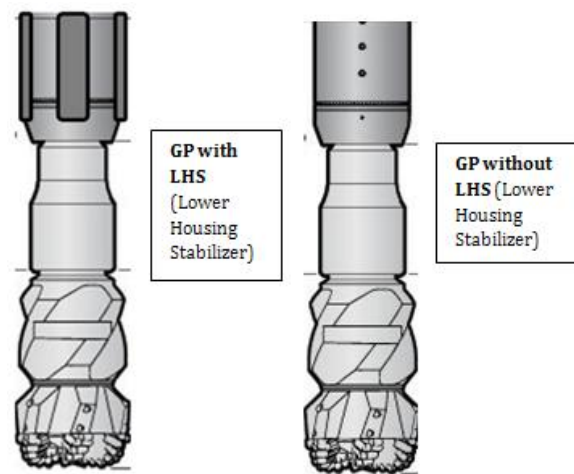


Figure 7, GP with and without LHS

Reference stabilizer, is the part that prevent the housing from rotating and therefore assures the directional control. It is composed of four sets of discs, called pizza cutters that have springs that push them against the formation thus fixing the housing and preventing rotation.

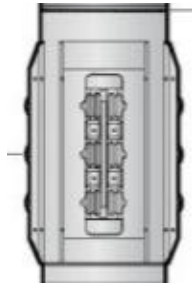


Figure 8, Non-rotating housing [7]

2.2.3 Surveys

Sperry Drilling's GABI™ (azimuthal gamma ray and at-bit inclination) sensor is a tri-axial accelerometer package that mounts on the bit box of a steerable assembly and communicates data across the directional tool (Geo-Pilot™, Motor or Turbine) to the main MWD tool via an acoustic telemetry link. The GABI™ service provides Inclination, Azimuth and Gamma ray measurements that are taken as close as 3 ft from bit that can generate a gamma ray image for geosteering.

Directional sensors consist of tri-axial accelerometers and magnetometers (based on gravitational and magnetic fields) and gyro service based on rate-gyro steering to avoid the influence of magnetic sources.

PWD (Pressure While Drilling), consists of quartz gauges that measure the annular and bore pressure. These allow to estimate the down hole ECD, kick detection, swap and surge pressure variations, etc. They also help in the calibration of downhole WOB, TQB and bending sensor tools such as Drill DOC (Downhole Optimization Collar) tool.

Drilling vibration sensors, these sensors can recognize the different torsional, lateral and axial accelerations and then if the drillstring vibration approaches the operational limits, corrective actions can be taken.

AcousticCaliper sensor, consists of three 120 degrees apart transducers that generate real-time caliper logs, This provide insight information regarding borehole stability, under gauge condition or washouts in the borehole. [11]

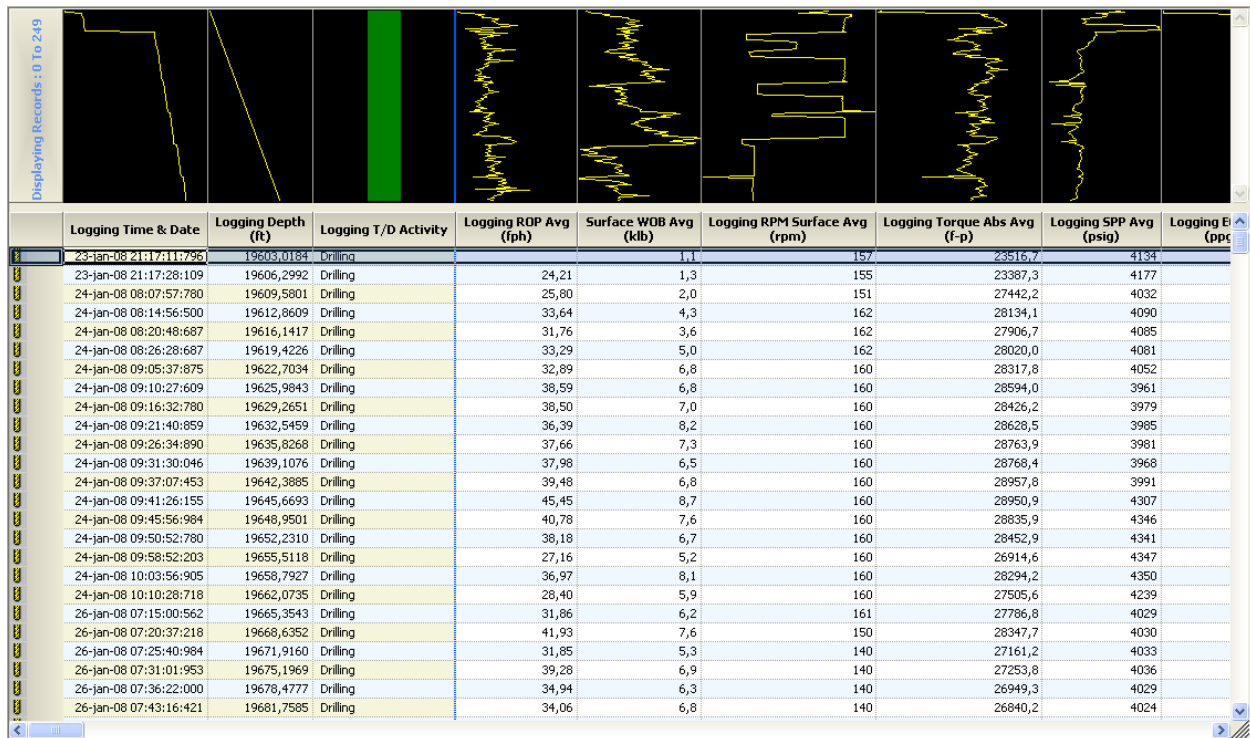


Figure 9, L/MWD datasets example "Insite" [9]

2.3 Fixed cutters bits

2.3.1 Range of applications

a) PDC

- a) Medium to high abrasiveness.
- b) Siliceous content (from shale, lime stone to 100% sandstone, quartzite).
- c) Shearing action.
- d) Used in long runs.
- e) Soft to hard formations.
- f) Low to medium RPM.



Figure 10, Standard PDC bit [10]

b) Impregnated

- g) High to very high abrasiveness.
- h) Siliceous content (from shale, lime stone to 100% sandstone, quartzite)
- i) Compression, plighting and scraping action.
- j) Hard very abrasive formations.
- k) High RPM (turbine)



Figure 11, Impregnated Bit [10]

2.3.2 Bit Nomenclature

Is the general commercial classification, as: FM2000, FM3000, FX, etc. series. Where the zeros “0” define some features of the bit as described in the following picture:

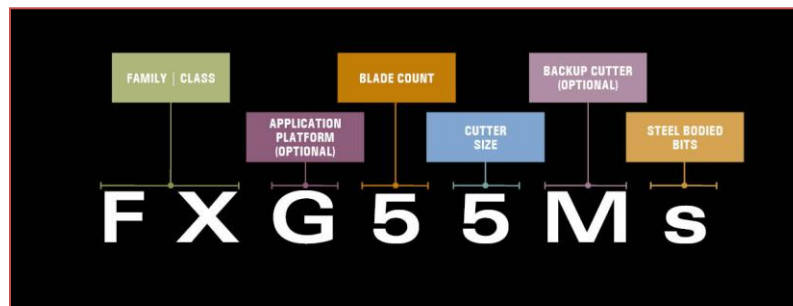


Figure 12, Nomenclature example [7]

As can be seen from Figure 12 the additional information that can be known from the bit nomenclature is about the number of blades, the main cutter size and the profile type. These basic features are designed to balance the requirements of the application to be drilled.

2.3.3 Material number and Serial number

The material number refers to every single design regarding any change in any feature of the bit. This means that a bit type can have many small (but important modifications) and each modification represents a new material number. These modifications can be:

- Change in cutters design (shape, size, technology type).
- Addition of backup options: R1 cutters, Double row of cutters, Diamond domes, impact arrestors.
- Passive/active gage pad
- Sleeve configuration
 - o Length, width
 - o Tapered
 - o Steps, etc

The list above is only an example and many other features can be added/modified.

The bit serial number is the identification of every single bit that has been manufactured. In that sense it is unique number.

2.3.4 Bit selection

The bit selection is made according to the various challenges and the application to be drilled. The main selection criteria include the following parameters:

- Formation hardness.
- Formation abrasiveness.
- Inter bedding, stringers.

- Run length (bit life).
- BHA (motor, RSS)
- Well profile (straight, directional)
- ROP limitations (hole cleaning)

2.3.5 Bit Features

a) Bit profile

The bit profile represents the shape of the blades from the center of the bit (cone) to the gauge. It is an important part of the design; it will partly dictate the bit cutting action. Below are described the two main types of behaviors and their general guidelines of design:

- Aggressive/less stable
 - Shallow cone angle
 - Small nose radius
 - Short profile
- Non aggressive/more stable
 - Deep cone angle
 - Large nose radius
 - Longer profile

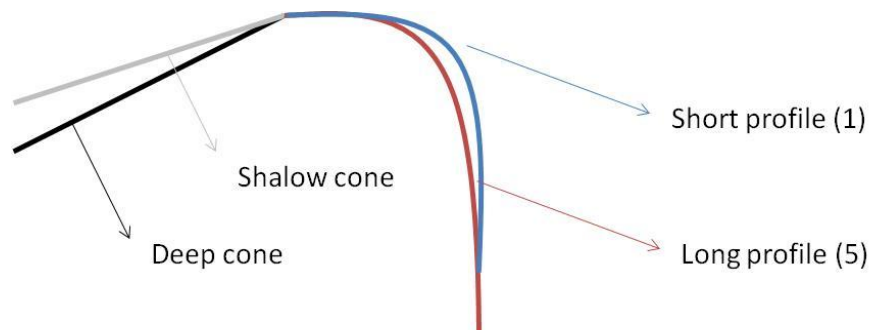


Figure 13, Bit profiles and Cone design

b) PDC cutters

PDC cutters are the major element in a PDC bit, and its many design features will also partly dictate the bit behavior.

- Size
 - Increasing size
 - More aggressive.
 - Decreased durability.
 - Lower cutter counts.
 - Decreasing Cutter size
 - Less aggressive.

- Increased durability.
- Higher cutter counts.
- Shape: Cylindrical, bullet, round or cube. For example scribe cutters for hard and brittle formations. These present a point loading effect, this is stresses in the formation are released. Formation is easier to shear resulting in a increase in ROP.
- Position
 - Face, nose, shoulder, gage
- Orientation, more aggressive less WOB needed
 - Back rake, is the angle between a vertical plane and the cutter as show in Figure 14. At lower back rake angle → more aggressive/less stable.

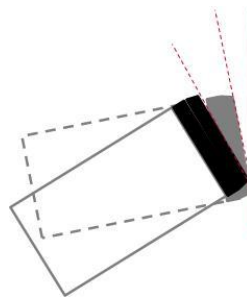


Figure 14, Back rake [14]

- Chamfer: is the tapered section of the PDC cutter. As in figure 15, smaller chamfer results in a higher depth of cut then the bit is more aggressive.

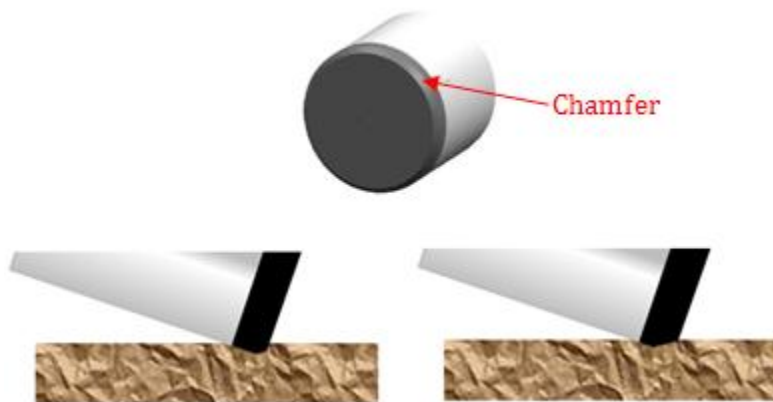


Figure 15, Small chamfer left (Higher depth of cut) [14]

- Cutters Material

During the development of the cutters technology there have been many materials and commercial names released to the market. Among those, the two most recent are Z3, then X3 cutters. The main challenges that the different technologies aim at improving are:

 - Impact resistance: ability to resist chipping and breakage.
 - Abrasion resistance: ability to stay sharp and slower cutters worn action.

- TMI (Thermal Mechanical Integrity): ability of the cutter to avoid degradation of the diamond bonds during high frictional heat during drilling.

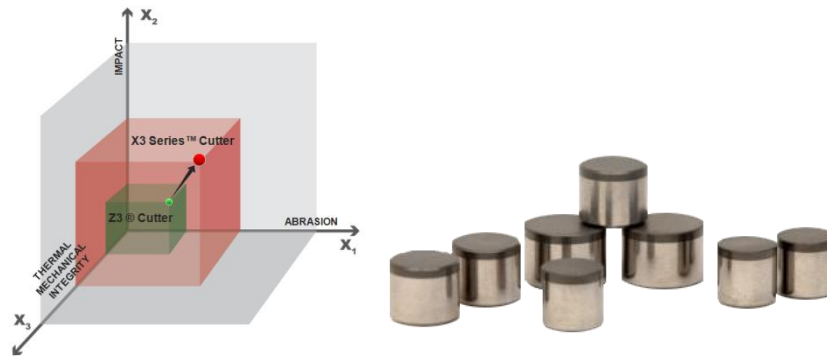


Figure 16, Cutters materials

c) Blades layout

- Symmetric design: generates lobes. Angle between the blades. For 3 blades at 120deg each.
- Asymmetric design: better resistance for lobe generation, smoother bore and less tendency for vibration (whirl).

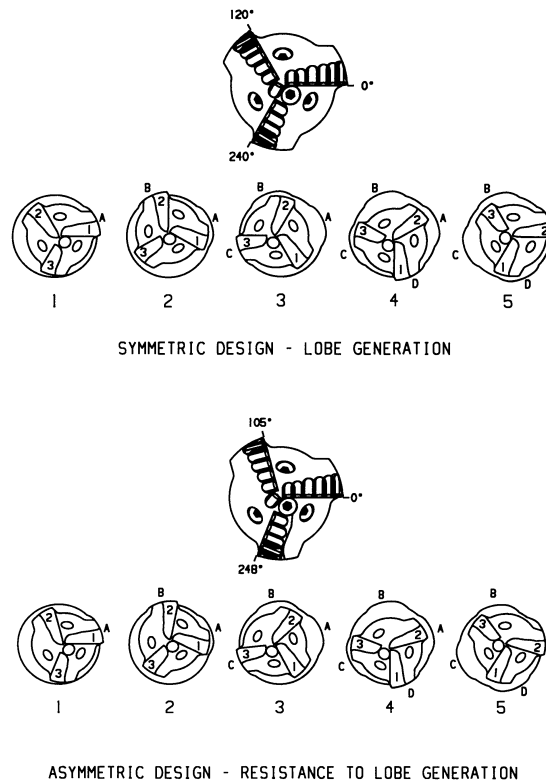


Figure 17, Blades, symmetric and asymmetric designs

- Spiraling vs. Straight: with spiraling less resistance from bore walls/bit interaction. Same torque but less variance, smoother drilling.



Figure 18, Spiraled (left) and Straight (right) blades

- Count
 - Higher number of blades and Higher cutter count → more stable/less aggressive.
 - Lower number of blades and Lower cutter count → more aggressive/less stable.
- MEG
 - Gap between gage pad and gage sleeve.
 - To improve hydraulics, hole cleaning.

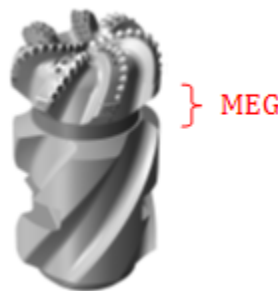
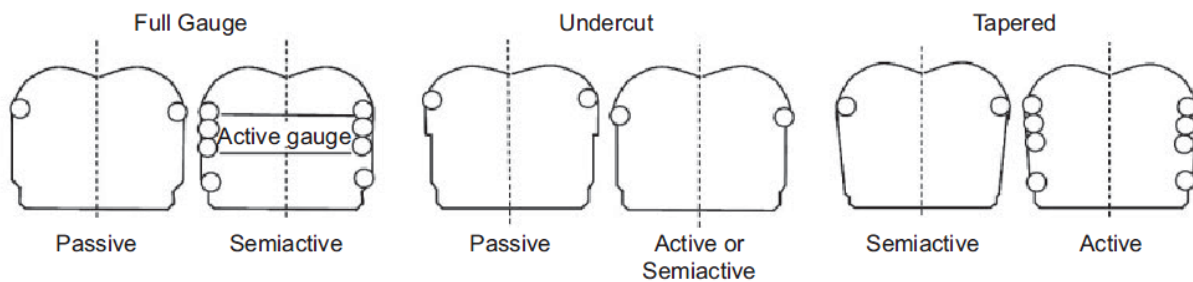


Figure 19, MEG (Modified Extended Gage)

- Gauge sleeve
 - Spiral, Straight, full gage, tapered,
 - Longer, more stable drilling, better hole quality.
 - Shorter, more steerable.
 - The higher the number of blades and the spiral angle, smoother drilling. This is achieved by the same torque but less variation.



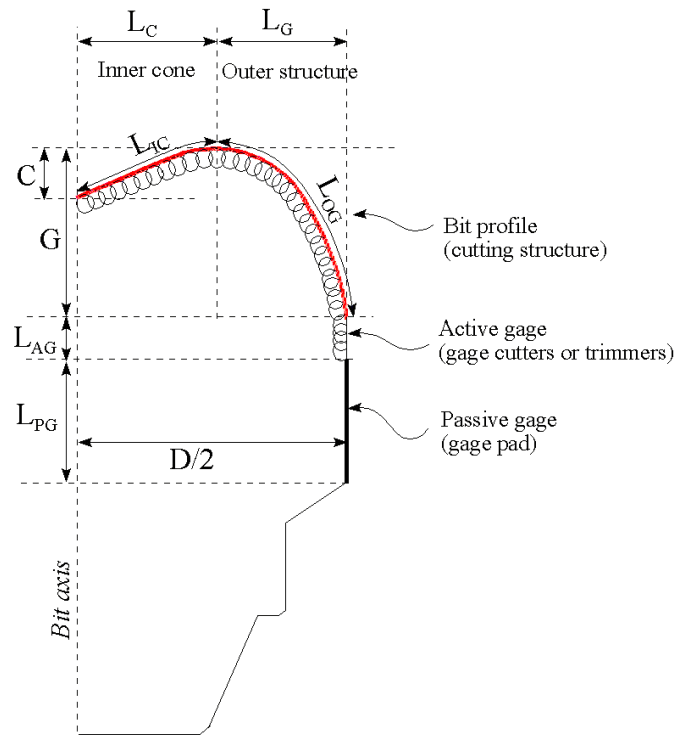


Figure 20, Gage pad and Gage sleeve design [12], [13]

As seen in the description of cutters and blades layout, aggressiveness depends mainly in:

- Blades design (count, shape, size, spiraling)
- Cutters design (count, size, shape, orientation)

d) Bit body material

- Matrix body type: It is made of tungsten carbide and powder particles which are cooked & bonded together by the carbide. Some important features include:
 - Faster manufacturing.
 - Less resistant to abrasion and wear.
 - Brittle.
- Steel body type: it is machined entirely from a carefully selected steel material.
 - Due to a more ductile behavior than matrix it allows higher blade stand offs. That means an improvement in flow dynamics, better cleaning.
 - Normal steel has lower resistance to wear and erosion. However with tungsten pebbles or diamond hard facing this is improved.
 - More Ductile.
 - Anti balling coating can be added

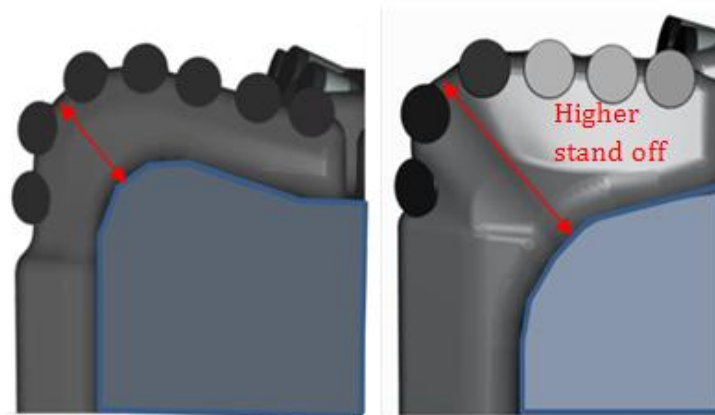


Figure 21, Standard matrix body (left) , Steel bullet body (right) [15]

e) Other features

- Fluid dynamics: PDC bits are built with nozzles where the drilling fluids exit from, ensuring:
 - Assure hole cleaning
 - PDC cutters cooling

Improved nozzles are designed to increased turbulence helping lift the cuttings.

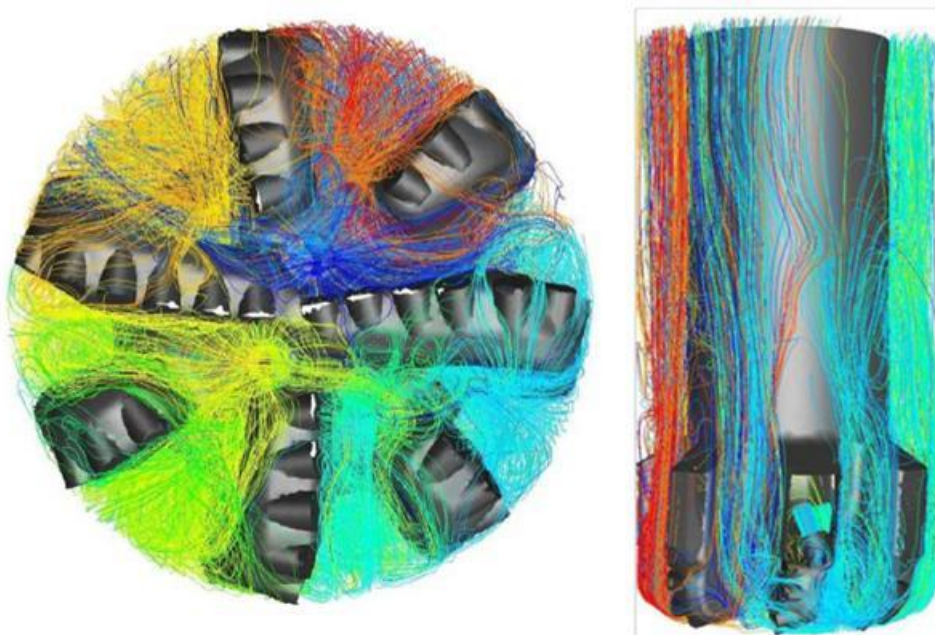


Figure 22, CFD Computational Fluid Dynamics [15]

- Special designs
 - With R1 (impact arrestors)
 - Dual row (for abrasive formations)

- With MDR (Modified Diamond Reinforcement) and Depth of Cut (DOC) control, limits over engagement.
- With impregnated diamond backup (for abrasive formations)

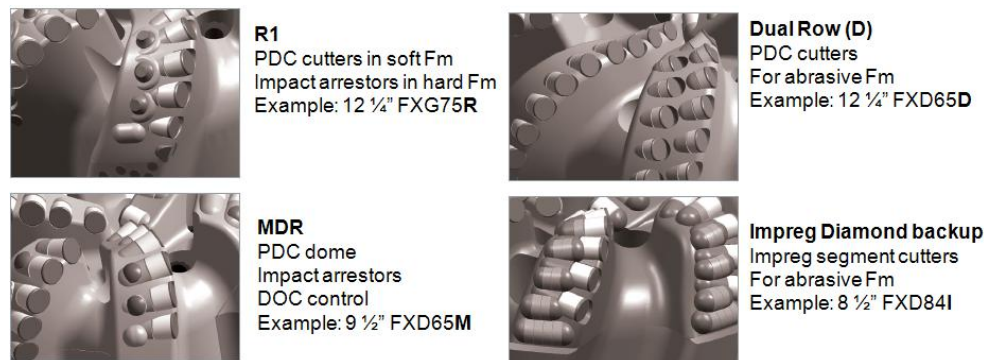


Figure 23, Special designs [14]

Cutter and blades layout are designed in order to maximize stability, durability, steerability and drilling speed. All these performance criteria come to a compromise to each other. Then, to obtain the optimum conditions, the following processes are applied:

f) Force balancing

- Includes: Drag, Radial, Axial forces analysis.
- Aim is to reduce the drag and radial forces to zero, and maximize the axial force. By doing so the risk of lateral/axial vibrations is decreased.

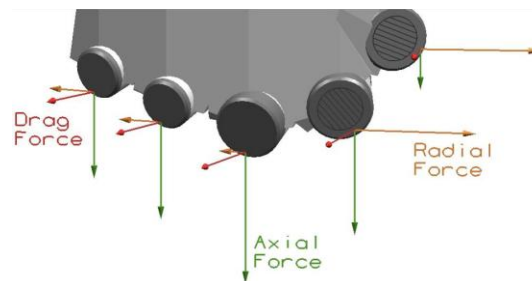


Figure 24, Force Balancing

g) Energy balancing

- Equally distribution of individual forces on cutters across the bit face, so cutting torque is smooth. All cutters are supported by each other.
- Aim to reduce impact damage and uneven wear while promoting improved ROP.

2.4 Steerability

According to S. Barton [16], S. Menand and H. Sellani [17], steerability was modeled on a basis of lateral ROP. This means that DLS was represented by lateral ROP. However the model is misleading

and the recently approach is considering parameters including: side force, tilt rate, tilt length, RPM and ROP.

What's more, generally three ideal drilling modes are considered:

- DLS = 0, vertical mode, bit kinematics determined only by ROP and RPM.
- DLS = Constant, ideal building/dropping.
- DLS ≠ Constant, kick off mode, sidetrack events, geosteering, etc

From operations and survey reports data, the mode that is the closest to the real world conditions is kick off. Thus, the focus of the study is in this drilling mode and the simulations were run only in this mode.

In most analytical and controlled laboratory conditions, bit steerability ^[18] (steer index) is a function of lateral drillability and axial drillability as

$$BS = \frac{\text{Lateral Drillability}}{\text{Axial Drillability}}$$

Where:

LD : mm of displacement over one revolution/side force

AD : mm of displacement over one revolution/WOB

Another approach to assess steerability is presented by Stephen Ernst, Paul Pastusek, and Paul Lutes ^[19] where bit steerability is evaluated in terms of side cutting (tilt) angle gain β at different ROPs and RPMs. In this paper the effects of ROP and RPM are presented. And as other sources stated as well: "most WOB effects are actually due to its influence on ROP and bit tilt". In the study, the analysis of data starts from that premise and continue to assess the performance of the RRS point the bit-and long gage bit. Where the ROP and RPM are carefully distinguished and filtered so more accurate conclusions can be obtained from real field data.

Another important conclusion from the different papers consulted and literature in the industry is the close relationship ROP-WOB. This relationship allows the model used for the simulation and others used in the industry to analyze steerability either in terms of ROP or WOB. If one parameter is defined the other is related and calculated and does not need to be explicitly defined. Therefore the thesis work analyses ROP and RPM. The WOB was willingly omitted as literature suggest an also because data is only from surface WOB which is not accurate in highly deviated wells. In future studies where downhole WOB (D-WOB) will be available from tools such as Sperry's DrillDOC®, the use of D-WOB and bending data will be very valuable to such project.

The impact of high RPM and lower ROP will be verified and validated with field data. In addition, with the aim to complement the ROP and RPM impact, another approach considering steering behaviors will be implemented and further explained in the methodology part of the study.

2.5 Description of variables

2.5.1 Side cutting

Side cutting is the action of a bit which drills with a lateral penetration (displacement); however it implies a very difficult control, tendency to whirl and create spiraling holes of poor quality. Therefore it is an action of the bit that is carefully implemented and tested to balance the downsides and upsides of such action.

2.5.2 Bit Side Force

The force at the bit that is perpendicular to the well path direction. The resulting side force will determine a build tendency (+) or a dropping tendency (-). The purpose of the deviation mechanisms is to create a large side force at the bit that will deviate the BHA laterally. Therefore in general terms the DLS that a system can achieve is a function of the bit side force applied.

Side force is largely generated by strain energy, the BHA bents into a curve. This deflection is the result of BHA geometry and WOB.

In order to maintain the side force in a given section, the curvature of that section must be kept. This is achieved by reducing the side cutting capability of bit to the maximum. Then the BHA will not be able to return to its normal straight position. If the bit side-cuts then the curvature will not be maintain and the strain energy will be released. Then, the DLS will tend to diminish.^[20]

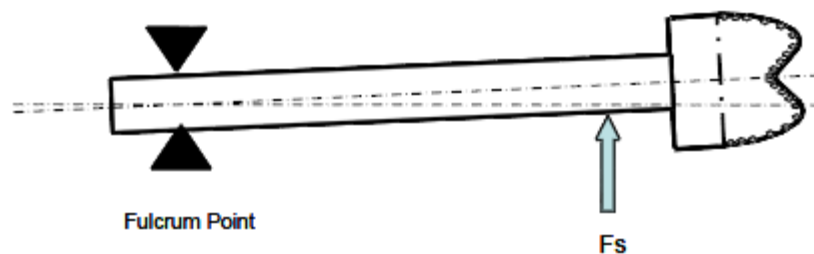


Figure 25, Side force F_s ^[20]

2.5.3 Dog Leg capability of BHA

The DLS capability of a BHA can be defined by the following parameters: BHA design, hole curvature, wellbore inclination, WOB and formation anisotropy. And it is usually proportional to bit side force. During the planning of a well the service companies defined the tools required for a given run. With that information the max loads and DLS that BHA can withstand are estimated and also define some directional tendencies of the assembly.

2.5.4 Dog-Leg Severity (DLS)

DLS is the ratio of dog leg angle to the course length and is commonly expressed in degrees per 100 ft or degrees per 30meter.

$$DLS = 100 \frac{\varphi}{\Delta MD} [\text{deg./100ft}]$$

Where the dog leg angle is:

$$\varphi = \cos^{-1} \cos I_1 \cos I_2 + \sin I_1 \sin I_2 \cos Az_2 - Az_1$$

And:

I : Inclination [deg.]

Az : Azimuth [deg.]

ΔMD : Course measured length [ft.]

1,2 : Previous and current survey points.

2.5.4 Geo-Pilot™ deflection

This variable is defined in a percentage range [%]. The result of the deflection is the tilt angle created between the hole's axis and the bit's angle.

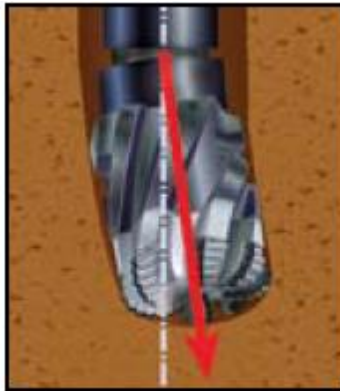


Figure 26, Tilt angle

3 Methodology

3.1 Structure of the Analysis

The methodology used to develop the study has a deductive base. In that sense, first a geological setting is identified and described in all the cases, then a production field within the NCS chosen, wells selected, sections and specific drilling parameters identified and used in the analysis.

The methodology can be summarized in three parts:

- Generation of field tendencies
- Generation of model tendencies
- Correlation of tendencies and validation of model

The field tendencies are generated following the next steps:

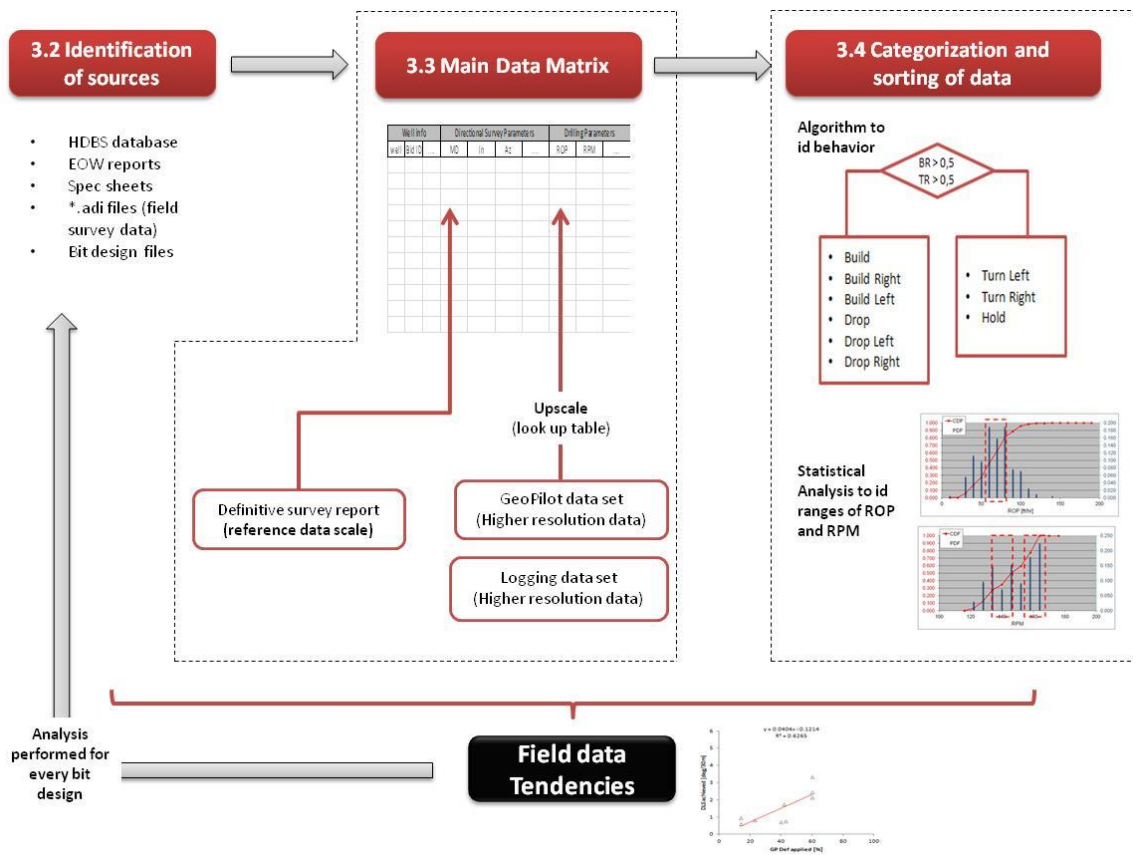


Figure 27, Field data tendencies flowchart

As shown in Figure 27 initially, all the relevant sources of data are identified and described. These descriptions summarize the types and resolution of data found in each source.

Then, the data gathering process is explained in the construction of the Main Data Matrix. In this part of the methodology the way to handle the different data resolutions is explained.

The next step is to categorize and sort data in a relevant way, so the analysis can be performed and more accurate results presented.

Finally, after sorting and filtering the main data, field tendencies are generated. These field tendencies are the base of comparison to correlate the theoretical model.

After assessing the field data, the second part of the study is to get the model tendencies. In order to run the simulations two main activities have to be carried on.

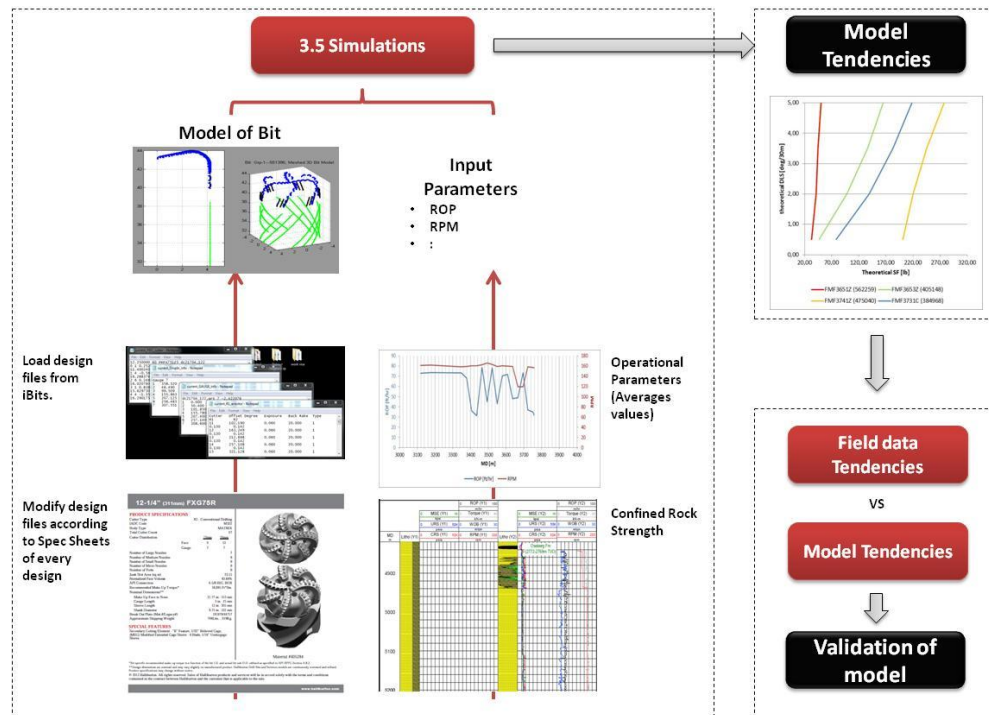


Figure 28, Model tendencies and Validation

As shown in Figure 28, first, a 3D model of the bit is generated. This is done with the iBits design files of each bit and the information gathered from the specification sheets.

Second, the input parameters are defined as a function of the ranges identified from the field data, analysis of ROP, RPM and CRS profiles is done and averages values are taken.

Once field tendencies and model tendencies are generated these can be compared. In this analysis the main features of each design are pointed out and performance is assessed from a theoretical and field point of view.

3.2 Identification of Data Sources

When collecting the data, the sources used where the following:

3.2.1 Use of DBS (Drilling Bits and Services) data base

- The data base has records of all the bit runs of the region.
- Useful to locate the well name, rig, RSS type, bit type/size.
- From this info a master report can be exported to Excel.

SERIAL	BIT TYF	BIT DIMENS	MANUFACT	CUSTOMER	RIG	WELL	DRIVE SYST	DEPT	DEPT OI	TVI	TVD OI	METERS D					
10644133	FMF3731C	8 1/2"	SDBS	NORSK HYDRO	OSEBERG C	30/6-C-8CT2	Geo-Pilot	4244	13920.3	4997	16390.16	2622.6	2663.4	75:			
10698367	FMF3653Z	8 1/2"	SDBS	NORSK HYDRO	OSEBERG C	30/6-C-8C	Geo-Pilot	3763	12342.6	4516	14812.48	2621.8	2635.8	75:			
10745126	FMF3653Z	8 1/2"	SDBS	NORSK HYDRO	OSEBERG C	30/6-C-8A	Geo-Pilot	2819	9246.32	3465	11365.2	2104	2457.6	64:			
10745126	FMF3653Z	8 1/2"	SDBS	NORSK HYDRO	OSEBERG C	30/6-C-8A	Geo-Pilot	3567	11699.8	3920	12857.6	2512.9	0	35:			
10881263	FMF3741Z	8 1/2"	SDBS	NORSK HYDRO	OSEBERG C	30/6-C-15C T6	Geo-Pilot	4005	13136.4	4520	14825.6	2706.6	2705.1	51:			
10881263	FMF3741Z	8 1/2"	SDBS	NORSK HYDRO	OSEBERG C	30/6-C-15C T7	Geo-Pilot	4267	13995.8	4634	15199.52	2707.7	2705.2	36:			
10948194	FMF3653Z	8 1/2"	SDBS	NORSK HYDRO	OSEBERG C	30/6-C-15C	Geo-Pilot	2581	8465.68	2674	8770.72	2529	2595	93			
10932827	FMF3651Z	8 1/2"	SDBS	NORSK HYDRO	OSEBERG C	30/6-C-15CT2	Geo-Pilot	2988	9800.64	3406	11171.68	2700.4	2721.3	41:			
10932827	FMF3651Z	8 1/2"	SDBS	NORSK HYDRO	OSEBERG C	30/6-C-15C	Geo-Pilot	2813	9226.64	3572	11716.16	2666.9	2739.5	74:			
10984824	FMF3651Z	8 1/2"	SDBS	NORSK HYDRO	OSEBERG C	30/6-C-15C T4	Geo-Pilot	2620	8593.6	3368	11047.04	2554.3	2722	76:			
DRILL	HOU	RC	RPM M	RPM M/	WOB M	WOB M/	FLOW M	FLOW M/	PRESSURE M	PRESSURE M/	TRQ ON E	INCL	INCL OI	AZIMUTH	AZIMUTH OI		
753	46	16	145	145	3	12	1800	2070	197	237	33kNm	89.6	84	326.7	16.9		
753	46.9	16.1	120	160	1	10	1800	2200	195	230	22-29kNm	87.8	86.1	310	350		
346	32.3	20	80	150	2	7	1976	1976	171	171	16-22kNm	56	57.2	324.3	322.2		
353	19.4	18.2	135	140	3	7	2190	0	217	0	0	57	55.6	323.6	321.3		
515	26.4	19.5	150	160	4	12	2200	2200	224	224	0	90.1	92.5	342	354		
367	20.5	17.9	160	160	1	4	2100	2200	220	220	29	89.9	93.5	347	336		
93	6.8	13.6	100	100	3	8	2000	0	141	0	11-14kNm	41	48	39.5	41		
418	26.7	15.7	120	120	3	8	1750	2200	138	208	18-21kNm	86.3	91.1	36.6	5.3		
749	32.2	23.6	120	120	3	8	1600	2200	138	198	12-17kNm	69.5	83.5	37	3		
768	67.7	11.3	140	160	6	12	2500	2800	180	209	17-28kNm	51.2	90	33	350		
MUD TYF	MUD WEG	TFA	NOZZLES	OF	CHAI	LC	BR	GA	CHAR	POK	RECOMMENDATIC	DULL REMARKS	CUSTOMER IADC DUL	COMMENT	IADC BITCOI		
OBM	1.25	0.804	2x18, 1x20	8	4	CR	A	X	I	WT	TD	SCRAP	Bit cored in center	8-3-RO-C--X-ILT-TD	M422		
OBM Versawert	1.25	0.778	6x13	3	4	CT	A	X	I	LT	TD	SCRAP	Looks like junk damage. Starting to ringout	3-2-CT-N-X-ILT-DTF	M423		
OBM	1.45	0.778	6x13									REPAIRABLE	Sent to brussels for hardfacing on sleeve	1-1-WT-A--X-I-NO-TD	M423		
OBM	1.46	0.778	6x13	1	1	WT	S	X	I	NO	TD	REPAIR		1-1-WT-A--X-I-NO-TD	M423		
OBM	1.2	0.99	4x18									N/A	not seen - OH sidetrack		M432		
OBM	1.2	0.99	4x18	3	2	WT	A	X	I	NO	TD	REPAIRABLE		3-1-BT-N--X-I-WT-TD	M432		
OBM	1.35	1.18	6x16	2	2	CT	A	X	I	WT	TD	BHA	REPAIRABLE	1-0-PN-C-X-CT-BHA	M423		
OBM	1.35	1.035	6x15	2	2	CT	A	X	I	NO	TD	REPAIR		3-2-WT-N--X-I-NO-TD	M423		
OBM	1.35	1.04	6x15									N/A	sidetrack, not seen		M423		
OBM	1.35	1.18	6x16	0	0	WT	A	X	I	NO	TD	REPAIRABLE	as new	0-0-NO-A-X-I-NO-TD	M422		
REMARKS																	
Drilled sidetrack after several attempts - chased the weight as soon as any weight was recorded. No vibrations during run. Several pressure peaks - bit condition on surface explained this. 4200m approx. Hole cleaning good. Good sand. Circulate hole clean prior to drill fault at 4278m. Drilled through without problems. Slower ROP in lower Ness. Hit coal and decided to pull back and perform an open hole sidetrack. (this ST 4335-4346m was not identified as TZ, as the roof fell down after only 10m.)																	
CBIs. Big casing size 13 3/8" - carefully reamed and drilled until all states inside open hole. No problems. Drilled to first core point. No bit related problems. Bit run after last core in section.																	
12. available, in case of OH Sidetrack. At 3660m a survey was taken to verify the BHA was in T6 before carrying on in hole to 3950m where the interval from 3950m to 4004m was relogged where the ALD sensor had failed. Drilling commenced at 4004m. Geosteering according to and the ROP limited to 20 m/hr. At 4452m, due to a decreasing trend in resistivity the inclination was increased to 92 degrees and held there. It was thought the wellbore was approaching the oil water contact. However the T6 wellpath exited the roof of the Etna formation and encountered coal at 4998m MD. TD was called for the T6 wellpath at 4520m and it was decided to pull back to do an open hole sidetrack.																	
Problem to build as planned.																	
Drilled into OWC, pulled back to do a OH ST. Reamed 2979-2988m to create ledge for Shrs. Timedrilled OH sidetrack in 3-4 hrs. Continued drilling 8 1/2"hole...tbc																	
Drilled into oil/water contact. Performed successful open hole sidetrack. with XR800, modified GP no press indication on active-set reamer. Shoulder verified.																	
HOLE DIAMET	DATE I	FORMATION NAME	LITHOLOGY	MAX DOGL	BHA	DRILLED SH	TA										
8 1/2"	5/19/2006	tba	tba	5.7													
8 1/2"	5/8/2006	Ness, Etna	sand, silt	4			No										
8 1/2"	2/27/2006	Hordland, Shetland	tba	1.2	bit-GP-Flexsub-Stab-MWD-MWD-PWD-XO-MWD-MWD-Stab-MWD-float-HWDP-Jar-HWDP		no										
8 1/2"	3/11/2006	Shetland, Dunlin	tba	1.34			no										
8 1/2"	8/16/2007	Etna	Sandstone	4.5	Bit, GP7600, flex, 8.44stab, MWD, sub, 8.25stab, float, HWDP, jar		No										
8 1/2"	8/16/2007	Etna, Ness	Sandstone	4.74	Bit, GP7600, flex, 8.44stab, MWD, sub, 8.25stab, float, HWDP, jar		No										
8 1/8"	4/25/2007	Jurassic: Viking, Heather, Brent, Tarbert		7.34	bit-GP-flex-8.405stab-mwd-float-dc-hwdp-jar-hwdp		no										
8 1/2"	5/6/2007	Brent, Ness	Sandstone, claystone	4.68	nit-GP7600-flex-8.405stab-mwd-float-dc-hwdp-jar-hwdp		no										
8 1/2"	5/1/2007	Brent, Ness	Sandstone, claystone	4.68	Bit, motor, flex, stab, MWD, sub, float, flex, xo		no										
12 1/4"	6/19/2007	Etna	claystone, sandstone	4.7	Bit, GP, flex, stab, MWD, sub, XR800, 8.5stab, DC, xo		No										
TAGGED TC	HRS UNT	UBR SENT DA	EWO REPO	RENT	COUNT	GRADING DA	UI	BITSTATU	BIT	DATE INTO COUNT	MOT	PDC	STORAGE PLA	UNDER CONTRA	ASSY	NO	BITRUN
0	0			Yes	Norway	6/14/2006			12992	6/16/2004		PDC	Tananger	Yes	384968	RR12	36253
0	0				Norway	6/29/2006			13244	1/14/2005		PDC	Tananger	Yes	405148	7	35996
0	0				Norway	13392			13392	8/1/2005		PDC	Tananger	Yes	405148	RR3	34973
0	0				Norway	13392			13392	8/1/2005		PDC	Tananger	Yes	405148	RR3	35353
0	0			Yes	Norway	13550			13550	9/20/2006		PDC	Tananger	Yes	475040	RR4	40783
0	0			Yes	Norway	13550			13550	9/20/2006		PDC	Tananger	Yes	475040	RR1	40812
0	0			Yes	Norway	13705			13705			PDC		Yes	435410		40233
0	0			Yes	Norway	13706			13706			PDC		Yes	487256	RR1	40293
0	0			Yes	Norway	13706			13706			PDC		Yes	487256	RR1	40483
0	0			Yes	Norway	13749			13749	8/8/2007		PDC	Tananger	Yes	487256		40482

Figure 29, Example of master report

This master report gives summary information about any bit run. This includes: Serial No, Bit Type, Bit dimension, Manufacturer (only SDBS taken), Customer, Rig, Well, Drive system, Depth in, depth out (MD), Meters drilled, Hours, ROP, RPM min, max, WOB min, max, Flow min, max, Pressure min, max, Torque on bit, Inclination in, out, Azimuth in, out, Mud type, weight, TFA, Nozzles, Dull grading, remarks, Hole diameter (run with Reamer), Formation name, Lithology, Max DLS, BHA,

Assembly No (material No.) And from here the most relevant runs can be selected. The main criteria are:

- The runs must be longer than 3 average survey points. That is, longer than 90m MD (measured depth)
- Within similar TVD (True Vertical Depth).
- With important change in inclination and azimuth, to capture the directional responsiveness.

During this process bit runs are selected, wells are identified and further information about the run is collected from the EOW reports

3.2.2 EOW reports

With the group of wells selected the next step is to get the DD EOW (Directional Drilling End of Well) report to complement and validate the information from the HDBS data base. The same is done with the SDL (Surface Data Logging) and MWD (Measurements While Drilling) reports.

3.2.2.1 DD (Directional Drilling) reports

From this report the following info was gathered and analyzed:

- *BHA (Bottom Hole Assembly) tally analysis and summary.* Contains schematics of the BHA used in each run are detailed, summary of parameters In and Out, and the results of the run are described. These include details regarding the trip in, operations and trip out. From that insight each run can be validated for the analysis.
- *Summary of BHA, motor and bit run.* This section shows a summary of the statistics regarding the time spend in the different operations (Drilling, circulating, tripping, etc) of all BHAs used in the well. This info can be used to compare the performance of each BHA within the different activities of the well, besides problematic runs and special operations are also point out here.
- *Summary of MWD runs.* Usually this info is included here otherwise the runs can be found in the MWD EOR. The run code number and depth in/depth information is identified to further load the corresponding ADI file (described in 3.2.4) in the Data Manager application of Insite.
- *Survey management program.* This part of the reports is done with the collaboration of the survey management team and RTOC (Real Time Operations Centre) in Alaska or Norway.

The main information described here is:

- Geomagnetic reference and azimuth correction data.
- Well position tie in points.

This data processing allows the correction of azimuth, and help to identify the tie-in points for the well that was drilled.

- *Definitive Survey data.* It is the part of the report that contains the inclination, azimuth, DLS (Dog Leg Severity), and most of the directional information used for the study and that will help to identified similar conditions and the most significant points for the study. Definitive survey refers to the final data measured, corrected and verified by the magnetic survey program. It is different from planned survey and represents the best approximation (applying the survey calculation method of minimum curvature) to the real trajectory followed subsurface.

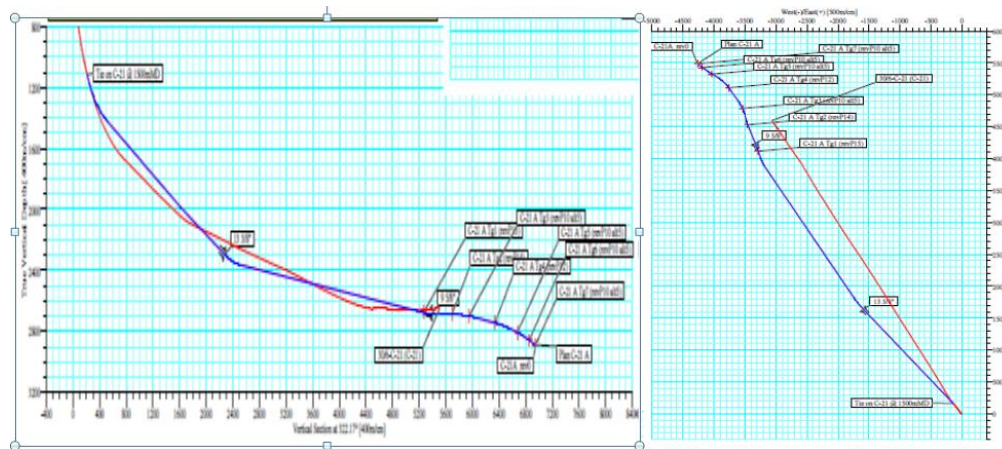


Figure 30, Example of planned (red) and real trajectory followed (blue)

Company: StatoilHydro		Date: 02-05-2008		Time: 15:06:41		Page: 5				
Field: Oseberg		Co-ordinate(NE) Reference: Oseberg C, Grid North		Site: Oseberg C, Grid North						
Site: Oseberg C		Vertical (TVD) Reference: Oseberg C 62.3		Section (VS) Reference: Well (-1.00N,-6.68E,322.17Azi)						
Well: 30/6-C-21		Survey Calculation Method: Minimum Curvature		Db: Sybase						
Wellpath: C-21 A										
Survey										
MD	Incl	Azimu	TVD	+N-S	+E-W	VS	DLS	Build	Turn	Tool/Comment
m	deg	deg	m	m	m	m	deg/30m	deg/30m	deg/30m	
4464.00	82.97	325.02	2436.66	2349.91	-2132.22	3160.47	1.933	-1.915	-0.266	IIFR Norway Standard
4494.10	84.36	325.34	2439.98	2374.47	-2149.30	3190.34	1.421	1.385	0.319	IIFR Norway Standard
4523.00	83.86	326.76	2447.04	2368.76	-2165.46	3210.03	1.063	0.510	0.065	IIFR Norway Standard

Figure 31, Example of definitive survey report

3.2.2.2 SDL (Surface Data Logging) reports

These reports contain general well and rig information, Geological and Drilling discussion section by section, BHA and bit summaries, Hole cleaning plots, Slack off, pick up and off bottom loads and torque, flow and pressure plots and RPM plots.

This information helps to identify the formations drilled, the type of rocks and also verified the normal conditions of the each run (Hook load, Torque and drag expected and actual graphs). If a section of the well was troublesome or the expected and current drilling conditions were very different then that section was not considered in the study. This initial analysis helps to get more accurate and reliable information for the analysis.

Figure 32, shows an example of a normal run. It can be seen that the calculated values are close to the measured ones. That behavior is an indication that the run was trouble free and therefore will

be considered in the analysis. Figure 33, summarizes the depth of the formations top expected and actual encountered on the field. This info is very useful when comparing well to well if those wells drilled the same formations and at similar depths. That also validates the fact of considering a constant rock strength for the simulations.

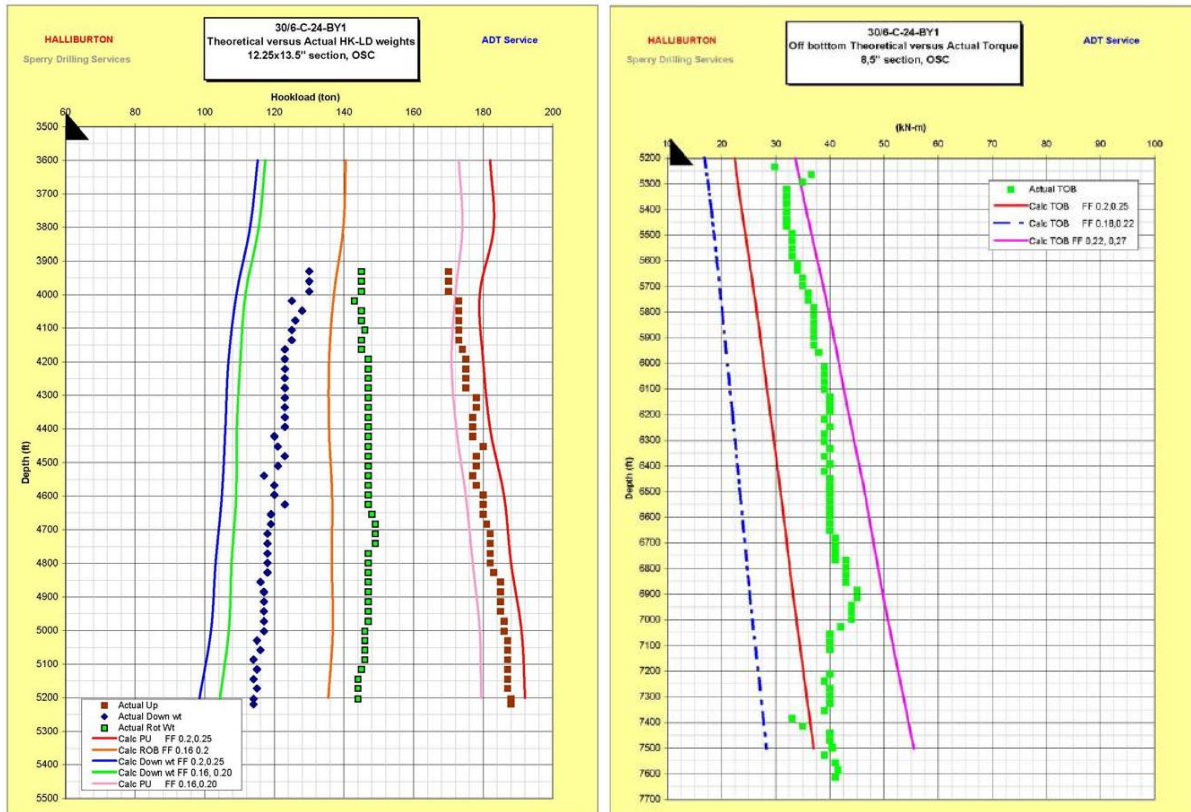


Figure 32, Example of theoretical and actual Hook load and Torque.

Predicted and actual (preliminary) tops of well Stratigraphic Top	Predicted Top		Actual (Provisional) Top	
	MD RKB (m)	TVD RKB (m)	MD RKB (m)	TVD RKB (m)
	K.O.F. from C24A	1140	1076	1133
Top Oligocene Str	1395	1250	1510	1334
Base Oligocene Str	1978	1615	1780	1604
Top Green Clay	2130	1711	2128	1717
Brown Clay	n/a	n/a	2632	2027
Top Balder	2698	2066	2688	2061
Sele	n/a	n/a	2817	2140
Lista	n/a	n/a	2858	2166
Våle	n/a	n/a	3116	2327
Top Shetland	3136	2341	3141	2343
Top Draupne	3358	2479	3348	2472
Top Heather	3377	2492	3378	2490
Top Brest Gr.	3601	2630	3580	2619
Top Tarbert	3601	2630	3580	2619
Top LT	3621	2642		
Top Ness	3641	2652	3622	2644
Top UN1	3652	2658		
Top LN3-5	3703	2682		
Top LN2_2	3756	2703		
Top LN2_1	3767	2708		
Top LN1	3777	2711		
Top Etive	3785	2714	3820	2726
Top Rannoch	3823	2726	3822	2727
Top Oseberg	3840	2730	3827	2729
Base Rannoch	4281	2753	4282	2753
Base Etive	4394	2754	4411	2754
Top Rannoch	4587	2760	4551	2757
Top Oseberg	4613	2762	4602	2761
Base Rannoch	5071	2776	5157	2770
Base Etive	5136	2770	5302	2766
Top Rannoch			6170	2769

Figure 33, Example of Lithology Summary

3.2.2.3 MWD (Measured While Drilling) reports

They summarize the BHA tally and tools used. The aim of analysis this information was to verify and get the Run No. so then the data can be extracted from the corresponding well database and run logging record. Figure 34 shows an example of the run summary and the information used:


Run No.	Bit No.	Hole Size (in)	MWD Service	Start Depth (m)	End Depth (m)	Drill/Wipe Distance (m)	Run Start Date Time	Run End Date Time	BRT Hrs.	Oper. Hrs.	Circ. Hrs.	Max Temp. (degC)	Serv. Int.	Trip for MWD
300	4	12.250		1122.000	1667.000	545.000	06-Apr-07 21:00	12-Apr-07 10:50	133.83	133.000	103.000	75.00	No	No
400	6	12.250		1667.000	2573.500	906.500	13-Apr-07 15:50	18-Apr-07 10:45	114.92	116.000	74.600	82.00	No	No
600	7	8.500		2581.000	2674.000	93.000	26-Apr-07 20:40	27-Apr-07 21:42	25.03	45.450	15.800	92.00	No	No

Figure 34, Example of MWD run summary

3.2.3 Specifications Sheets

These documents present the product specifications and special features of every bit design (material #), important information such as cutters type, nozzles, connection type, gage geometry, etc. can be found in these sheets as show in figure 35.

8-1/2" (216mm) FMF3651Z

<p>PRODUCT SPECIFICATIONS</p> <table border="0" style="width: 100%;"> <tr> <td style="width: 35%;">Cutter Type</td> <td colspan="2">X2 - Tough Drilling</td> </tr> <tr> <td>LADC Code</td> <td colspan="2">M422</td> </tr> <tr> <td>Body Type</td> <td colspan="2">MATRIX</td> </tr> <tr> <td>Total Cutter Count</td> <td colspan="2">48</td> </tr> <tr> <td>Cutter Distribution</td> <td style="text-align: center;"><u>13mm</u></td> <td style="text-align: center;"><u>16mm</u></td> </tr> <tr> <td style="padding-left: 20px;">Face</td> <td style="text-align: center;">6</td> <td style="text-align: center;">24</td> </tr> <tr> <td style="padding-left: 20px;">Gauge</td> <td style="text-align: center;">18</td> <td style="text-align: center;">0</td> </tr> <tr> <td>Number of Standard Nozzles</td> <td colspan="2" style="text-align: right;">6</td> </tr> <tr> <td>Number of Small Nozzles</td> <td colspan="2" style="text-align: right;">0</td> </tr> <tr> <td>Number of Ports</td> <td colspan="2" style="text-align: right;">0</td> </tr> <tr> <td>Junk Slot Area (sq in)</td> <td colspan="2" style="text-align: right;">13.76</td> </tr> <tr> <td>Normalized Face Volume</td> <td colspan="2" style="text-align: right;">40.2%</td> </tr> <tr> <td>API Connection</td> <td colspan="2" style="text-align: right;">4-1/2 LF. BOX</td> </tr> <tr> <td>Recommended Make-Up Torque*</td> <td colspan="2" style="text-align: right;">25,000 Ft*lbs.</td> </tr> <tr> <td>Nominal Dimensions**</td> <td colspan="2"></td> </tr> <tr> <td style="padding-left: 20px;">Make-Up Face to Nose</td> <td colspan="2" style="text-align: right;">14.86 in - 377 mm</td> </tr> <tr> <td style="padding-left: 20px;">Gauge Length</td> <td colspan="2" style="text-align: right;">1.5 in - 38 mm</td> </tr> <tr> <td style="padding-left: 20px;">Sleeve Length</td> <td colspan="2" style="text-align: right;">8 in - 203 mm</td> </tr> <tr> <td style="padding-left: 20px;">Shank Diameter</td> <td colspan="2" style="text-align: right;">6.25 in - 159 mm</td> </tr> <tr> <td>Break Out Plate (Mat.#/Legacy#)</td> <td colspan="2" style="text-align: right;">181975/44745</td> </tr> <tr> <td>Approximate Shipping Weight</td> <td colspan="2" style="text-align: right;">256Lbs. - 116Kg.</td> </tr> </table> <p>SPECIAL FEATURES P-100. Active Gage. .1/32" Relieved Gage. 1/16" Undergage Sleeve</p>		Cutter Type	X2 - Tough Drilling		LADC Code	M422		Body Type	MATRIX		Total Cutter Count	48		Cutter Distribution	<u>13mm</u>	<u>16mm</u>	Face	6	24	Gauge	18	0	Number of Standard Nozzles	6		Number of Small Nozzles	0		Number of Ports	0		Junk Slot Area (sq in)	13.76		Normalized Face Volume	40.2%		API Connection	4-1/2 LF. BOX		Recommended Make-Up Torque*	25,000 Ft*lbs.		Nominal Dimensions**			Make-Up Face to Nose	14.86 in - 377 mm		Gauge Length	1.5 in - 38 mm		Sleeve Length	8 in - 203 mm		Shank Diameter	6.25 in - 159 mm		Break Out Plate (Mat.#/Legacy#)	181975/44745		Approximate Shipping Weight	256Lbs. - 116Kg.		 <p style="margin-top: 10px;">Material #487256</p>
Cutter Type	X2 - Tough Drilling																																																																
LADC Code	M422																																																																
Body Type	MATRIX																																																																
Total Cutter Count	48																																																																
Cutter Distribution	<u>13mm</u>	<u>16mm</u>																																																															
Face	6	24																																																															
Gauge	18	0																																																															
Number of Standard Nozzles	6																																																																
Number of Small Nozzles	0																																																																
Number of Ports	0																																																																
Junk Slot Area (sq in)	13.76																																																																
Normalized Face Volume	40.2%																																																																
API Connection	4-1/2 LF. BOX																																																																
Recommended Make-Up Torque*	25,000 Ft*lbs.																																																																
Nominal Dimensions**																																																																	
Make-Up Face to Nose	14.86 in - 377 mm																																																																
Gauge Length	1.5 in - 38 mm																																																																
Sleeve Length	8 in - 203 mm																																																																
Shank Diameter	6.25 in - 159 mm																																																																
Break Out Plate (Mat.#/Legacy#)	181975/44745																																																																
Approximate Shipping Weight	256Lbs. - 116Kg.																																																																

*Bit specific recommended make-up torque is a function of the bit I.D. and actual bit sub O.D. utilized as specified in API RP7G Section A.8.2.
 **Design dimensions are nominal and may vary slightly on manufactured product. Halliburton Drill Bits and Services models are continuously reviewed and refined. Product specifications may change without notice.
 © 2012 Halliburton. All rights reserved. Sales of Halliburton products and services will be in accord solely with the terms and conditions contained in the contract between Halliburton and the customer that is applicable to the sale.

www.halliburton.com

Figure 35, Spec Sheet

3.2.4 ADI files

These files are from the logging data base and contain the information gathered on the field by all the tools deployed in each run. The data can be arranged by time or depth and displays the records for all the activities in the hole. These activities can be tripping in, drilling, tripping out. As the analysis was done when the tool was drilling only drilling data was gathered.

The information held in these files is managed by the Insite software applications. The main applications used were the Data Manager and the Export tool. Screen shots of the software can be seen in Figure 36.

It is important to point out the large amount of data contained in these files, that is why is critical to identified the relevant runs, so only those runs are loaded. In addition, not all the data sets should be extracted, only the ones that are important for the analysis were loaded then the time required for these extraction was in the range of 3 to 5 minutes per run.

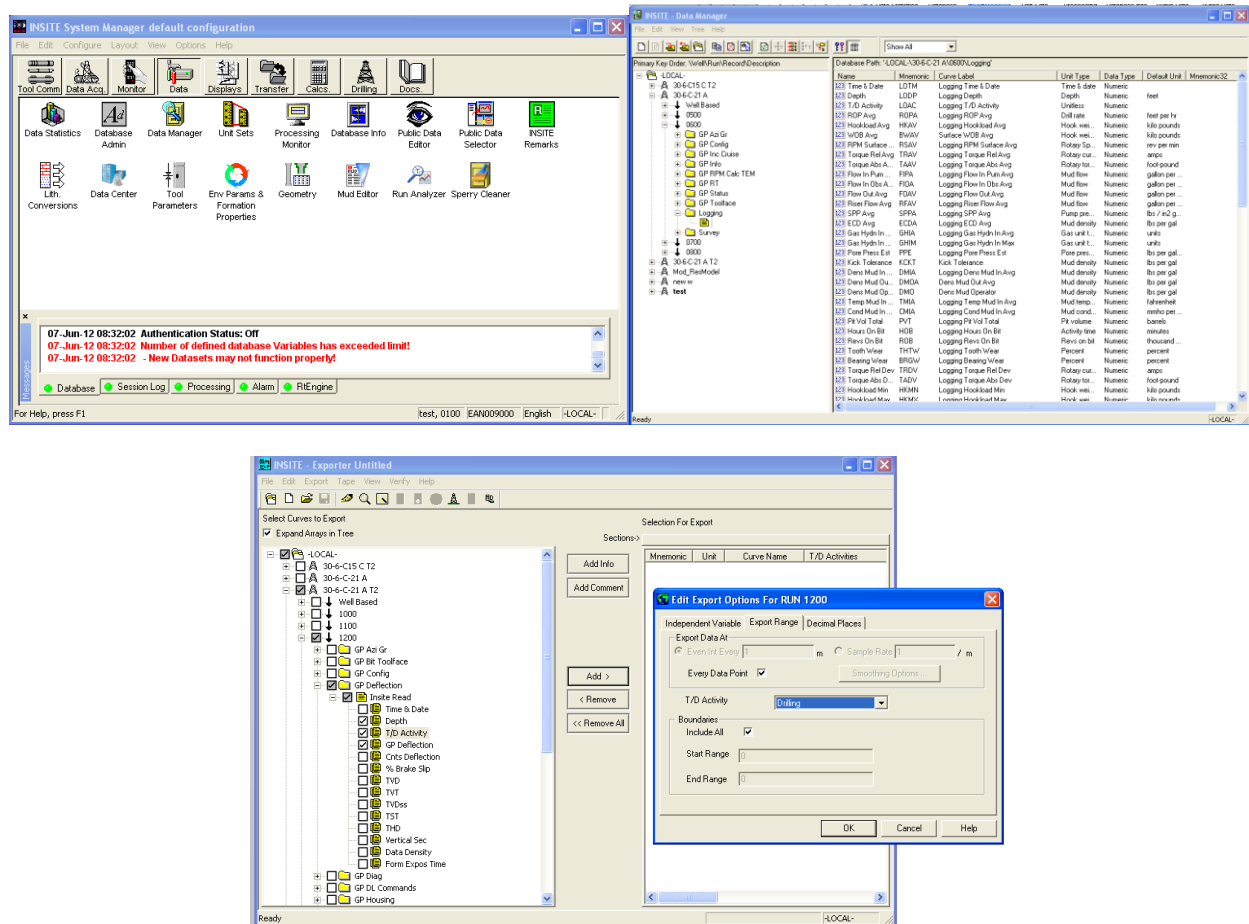


Figure 36, Insite environment

3.2.5 Bit design files

The design files are gathered from the designers which have access to the iBits platform and are able to generate these files associated with different bit designs. The information needed to identify the files and request those to the designers is collected from the SAP interfaces (Figure 37) where the material number is the reference and the manufacture plant can be tracked and selected together with the design file that will be used later in the simulations.

Display material BOM: General Item Overview

Material: 405148 1/2 FMF36532 FIX CUTTER BIT
Plant: 2130 Halliburton O&S Houston Mfg
Alternative BOM: 1

Item	CT	Component	Component description	Quantity	Un	A...	Sl	Valid From	Valid to	Change No.	P...	SortString	Item ID	Chg No.	To
0130	L	179728	BRAZE WIRE - SILVER SOLDER	8.200			TOZ	11/23/2004	12/31/9999				00000012		
0140	L	405148	CUTTER KIT 405148	1.00			EA	11/23/2004	12/31/9999				00000013		
0150	L	179726	TSP DISC 6.5MM DIA X 3.3MM LG	90.00			EA	11/23/2004	12/31/9999				00000014		
0160	L	179824	SINT DISK NATURAL ROUND 13X08 BABW/00412	24.00			EA	11/23/2004	12/31/9999				00000015		
0170	L	179804	1613 SAND PLUG	24.00			EA	11/23/2004	12/31/9999				00000016		
0180	L	179738	1313 SAND PLUG	12.00			EA	11/23/2004	12/31/9999				00000017		
0190	L	179680	1308 DROP IN PLUG	6.00			EA	11/23/2004	12/31/9999				00000018		
0191	L	418525	CUTTER 1308 CT31-T1 DROP-IN (JUMIN)	6.00			EA	06/07/2006	12/31/9999				00000038		
0200	D		DC11389 FACE	1			PC	11/23/2004	12/31/9999				00000019		
0210	D		DL11390 LOC SHT	1			PC	11/23/2004	12/31/9999				00000020		
0220	D		DR11391 MOLD	1			PC	11/23/2004	12/31/9999				00000021		
0230	D		DR11392 BLANK	1			PC	11/23/2004	12/31/9999				00000022		
0240	D		DY11395 ASSEMBLY	1			PC	11/23/2004	12/31/9999				00000023		
0250	D		DR11394 J S MOLD *TRASHED*	1			PC	11/23/2004	12/31/9999				00000024		
0260	D		DR11393 J S PLUG *TRASHED*	1			PC	11/23/2004	12/31/9999				00000025		
0270	D		SH465 TURNING DETAIL REV A	1			PC	11/23/2004	12/31/9999				00000026		
0280	D		SJ11396 MILLING DETAIL	1			PC	11/23/2004	12/31/9999				00000027		
0290	D		SS11397 FINAL ASSEMBLY	1			PC	11/23/2004	12/31/9999				00000028		
0320	D		SS093 DOME HOLE DETAIL REV H	1			PC	11/23/2004	12/31/9999				00000031		
0330	D		SS132 LOCATION PIN REV D	1			PC	11/23/2004	12/31/9999				00000032		
0340	D		DG015 Ø 1/2 RING GAGE REV F	1			PC	11/23/2004	12/31/9999				00000033		
0341	D		H411456 BREAKOUT COLLAR Ø 1/2 TURBOSLVE	1			PC	12/21/2004	12/31/9999				00000036		

Figure 37, SAP

These files are generated from the iBits software, which is the environment where bits are designed. The files collect all the data regarding the position and geometry of the bit. All the features are captured in these files and used in the simulator DxD (Direction by Design).

The cutter structure is defined by the position of each blade, each cutter and each special feature added to the bit. The gage is also described in more detail; every blade can be calibrated to match the specifications of any design. This is, the under gage feature of a bit can be modified here, modifying the numerical information of the files. Figure 38 shows an example screenshot of the design files.

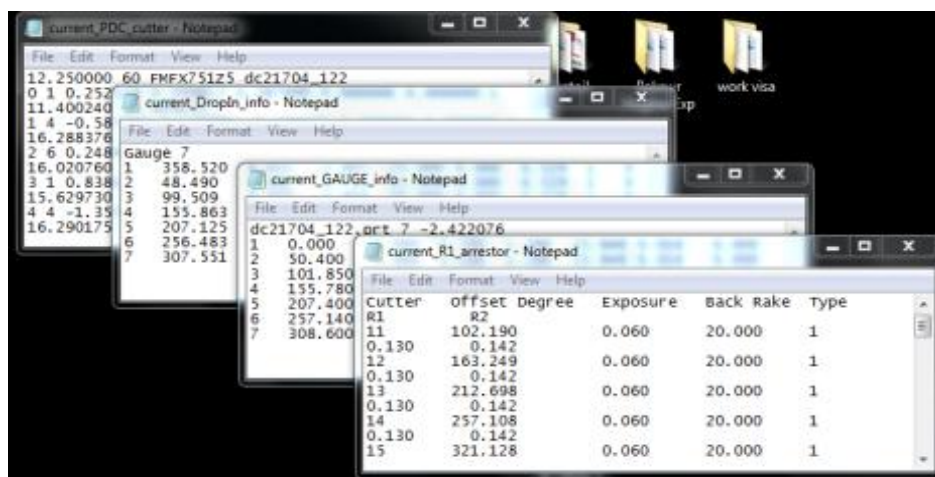


Figure 38, iBits design files

3.3 Construction of the Main Data Matrix

After checking all those important features of each run the directional information can be gathered from the corresponding survey report: inclination, azimuth, building rate, turning, rate, DLS, X, Y, Z. However for the operational parameters the information is in different sources and at different resolutions.

3.3.1 Data from the definitive survey reports

The survey data was easily extracted from the DD EOW report, first exporting to a *.txt format and then to the corresponding spread sheet in Excel. This data got a flag for each bit design ran then this can be analyze separately or in bulk.

3.3.2 Data from logging records

For the drilling parameters and Geo-Pilot™ settings however, the process was more complex since the data in this case is at different resolution. In order to handle this and upscale the data from logging records a look up table (spread sheet with macros) was created. Figure 39 displays this spread sheet:

Figure 39, Look up table

Reference data points are the survey information this will be the target resolution (around every 5 to 9 or 12m). Then the ROP and RPM datasets between other drilling parameters where exported and finally data points at each survey depth were extracted with the help of a look up table build for that purpose with Excel macros (Code in Appendix A). This process involved the following tools, Insite Data manager and Insite Data exporter. From software definition when doing these loading and exporting activities one should be careful when selecting only the drilling tag for the records. That means, the data considered and displayed will be only be the one when the drilling string was breaking through the formation.

Description of template:

- The **source** table contains the information from Logging database of surveys (Data exported from ADI files). High definition data in steps of 1m. Data from logging dataset (ROP, WOB, RPM, torque, SPP, ECD, flow at bit, etc). These records are in the range of hundreds and reaching even thousands records for some runs. A manual approach was very time consuming and not effective, that was one of the main reasons for developing the look up table (Code in appendix A). Also only drilling data was considered. That is, the data considered is only when the tool was drilling and breaking through new formations.
- The **Reference** table contains the survey points from the DD EOW report and the resolution is in the range of every 5 to 12m (target resolution). In addition, its depth intervals are not regular and a fix step solutions was not delivering good results. Therefore the necessity of this reference table. Then data points can be extracted as closest to each survey depth as possible, therefore a more accurate data selection was performed.
- The **Extracted** data, displays the results of running the algorithm; the difference between reference depths and extracted depths is generally below the 2%.

3.4 Categorization and sorting of data

The data selection for the analysis considers to main criteria:

- The behavior identification criterion.
- ROP and RPM ranges criterion.

3.4.1 Algorithm to identify the behavior

As known in the industry the parameter DLS is the global representation of the directional response of the tools involved in the drilling process. However, this DLS is the sum of a build/drop and turn behaviors of the system.

The algorithm Figure 40 (code in appendix), developed identifies the main behaviors and tag each survey point with a behavior. There are 9 behaviors considered in the analysis: building, building left, building right, dropping, dropping left, dropping right, turning left, turning right or holding behaviors.

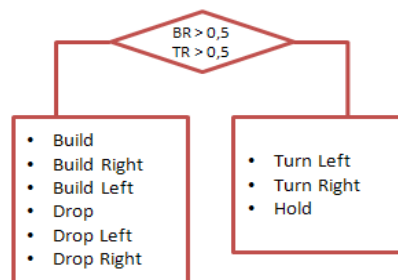


Figure 40, Behaviors algorithm

Once the tag is applied then a filtering process can be defined and only relevant behaviors are considered. For example an initial correlation of DLS achieved and Geo-Pilot™ deflection for all the behaviors is shown in Figure 41.

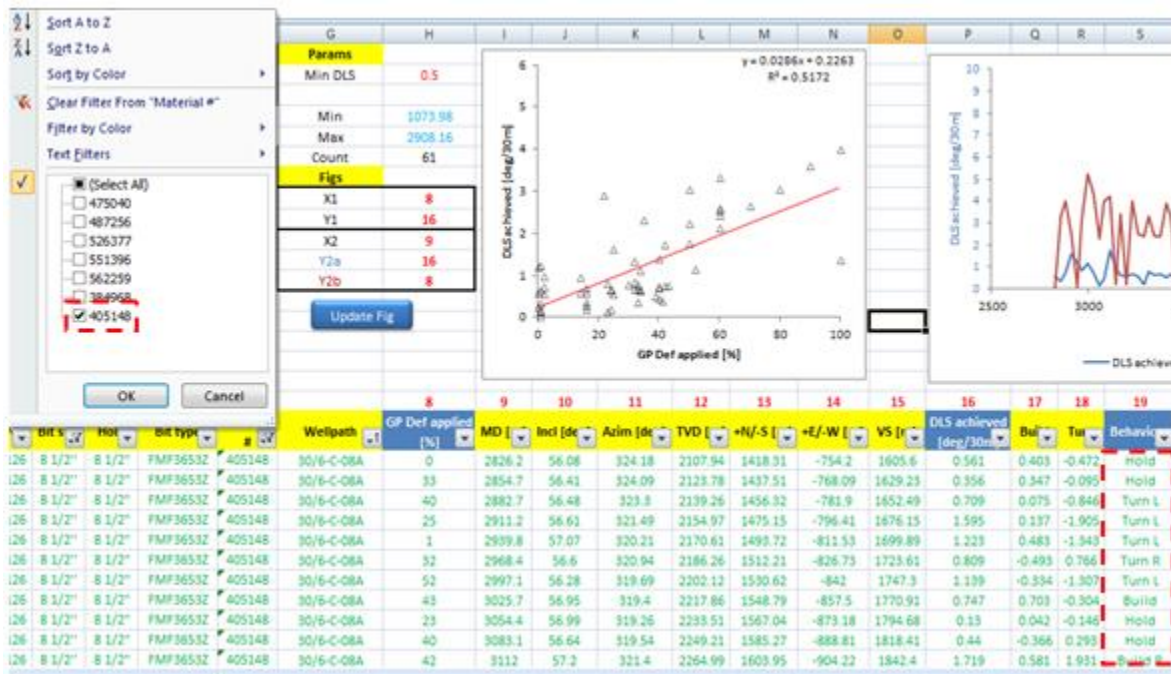


Figure 41, All data points in a run.

The red dotted boxes show, on the left, the design selected and on the right the box highlighting the column where all behaviors are displayed and not filter apply yet.

One the filter is applied only the relevant behaviors are shown:

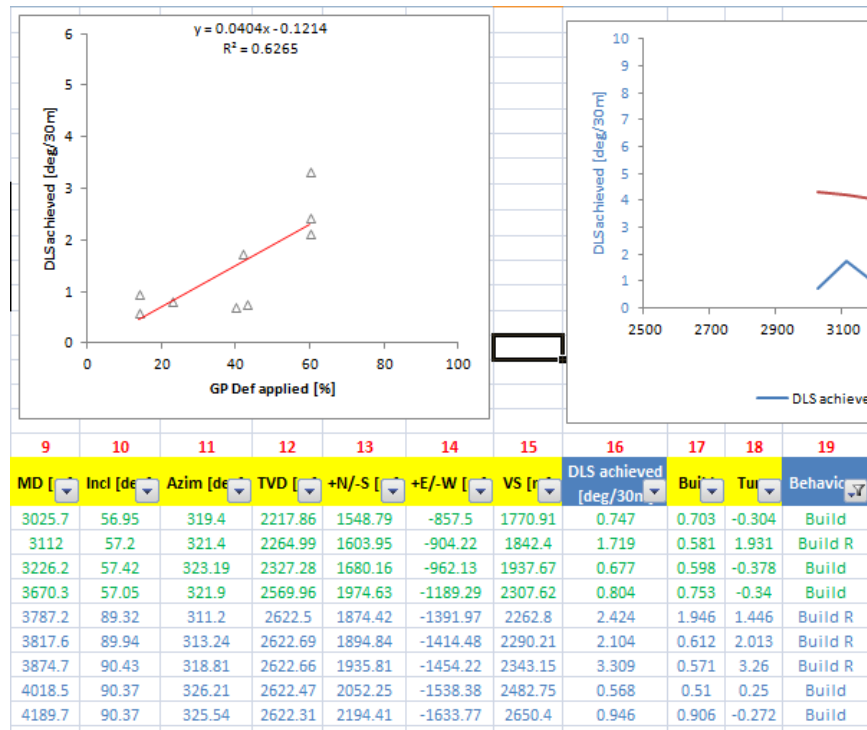


Figure 42, Filtered only building behavior.

As can be seen in this case the database is showing only building data points. This process of behavior filtering is used to describe in more detail the performance of the system on the field. Walking tendencies can clearly be seen and the figures described in the data analysis chapter will further discuss these results.

3.4.2 Statistical analysis to identify the relevant ranges of ROP and RPM

The next step is to perform a statistical analysis. The approach taken is to identify the ranges of ROP (Rate of Penetration) and RPM (Revolutions per Minute) most populated with the behavior data defined in the previous step. This means that ranges with more data points will be considered and groups of analysis defined.

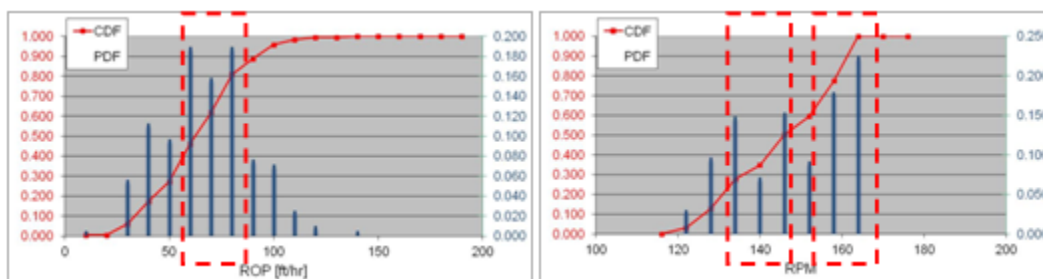


Figure 43, Examples of ROP and RPM distribution

The distributions for all designs are plotted and one or two common ranges are selected to begin the study. These ranges are short enough to be representative groups of categories such as low, medium and high. For example medium ROP between 50 to 70 ft/hr or high RPM of 140 to 170 RPM are common ranges identified.

3.5 Simulation in Direction by Design DxD™

3.5.1 Introduction [24]

3.5.1.1 Capabilities of Direction by Design

Given a bit design and operational conditions, Direction By Design calculates the following parameters:

- ROP / WOB, TOB: magnitude and variation;
- Bit Side Force required to reach a given DLS
- Bit walk force, walk rate and walk direction
- Gage pad / hole wall interaction and force distribution along gage pad

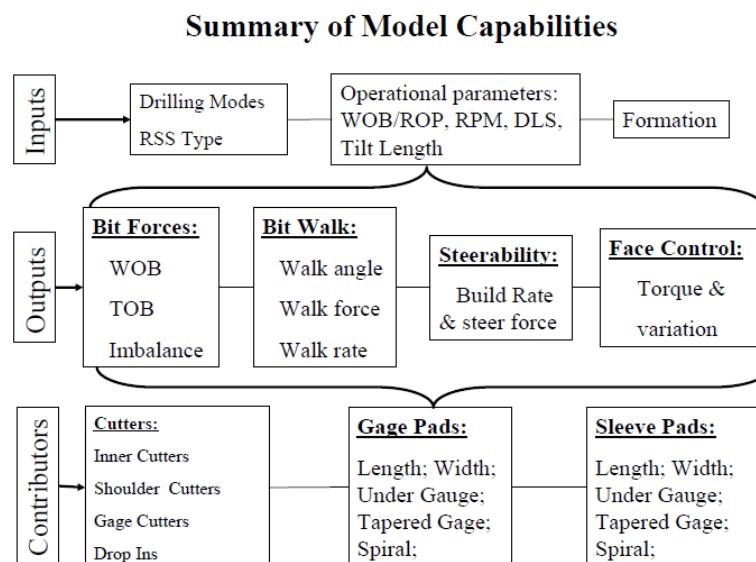


Figure 44, Capabilities of DxD [24]

As displayed in Figure 44, the main inputs and sources are summarized in the following list:

- Bit:
 - Info from Specification sheets (appendix with all designs)
 - Design files from iBits.
- Formation: Description of formations in terms of lithology as the main feature to distinguish variation in CRS. This info is process and gotten from other logs
 - From offset wells.

- At specific depths and formations
 - Drilling parameters: ROP, RPM
 - RSS type: point the bit, push the bit.
 - Directional mode: Kick off, Equilibrium.

3.5.1.2 Applications

Optimal design of bit steerability: one can change a bit's cutting structure (profile, cutter distributions, back rake and side rake) and gage pad geometry (number of gage pad, length, width, taper or UG, aggressiveness) to increase or decrease bit's steerability.

Bit steerability selection: if there are several bits available for a directional application, Direction By Design may be used to select the best suitable bit by running the software for each bit under the same operational conditions.

Optimization of RPM/ROP, RPM/WOB: RPM, ROP or WOB have significant effects on bit steerability. Direction By Design may be used to determine the best RPM/ROP or RPM/WOB based on bit steerability.

3.5.1.3 Input Mode

ROP / DLS

In this input mode, bit motion is fully determined and all the calculations are forward. If bit cutting structure is fixed for all case studies, then this input mode calculates the bit steerability faster and more reliable compared to the 2nd input mode because no iterations are needed. This input mode may be used if the purpose is to design the gage geometry without changing the cutting structure, or to see the effects of RPM and/or ROP on bit steerability.

WOB / DLS

In this input mode, the ROP is first estimated by an iteration algorithm. The estimated ROP is convergent if its associated WOB is close to the input WOB. Therefore, the calculation procedure is slower. This input mode may be used to compare steerability for different types of bits having different cutting structure. This input mode may also be used to compare the effects of formation type on bit steerability.

3.5.2 Simulation Process

3.5.2.1 Generation of bit files from iBits ^[21]

In iBits software (Figure 45), the bit design files are generating when running the Force Analysis. Four files are generated ^[21]:

- current_PDC_cutter.txt: contains all cutter geometries
- current_DropIn_info.dat: contains all drop-in cutters
- current_R1_arrestor.dat: contains all R1 cutter geometry
- current_GAUGE_info.dat: contains gage pad geometry

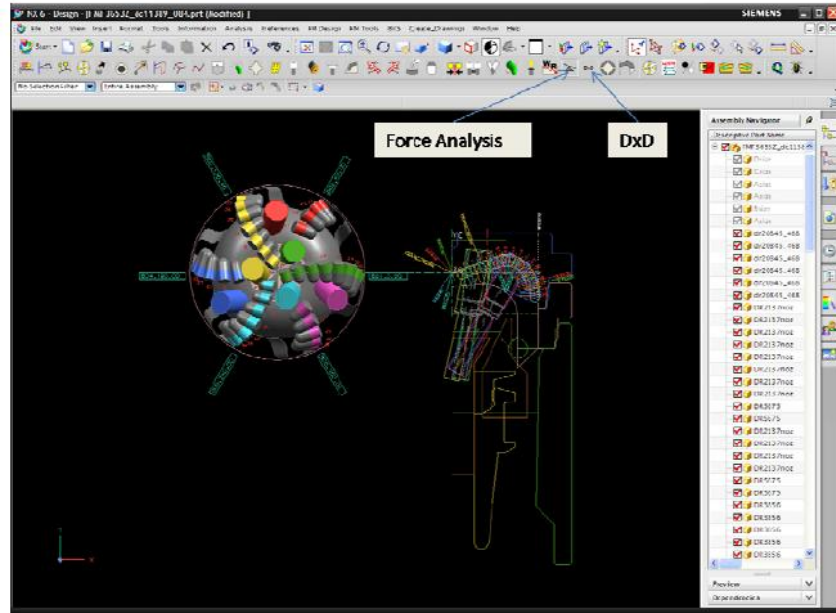


Figure 45, iBits Software [21]

3.5.2.2 Design of gage pad and gage sleeve in DxD

Before opening DxD software one important step must be carried on. The file: *current_GAUGE_info.dat*, has to be modified if there is a incongruence with the specification sheets. Figure 46, show the column where the gage pad can be set to under gage by changing the 0 value to for example 1/32" or 1/16" (under gage in diameter). The values introduced in the table are in radius, so the corresponding value should be divided by two.

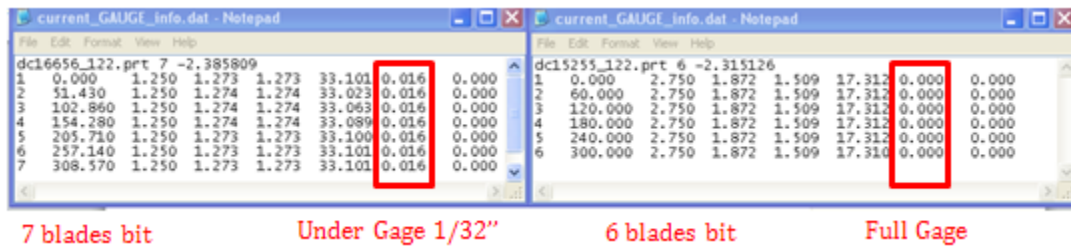


Figure 46, Gage design

Once this is done, the program can be opened and the application will automatically load the design files. Other details of the sleeve gage can be design in the "Add cut parts and Design Sleeve Pads" window. This is done with the criteria of matching the specifications of a specific bit. In Figure 47

this match can be seen by comparing the specification sheet with the model generated by the software.

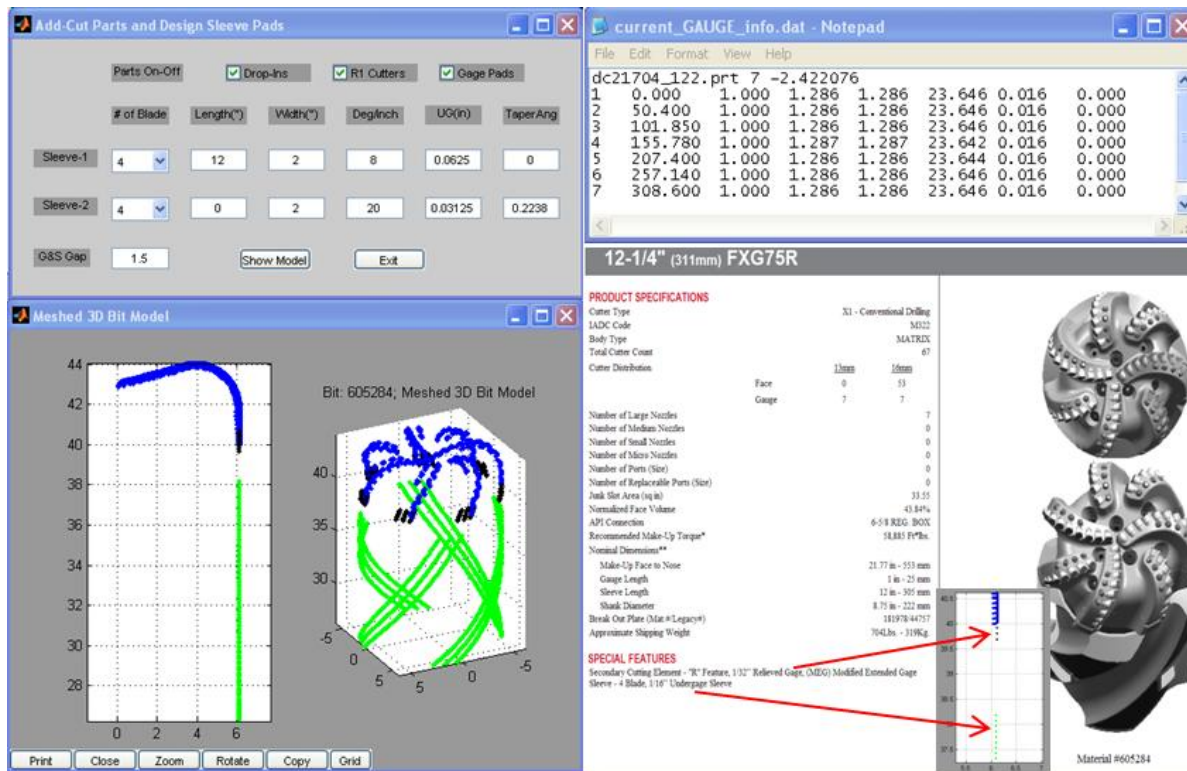


Figure 47, Desing of Gage Pad and Sleeve

3.5.2.3 Defining input parameters and Simulation

The input parameters are defined in the section "BHA Geometry & Operational Parameters". Figure 48 show the window and the description of an important parameter tilt length.

What's more, in order to generate tendencies for different DLS, sensitivity in this parameter was performed in every simulation. Figure 48 as well shows that setting.

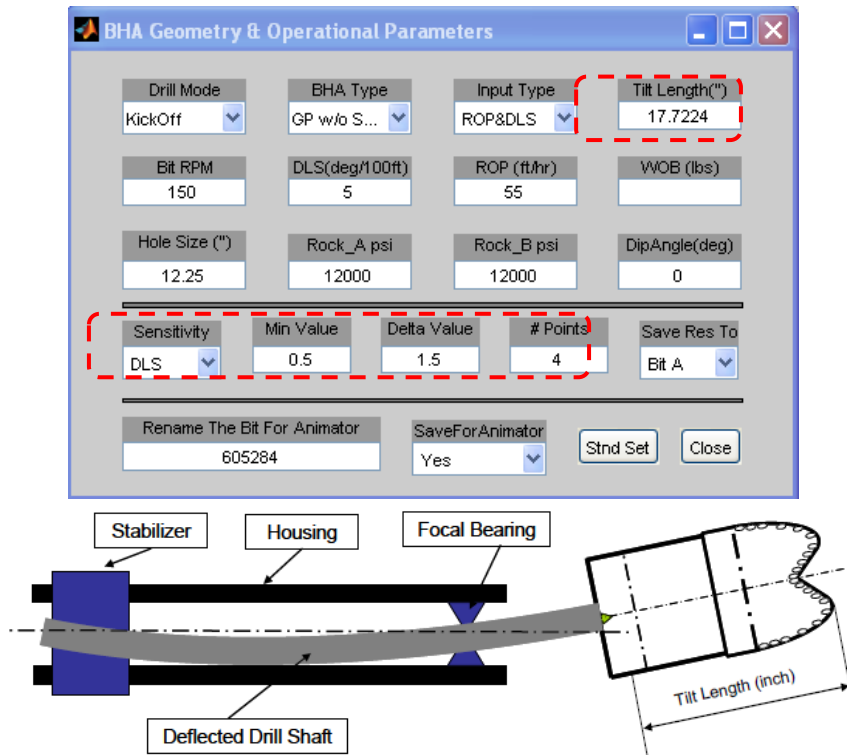


Figure 48, Input parameters

Finally the simulation can be performed and the results exported to the Spread Sheet.

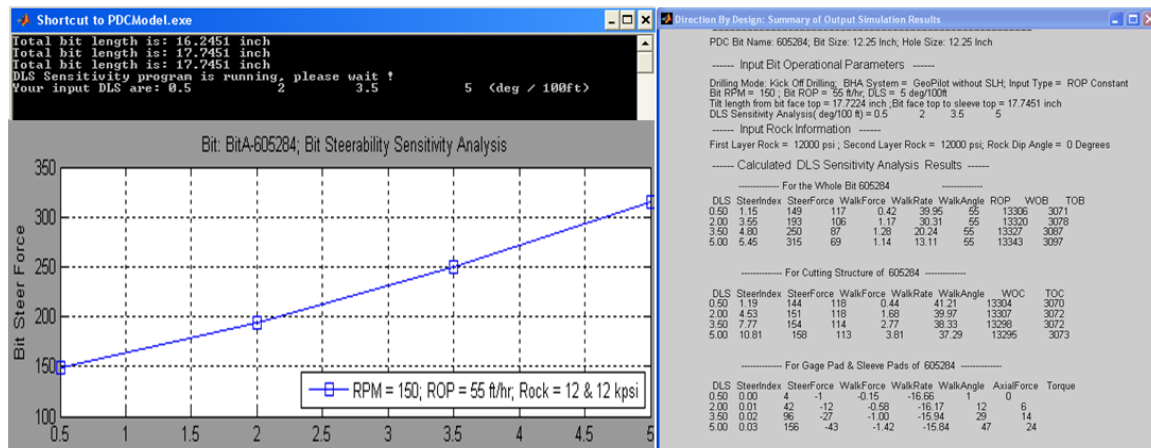


Figure 49, Simulation results

In order to compare different designs a have a better display of the results the information is exported and handle in excel

3.6 Validation of model

In this last step the tendencies generated from field data are compared with the tendencies got from the simulator runs. The tendencies gotten from field are in the form

DLS achieved vs GP deflection Applied

And the tendencies from simulation (Figure 49) are:

Bit steer force vs DLS

As can be seen the logic of the simulator is that computes the side force (steer force) required for a given DLS. From field data analysis the DLS achieved in the wells analyzed from Oseberg field are in the range of 0 to 5 deg/30m. That is why the simulations are performed in this range and with steps of 1.5 deg/30m. That step interval was chosen as the tendencies are in most of the cases linear and the time of simulation is not that long for 4 points sensitivity (each simulation takes around 5 minutes).

In order to compare Field data and Simulator results the tendencies from simulator were plotted in inversed axis, then having:

DLS vs Side force

In this way the qualitative process of comparison can be performed. The main points of comparison are:

- Slope of field tendencies, simulator results.
- Maximum DLS from field and from simulation.

The values of side force are reference and there is no possible way yet to measure that parameter from field (as previously explained as well in scope and limitations).

From field data tendencies, the best designs can be identified and correlated to what the model predicted. This is done in a qualitative way only as not magnitudes can be compared. However, some other features can also be analyzed, changes in bit design impacts are also pointed out and some insights about the improvements expected with the simulator can also be confirmed.

4 Data analysis & Interpretation

In this section the field chosen for the study is described. General information and geological description of the Oseberg field follows in 4.1.

Then a hypothesis is explained before the case studies are developed. A case study analysis was chosen as the data is for different sections and different conditions. Then 12 $\frac{1}{4}$ and 8 $\frac{1}{2}$ cases are analyzed.

As explained in the methodology and objectives, the main objective is to analyze the different bit designs performance in the field versus the model results. In that sense, the methodology to filter and categorize data as described in the 3. Methodology is applied.

4.1 Oseberg Field

Oseberg field is located in the Norwegian North Sea approximately 140 km northwest of Bergen, Norway. It was discovered in 1979 and was put onstream on December 1, 1988. The reserves are estimated to be 231.6 million standard m³ (1457 million STB) of oil and 92 billion standard m³ (3.25 trillion standard ft³) of gas.

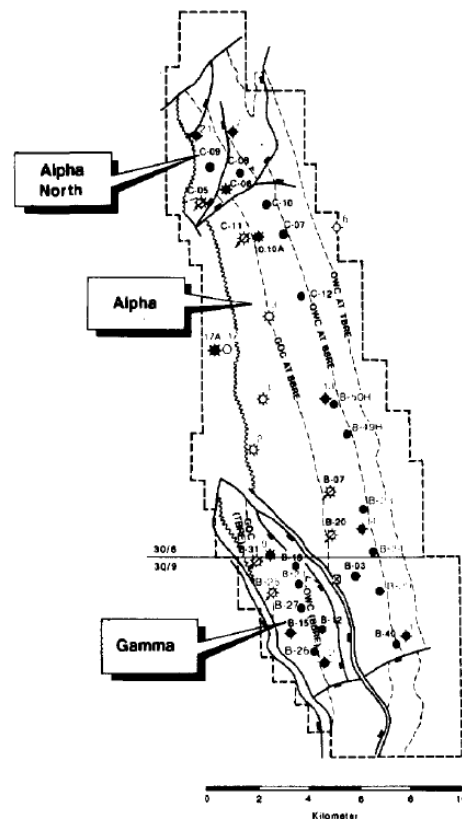


Figure 50, Oseberg field structural map [22]

4.1.1 General Information

1st well, Gas-bearing sandstones were found in the Middle Jurassic Brent Group, but the gross thickness was only 68.5 m. In addition, the reservoir properties were moderate. Furthermore, the Paleocene had no significant sandstone development, and the Lower Jurassic Statfjord Formation was water bearing

4th well, first oil discovery made in 1981. This well, located in a downdip position on the Alpha structure, showed a significant thickening of the reservoir rocks. Gross thickness was 88 m. reservoir quality was far better than that intersected by the first three wells.

5th well, established the free water level (FWL) in 1982. The vertical hydrocarbon-bearing section measured approximately 600 m, from the crestal position at about 2120 m MSL to the FWL (free water level) at about 2719 m MSL. The extension of the Alpha structure alone was about 22 km, and the width was as great as 5 km. Block 30/6, show several eastward-dipping structures.

Oseberg C lies 10 km north of the Oseberg field centre, and is an integrated accommodation, production and drilling platform with a steel jacket. Oil is produced from 18 wells. From three of the wells crude oil is sent in a multiphase pipeline to the field centre for processing.

Water is injected into three wells and gas into five wells to improve the oil recovery rate. Around 25,000 - 30,000 barrels of oil is produced from the field per day.

The initial production strategy was composed of:

- Multi objective horizontal wells close to OWC (3-8m), to avoid gas conning and optimize production (larger drainage area). Multi fo systems, channel sands systems (Ness).
- Horizontal sections between 1500-2000ft. 13 oil producers. [22]

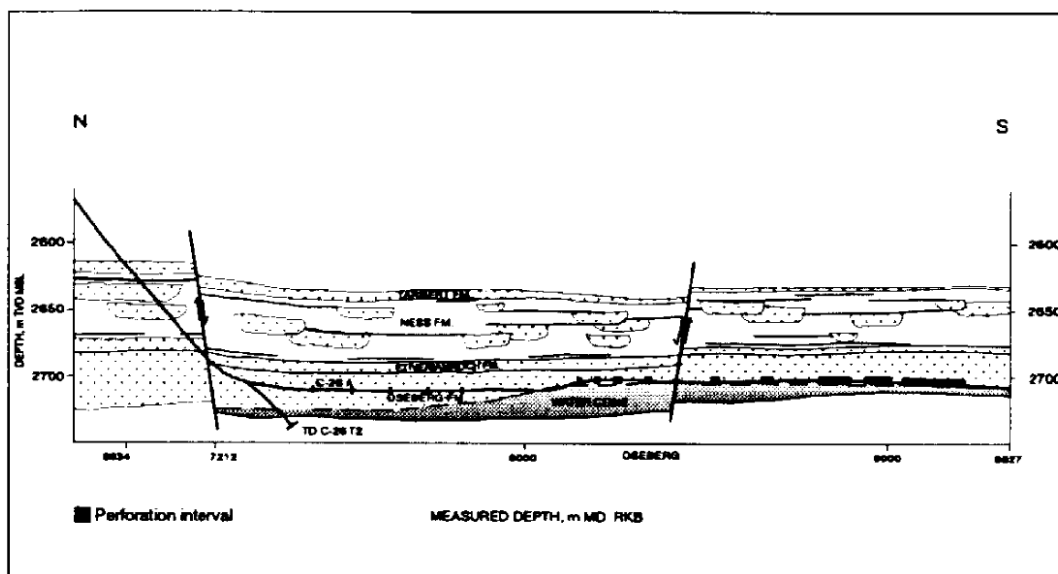


Figure 51, Example of cross section in Oseberg field [22]

4.1.2 Formations drilled

4.1.2.1 The 12 ¼ section

The main geological features are: CCS (Confined Compressive Strength) around 15000 psi, and lithology:

Lista Formation: comprised by claystone, tuff and some limestone stringers. It is present in the range of 2130 – 2265 m TVD along the wells analyzed.

Vale Formation: mainly claystone. Present in the interval 2265 – 2280 m TVD.

Shetland group: The Shetland Group consisted of calcareous claystone, limestone beds and dolomite and in occasions thick limestone beds appeared in the lowermost part of the interval. This formation is present in the interval 2280 – 2540 m TVD.

Viking group: comprised Heather Fm consisting in mainly siltstone and present in the interval 2520 – 2550 m TVD.

Brent group: comprise only of Tarbert Fm (formation) a sandstone Fm present in the interval 2550 – 2600 m TVD.

4.1.2.2 The 8 ½ section

The main geological features are: confined rock strength around 1000 psi, and lithology mainly: Claystone-siltstone, coal, sandstone. One example of CCS log can be found in Appendix C.

Tabert:

- fair to good sand.
- h=40m
- 1000-4000 mD (good sand), 100mD (poor sand)

Ness:

- Delta plain channels sandstones, interbedded with fine sediments and coal beds.
- 1mD-Several darcies.

Etive:

- 500-1500 mD

Rannoch:

- Interbedded fine to medium grained sandstone.
- Acts as a flow restriction between Oseberg and Etive formations.

Oseberg:

- Medium to coarse grained fan-delta sandstones.
- h = 20-60 m.
- 500-6000 mD.

4.2 Hypothesis

The field data tendencies will be qualitative similar to those generated by the simulator. This premise will be check using the method developed and also describing the relevancy of applying this methodology when analyzing directional data from real wells and not from laboratory controlled conditions.

4.3 Case studies

Although all the variables considered, and the approach taken to analyze them, are described in the scope and methodology section. It is important to make some additional comments about the information presented in the case studies:

- The wells considered in the different sections are from the same field and within a narrow range of TVD, trying to consider the same formations with similar properties.
- The BHA designs for all wells in the data set are almost the same, where only the bit design changes and therefore the impact of that change is the one to be described and quantified. To support this some BHA designs of this section are presented in the appendix part.
- The study is aware of the different trajectories of each well however, the aim is not analyze well by well, but bit design by bit design. Therefore the information presented is displayed in that format.
- The drilling parameters are changing all the time in order to optimize the activities on the rig. In that sense a statistical approach was taken when analyzing the two parameters considered, ROP and RPM.

	8 1/2 section				12 1/4 section	
	Case A	Case B	Case C	Case D	Case E	Case F
Description of case	-Bits with more available data. -To display and show the relevancy of identifying the different steering behaviors.	-Low ROP range considered. -Focus on a single feature change MEG.	-Medium ROP range considered. -Data allowed to analyse different behaviors.	-High ROP range considered. -Data allowed to analyse different behaviors.	-Mainly building section. -No reamer used hole 12 1/4.	-Mainly building section. -Section reamed to 13 1/2.
Bit designs considered	FMF3651Z (487256) FMF3653Z (405148)	FMF3651Z (487256) FMF3653Z (551396)	FMF3651Z (487256) FMF3653Z (551396) FMF33653Z (405148) FMF3741Z (475040)	FMF3741Z (475040) FMF3731C (384968) FMF3651Z (562259)	FMF3643ZS (438320) FMF3643ZS (411639) FMF3643CS (375525)	FXG75 (605284) FMF3751 (585609) FMF3661ZR (478186) FMF3751ZR (422785)
Analysis done	-Comparisson behavior by behavior. -Turning behavior qualified for comparison Field vs. Model.	-Range of ROP identified from statistics. -Same RPM for cases B, C and D. -Turning left behavior qualified for comparison Field vs. Model.	-Range of medium ROP identified from statistics. -Same RPM for cases B, C and D. -Building, Turning left and Turning right behaviors qualified for comparison Field vs. Model.	-Range of HIGH ROP identified from statistics. -Same RPM for cases B, C and D. -Building, and Turning right behaviors qualified for comparison Field vs. Model.	-Ranges of ROP and RPM identified from statistics. -Building behavior qualified for comparison Field vs. Model.	-Ranges of ROP and RPM identified from statistics. -Building behavior qualified for comparison Field vs. Model.
ROP range [ft/hr]	61 - 76	40 - 55	55 - 70	70 - 85	40 - 70	40 - 70
RPM range	132 - 162	140 - 170	140 - 170	140 - 170	130 - 170	130 - 170

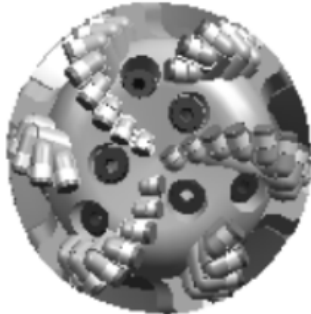

4.3.1 Case A - 8 1/2 section, FMF3651Z (487256) vs FMF3653Z (405148)

Initially each design is analyzed independently. General information regarding drilling parameter is summarized and the main objective is to show the importance of identifying the different steering behaviors (building, dropping, and holding) are described in detail.

Once the behavior most representatives is identified the field tendencies are generated. Then, the simulations are performed with the averages of the ranges selected. Finally a comparison between field and simulation is performed.

The bits analyzed in this case are show in Figures 52 and 53, these are the screenshots of the specification sheets. The most relevant info for the analysis is also highlighted.

PRODUCT SPECIFICATIONS			
Cutter Type		X2 - Tough Drilling	
IADC Code		M422	
Body Type		MATRIX	
Total Cutter Count		48	
Cutter Distribution		<u>13mm</u>	<u>16mm</u>
	Face	6	24
	Gauge	18	0
Number of Standard Nozzles		6	
Number of Small Nozzles		0	
Number of Ports		0	
Junk Slot Area (sq in)		13.76	
Normalized Face Volume		40.2%	
API Connection		4-1/2 I.F. BOX	
Recommended Make-Up Torque*		25,000 Ft*Ibs.	
Nominal Dimensions**			
	Make-Up Face to Nose	14.86 in - 377 mm	
	Gauge Length	1.5 in - 38 mm	
	Sleeve Length	8 in - 203 mm	
	Shank Diameter	6.25 in - 159 mm	
Break Out Plate (Mat.#/Legacy#)		181975/44745	
Approximate Shipping Weight		256Lbs. - 116Kg.	
SPECIAL FEATURES			
P-100, Active Gage, , 1/32" Relieved Gage, 1/16" Undergage Sleeve			

Material #487256

Figure 52, FMF3651Z (487256)

PRODUCT SPECIFICATIONS

Cutter Type			Z3®
IADC Code			M423
Body Type			MATRIX
Total Cutter Count			42
Cutter Distribution		<u>13mm</u>	<u>16mm</u>
Face	6		24
Gauge	12		0
Number of Standard Nozzles			6
Number of Small Nozzles			0
Number of Ports			0
Junk Slot Area (sq in)			13.12
Normalized Face Volume			54.64%
API Connection			4-1/2 I.F. BOX
Recommended Make-Up Torque*			25,000 Ft*lbs.
Nominal Dimensions**			
Make-Up Face to Nose	15.28 in - 388 mm		
Gauge Length	2 in - 51 mm		
Sleeve Length	8 in - 203 mm		
Shank Diameter	6.25 in - 159 mm		
Break Out Plate (Mat.#/Legacy#)			407013/4411456
Approximate Shipping Weight			400Lbs. - 181Kg.

SPECIAL FEATURES

FullDrift Design, Tapered to 1/16" Under Gauge, P100, *** REQUIRES SPECIAL BIT BREAKER ***



Material #405148

Figure 53, FMF3653Z (405148)

a) FMF3651Z (487256) data analysis

For this design there were 8 well-paths of data available. An example of the well-paths covered in the study can be seen in Figure 54.

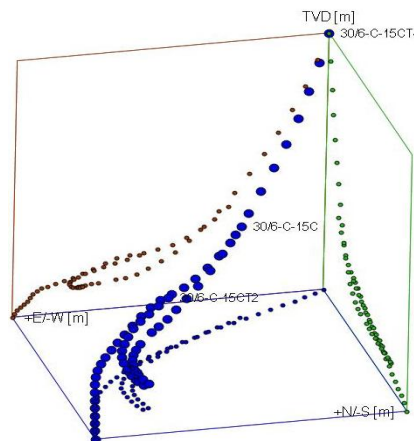
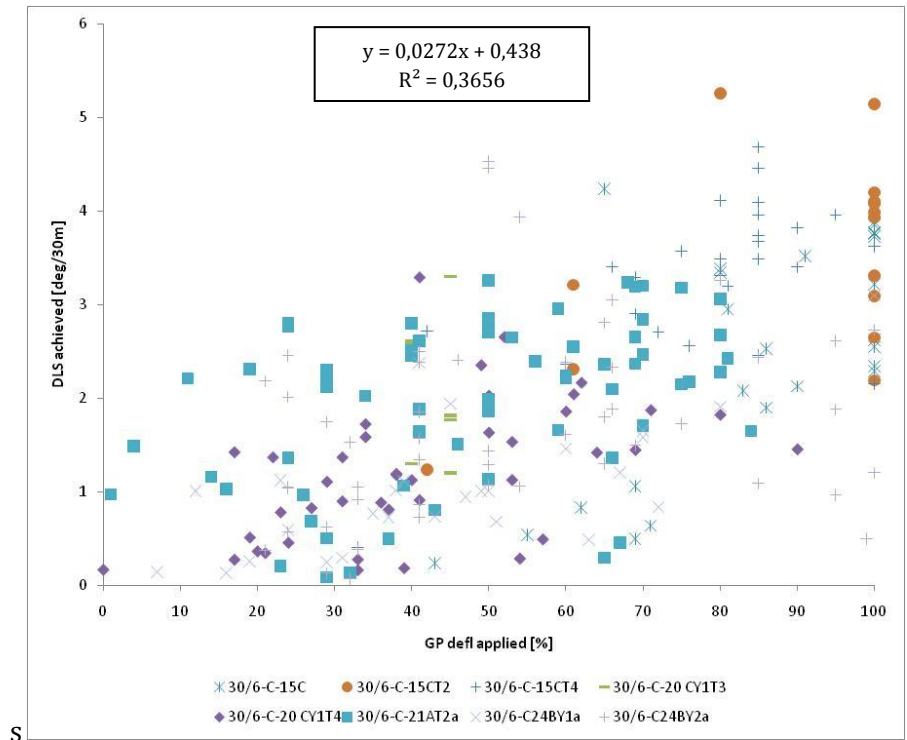


Figure 54, Example of well paths analyzed

Then an initial correlation DLS achieved vs GP deflection applied is plotted in Figure 55. This correlation considers the eight wells paths (258 data points) drilled from Oseberg C. The first analysis discloses a cloud of data with positive tendency. However, there are many spread points despite the fact that the data is taken mainly at reservoir level within a range of TVD 2560m to 2910m, with the same directional tool and same bit design.



S

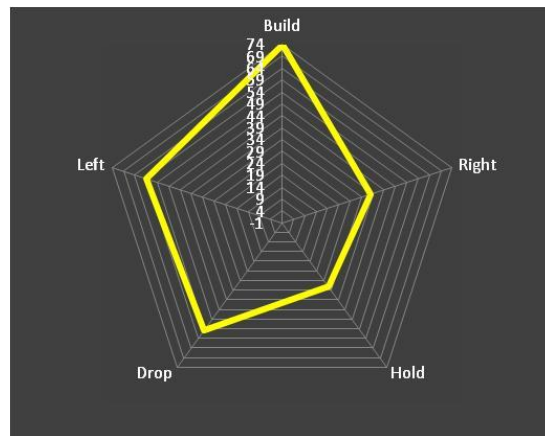


Figure 55, FMF3651Z (487256) all data points

Table 2, Summary design (487256) all data points

	Av	Min	Max
ROP [ft/hr]	53,41	6,0149	100,38
RPM	139,00	98	163
Count	258		

Table 2 shows the drilling conditions for the whole data sample of design FMF3651Z (487256). The sample consists of 258 data points. The minimum and maximum value for each variable was identified and a geometric average calculated.

In order to obtain better correlations and more insight about the directional behavior of the system, the methodology proposed in chapter 3 will be applied.

i) Identification of Behaviors

The sensitivity of the look up table constructed was set to +/-0,5 deg/30m. This is, all the values of build, dropping or turning below this threshold are considered holding. For example:

- If turning or dropping have an absolute value lower than 0,5 deg/30m. The lookup table will consider that survey as holding. The same for turning, if left or right are below 0,5 deg/30m absolute, then the outcome is holding.
- In order to get holding as a flag, both building and turning must be lower than 0,5 deg/30m.

Example of the criteria:

- If turning -0,6 and build -0,4 then the behavior is (Turning Left)
- If turning 0,55 and build 0,6 then the behavior is (Building Right)

Figures 56-60 shows the filtered data for the different directional behaviors. In these figures no restrictions on ROP or RPM are apply yet. These behaviors are:

- Building: it is composed of: building right, building left and only building.
- Dropping: it is composed of: dropping right, dropping left and only dropping.
- Turning: it is composed of both turning left and right.
- Turning left: only turning left.
- Turning right: only turning right.
- Holding: with a building and absolute turning value below 0.5 deg/30m.

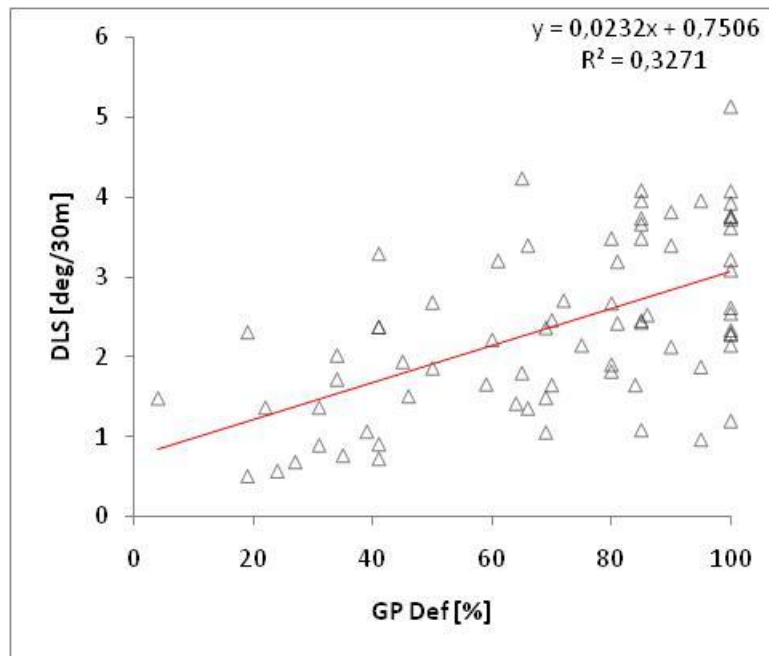
Building

Figure 56, FMF3651Z-487256 building @ all ROP and RPM

In order to understand the algorithm of the filtering process, the data contained in Figure 56 is as follows:

- Building left: building rate higher than 0.5 deg/30m and turning negative below -0.5 deg/30m.
- Building right building rate higher than 0.5 deg/30m and turning rate positive above 0.5 deg/30m.
- Building: building rate higher than 0.5 deg/30m and turning rates below 0.5 deg/30m.

In this case the sample data is reduced from 258 to 74 data points.

Dropping

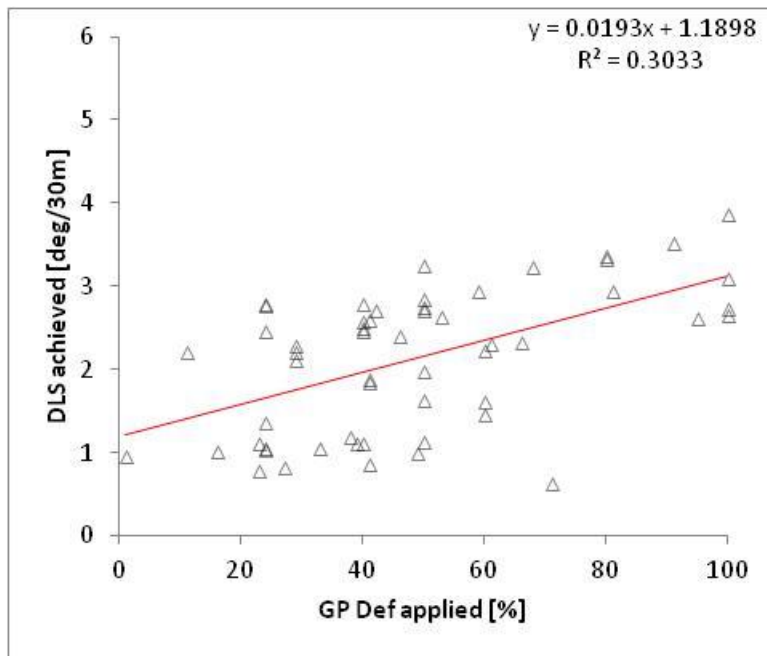


Figure 57, FMF3651Z-487256 dropping @ all ROP and RPM

In dropping, the dataset is reduced to 55 data points

Turning both right and left

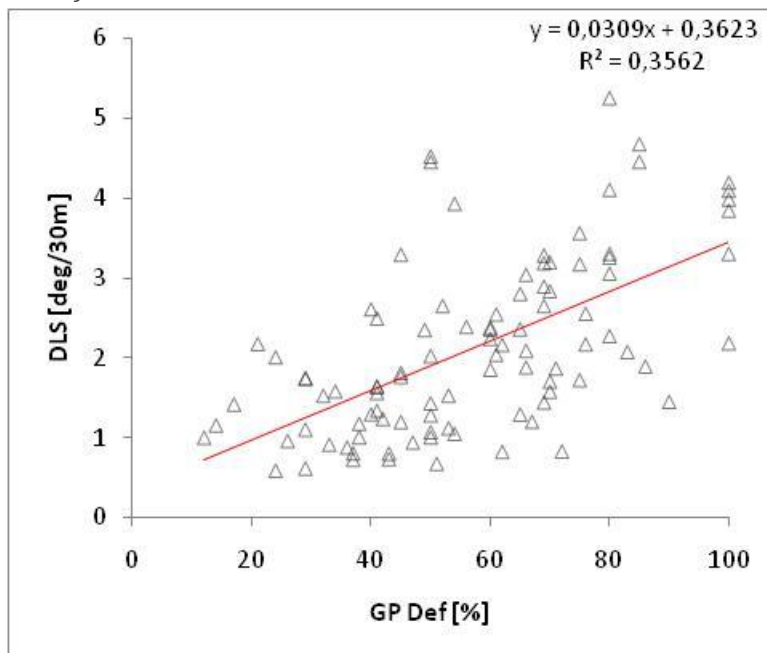


Figure 58, FMF3651Z-487256 turning @ all ROP and RPM

The filtered data comprises 97 data points. It considers both turning left and turning right were building or dropping were less than 0,5 deg/30m.

Turning only right

The data shown represents 38 data points.

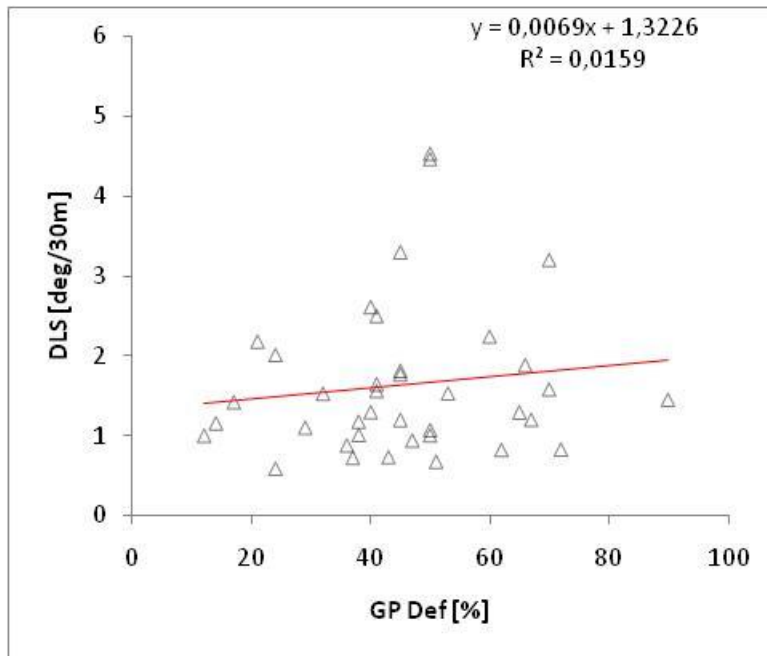


Figure 59, FMF3651Z-487256 T right @ all ROP and RPM

Turning only left

The data shown represents 59 data points.

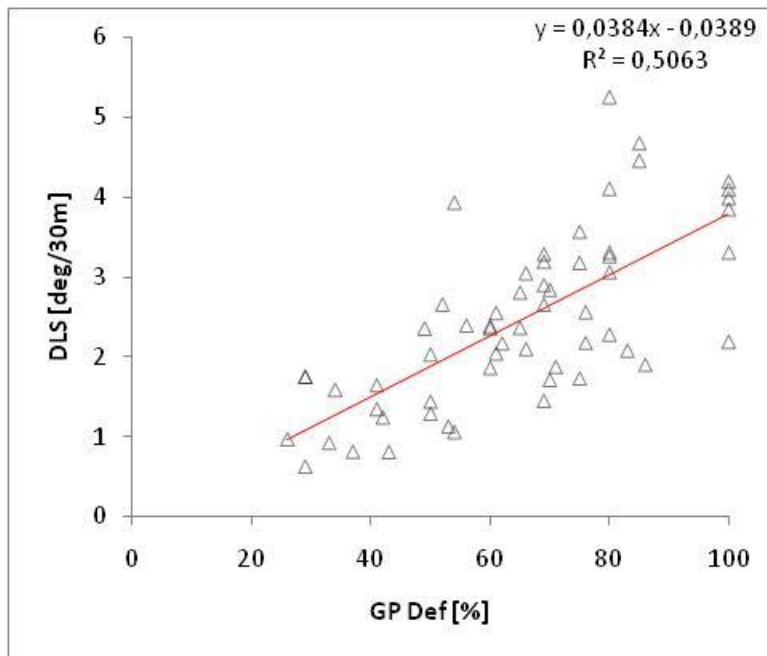


Figure 60, FMF3651Z-487256 T left @ all ROP and RPM

When comparing only by direction, is clear that turning left has a better response from the system. The slope of turning left is more than 400% higher than the one for turning right. This can be explained by the geological tendencies, the operative conditions and the bit design walk tendency.

Only Holding

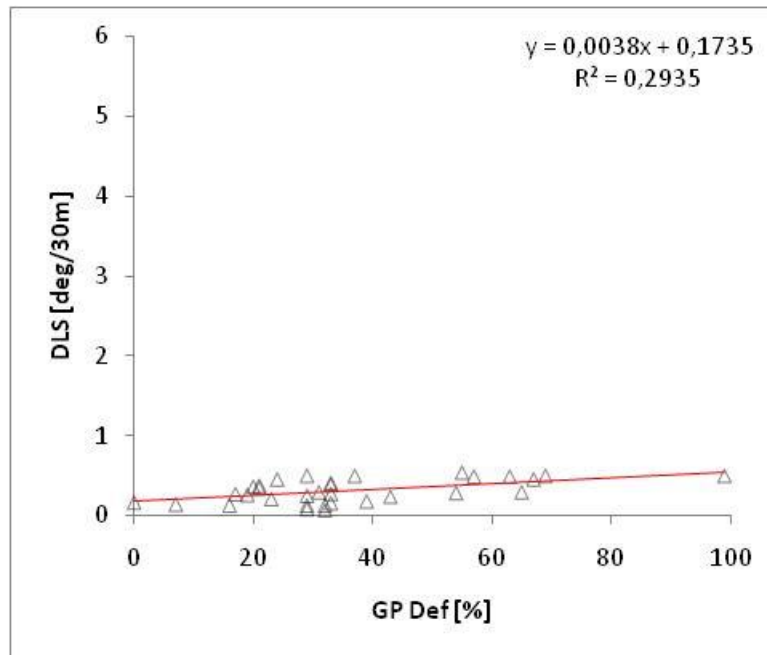


Figure 61, FMF3651Z-487256 holding @ all ROP and RPM

General observations/Preliminary Conclusions

Taking the slope of the trend lines as the criteria for describing the steerability capacity of the system, the following can be pointed out:

- Building has a higher slope than dropping. Then a change in GP deflection has a better response in building. Although at maximum deflections the build and drop rate are around 3 deg/30m, the slope of building is 20% higher.
- In turning the slope is 60% higher than the average. From this finding it can be conclude that at the conditions of this data the steering capability of the system for the turning application has a better response. Additionally turning left has a much higher slope than turning right. Then the system must have a walk tendency to the left.
- In order to hold angle at a range below 0,5 deg/30m between survey points a deflection of even around 70% was needed. This means that the geological tendencies or drilling parameters did not allow an optimum response from the system when holding.

ii) Identification of ROP and RPM ranges

As an intuitive approach and considering that design 487256 has large amount of data points. The identification of the ranges of ROP and RPM for this case where selected from the conditioning set

of data of design 405148 (61 data-points). A tolerance of +/-10% from the average was considered as the range of study. Table 3 shows the information of design 405148 and Table 4 displays the range of study that will be common for both designs.

Table 3, Summary design (405148) all data-points

	Av	Min	Max
ROP	68,86	30,86	128,22
RPM	147,07	82	162
Count	61		

Table 4, Case A, Ranges for FMF3651Z vs FMF3653Z

	10% Range	
ROP [ft/hr]	61.00	76.00
RPM	132.00	162.00

Then after applying those ranges of ROP and RPM Figure 62 is generated. This plot considers **all the directional behaviors**. However, only data points within 61 to 76 ft/hr and between 132 and 162 RPM were considered. In this case the dataset consists of 26 data points.

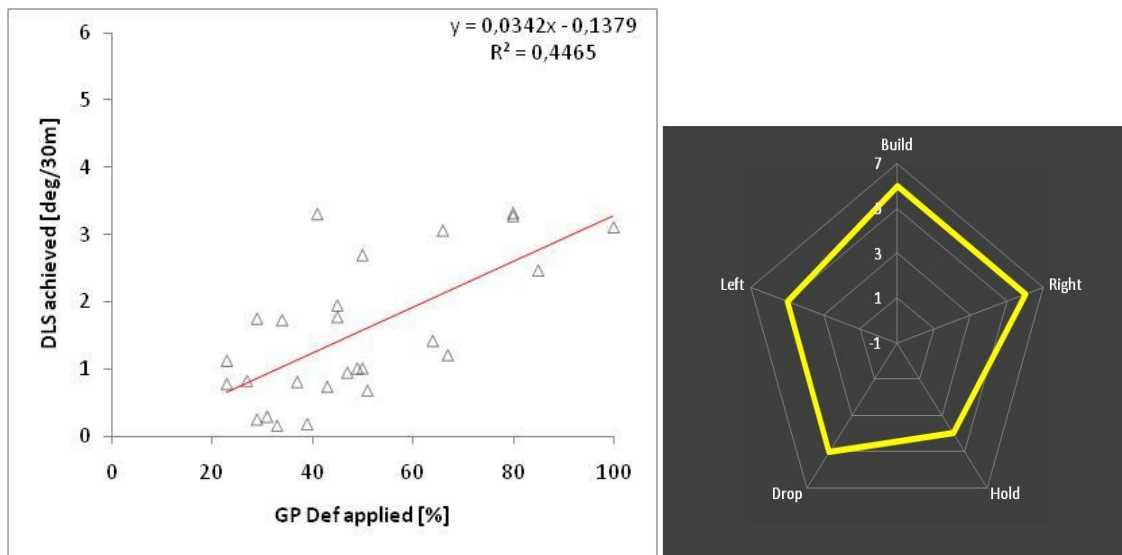


Figure 62, FMF3651Z-487256 all behaviors @ Range A

iii) Filtering by Steering behavior and Drilling parameters

Now that the impact of the directional behaviors and drilling parameters has been presented, the next step is to combine both criteria to obtain the final tendencies from field data.

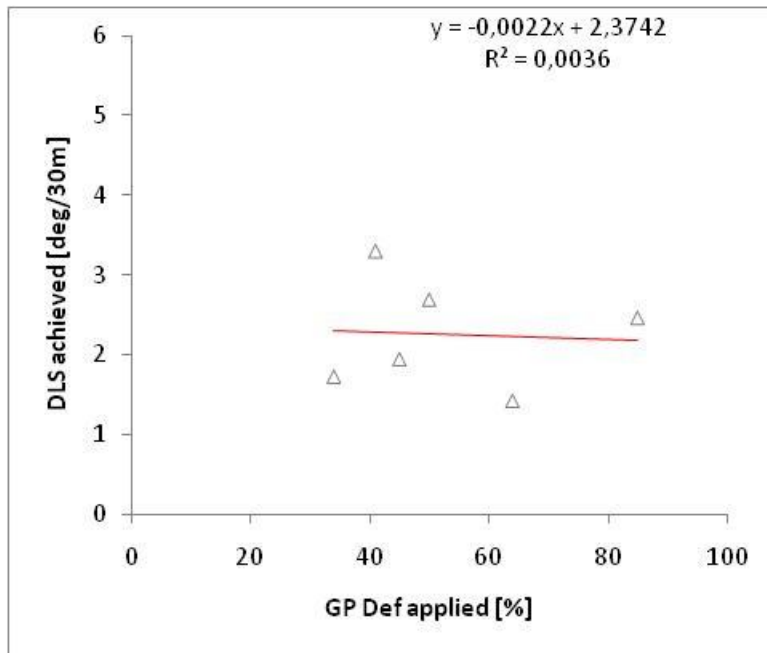


Figure 63, FMF3651Z-487256 building @ Range A

Within Range 1 of parameters (Table 4) the building behavior is very poor. The response to the GP setting as can be noticed from Figure 63 is very low, the slope is close to zero. This is true even for settings above 50% deflection.

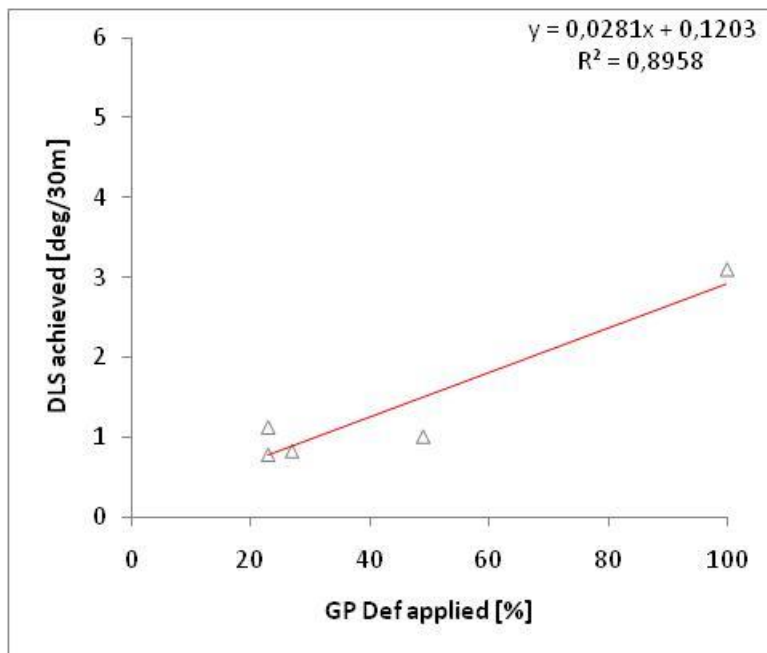


Figure 64, FMF3651Z-487256 dropping @ Range A

The tendency for dropping Figure 64, in the other hand is well correlated as a positive straight line. The response was much better than in building.

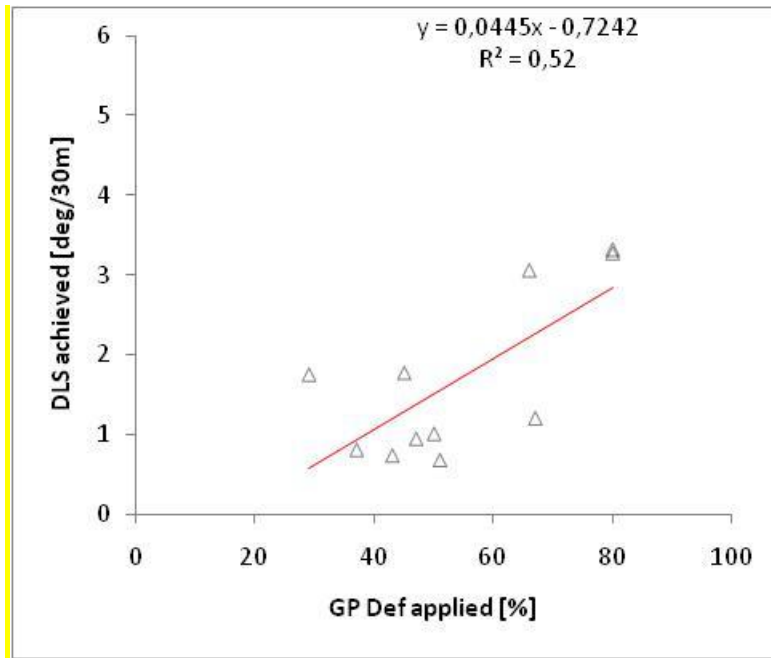


Figure 65, FMF3651Z-487256 turning @ Range A

The turning behavior (Figure 65) is directly influenced by turning left, given that turning right is almost not responsive. Figure 66 and 67 show that clearly. In addition, as building behavior for this design is not conclusive, **turning will be the tendency relevant for the comparison** with the next design and both tendencies will be finally compared with the simulations results.

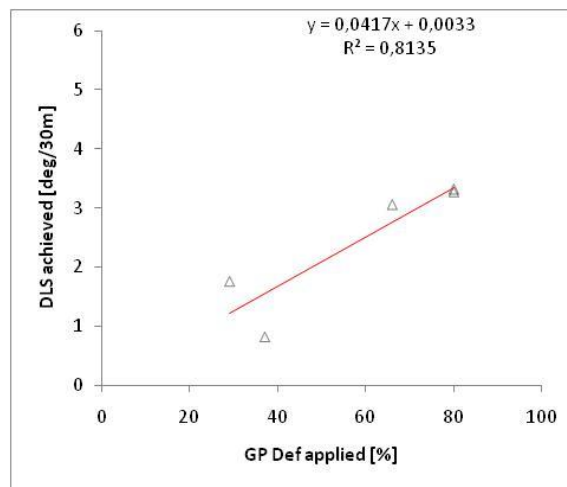
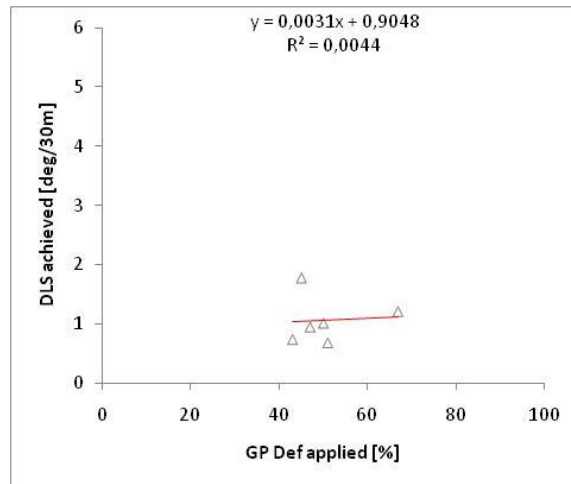


Figure 66, FMF3651Z-487256
Turning left @ Range 1



**Figure 67, FMF3651Z-487256
Turning right @ Range 1**

b) FMF3653Z (405148) data analysis

Table 5 shows the summary of the drilling conditions for the whole sample data of design FMF3653Z (405148). The sample consists of 61 data points. The minimum and maximum value for each variable was identified and a geometric average calculated.

Table 5, Summary design (405148) all data points

	Av	Min	Max
ROP	68,86	30,86	128,22
RPM	147,07	82	162
Count	61		

The Figure 68 shows the correlated data DLS achieved vs. GP deflection applied of all the data from the two well-paths drilled with bit design 405148. There are still a lot of spread data points despite the fact that it is taken mainly at reservoir level within a range of TVD 2100m to 2710m, with the same directional tool and same bit design.

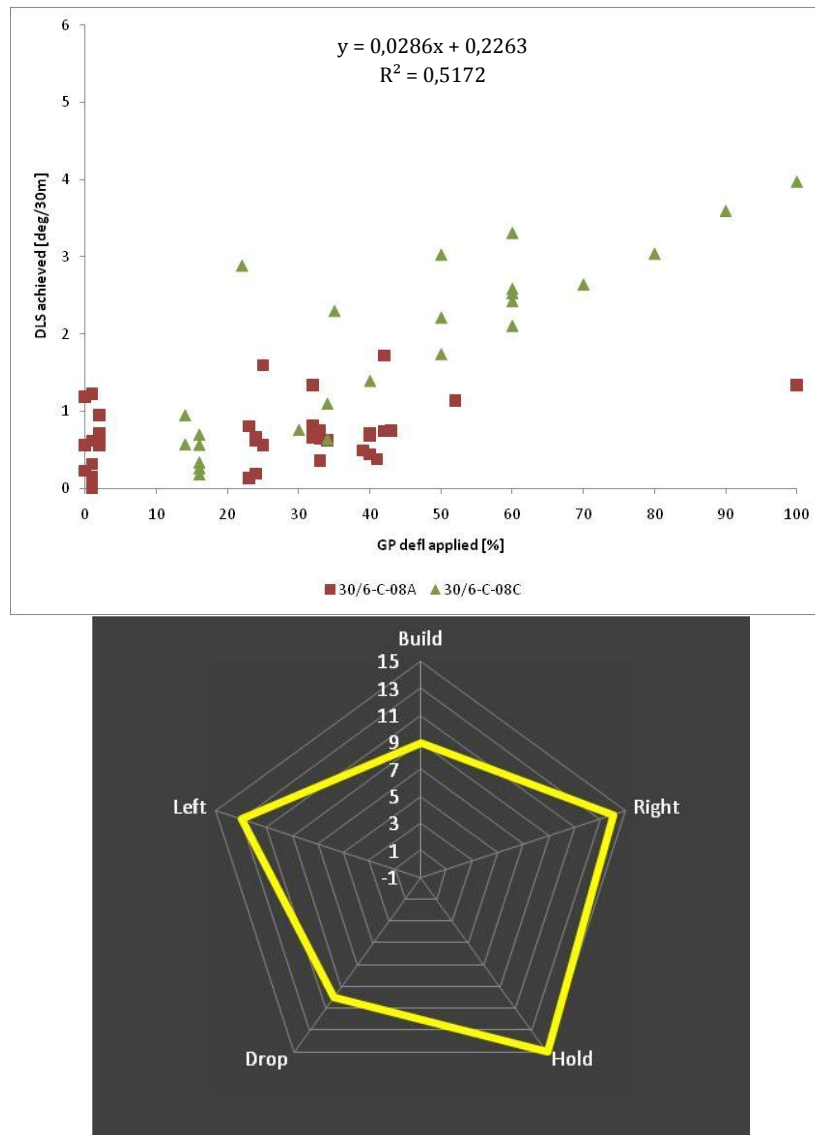


Figure 68, FMF3653Z (405148) all data

i) Identification of behaviors

Again the steering behaviors criterion is the same as for the previous design. Look up table sensitivity set to 0,5 deg/30m. Applying the algorithm the different results are displayed behavior by behavior.

Building

Figure 69 shows the filtered data for only building behavior of all dataset (all ROP and RPM). That is, no dropping, turning or holding data points are considered. It also shows the tendency line generated. And the total data points are 9.

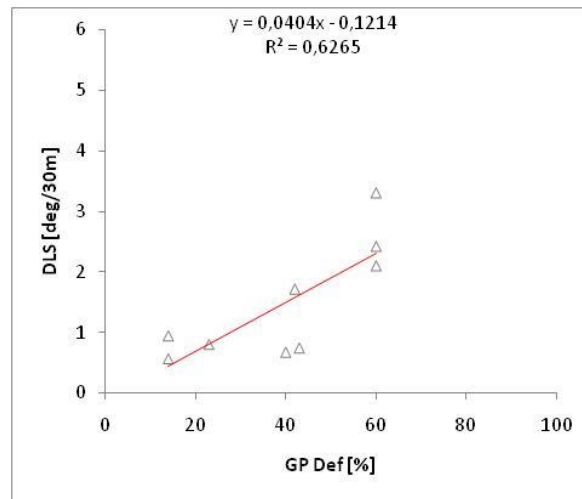


Figure 69, FMF3653Z-405148 building @ all ROP and RPM

Dropping

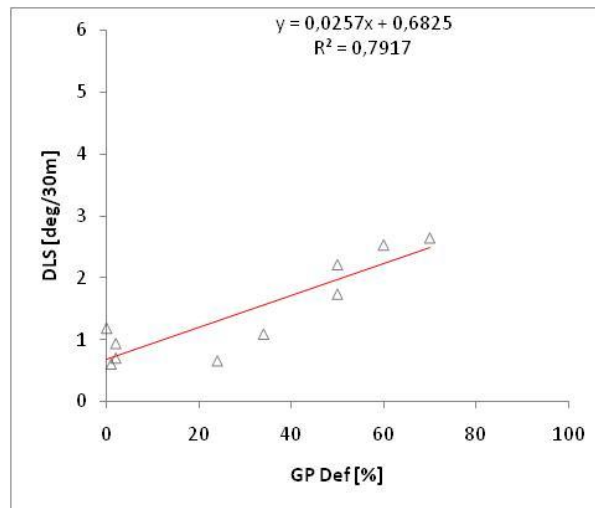


Figure 70, FMF3653Z-405148 dropping @ all ROP and RPM

In dropping, the dataset is reduced to 10 data points.

Turning both right and left

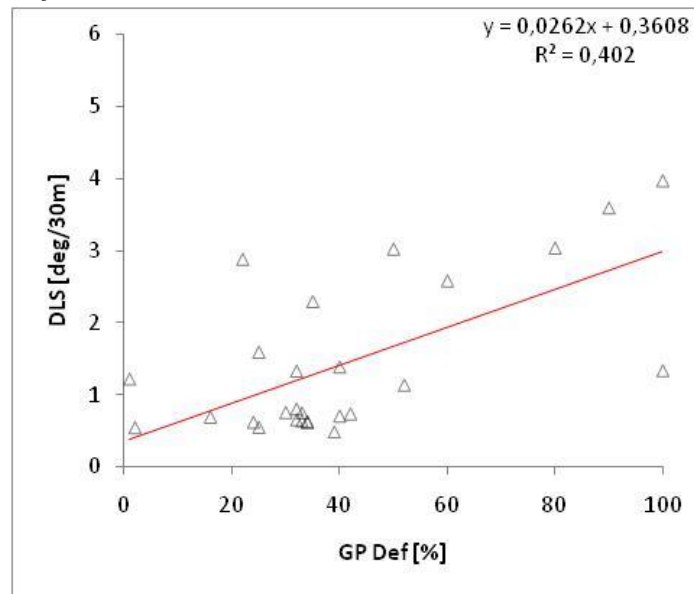


Figure 71, FMF3653Z-405148 turning @ all ROP and RPM

The filtered data comprises 27 data points. It considers both turning left and turning right where building or dropping were less than 0,5 deg/30m.

Turning only right

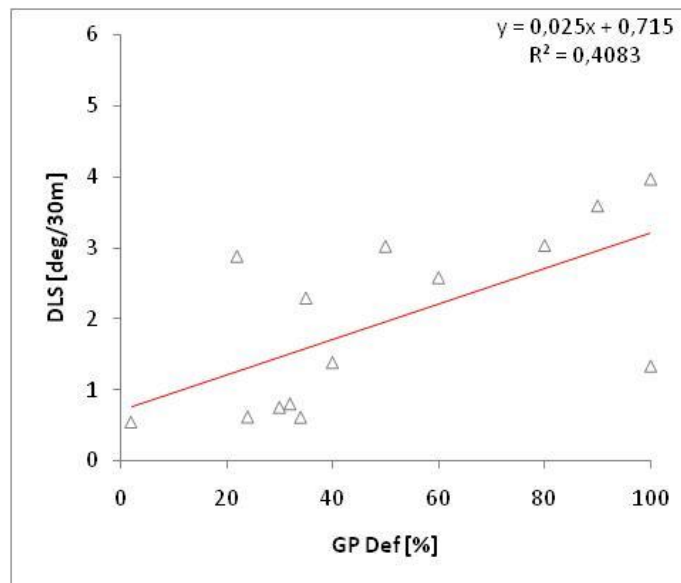


Figure 72, FMF3653Z-405148 T right @ all ROP and RPM

Turning right comprises 14 data points. The data show a good level of correlation between GP deflection and DLS achieved, what is not the case in the next scenario.

Turning only left

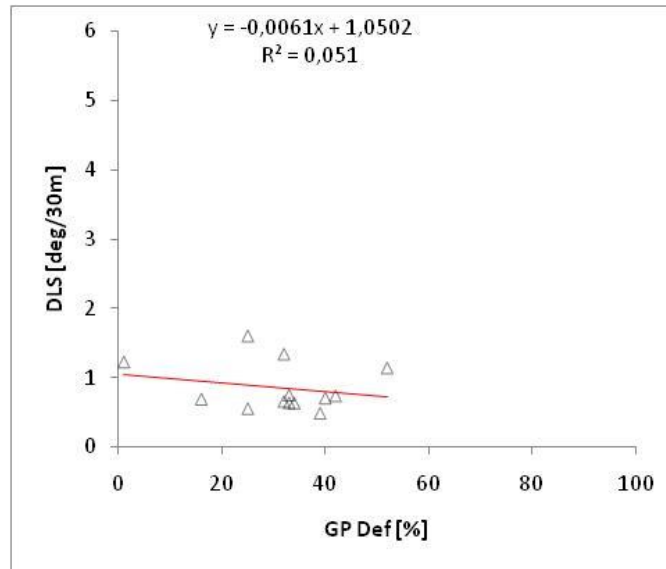


Figure 73, FMF3653Z-405148 T left @ all ROP and RPM

When comparing only by direction, the sample has almost 50% right and 50% left turning. However, turning right has a better response from the system. The slope of turning left is close to zero. This can be explained by the geological tendencies, the operative conditions and the bit design walk tendency.

Holding

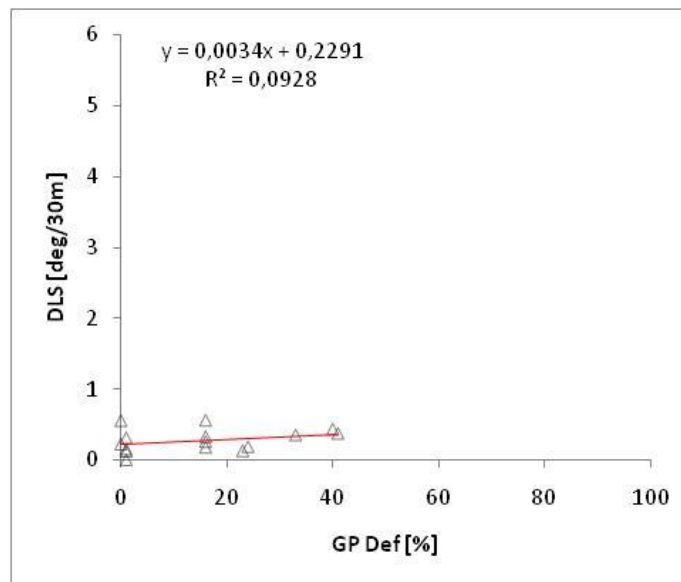


Figure 74, FMF3653Z-405148 holding @ all ROP and RPM

General observations and preliminary conclusions

Taking the slope of the trend lines as the criteria for describing the steerability capacity of the system, the following can be pointed out:

- Building has a good performance; the average slope is 0,040, however, the dropping slope is 50% lower. And when comparing maximum values, the one of building reach around 3,2 deg/30m while that of dropping reach around 2,7 deg/30m.
- Turning presents a slope of 0,026. However, the left and right behaviors have very different responses. The left response is poor, this can be explained by the geological features or other drilling parameters, such as WOB. And the right response has a good correlation with GP deflection.
- Finally, in holding, it can be seen that a 40% deflection had to be applied in order to hold angle.

ii) Identification of ROP and RPM ranges

The data-points considered are within the same range as for the previous design. Range A defined in Table 4, and repeated here:

Range A

	10% Range	
ROP [ft/hr]	61.00	76.00
RPM	132.00	162.00

The following fig. shows all the steering behaviors (Building, dropping, turning and holding) at the range of ROP [61-76] ft/hr and RPM [132-162].

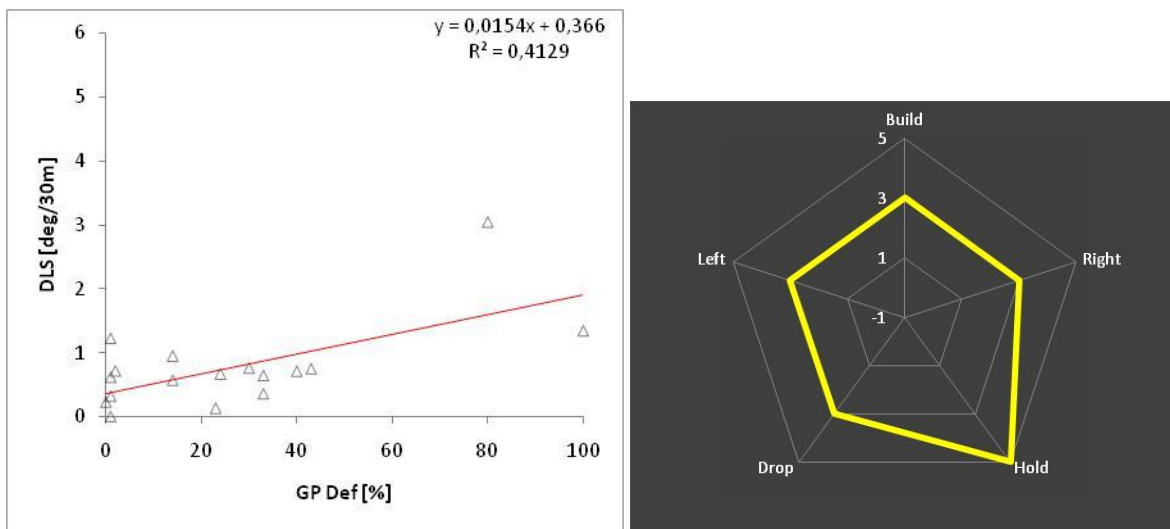


Figure 75, FMF3653Z-405148 all behaviors @ Range A

iii) Filtering by Steering behavior and Drilling parameters

The following Figures show the different behaviors responses within the Range A of drilling parameters.

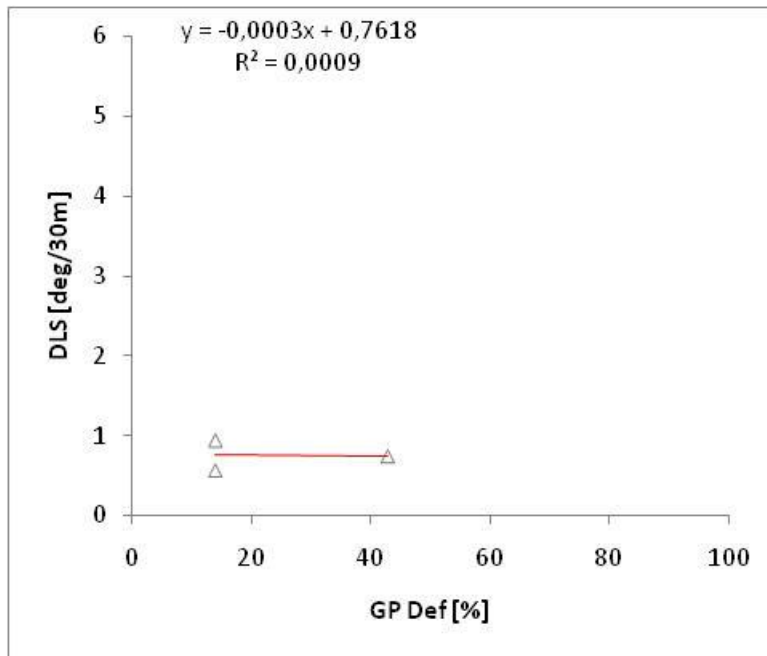


Figure 76, FMF3653Z-405148 building @ Range A

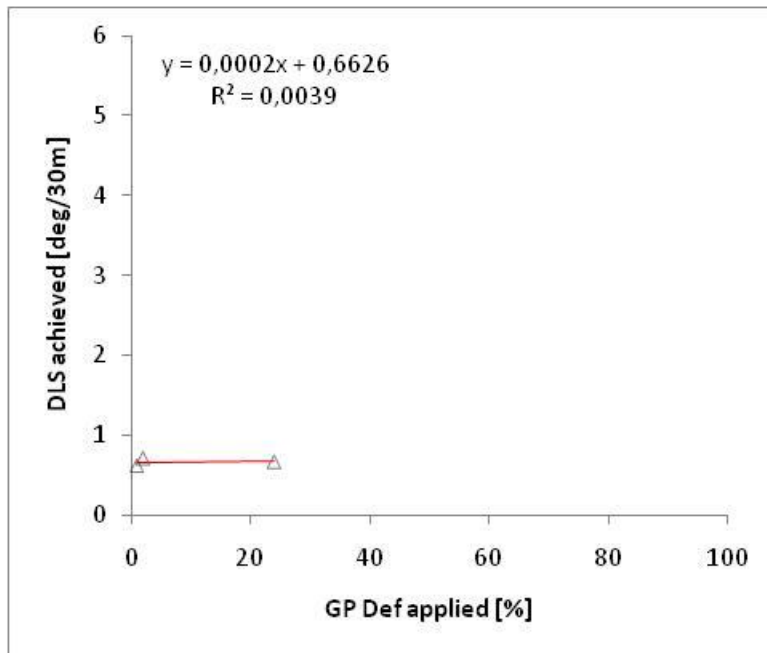


Figure 77, FMF3653Z-405148 dropping @ Range A

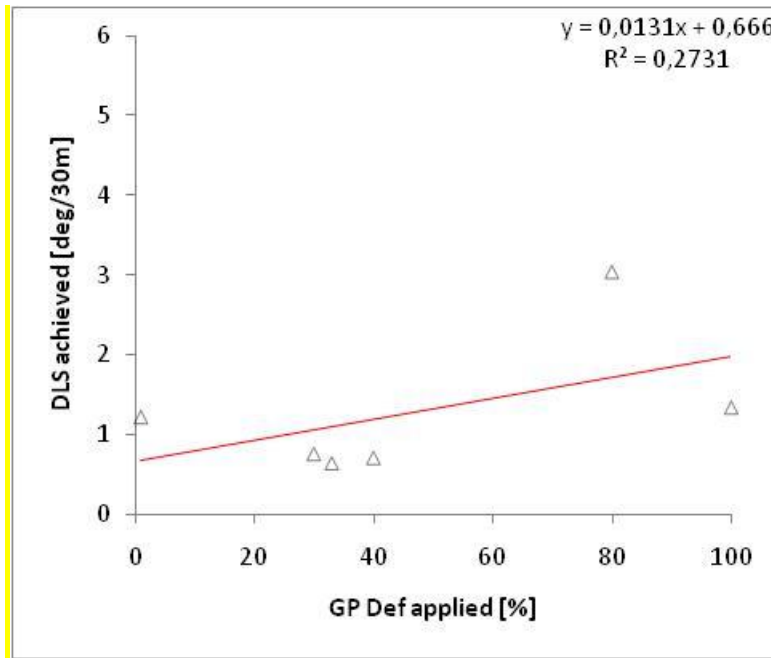


Figure 78, FMF3653Z-405148 turning @ Range A

Building again in this case is not conclusive then the behavior selected for the analysis is turning. Figure 78 shows the field tendency of design 405148 that will be relevant for the comparison with simulation.

In addition, the difference between turning left and right can be seen in Figures 79 and 80. Turning right has a much better performance.

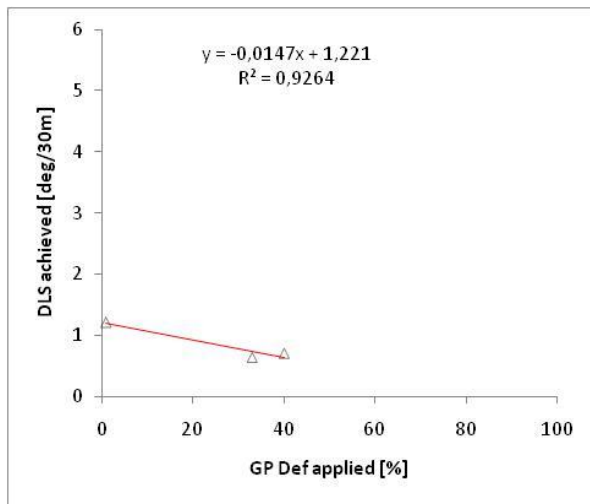


Figure 79, FMF3653Z-405148 T left @ Range A

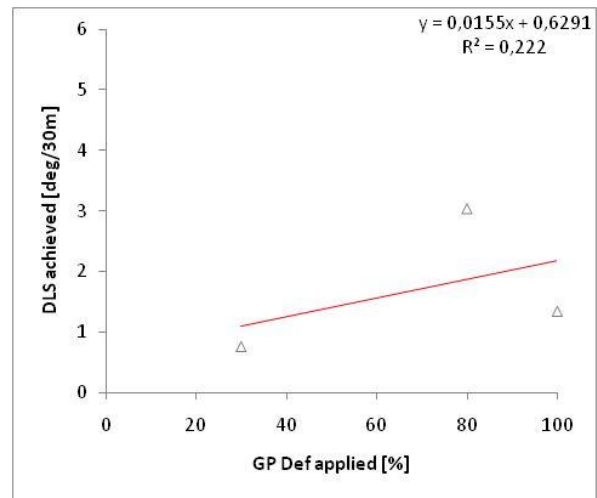


Figure 80, FMF3653Z-405148 T right @ Range A

c) Field Tendencies

After this analysis we can put together the information generated from both designs. These field tendencies will be the base for the comparison with the simulation. Figure 81 considers not only the same steering behavior but also the same ranges of ROP and RPM for both designs. This is the final result of the analysis of field data, the **Field Tendencies** for Case A.

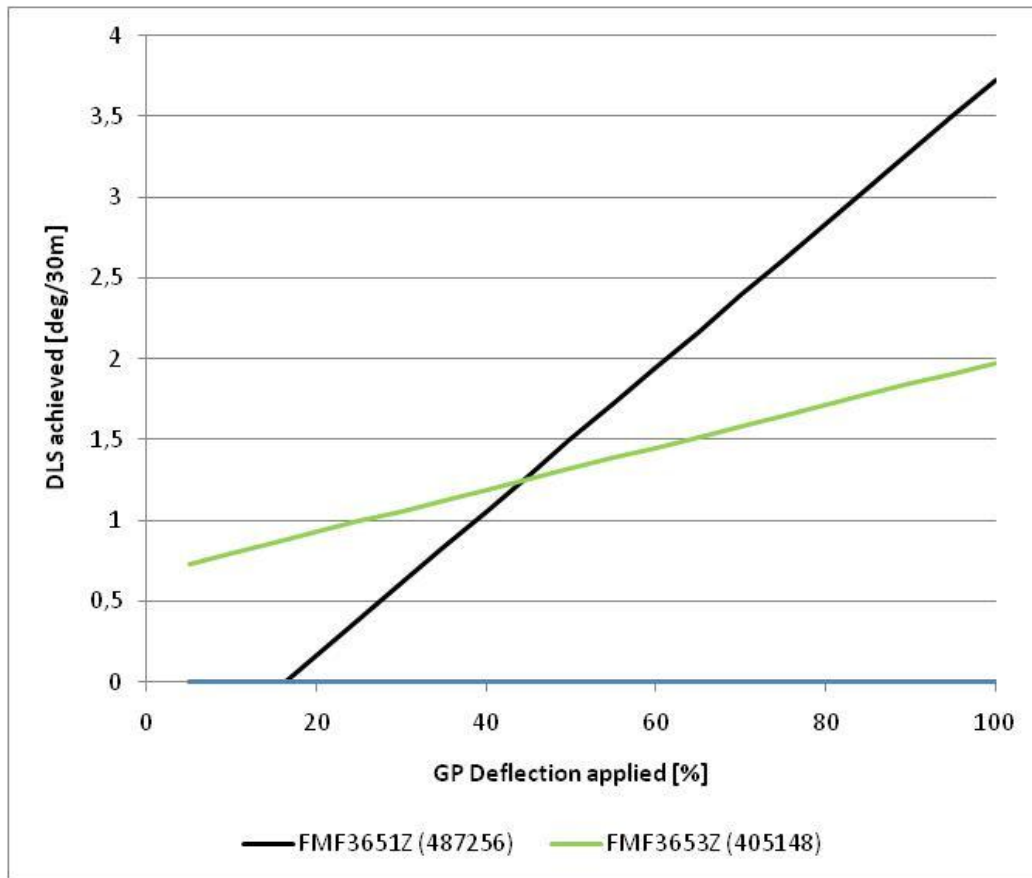


Figure 81, Design 487256 and 405148 field tendencies (turning)

From this figure is clear that under similar conditions (operative and steering behavior), the design (487256) – FMF3651Z is more steerable than (405148) – FMF3653Z. At maximum deflection FMF3651Z can achieve 88% higher DLS than FMF3653Z.

d) Simulation and Model Tendencies

The simulation is performed as described in 3.5. The input parameters for each design are described in tables. In addition, a picture of the bit is also attached to verified the model used in the simulation.

To understand the model of the gage and sleeve Figure 82 shows the parts designed.

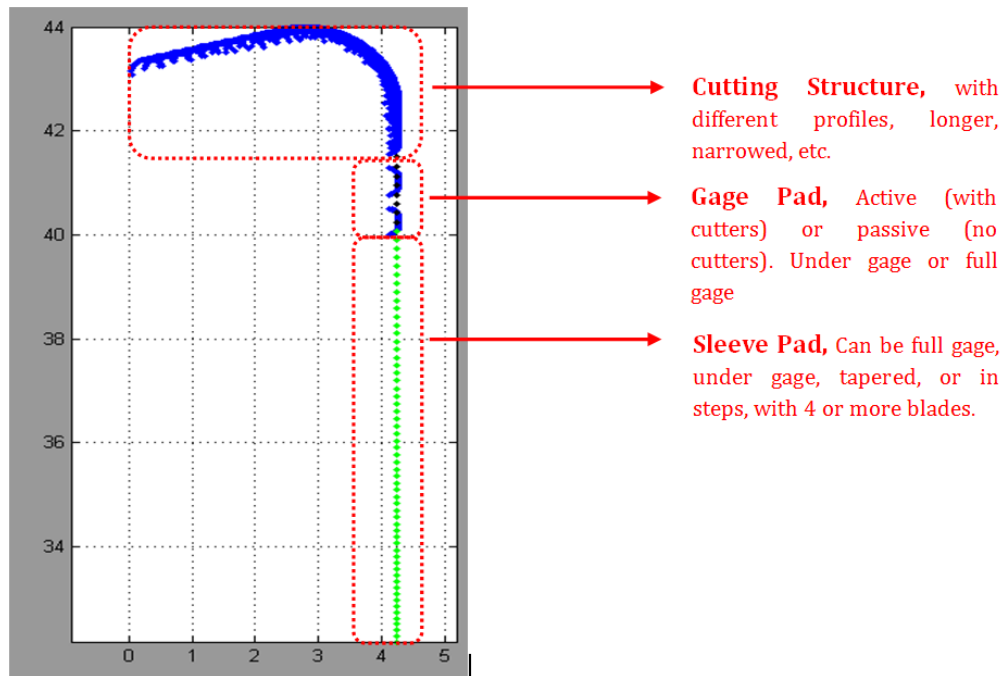


Figure 82, Bit parts.

And the input parameters are defined as explained in 3.5. ROP is the average of the range identified and the same for RPM. Figure 83 displays the input boxes of these parameters.

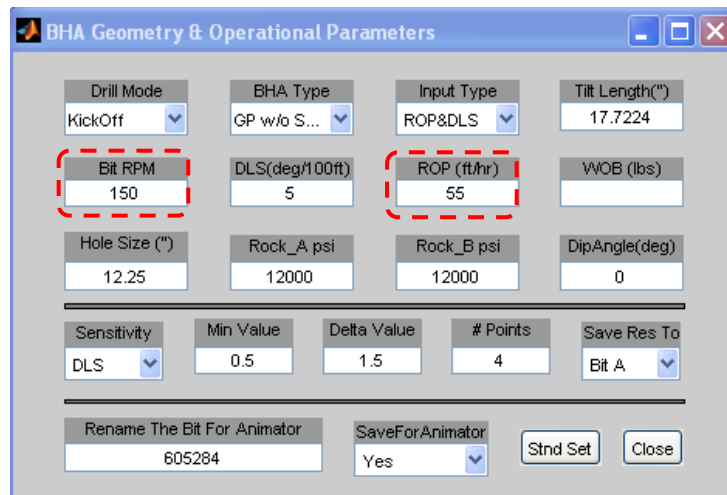
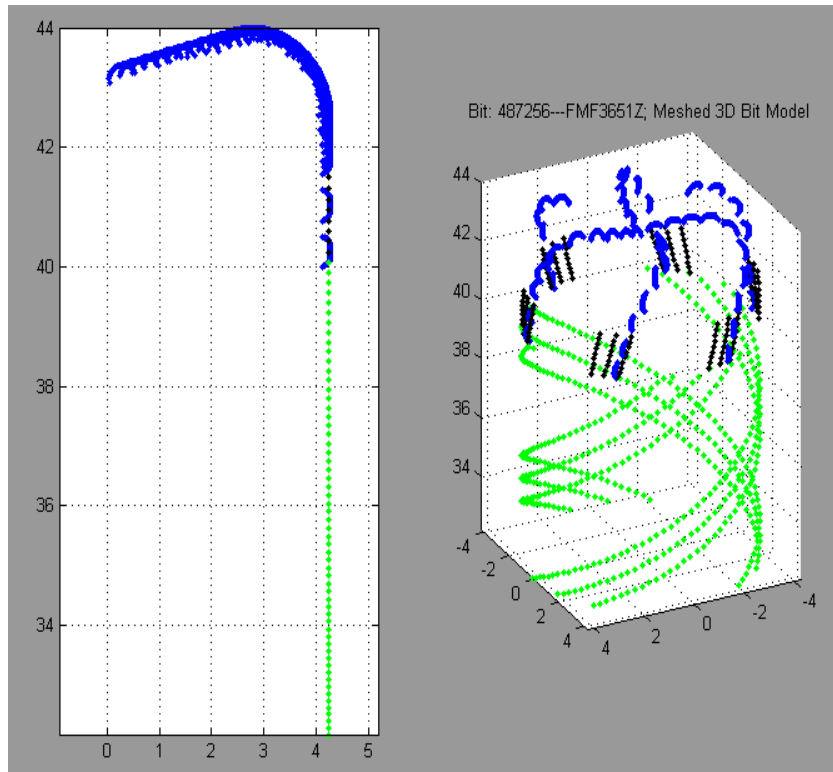
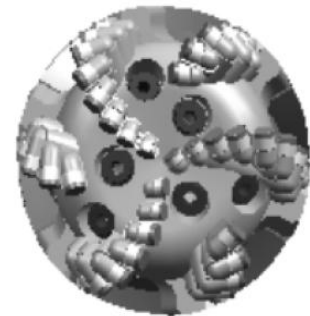


Figure 83, Input parameters

487256 - FMF3651Z

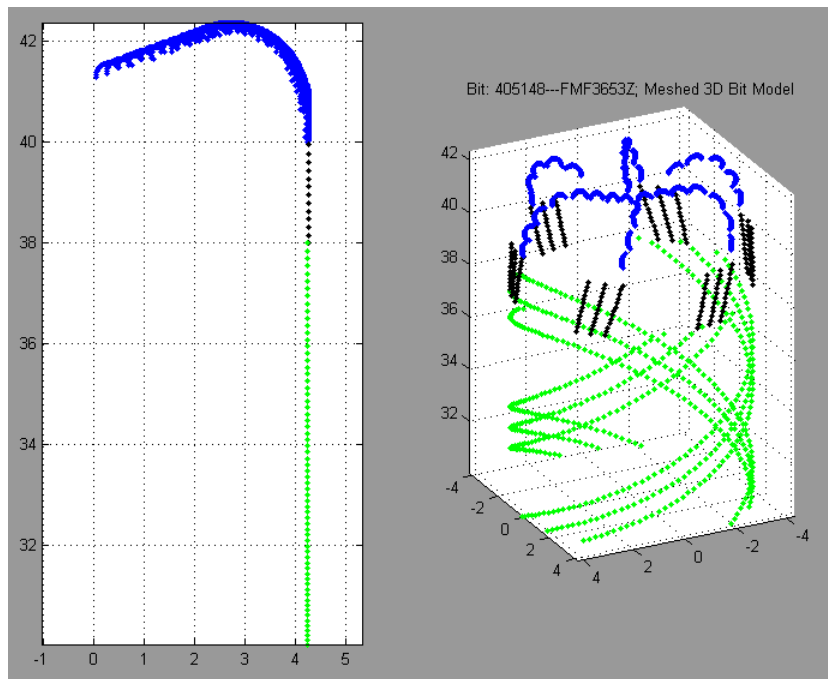
Input Data	
Bit type	487256 - FMF3651Z
Drill mode	Kickoff
BHA type	GP w/o SLH
ROP [ft/hr]	69
RPM	147
Tilt Length ["]	13,3979
Hole size ["]	8,5
Rock Strenght [psi]	10000
Dip angle [deg]	0
Gage pad length ["]	1,5
Undergage 1/ ["]	32
Sleeve blades	4
Sleeve blades angle	20
Sleeve gage length ["]	8
Undergage 1/ ["]	16
Tapered angle [deg]	0
Comment	Active Gage Pad



Material #487256

405148 - FMF3653Z

Input Data	
Bit type	405148 - FMF3653Z
Drill mode	Kickoff
BHA type	GP w/o SLH
ROP [ft/hr]	69
RPM	147
Tilt Length ["]	12,3348
Hole size ["]	8,5
Rock Strenght [psi]	10000
Dip angle [deg]	0
Gage pad length ["]	2
Undergage 1/ ["]	0
Sleeve blades	4
Sleeve blade angle	20
Sleeve gage length ["]	8
Undergage 1/ ["]	0
Tapered angle [deg]	0,2238
Comment	Passive gage Sleeve taperd 1/16



Material #405148

e) Results and comparison

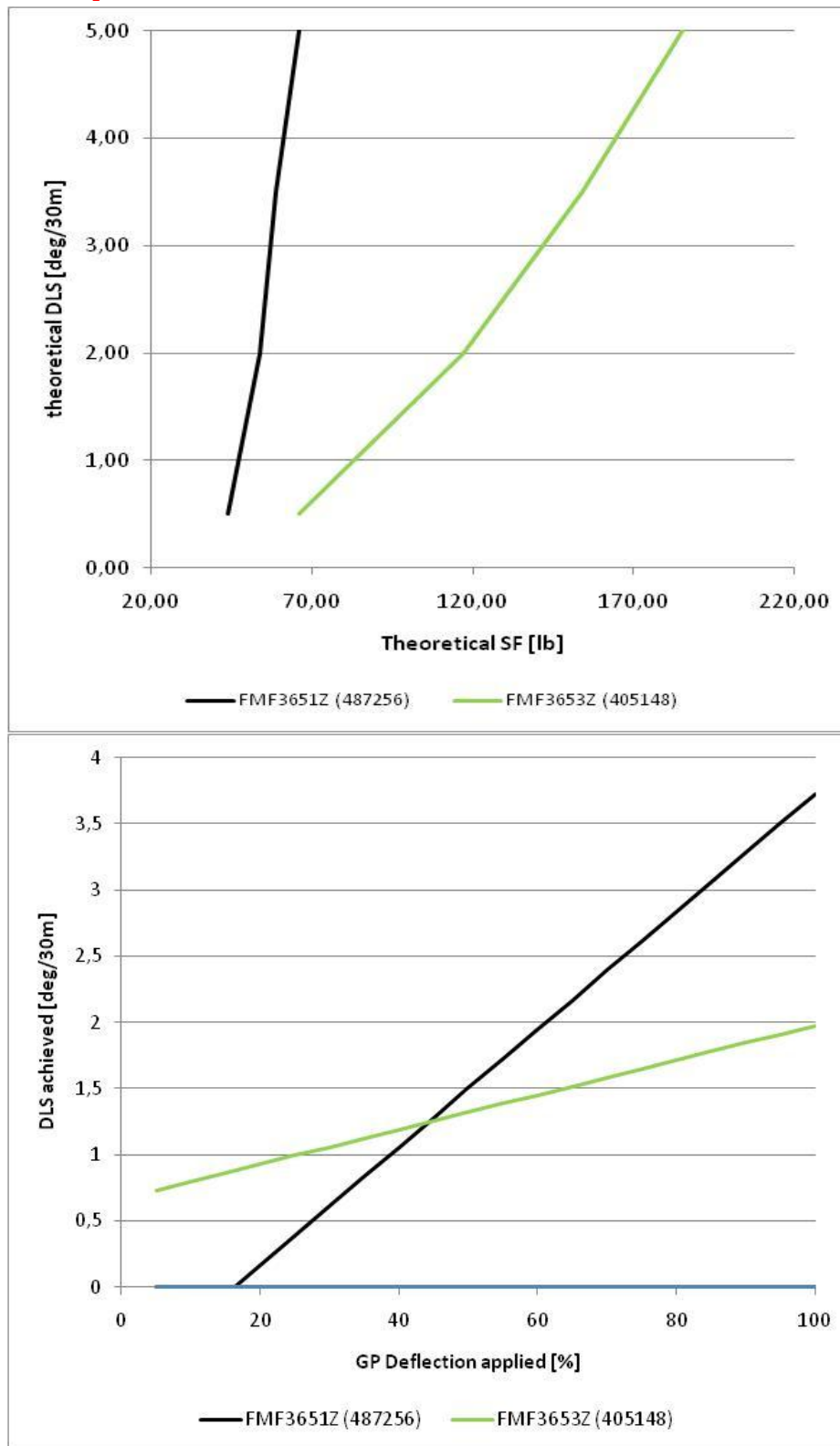


Figure 84, Designs 487256 and 405148 simulation (top) and field data (bottom) comparison

As can be seen in Figure 84, the tendencies displayed by the simulator and from field data correlate. Bit FMF3651Z is much more steerable than FMF3653Z. From the simulation, design (487256) requires a considerable lower side force than (405148) to achieve the same DLS.

The field response is more complex than the simulator:

- If only considering the slope of the tendencies of the field results, design 487256 has a response 300% higher than 405148.
- Regarding the DLS achieved at maximum deflection, design (487256) reached 3,7 deg/30m while (405148) only 2 deg/30m.

These results validate the relevancy of considering different bit behaviors and specific ranges of ROP and RPM. The addition of an active gage and a flatter bit profile had a positive impact in steerability. G. Mensa-Wilmot^[23] also explains the effect of active gage and the impact on steerability.

4.3.2 Case B – 8 ½ section, Low ROP

After analyzing the whole data available for this section, it was decided to make the study in three ranges of ROP and a constant range of RPM. This was possible after checking the distributions of the data. This distributions analysis also defined the designs considered in each range of ROP.

Initially each design is analyzed independently. General information regarding the drilling parameters and behaviors is summarized. This big picture of both designs helps identify the most representative steering behavior and generate the field tendencies straight forward. However, the whole analysis behavior by behavior can be found in the appendix section.

Then, the simulations are performed with the averages of the ranges selected. Finally a comparison between field and simulation is performed.

All the data considered is taken at the following conditions:

Table 6, Case B, Ranges @ Low ROP, 8 ½ section

Case B	Min	Max	Av
ROP [ft/hr]	40	55	47,5
RPM	140	170	155

After filtering by these criteria two bits Figure 85 and 86 have enough data points to generate tendencies and elaborate the analysis of the most relevant steering behavior.

Table 7, Low ROP, bit designs

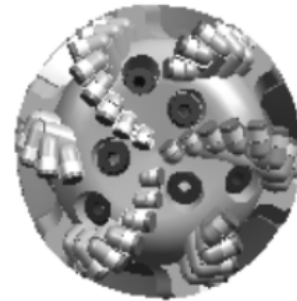
Type	Material #	Design
FMF3651Z	487256	A
FMF3651Z	531396	B

PRODUCT SPECIFICATIONS

Cutter Type	X2 - Tough Drilling	
IADC Code	M422	
Body Type	MATRIX	
Total Cutter Count	48	
Cutter Distribution	<u>13mm</u>	<u>16mm</u>
Face	6	24
Gauge	18	0
Number of Standard Nozzles	6	
Number of Small Nozzles	0	
Number of Ports	0	
Junk Slot Area (sq in)	13.76	
Normalized Face Volume	40.2%	
API Connection	4-1/2 I.F. BOX	
Recommended Make-Up Torque*	25,000 Ft*lbs.	
Nominal Dimensions**		
Make-Up Face to Nose	14.86 in - 377 mm	
Gauge Length	1.5 in - 38 mm	
Sleeve Length	8 in - 203 mm	
Shank Diameter	6.25 in - 159 mm	
Break Out Plate (Mat.#/Legacy#)	181975/44745	
Approximate Shipping Weight	256Lbs. - 116Kg.	

SPECIAL FEATURES

P-100, Active Gage, , 1/32" Relieved Gage, 1/16" Undergage Sleeve



Material #487256

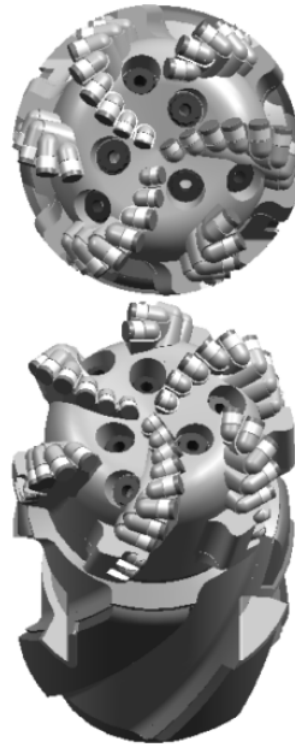
Figure 85, FMF3651Z (487256)

PRODUCT SPECIFICATIONS

Cutter Type	X2 - Tough Drilling	
IADC Code	M422	
Body Type	MATRIX	
Total Cutter Count	48	
Cutter Distribution	<u>13mm</u>	<u>16mm</u>
Face	6	24
Gauge	18	0
Number of Standard Nozzles	6	
Number of Small Nozzles	0	
Number of Ports	0	
Junk Slot Area (sq in)	13.76	
Normalized Face Volume	40.2%	
API Connection	4-1/2 IF. BOX	
Recommended Make-Up Torque*	25,000 Ft*lbs.	
Nominal Dimensions**		
Make-Up Face to Nose	14.69 in - 373 mm	
Gauge Length	1.5 in - 38 mm	
Sleeve Length	7 in - 178 mm	
Shank Diameter	6.25 in - 159 mm	
Break Out Plate (Mat.#/Legacy#)	181975/44745	
Approximate Shipping Weight	256Lbs. - 116Kg.	

SPECIAL FEATURES

P-100, Active Gage, 1/32" Relieved Gage, (MEG) Modified Extended Gage Sleeve - 4 Blade, 1/16" Undergage Sleeve



Material #551396

Figure 86, FMF 3651Z (551396)

a) Field Tendencies

An initial correlation of “DLS achieved vs GP deflection applied” is plotted for each design Figure 87 and Figure 88. This correlation considers all the behaviors within the Low ROP range in Table 7. The first analysis discloses a cloud of data with positive tendency. However, there are many spread points because of the different behaviors.

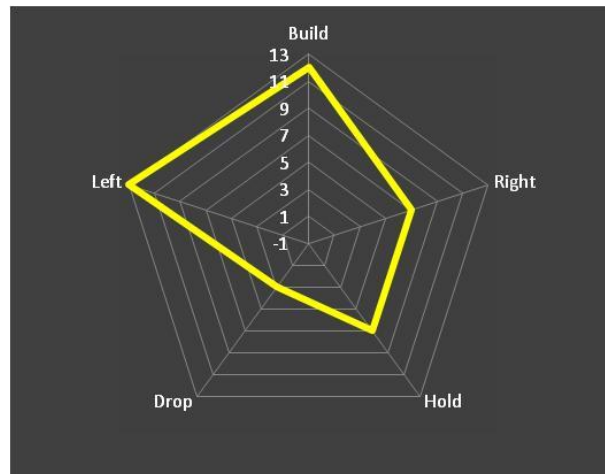
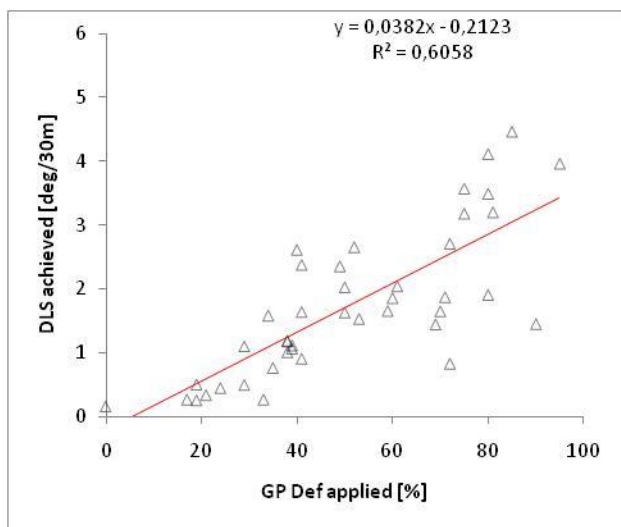


Figure 87, Design (A) steering response all behaviors

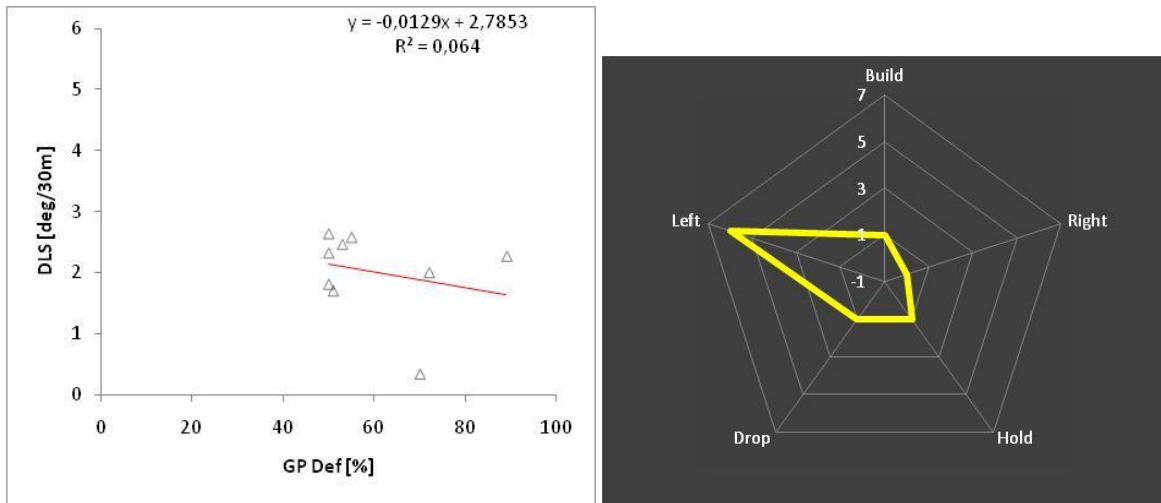


Figure 88, Design (B) steering response all behaviors

As can be seen from the figures it is much more meaningful to make the analysis in the turn left behavior in that way more data-points will be considered and the analysis more accurate.

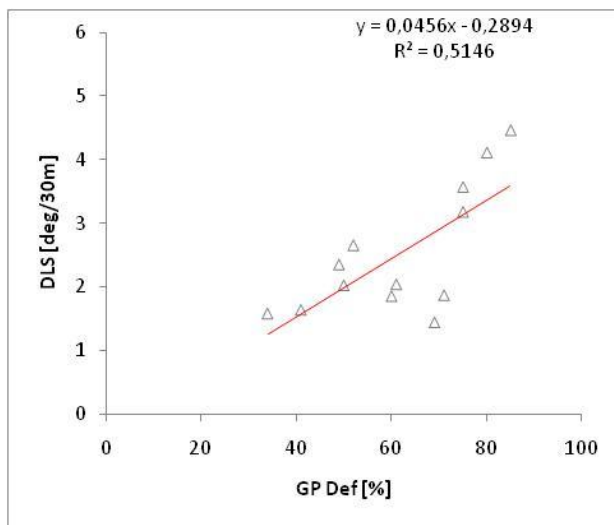


Figure 89, Design 487256

Turning left and operational parameters

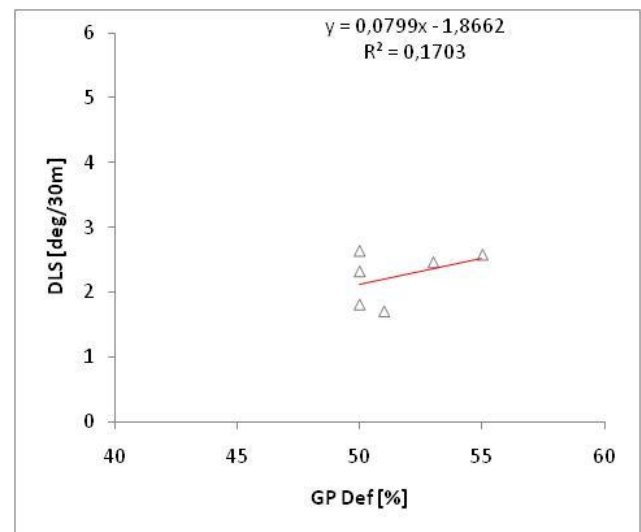


Figure 90, Design 551396

Turning left and operational parameters

Figures 89 and 90, display the field tendencies of both bit designs. Turning left and at the ranges of ROP and RPM specified at the beginning of the section. Now it is possible to compare both designs between each other and also with the results from the simulator.

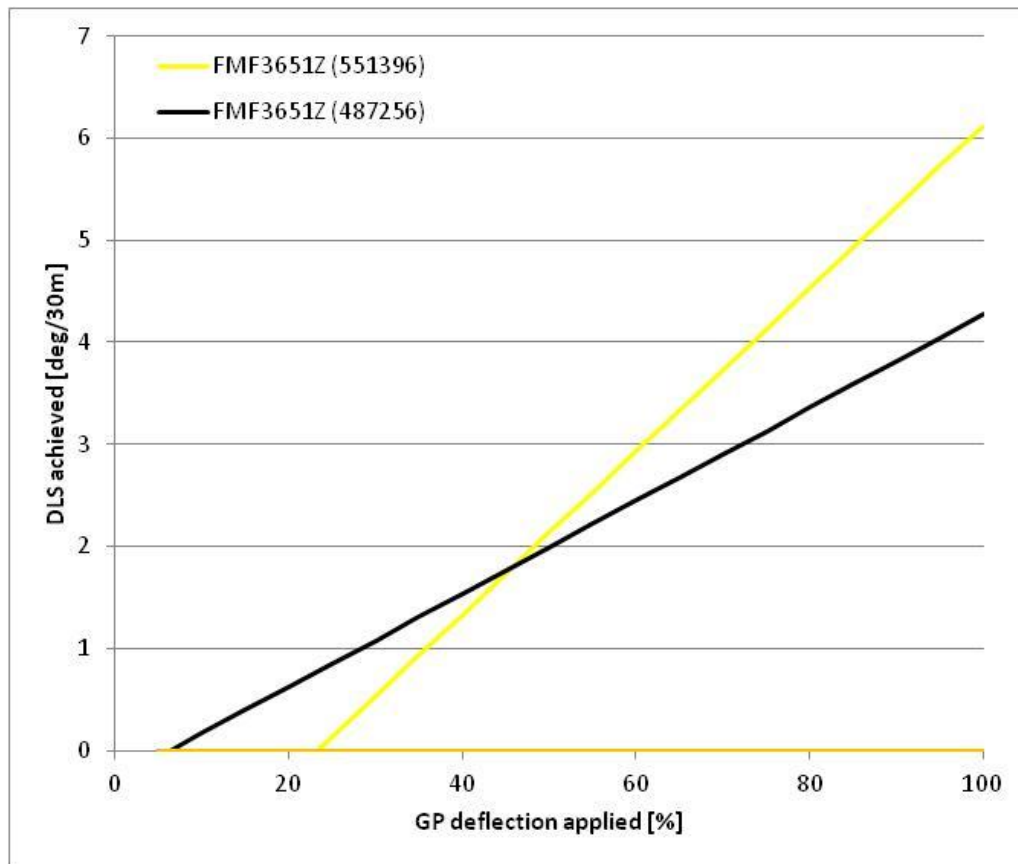


Figure 91, Field tendencies Case B, 8 ½ section

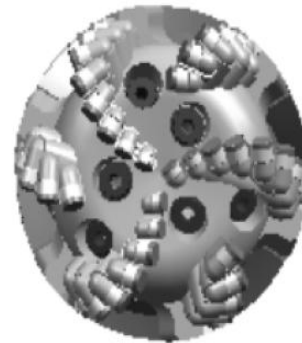
From Figure 91 it is clear that under similar conditions (operative and steering behavior) and for a deflection within 50%, design (487256) is more steerable than (551396). However, considering only the slope and maximum DLS achieved, design (551396) becomes the most steerable reaching 6,1 deg/30m at maximum deflection while the other design reaches only 4,2 deg/30m, what represents an improvement of 45% under the conditions describe before.

b) Simulation and Model Tendencies

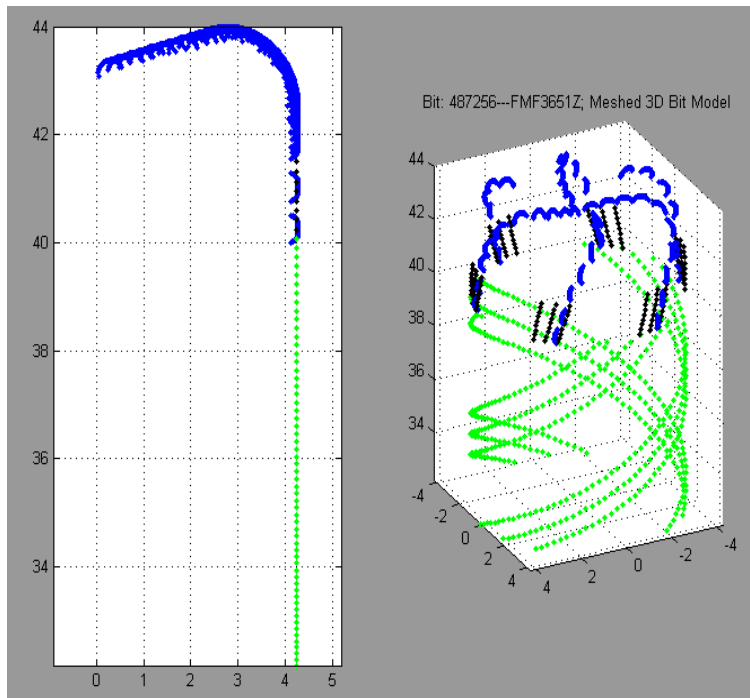
The simulation is performed as described in 3.5. The input parameters for each design are described in tables. In addition, a picture of the bit is also attached to verified the model used in the simulation.

487256 - FMF3651Z

Input Data	
Bit type	487256 - FMF3651Z
Drill mode	Kickoff
BHA type	GP w/o SLH
ROP [ft/hr]	47,5
RPM	155
Tilt Length ["]	13,6479
Hole size ["]	8,5
Rock Strenght [psi]	10000
Dip angle [deg]	0
Gage pad length ["]	1,5
Undergage 1/ ["]	32
Sleeve blades	4
Sleeve gage length ["]	8
Undergage 1/ ["]	16
Tapered angle [deg]	0
Comment	Active Pad gage

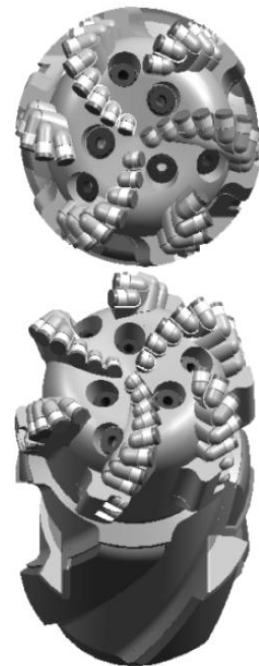
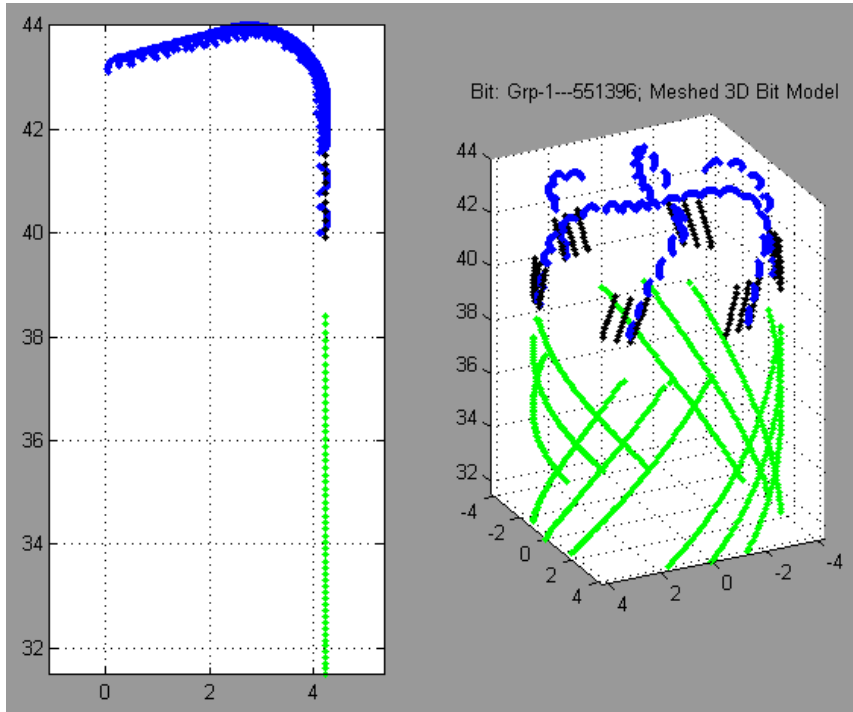


Material #487256



551396 - FMF3653Z

Input Data	
Bit type	135596 - FMF3651Z
Drill mode	Kickoff
BHA type	GP w/o SLH
ROP [ft/hr]	47,5
RPM	155
Tilt Length ["]	14,1479
Hole size ["]	8,5
Rock Strenght [psi]	10000
Dip angle [deg]	0
Gage pad length ["]	1,5
Undergage 1/ ["]	32
Sleeve blades	4
Sleeve gage length ["]	7
Undergage 1/ ["]	16
Tapered angle [deg]	0
Comment	Active gage MEG 1,5"



Material #551396

The tendencies displayed Figure 92, Simulator are very similar due to fact that the only change in design is the addition of the MEG feature in design 551396. This difference is almost constant along both lines. This is in correlation with other studies which state that a higher tilt length will reduce steerability.

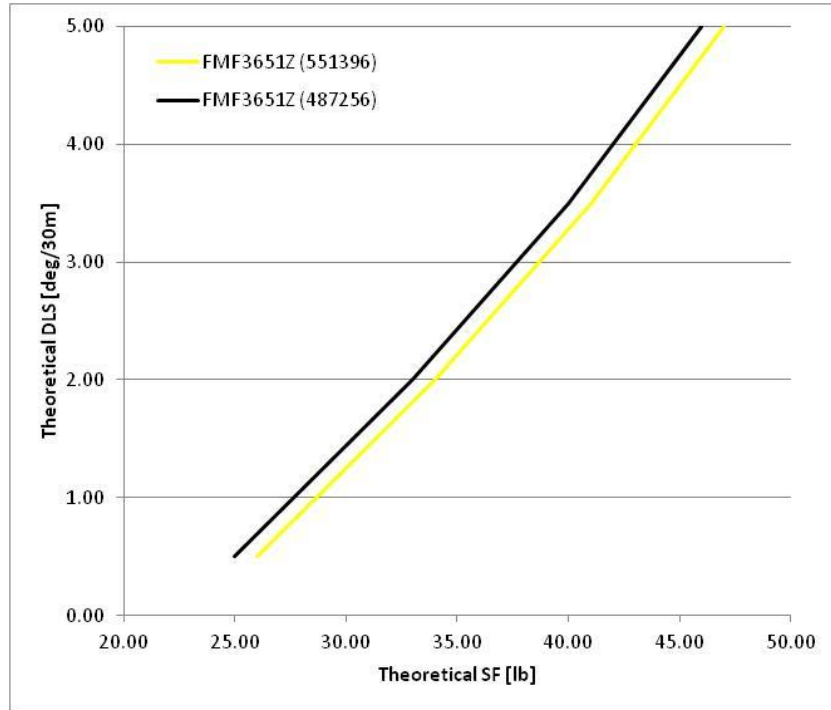


Figure 92, 487256 vs 551396 simulation results

c) Results and comparison

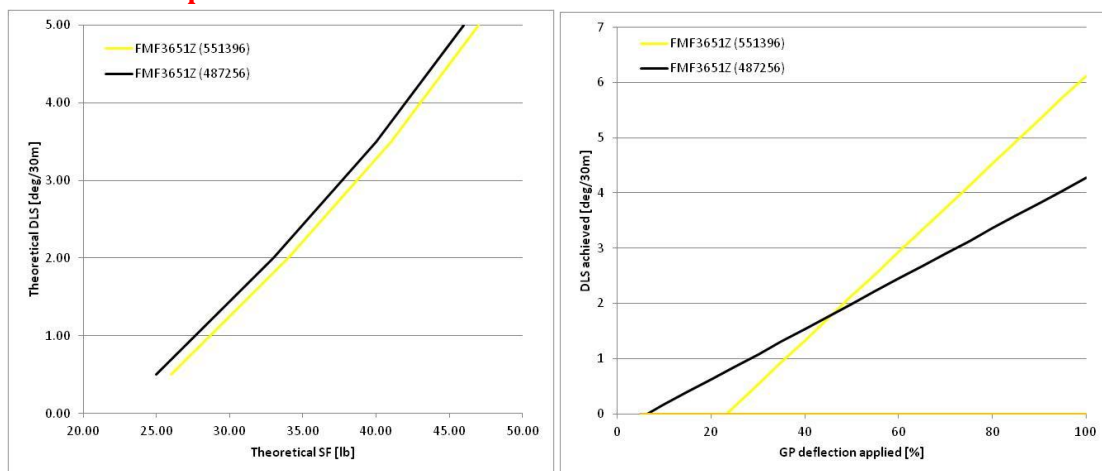


Figure 93 Model vs Field tendencies

When comparing both tendencies, the field data match the model within lower values of GP deflection until approximate 45% deflection. For higher values the simulator does not model the tendency seen at the field. Bit 551396 is more steerable than 487256 and reach a maximum DLS of 6 deg/30m where 487256 reach only 4.2 deg/30m. This can be explained partly by the modifications introduce in design 551396, the MEG (Modified Extended Gage), that improves flow and cleaning and also some other geological features as dipping or change in rock strength.

4.3.3 Case C – 8 ½ section, Medium ROP

The second group of data is taken at the following conditions:

Table 8, Case C, Ranges @ Medium ROP, 8 ½ section

Case C	Min	Max	Av
ROP	55	70	62,5
RPM	140	170	155

After filtering by this criterion, the following designs have enough data points to generate tendencies and elaborate the analysis by turning:

Table 9, Medium ROP, bit designs for turning analysis

Type	Material #	Design
FMF3651Z	487256	A
FMF3651Z	551396	B
FMF3653Z	405148	C
FMF3741Z	475040	D

And for analyzing building behavior:

Table 10, Medium ROP , bit designs for building analysis

Type	Material #	Design
FMF3651Z	487256	A
FMF3741Z	475040	D

Initially each design is analyzed independently. General information regarding the drilling parameters and behaviors is summarized. This big picture of the several designs helps identify the most representative steering behavior and generate the field tendencies straight forward. However, the whole analysis behavior by behavior can be found in the appendix section.

Then, the simulations are performed with the averages of the ranges selected. Finally a comparison between field and simulation is performed and explained.

Design A and B are already presented in Figures 85 and 86. Designs C and D are described in Figures 94 and 95.

PRODUCT SPECIFICATIONS

Cutter Type		Z3®	
IADC Code		M423	
Body Type		MATRIX	
Total Cutter Count		42	
Cutter Distribution		<u>13mm</u>	<u>16mm</u>
	Face	6	24
	Gauge	12	0
Number of Large Nozzles			6
Number of Medium Nozzles			0
Number of Small Nozzles			0
Number of Micro Nozzles			0
Number of Ports (Size)			0
Number of Replaceable Ports (Size)			0
Junk Slot Area (sq in)			13.12
Normalized Face Volume			54.64%
API Connection			4-1/2 I.F. BOX
Recommended Make-Up Torque*			25,000 Ft*lbs.
Nominal Dimensions**			
Make-Up Face to Nose			15.28 in - 388 mm
Gauge Length			2 in - 51 mm
Sleeve Length			8 in - 203 mm
Shank Diameter			6.25 in - 159 mm
Break Out Plate (Mat.#/Legacy#)			407013/4411456
Approximate Shipping Weight			400Lbs. - 181Kg.

SPECIAL FEATURES

FullDrift Design, Tapered to 1/16" Under Gage, P100, *** REQUIRES SPECIAL BIT BREAKER



Material #405148

Figure 94, FMF3653Z (405148)

PRODUCT SPECIFICATIONS

Cutter Type	X2 - Tough Drilling
IADC Code	M432
Body Type	MATRIX
Total Cutter Count	46
Cutter Distribution	<u>13mm</u>
	Face 32
	Gauge 14
Number of Large Nozzles	4
Number of Medium Nozzles	0
Number of Small Nozzles	0
Number of Micro Nozzles	0
Number of Ports (Size)	0
Number of Replaceable Ports (Size)	0
Junk Slot Area (sq in)	9.26
Normalized Face Volume	35.06%
API Connection	4-1/2 I.F. BOX
Recommended Make-Up Torque*	25,000 Ft*lbs.
Normal Dimensions**	
Make-Up Face to Nose	13.84 in - 352 mm
Gauge Length	1 in - 25 mm
Sleeve Length	8 in - 203 mm
Shank Diameter	6.25 in - 159 mm
Break Out Plate (Mat.#/Legacy#)	181975/44745
Approximate Shipping Weight	272lbs. - 123Kg.

SPECIAL FEATURES

FullDrift Design, 1/16" Under Gage, P100



Material #475040

Figure 95, FMF3741Z (475040)

a) Field Tendencies

Initial correlations of “DLS achieved vs GP deflection applied” is plotted for each design Figures 96-99. These correlations consider all the behaviors within the Medium ROP range defined in Table 8. The first analysis discloses a cloud of data with positive tendency. However, there are many spread points because of the different behaviors.

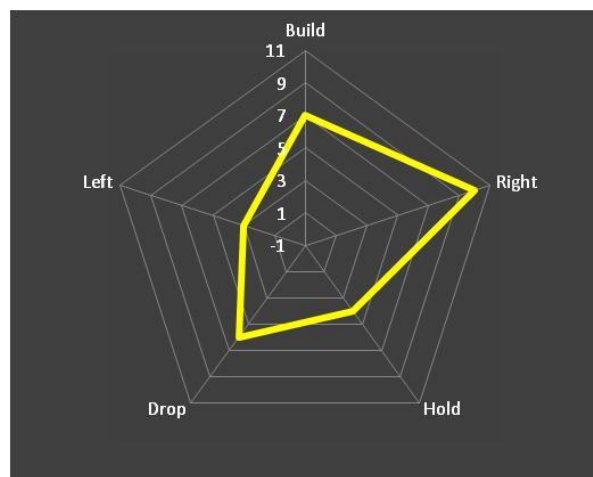
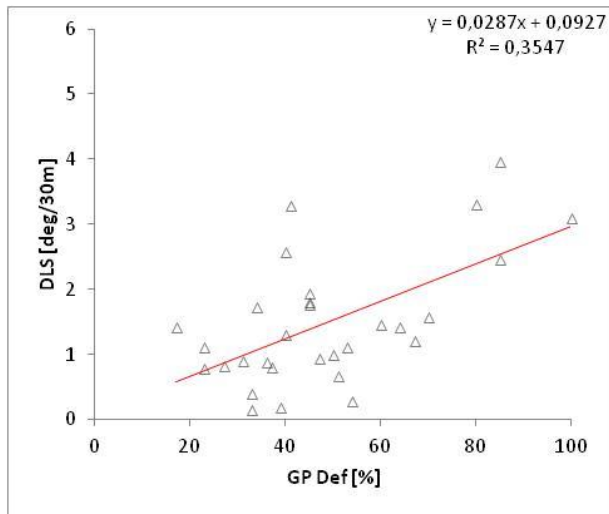


Figure 96 Design (A) steering response all behaviors all behaviors

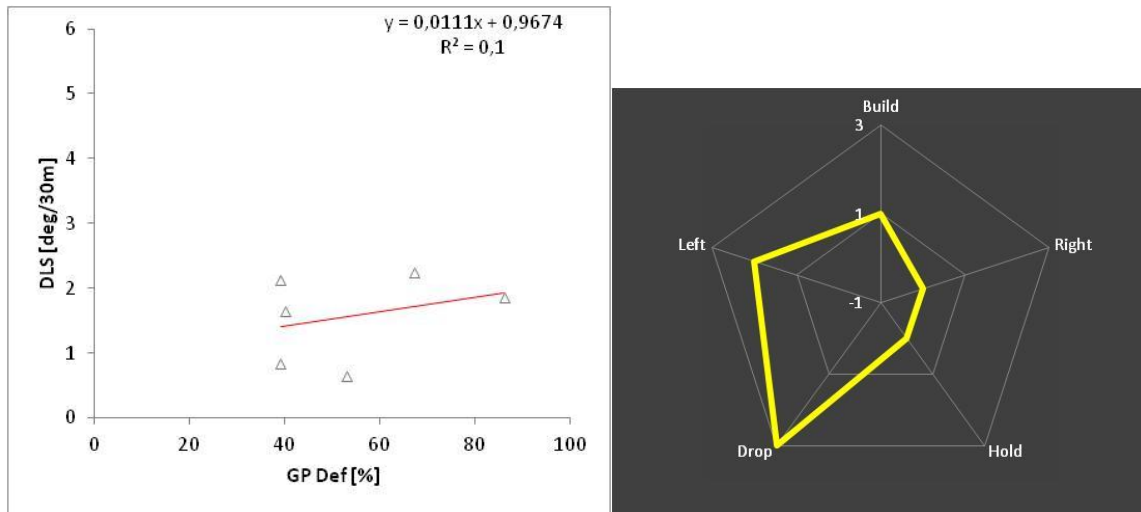


Figure 97 Design (B) steering response all behaviors

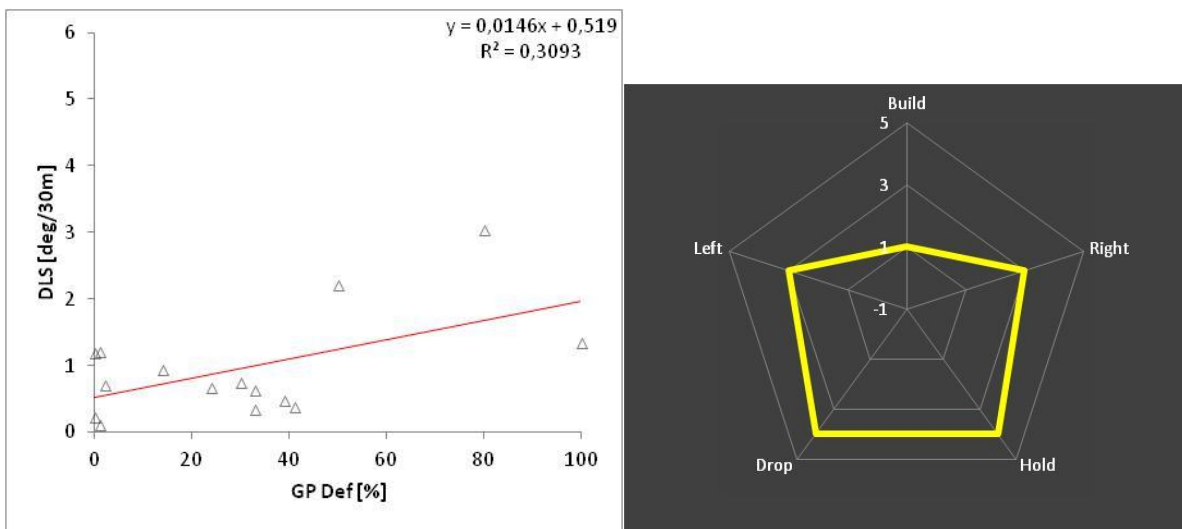


Figure 98 Design (C) steering response all behaviors

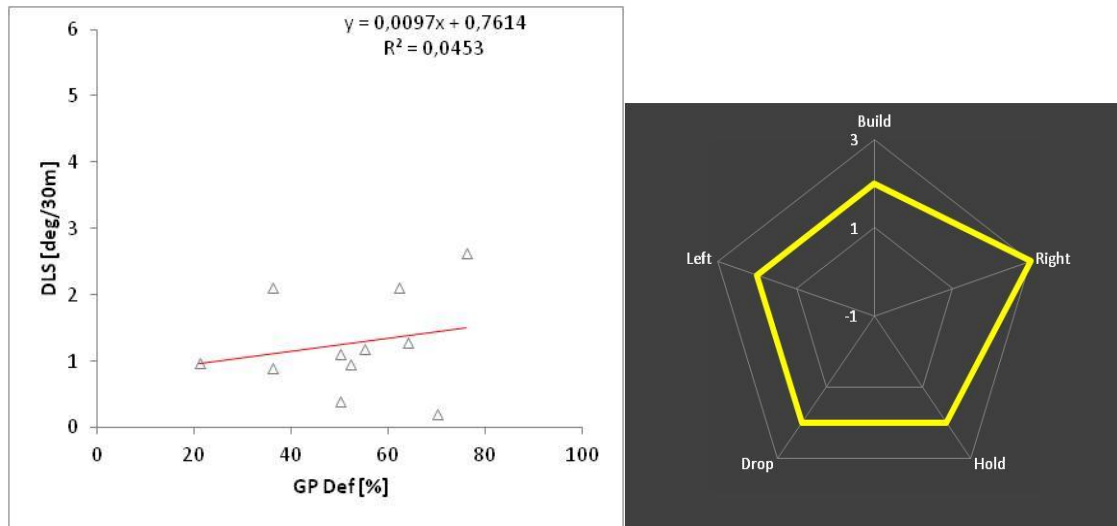


Figure 99 Design (D) steering response all behaviors

As can be seen from the Figures 96-99 it is much more meaningful to make the analysis separately for different behaviors.

Building analysis will be performed with bits (A) and (D), for turning left with bits (A), (B) and (D), and for turning right with bits (C) and (D).

- Building

Figures 100 and 101, display the field tendencies of design (A) and (D) for building at the ranges of ROP and RPM specified at the beginning of the section in Table 8. Now it is possible to compare both designs between each other and also with the results from the simulator.

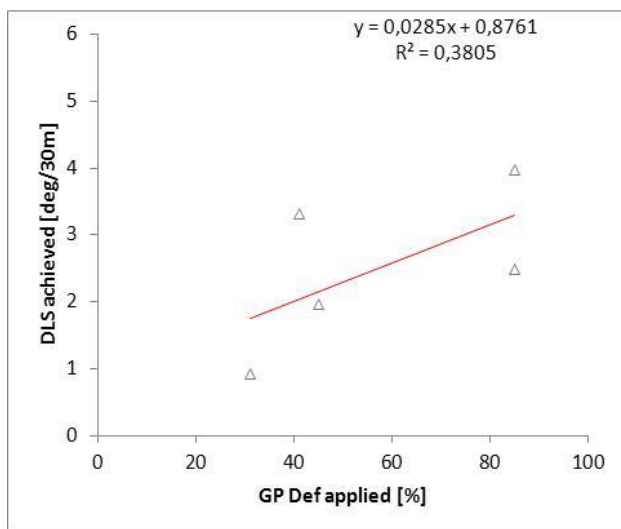


Figure 100, Design (A) building

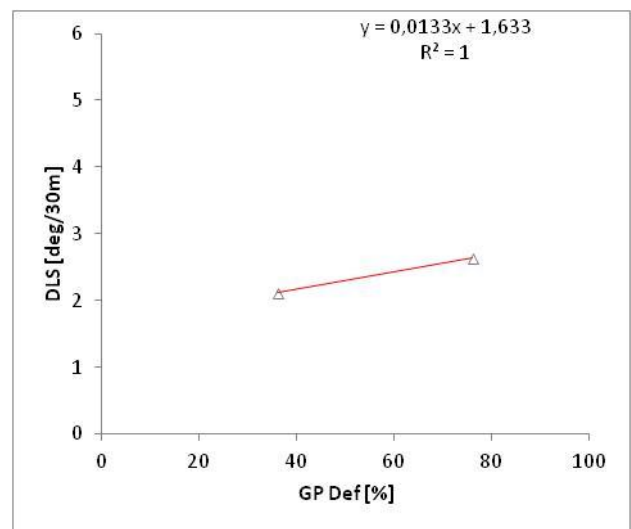


Figure 101, Design (D) building

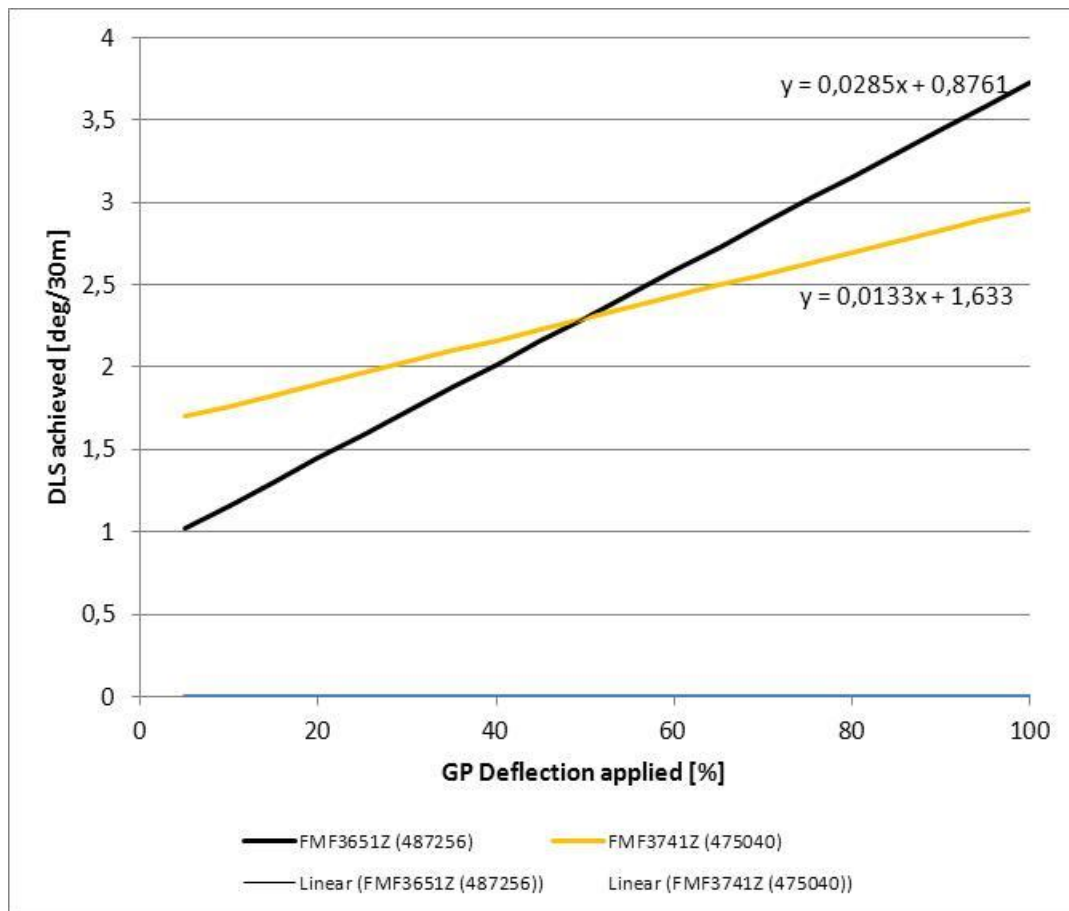


Figure 102, Building field tendencies @ Medium ROP

From Figure 102 it is clear that under similar conditions (operative and steering behavior) design (487256) is more steerable than (475040). Considering only the slope, design (487256) has an improvement of 114% and reach a DLS 28% than design (475040). At maximum deflection design (487256) reaches 3,7 deg/30m and the other design only 2,9 deg/30m.

- Turning left

Figures 103, 104 and 105, display the field tendencies of designs (A), (B) and (D) for turning left at the ranges of ROP and RPM specified at the beginning of the section in Table 8. Now it is possible to compare these designs between each other and also with the results from the simulator.

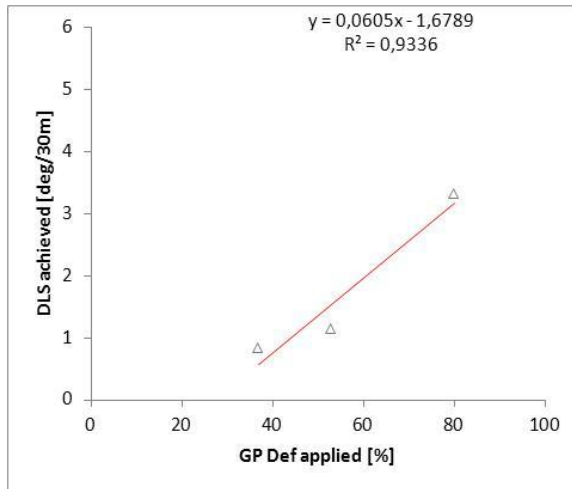


Figure 103 Design (A) turning left

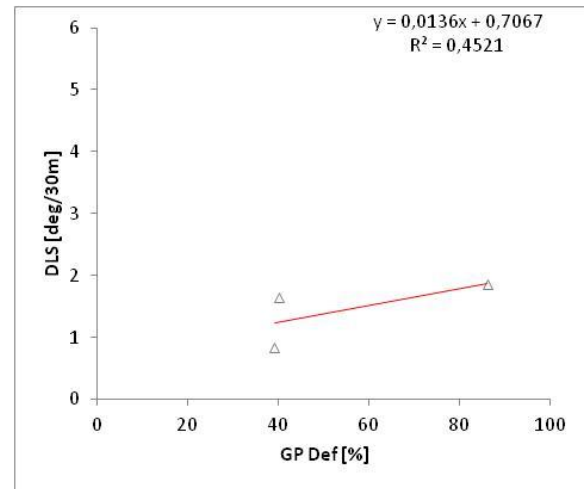


Figure 104 Design (B) turning left

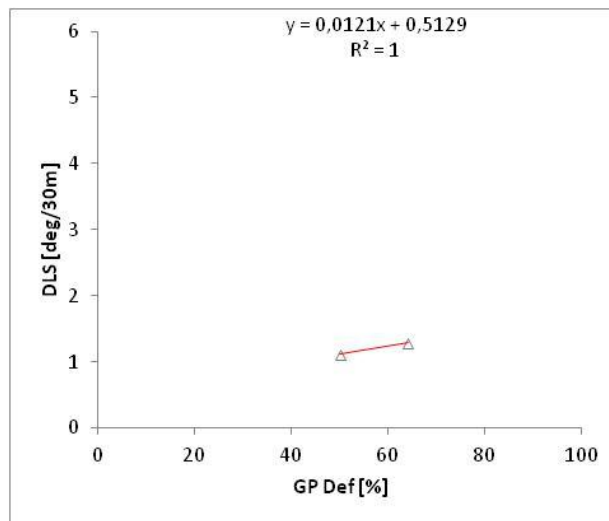


Figure 105 Design (D) turning left

From Figure 107 it is clear that under similar conditions (operative and steering behavior) design (487256) is more steerable than (551396) and (475040). Considering only the slope, design (487256) has an improvement much higher than the other two designs. Regarding the maximum DLS reached, for design (487256) approximate 4,4 deg/30m, design (551396) 2,1 deg/30m and design (475040) 1,2 deg/30m.

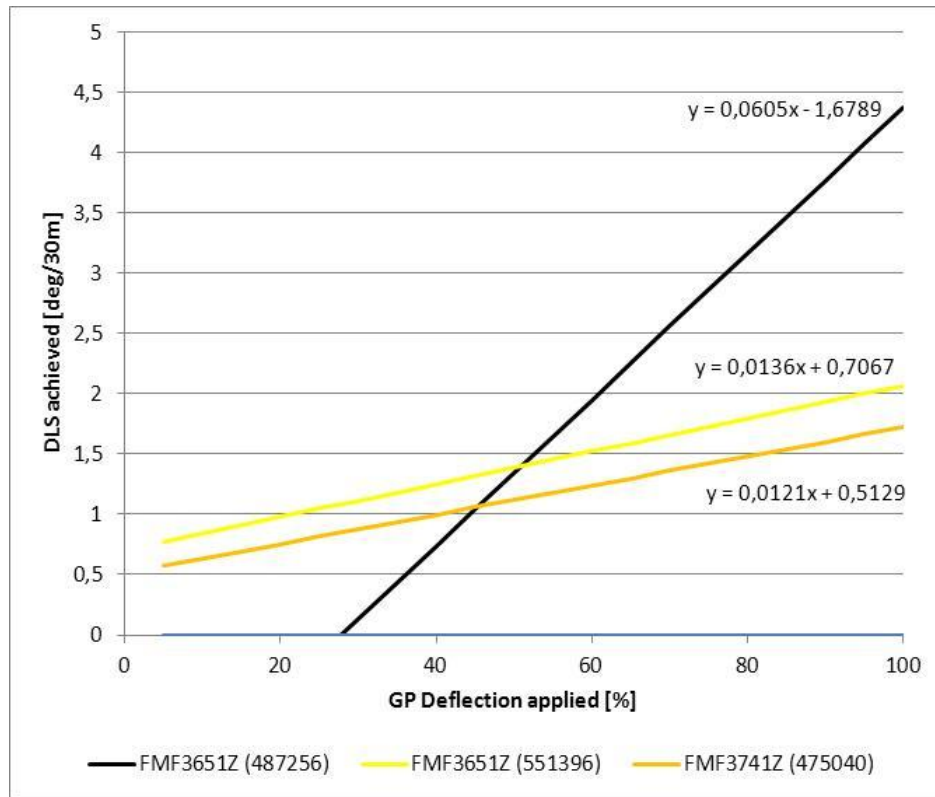


Figure 106, Turning left field tendencies @ Medium ROP

- Turning right

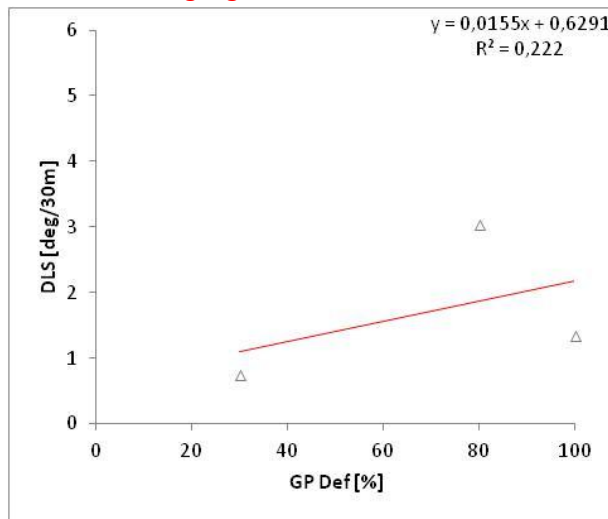


Figure 107 Design (C) turning right

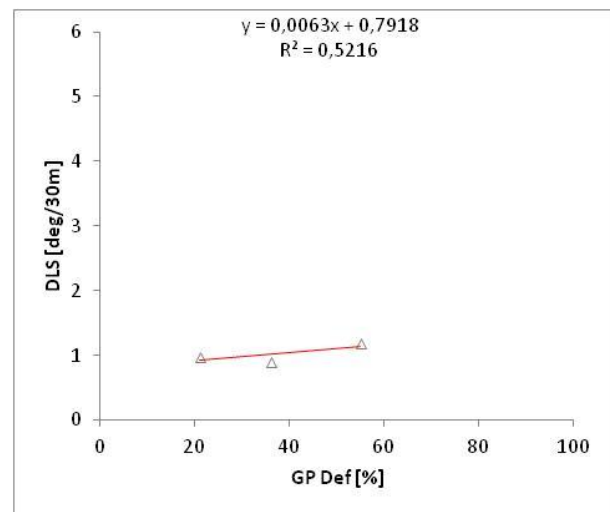


Figure 108 Design (D) turning right

Figures 107 and 108, display the field tendencies of designs (C) and (D) for turning left at the ranges of ROP and RPM specified at the beginning of the section in Table 8. Now it is possible to compare these designs between each other and also with the results from the simulator.

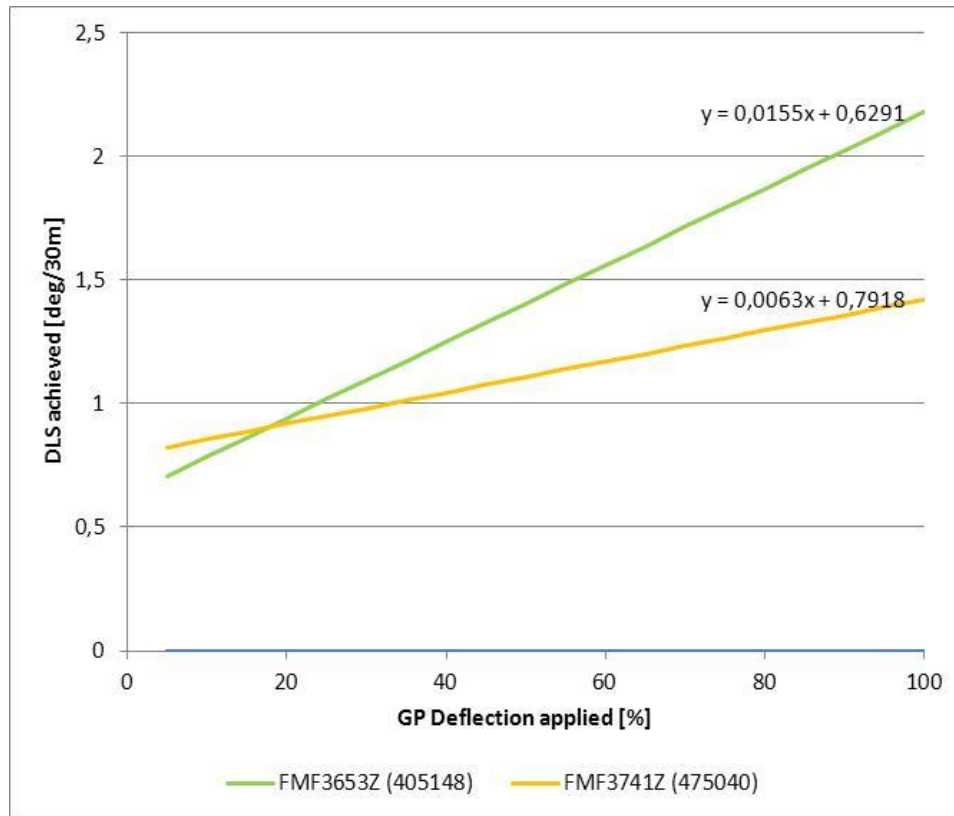


Figure 109, Turning right field tendencies @ Medium ROP

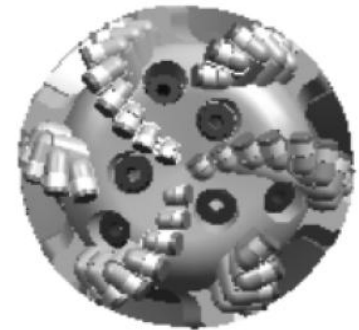
From Figure 109 it is clear that under similar conditions (operative and steering behavior) design (405148) is more steerable than (475040). Considering only the slope, design (405148) has an improvement of 146% over the other design. What's more, at maximum deflection design (405148) reaches 2,2 deg/30m and design (475040) only 1,4 deg/30m.

b) Simulation and Model Tendencies

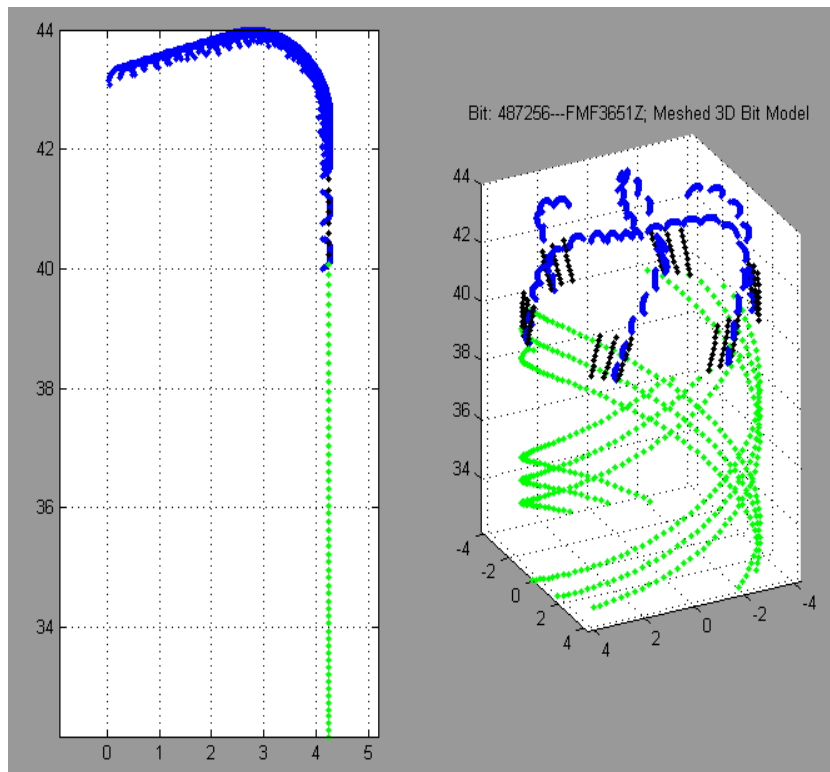
The simulation is performed as described in 3.5. The input parameters used in the simulation are the average of the ranges on Table 8.

Design A-FMF3651Z (487256)

Input Data	
Bit type	487256 - FMF3651Z
Drill mode	Kickoff
BHA type	GP w/o SLH
ROP [ft/hr]	62,5
RPM	155
Tilt Length ["]	13,6479
Hole size ["]	8,5
Rock Strenght [psi]	10000
Dip angle [deg]	0
Gage pad length ["]	1,5
Undergage 1/ ["]	32
Sleeve blades	4
Sleeve blades angle	20
Sleeve gage length ["]	8
Undergage 1/ ["]	16
Tapered angle [deg]	0
Comment	Active Pad gage

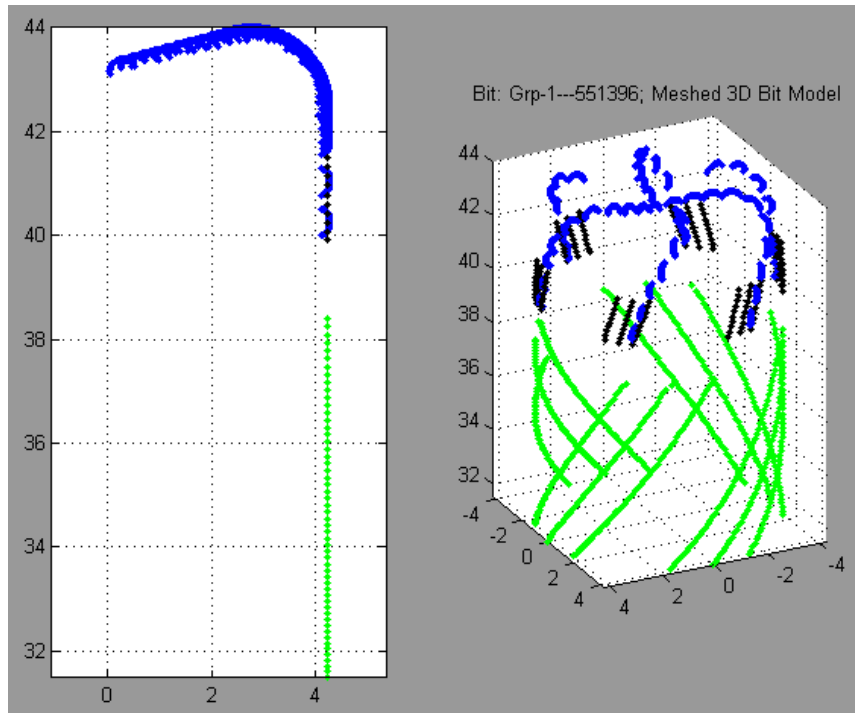
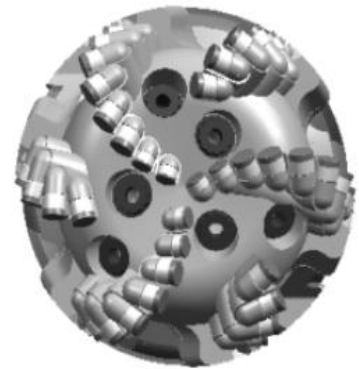


Material #487256



Design B-FMF3653Z(551396)

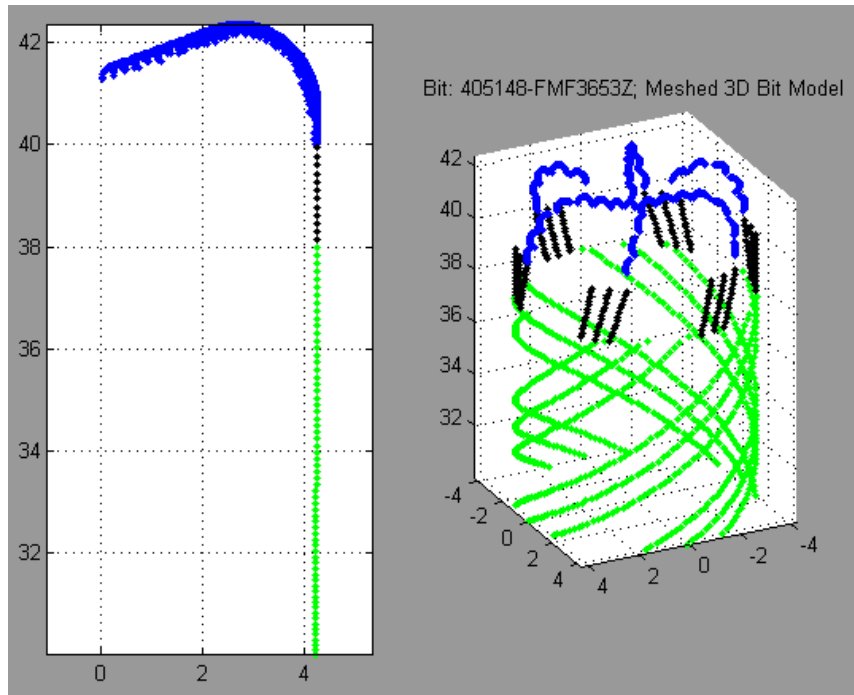
Input Data	
Bit type	551396 - FMF3651Z
Drill mode	Kickoff
BHA type	GP w/o SLH
ROP [ft/hr]	62,5
RPM	155
Tilt Length ["]	14,1479
Hole size ["]	8,5
Rock Strenght [psi]	10000
Dip angle [deg]	0
Gage pad length ["]	1,5
Undergage 1/ ["]	32
Sleeve blades	4
Sleeve blade angle	10
Sleeve gage length ["]	7
Undergage 1/ ["]	16
Tapered angle [deg]	0
Comment	Active gage MEG 1,5"



Material #551396

Design C-FMF3653Z (405148)

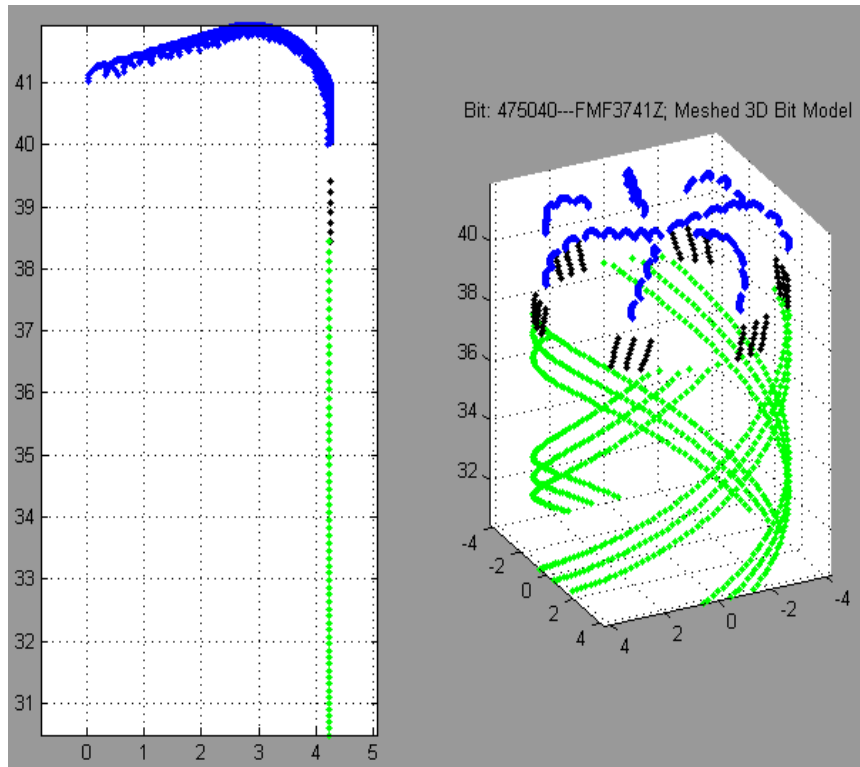
Input Data	
Bit type	405148 - FMF3653Z
Drill mode	Kickoff
BHA type	GP w/o SLH
ROP [ft/hr]	62,5
RPM	155
Tilt Length ["]	12,3348
Hole size ["]	8,5
Rock Strenght [psi]	10000
Dip angle [deg]	0
Gage pad length ["]	2
Undergage 1/ ["]	0
Sleeve blades	4
Sleeve blade angle	20
Sleeve gage length ["]	8
Undergage 1/ ["]	0
Tapered angle [deg]	0,2238
Comment	Passive gage



Material #405148

Design D-FMF3741Z (475040)

Input Data	
Bit type	475040 - FMF3741Z
Drill mode	Kickoff
BHA type	GP w/o SLH
ROP [ft/hr]	62,5
RPM	155
Tilt Length ["]	12,3348
Hole size ["]	8,5
Rock Strenght [psi]	10000
Dip angle [deg]	0
Gage pad length ["]	1
Undergage 1/ ["]	0
Sleeve blades	4
Sleeve blade angle	20
Sleeve gage length ["]	8
Undergage 1/ ["]	16
Tapered angle [deg]	0
Comment	Passive gage



Material #475040

c) Results and comparison

Building analysis

As can be seen from Figure 110, for the building analysis the theoretical results and the field data correlate. From a slope point of view design (487256) performs 114% better than (475040). And regarding the DLS achieved at maximum deflection design (487256) reaches 3,7 deg/30 while design (475040) reaches only 2,9 deg/30m.

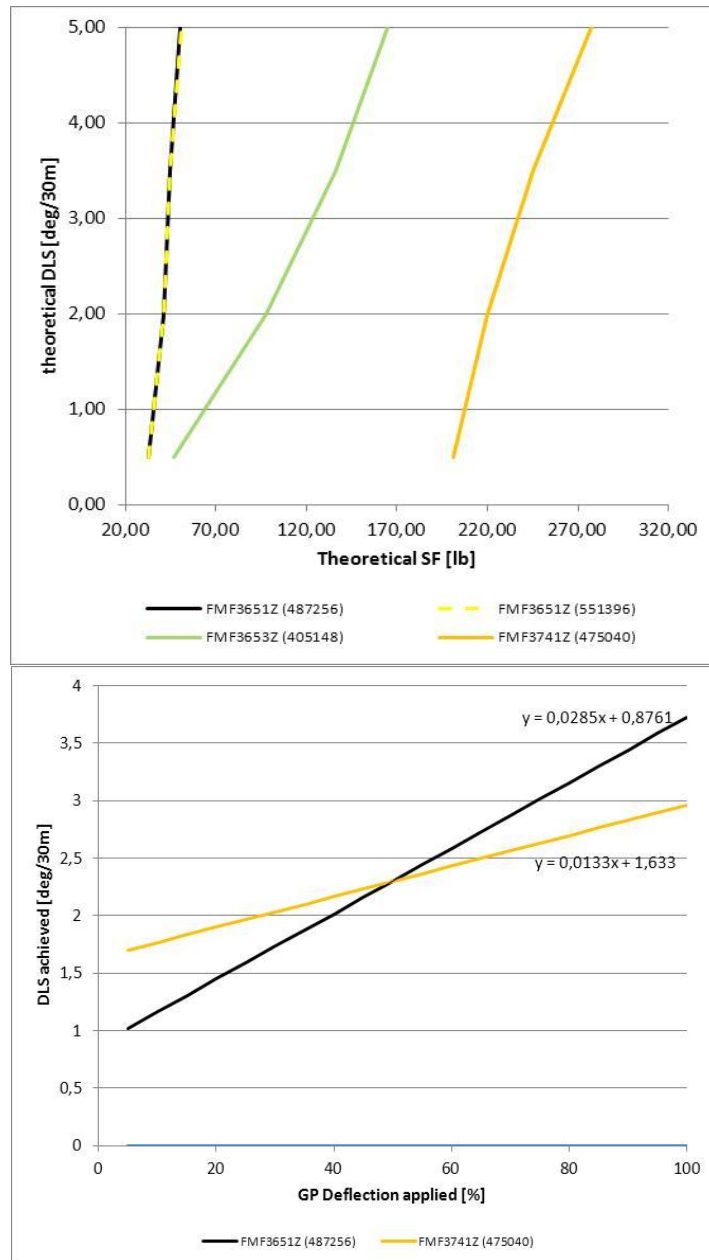


**Figure 110, Building at Medium ROP
Model (top) vs. Field Data (bottom) tendencies**

Turning left analysis

As can be seen from Figure 111, for the turning left analysis the theoretical results and the field data correlate quite well between design (487256) and (475040). From a slope point of view design (487256) performs much better than (475040). And regarding the DLS achieved at maximum deflection design (487256) reaches 4,4 deg/30 while design (475040) reaches only 1,7 deg/30m.

However for design 551396 the model and field data does not correlate.

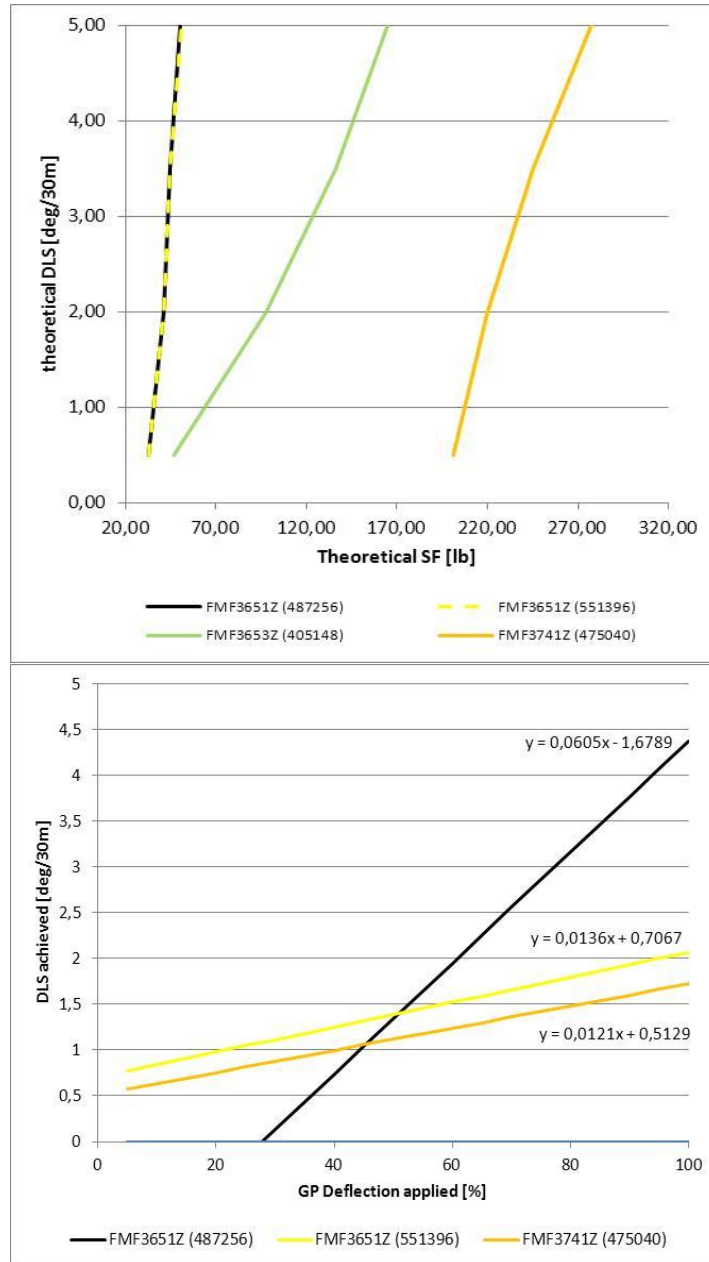


Figure 111, Turning left at Medium ROP Model (top) vs. Field Data (bottom) tendencies

Turning right analysis

As can be seen from Figure 112, for the turning left analysis the theoretical results and the field data correlate. From a slope point of view design (405148) performs 146% better than (475040). And regarding the DLS achieved at maximum deflection design (405148) reached 2,2 deg/30 while design (475040) reached only 1,4 deg/30m.

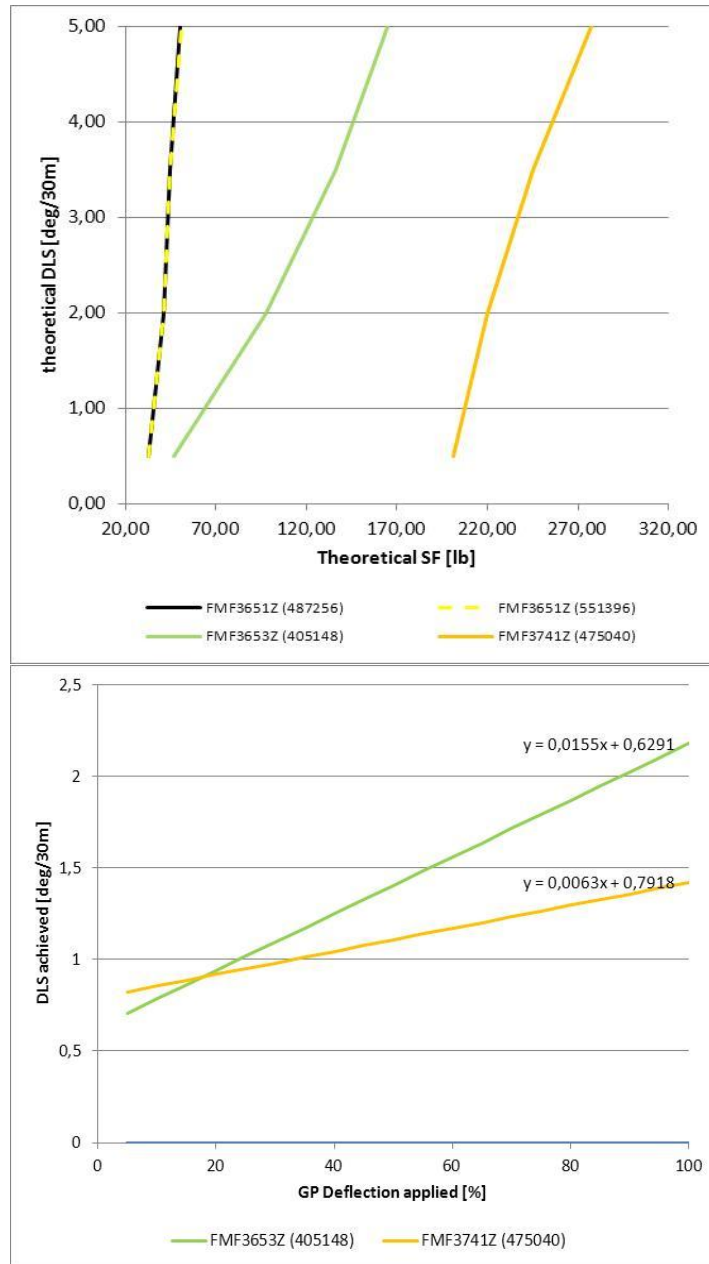


Figure 112, Turning right at Medium ROP Model (top) vs. Field Data (bottom) tendencies

4.3.4 Case D – 8 ½ section, High ROP

All the data considered is taken at the following conditions:

Table 11, Case D, Ranges @ High ROP, 8 ½ section

Case D	Min	Max	Av
ROP	70	85	77,5
RPM	140	170	155

After filtering by these criteria the following designs have enough data points to generate tendencies and elaborate the analysis by building:

Table 12, High ROP, Bit designs for building analysis

Type	Material #	Design
FMF3731C	384968	E
FMF3651Z	562259	F

And for analyzing building behavior:

Table 13, High ROP, bit designs for turning analysis

Type	Material #	Design
FMF3741Z	475040	D
FMF3731C	384968	E
FMF3651Z	562259	F

Initially each design is analyzed independently. General information regarding the drilling parameters and behaviors is summarized. This big picture of the several designs helps identify the most representative steering behavior and generate the field tendencies straight forward. However, the whole analysis behavior by behavior can be found in the appendix section.

Then, the simulations are performed with the averages of the ranges selected. Finally a comparison between field and simulation is performed and explained.

Design (A), and (D) are already presented in Figures 85 and 95. Design (E) and (F) are described in Figures 113 and 114.

PRODUCT SPECIFICATIONS

Cutter Type	X1 - Conventional Drilling		
IADC Code	M442		
Body Type	MATRIX		
Total Cutter Count	50		
Cutter Distribution	<u>10mm</u>	<u>13mm</u>	
Face	23	19	
Gauge	0	8	
Number of Large Nozzles	3		
Number of Medium Nozzles	0		
Number of Small Nozzles	0		
Number of Micro Nozzles	0		
Number of Ports (Size)	0		
Number of Replaceable Ports (Size)	0		
Junk Slot Area (sq in)	9.24		
Normalized Face Volume	38.06%		
API Connection	4-1/2 I.F. BOX		
Recommended Make-Up Torque*	25,000 Ft*lbs.		
Nominal Dimensions**			
Make-Up Face to Nose	14.97 in - 380 mm		
Gauge Length	2 in - 51 mm		
Sleeve Length	8 in - 203 mm		
Shank Diameter	6.25 in - 159 mm		
Break Out Plate (Mat.#/Legacy#)	407013/4411456		
Approximate Shipping Weight	400Lbs. - 181Kg.		

SPECIAL FEATURES

FullDrift Design, Tapered to 1/16" Under Gage, P100, Pocket Erosion Resistance, ***
REQUIRES SPECIAL BIT BREAKER ***



Material #384968

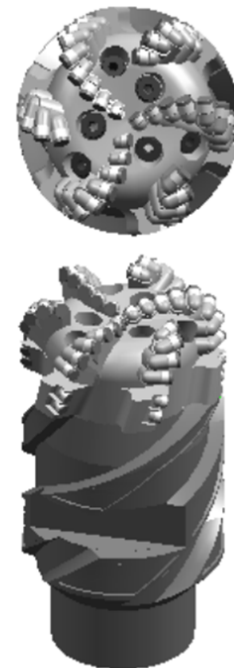
Figure 113, FMF3731 (384968)

PRODUCT SPECIFICATIONS

Cutter Type	Unavailable		
IADC Code	M422		
Body Type	MATRIX		
Total Cutter Count	48		
Cutter Distribution	<u>13mm</u>	<u>16mm</u>	
Face	6	24	
Gauge	18	0	
Number of Large Nozzles	6		
Number of Medium Nozzles	0		
Number of Small Nozzles	0		
Number of Micro Nozzles	0		
Number of Ports (Size)	0		
Number of Replaceable Ports (Size)	0		
Junk Slot Area (sq in)	13.76		
Normalized Face Volume	40.2%		
API Connection	4-1/2 I.F. BOX		
Recommended Make-Up Torque*	25,000 Ft*lbs.		
Nominal Dimensions**			
Make-Up Face to Nose	14.86 in - 377 mm		
Gauge Length	1.5 in - 38 mm		
Sleeve Length	8 in - 203 mm		
Shank Diameter	6.25 in - 159 mm		
Break Out Plate (Mat.#/Legacy#)	181975/44745		
Approximate Shipping Weight	256Lbs. - 116Kg.		

SPECIAL FEATURES

Active Gage, 1/32" Relieved Gage, 1/16" Undergauge Sleeve



Material #562259

Figure 114, FMF3651Z (562259)

a) Field Tendencies

Initial correlations of “DLS achieved vs GP deflection applied” is plotted for each design Figures 115-118. These correlations consider all the behaviors within the Medium ROP range defined in Table 8. The first analysis discloses a cloud of data with positive tendency. However, there are many spread points because of the different behaviors.

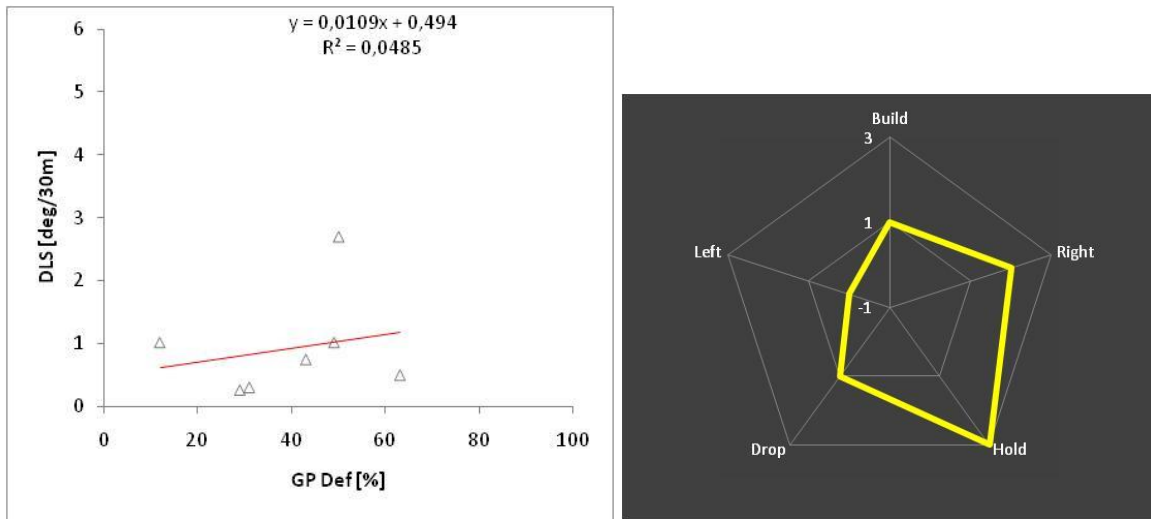


Figure 115 Design (A) steering response all behaviors all behaviors

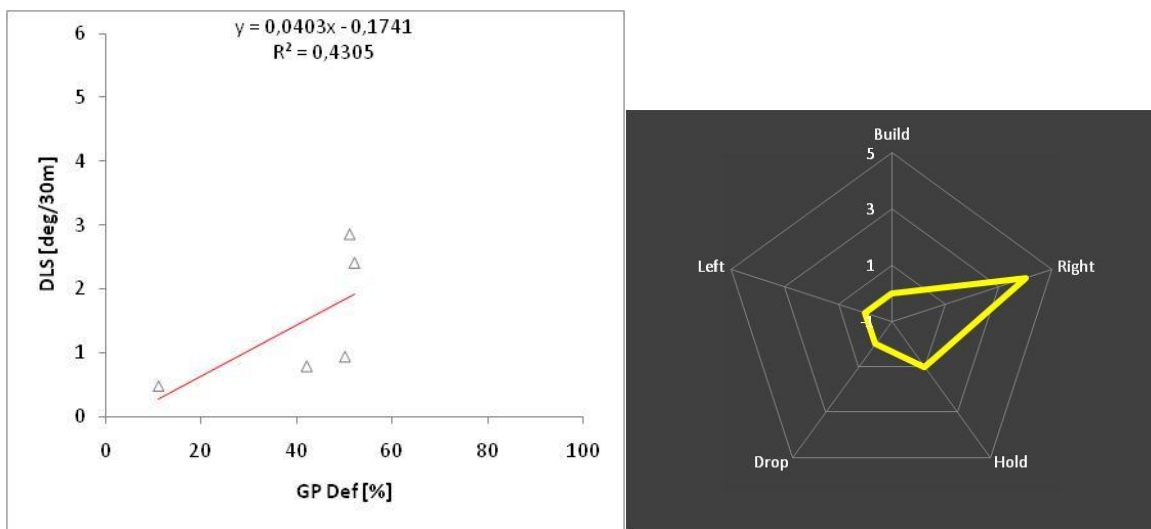


Figure 116 Design (D) steering response all behaviors

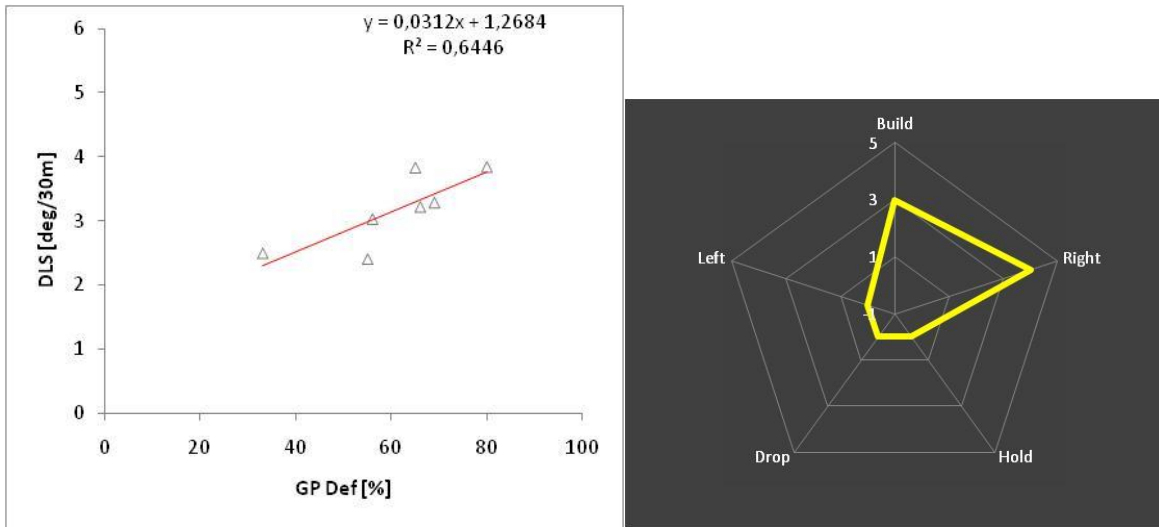


Figure 117 Design (E) steering response all behaviors

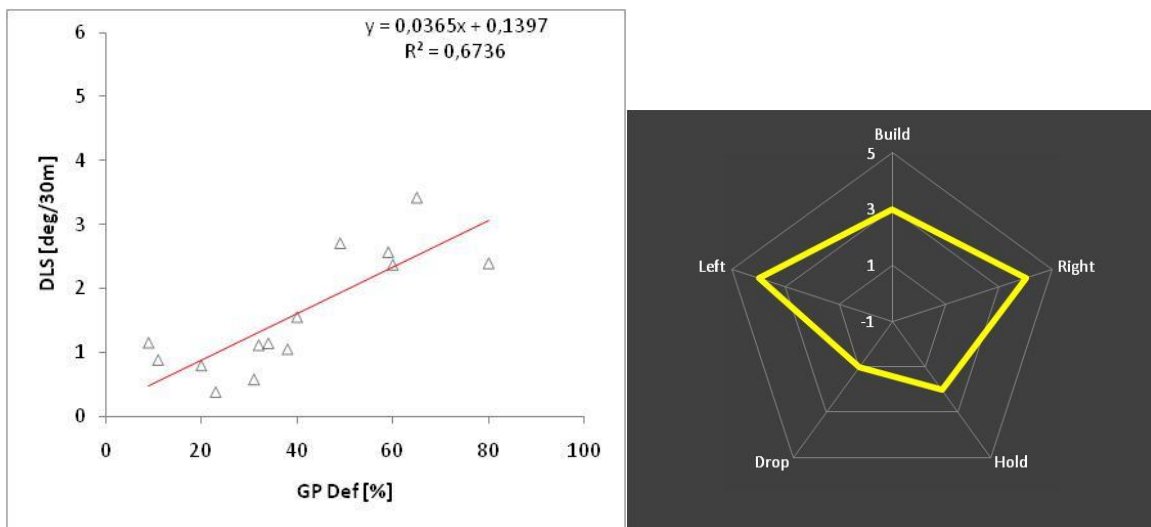


Figure 118 Design (F) steering response all behaviors

As can be seen from the Figures 115-118 it is much more meaningful to make the analysis separately for different behaviors.

Building analysis will be performed with bits (E) and (F) and turning right with bits (A), (D), (E) and (F).

- *Building*

Figures 119 and 120, display the field tendencies of design (E) and (F) for building at the ranges of ROP and RPM specified at the beginning of the section in Table 11. Now it is possible to compare both designs between each other and also with the results from the simulator.

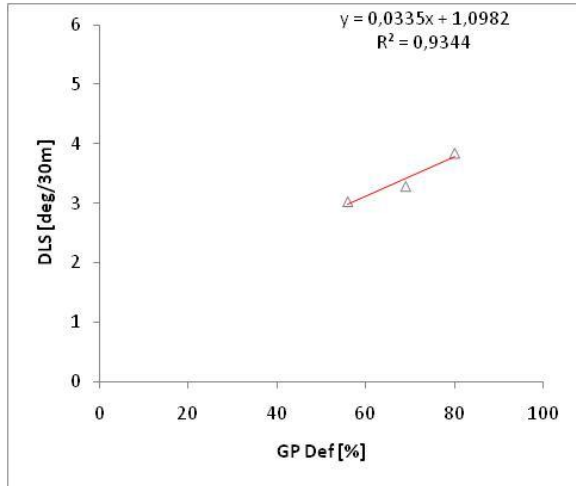


Figure 119, Design (E) building

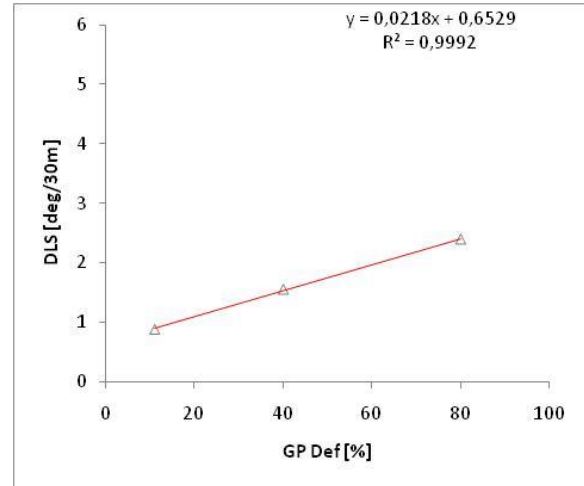


Figure 120, Design (F) building

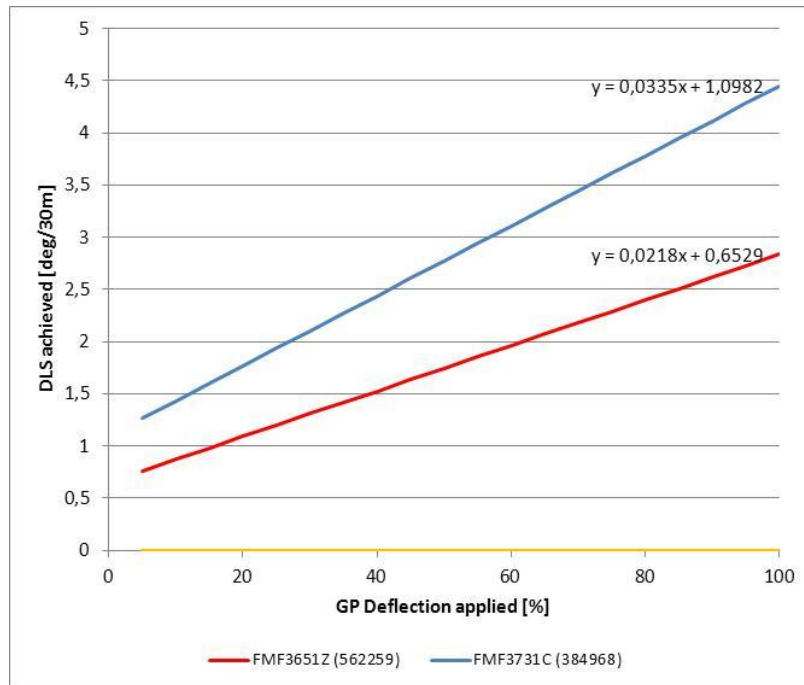


Figure 121, Building field tendencies @ High ROP

From Figure 121 it is clear that under similar conditions (operative and steering behavior) design (384968) is more steerable than (562259). Considering only the slope, design (384968) has an improvement of 154%. In addition, at maximum deflection design (384968) reaches a DLS of 4,4 deg/30m and the other design only 2,8 deg/30m.

- *Turning right*

Figures 122, 123 and 124, display the field tendencies of designs (D), (E) and (F) for turning right at the ranges of ROP and RPM specified at the beginning of the section in Table 11. Now it is possible to compare these designs between each other and also with the results from the simulator.

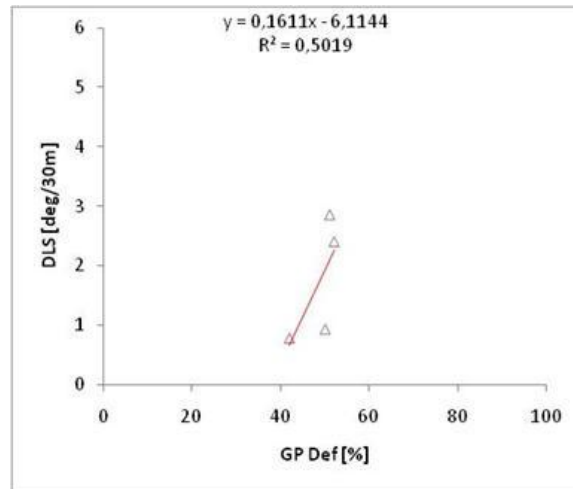


Figure 122 Design (D) turning right

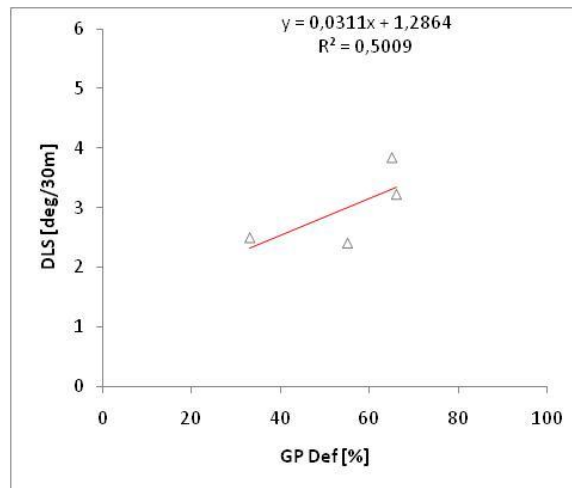


Figure 123 Design (E) turning right

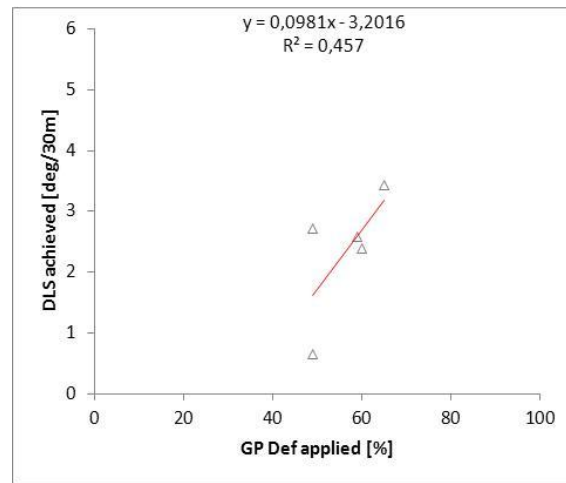


Figure 124 Design (F) turning right

From Figure 125 it is clear that under similar conditions (operative and steering behavior) design (475040) is more steerable than (562259) and (384968). Considering only the slope, design (475040) performed much better than the other two designs. Regarding the maximum DLS, design (475040) can achieve almost 10 deg/30m, design (562259) 6,6 deg/30m and design (475040) 4,4 deg/30m.

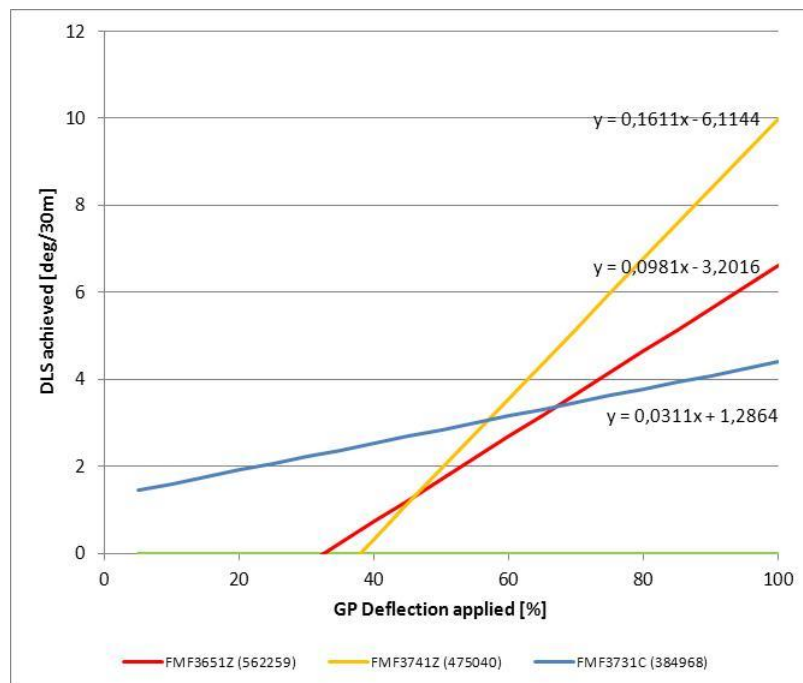


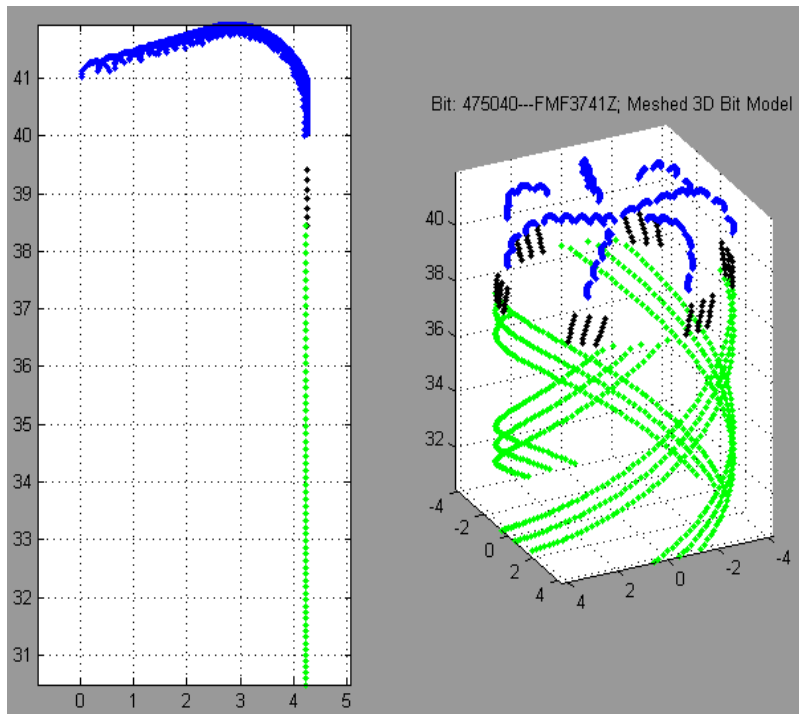
Figure 125, Turning right field tendencies @ High ROP

b) Simulation and Model Tendencies

The simulation is performed as described in 3.5. The input parameters used in the simulation are the average of the ranges on Table 11.

Design D-FMF3741Z (475040)

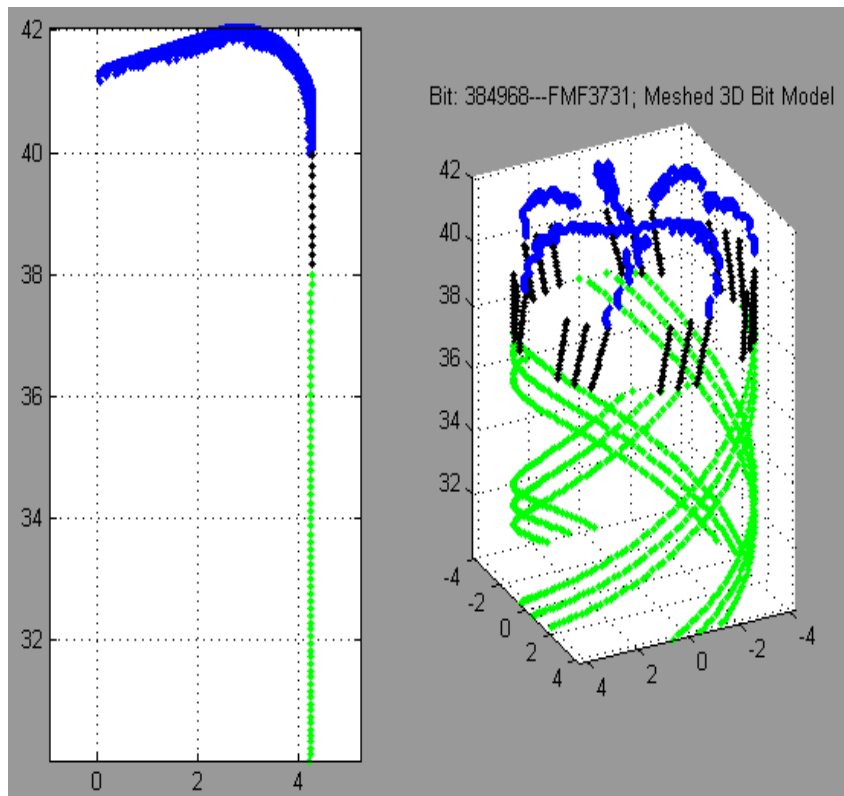
Input Data	
Bit type	475040 - FMF3741Z
Drill mode	Kickoff
BHA type	GP w/o SLH
ROP [ft/hr]	77,5
RPM	155
Tilt Length ["]	12,3348
Hole size ["]	8,5
Rock Strenght [psi]	10000
Dip angle [deg]	0
Gage pad length ["]	1
Undergage 1/ ["]	0
Sleeve blades	4
Sleeve blade angle	20
Sleeve gage length ["]	8
Undergage 1/ ["]	16
Tapered angle [deg]	0
Comment	Passive gage



Material #475040

Design E-FMF3731Z (384968)

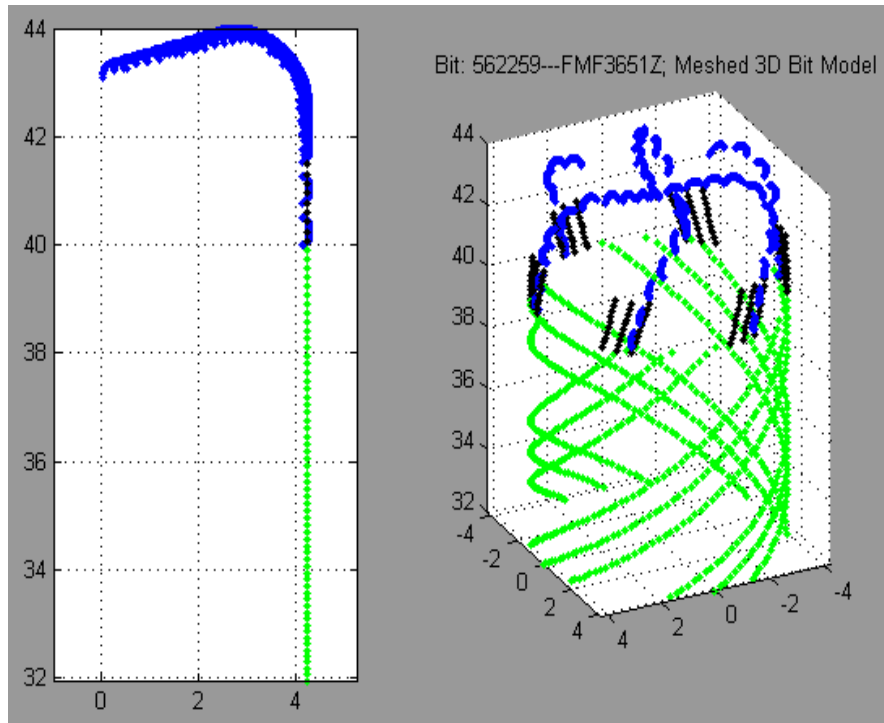
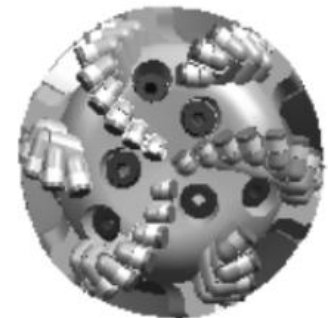
Input Data	
Bit type	384968 - FMF3731Z
Drill mode	Kickoff
BHA type	GP w/o SLH
ROP [ft/hr]	77,5
RPM	155
Tilt Length ["]	12,0103
Hole size ["]	8,5
Rock Strenght [psi]	10000
Dip angle [deg]	0
Gage pad length ["]	2
Undergage 1/ ["]	0
Sleeve blades	4
Sleeve blade angle	20
Sleeve gage length ["]	8
Undergage 1/ ["]	0
Tapered angle [deg]	0,2238
Comment	Passive gage Tapered to 1/16



Material #384968

Design F-FMF3651Z (562259)

Input Data	
Bit type	562259 - FMF3731Z
Drill mode	Kickoff
BHA type	GP w/o SLH
ROP [ft/hr]	77,5
RPM	155
Tilt Length ["]	13,6479
Hole size ["]	8,5
Rock Strenght [psi]	10000
Dip angle [deg]	0
Gage pad length ["]	2
Undergage 1/ ["]	32
Sleeve blades	4
Sleeve blade angle	20
Sleeve gage length ["]	8
Undergage 1/ ["]	16
Tapered angle [deg]	0
Comment	Active pad gage



Material #562259

c) Results and comparison

Building analysis

As can be seen from Figure 126, for the building analysis the theoretical results and the field data do not correlate. From a slope point of view design (384968) performs 54% better than (562259) from field data, however, from simulation this is the opposite. Regarding the DLS achieved at maximum deflection design (384968) reaches 4,4 deg/30 while design (562259) reaches only 2,8 deg/30m.

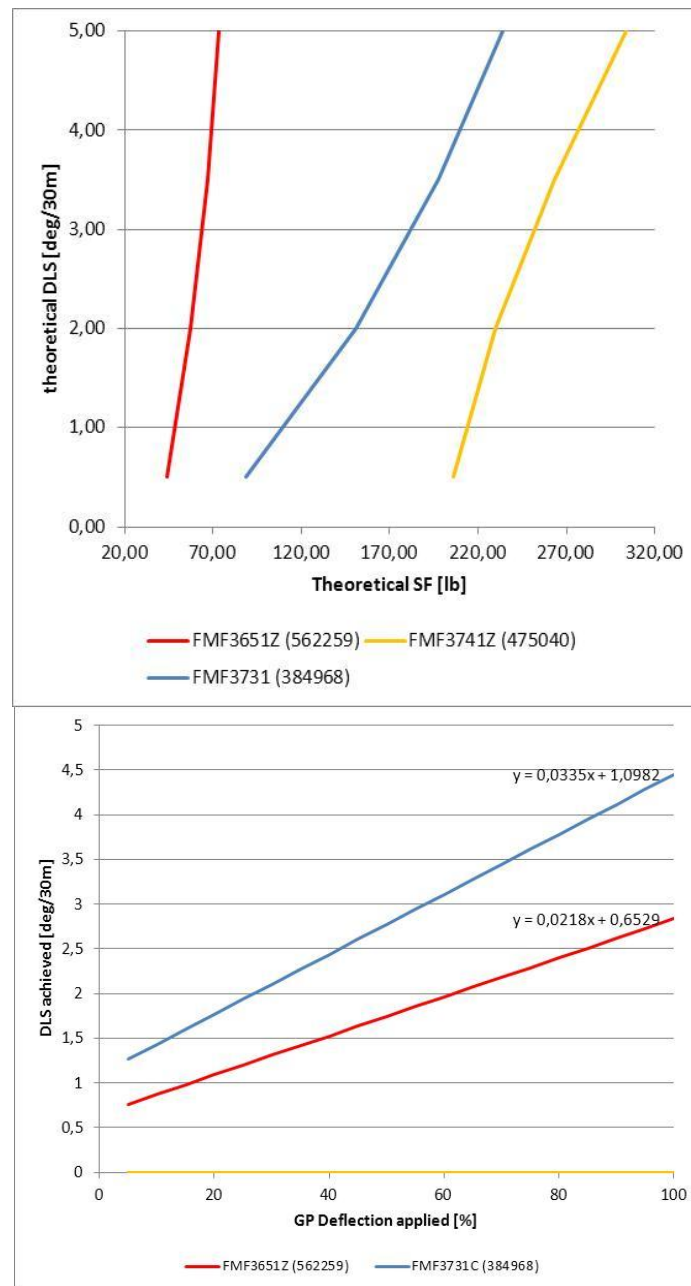


**Figure 126, Building at high ROP
Model (top) vs Field data (bottom) tendencies**

Turning right analysis

As can be seen from Figure 127, for the turning right analysis the theoretical results and the field data correlate when comparing designs (562259) and (384968). From a slope point of view design (562259) performs 215% better than (384968). Regarding the DLS achieved at maximum deflection design (562259) reaches approx. 6,8 deg/30 while design (384968) reaches only 4,5 deg/30m. However, design 475040 does follow the simulated behavior.

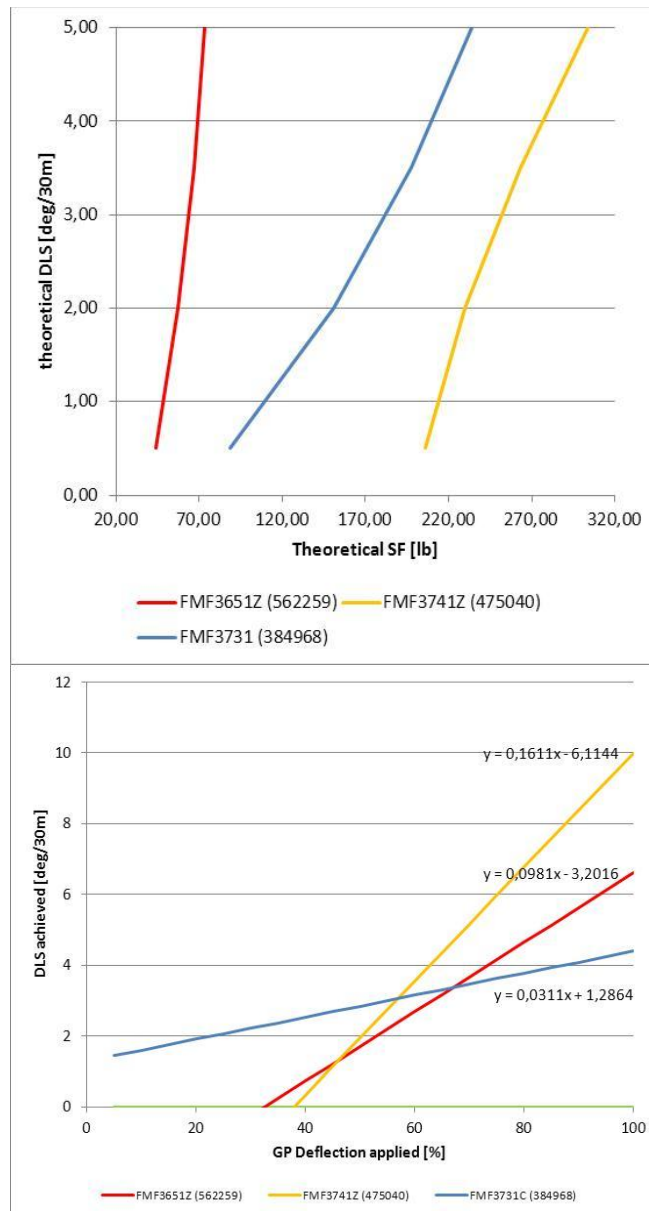


Figure 127, Turning right at High ROP Model (top) vs. Field Data (bottom) tendencies

4.3.5 Case E - 12 ¼" section

For this case, 3 bit designs bits were available. In order to support the decision of considering the building behavior, an initial correlation of "DLS achieved vs GP deflection applied" is plotted for each design Figures 128 - 130. These correlations consider all the behaviors and all ROPs and RPMs.

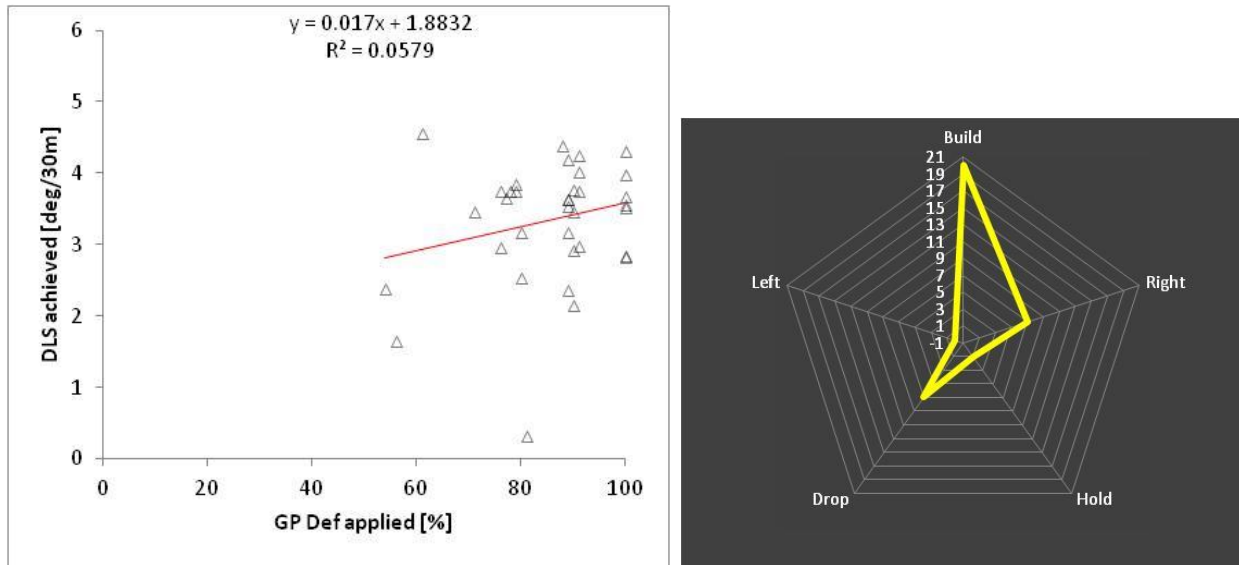


Figure 128, Design (375525) steering response all behaviors

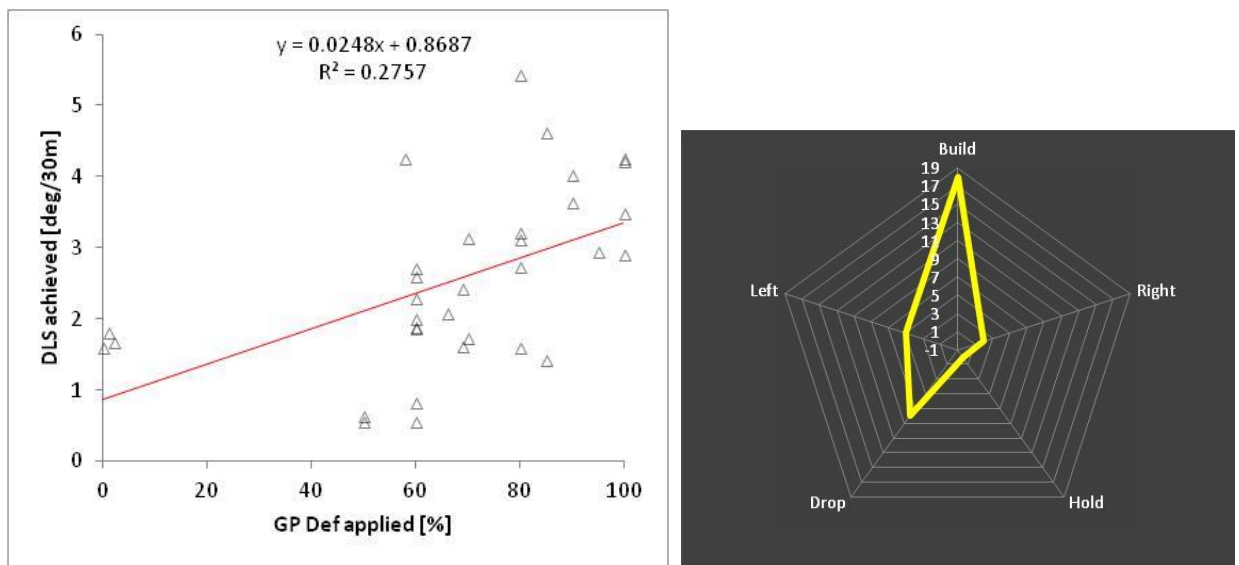


Figure 129, Design 411639 steering response all behaviors

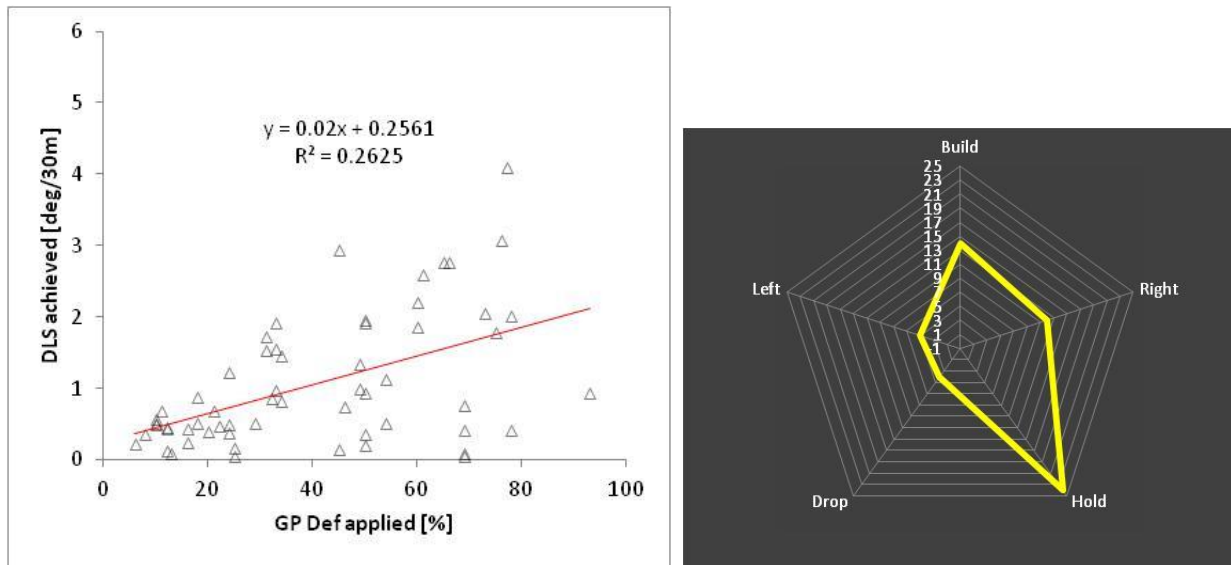


Figure 130, Design 438320 steering response all behaviors

As can be seen from the Figures 128 – 130 (behaviors), the main behavior displayed is building. Then, the analysis will be performed for building.

Table 14 summarizes the data of the three designs. The ROP is very spread from 7 to 232 ft/hr and RPM is between 121 and 167. Once the behavior is selected, as described in the methodology, a statistical analysis will be performed to select the ranges that have the most populated common regions with data.

Table 14, Case E - 12 ¼ section

FMF3643CS (375525)

	Av	Min	Max
ROP	62,32	6,9317	231,93
RPM	161,15	139,43	167,73
Count	35		

FMF3643ZS (411639)

	Av	Min	Max
ROP	68,49	31,435	134,57
RPM	156,94	119,33	165,94
Count	33		

FMF3643ZS (438320)

	Av	Min	Max
ROP	54,03	18,815	102,12
RPM	143,51	121,21	160,32
Count	59		

More details about these three designs can be found in Figures 131 - 133. The specification sheets show the cutting structure materials, gage design, sleeve design and special features of the bits.

PRODUCT SPECIFICATIONS

Cutter Type	X1 - Conventional Drilling
IADC Code	M133
Body Type	MATRIX
Total Cutter Count	68
Cutter Distribution	<u>13mm</u>
	Face 50
	Gauge 18
Number of Large Nozzles	6
Number of Medium Nozzles	0
Number of Small Nozzles	0
Number of Micro Nozzles	0
Number of Ports	0
Junk Slot Area (sq in)	35.1
Normalized Face Volume	46.5%
API Connection	6-5/8 REG. BOX
Recommended Make-Up Torque*	58,885 Ft*lbs.
Nominal Dimensions**	
Make-Up Face to Nose	24.37 in - 619 mm
Gauge Length	3 in - 76 mm
Sleeve Length	15 in - 381 mm
Shank Diameter	8.75 in - 222 mm
Break Out Plate (Mat.#/Legacy#)	181978/44757
Approximate Shipping Weight	1100Lbs. - 499Kg.

SPECIAL FEATURES

P100, 1/16" Under Gage Sleeve, Scribes in Center



Material #375525

Figure 131, Design 375525

PRODUCT SPECIFICATIONS

Cutter Type	X2 - Tough Drilling
IADC Code	M133
Body Type	MATRIX
Total Cutter Count	68
Cutter Distribution	<u>13mm</u>
	Face 50
	Gauge 18
Number of Large Nozzles	6
Number of Medium Nozzles	0
Number of Small Nozzles	0
Number of Micro Nozzles	0
Number of Ports	0
Junk Slot Area (sq in)	35.1
Normalized Face Volume	46.5%
API Connection	6-5/8 REG. BOX
Recommended Make-Up Torque*	58,885 Ft*lbs.
Nominal Dimensions**	
Make-Up Face to Nose	24.37 in - 619 mm
Gauge Length	3 in - 76 mm
Sleeve Length	15 in - 381 mm
Shank Diameter	8.75 in - 222 mm
Break Out Plate (Mat.#/Legacy#)	181978/44757
Approximate Shipping Weight	688Lbs. - 312Kg.

SPECIAL FEATURES

P100, 1/16" Under Gage Sleeve, Scribes in Center



Material #411639

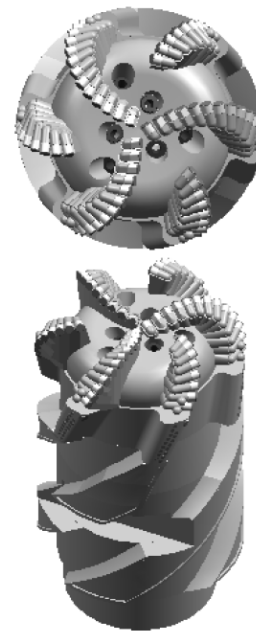
Figure 132, Design 411639

PRODUCT SPECIFICATIONS

Cutter Type	X2 - Tough Drilling
IADC Code	M133
Body Type	MATRIX
Total Cutter Count	68
Cutter Distribution	<u>13mm</u>
	Face 50
	Gauge 18
Number of Large Nozzles	6
Number of Medium Nozzles	0
Number of Small Nozzles	0
Number of Micro Nozzles	0
Number of Ports	0
Junk Slot Area (sq in)	35.1
Normalized Face Volume	46.5%
API Connection	6-5/8 REG. BOX
Recommended Make-Up Torque*	58,885 Ft*lbs.
Nominal Dimensions**	
Make-Up Face to Nose	21.37 in - 543 mm
Gauge Length	3 in - 76 mm
Sleeve Length	12 in - 305 mm
Shank Diameter	8.75 in - 222 mm
Break Out Plate (Mat.#/Legacy#)	181978/44757
Approximate Shipping Weight	688Lbs. - 312Kg.

SPECIAL FEATURES

FullDrift Design, 1/16" Under Gage Sleeve, 4 Bladed Sleeve, Scribes in Center, P-100



Material #438320

Figure 133, Design 438320

In this case there were three wells that provided the data. And the main formations drilled in terms of CCR (Confined Compressive Strength) were:

- Shetland : around 10 kpsi CCS (shale) with few stringers of limestone of 20-25 kpsi
- Viking : between 10 kpsi and 15 kpsi (sand)
- Brent/Tabert : 5 – 10 kpsi (sand)

a) Statistical Analysis

Once selected building as the behavior that will be analyzed, all the data-points in the main matrix were plotted in distributions for ROP and RPM. Figures 134 – 136 show the results.

As seen in the same Figures 134 – 136, there is one range identified for ROP and one for RPM. Those ranges define data considered for this case study.

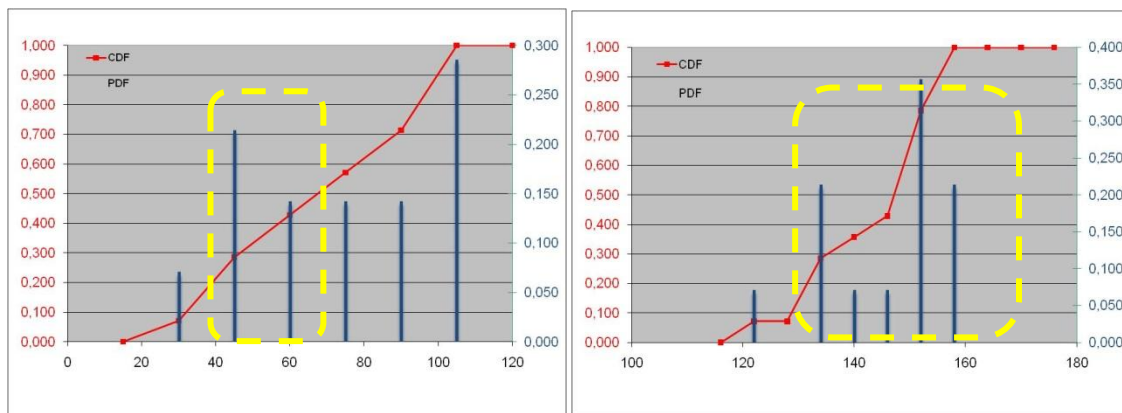


Figure 134, 438320 Building ROP (left) and RPM (right) stats

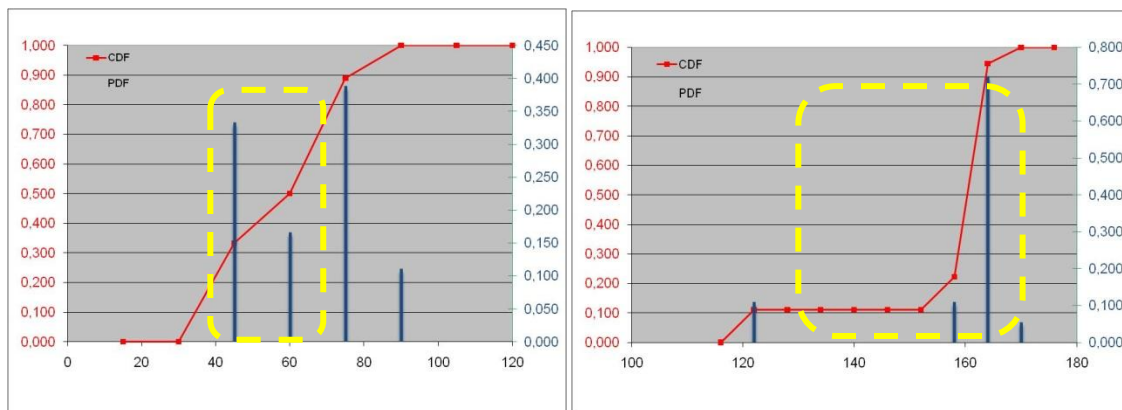


Figure 135, 411639 Building stats ROP (left) and RPM (right) stats

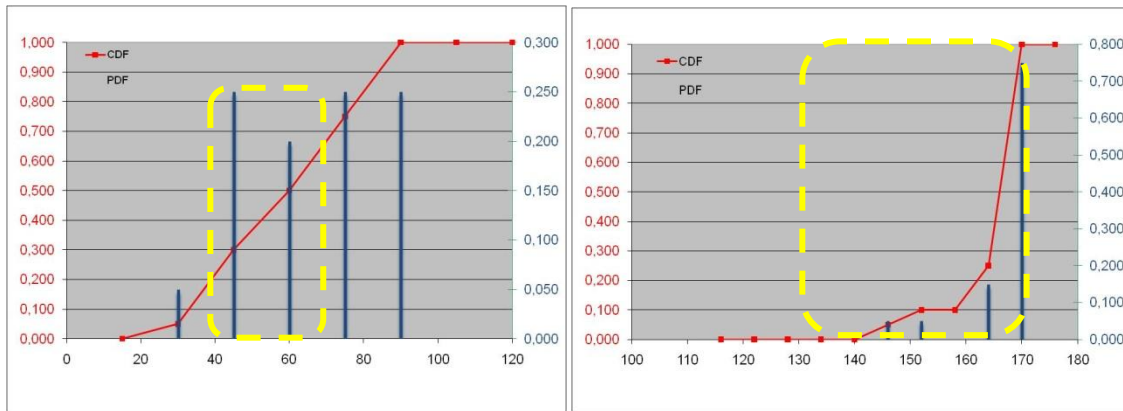


Figure 136, 375525 Building stats ROP (left) and RPM (right) stats

From that analysis, the following ROP and RPM ranges are selected to compare the building behavior for the three designs. Table 15 displays the ranges that contain more data-points regarding the building behavior.

Table 15, Case E, Ranges

Case E	Min	Max	Av
ROP	40	70	55
RPM	130	170	150

b) Field tendencies

As 12 ¼ section is mainly a building section, that behavior is analyzed. Figures 137 – 139, display the correlations observed for the three designs.

It is interesting to point out that building was responsive for deflections higher than 50 %. As discussed in the first cases studies and the appendixes, Low deflections usually represent only holding, that is the most likely interpretation for this case as well.

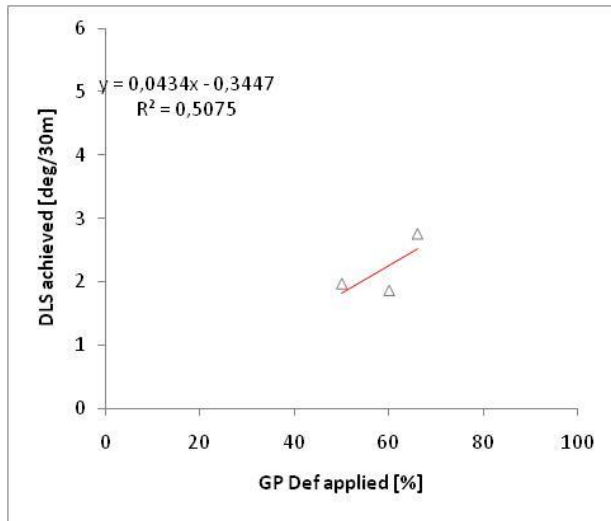


Figure 137, Design (438320) @ Range E

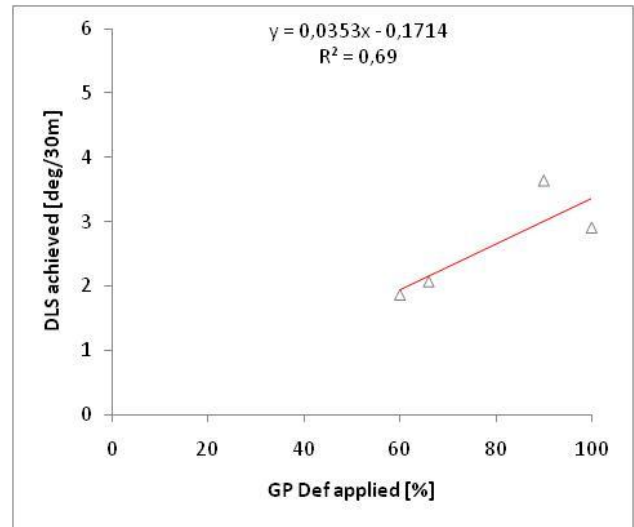


Figure 138, Design (411639) @ Range E

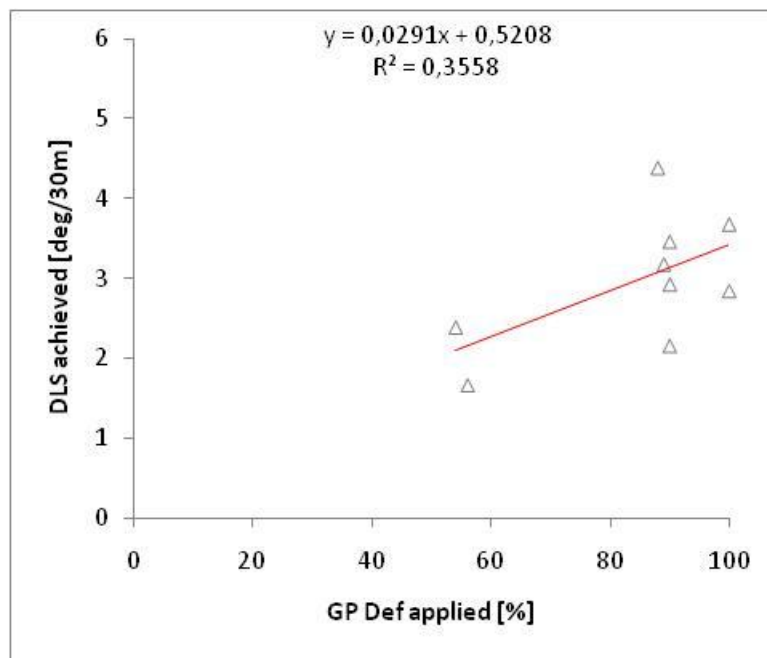


Figure 139, Design (375525) @ Range E

Figure 137 puts together the responses for the three designs. These are the final field tendencies for this case.

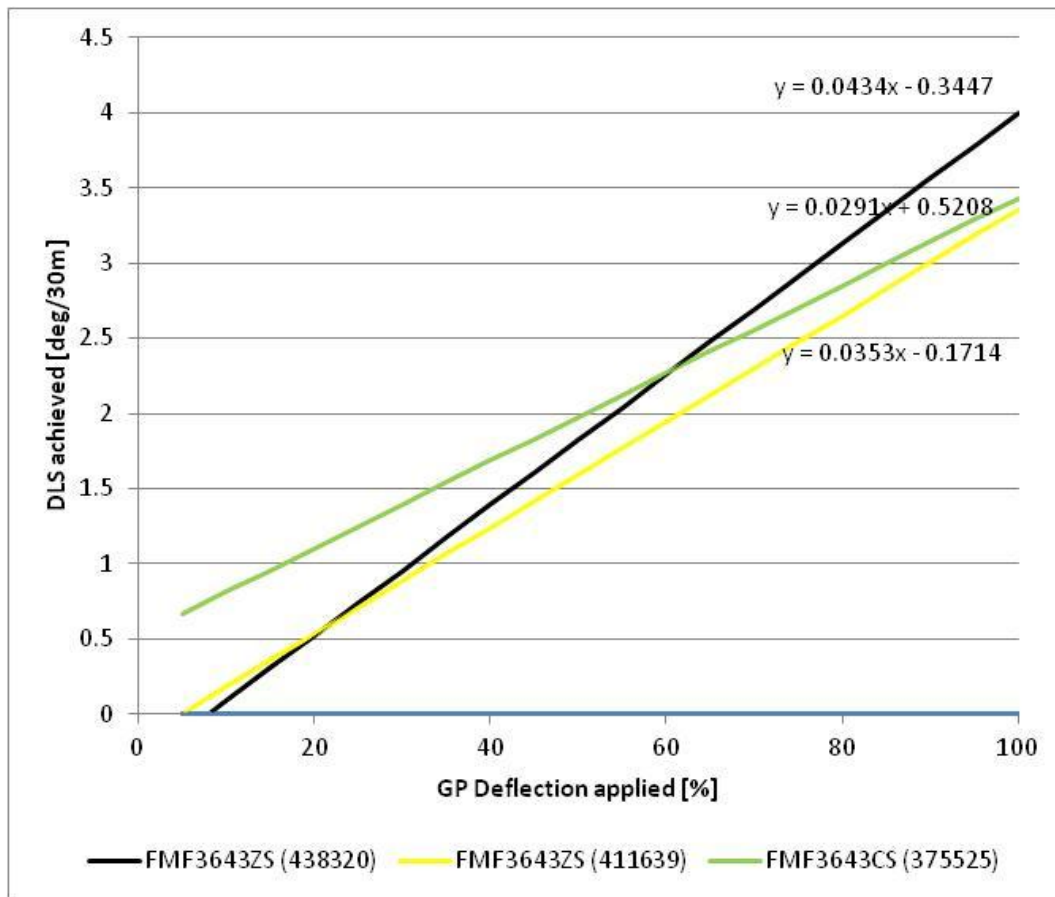


Figure 140 Building field tendencies 12 ¼ Case E

From this figure the study can point out the following observations:

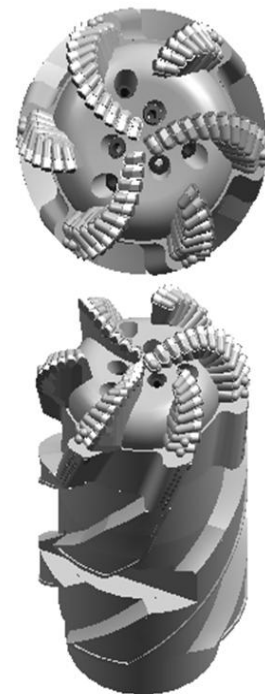
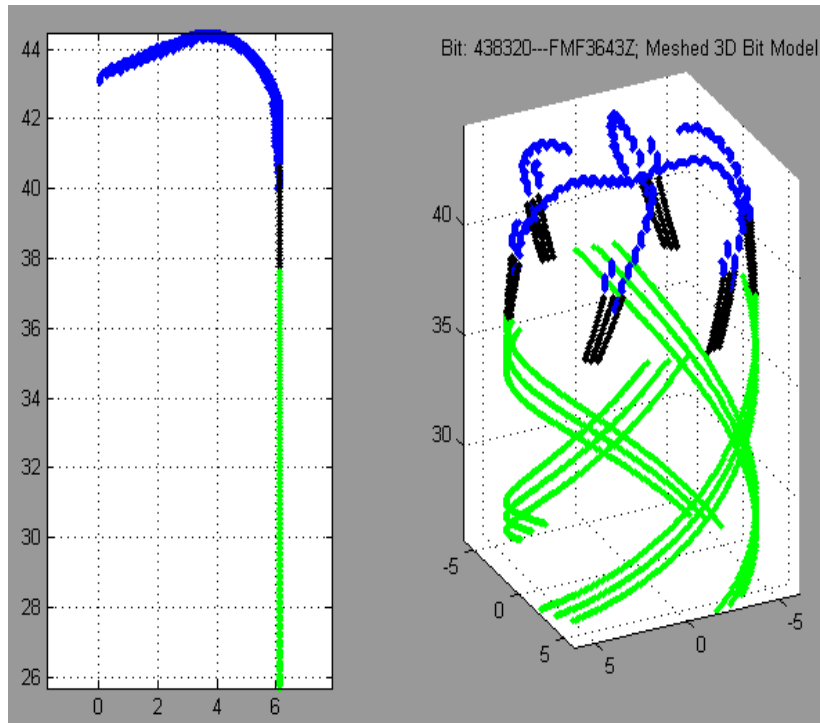
- There are three regions in the final figure. Above 60% deflection design (438320) displays the best performance among the group (4 blade and 12" sleeve). With a maximum DLS of 4 deg/30m. Designs 411639) and (375525) reach almost the same deflection around 3,4 deg/30m. This must be due to the fact that they have exactly the same geometry (6 blade longer 15" length sleeve), but different cutter materials.
- For deflections between 20-60 %. Design C (375525) has better performance
- And at very low deflection, below 20% design (375525) shows higher DLS than designs (438320) and (411639).
- If comparing only the slopes. Responsiveness of the system is as follows, design (438320) with ($m=0,0434$) 49% higher, design (411639) with ($m=0,0353$) 21% higher and Design (375525) ($m=0,0291$).

c) Simulation and Model Tendencies

The simulation is performed as described in 3.5. The input parameters used in the simulation are the average of the ranges on Table 15.

Design A-FMF3643Z (438320)

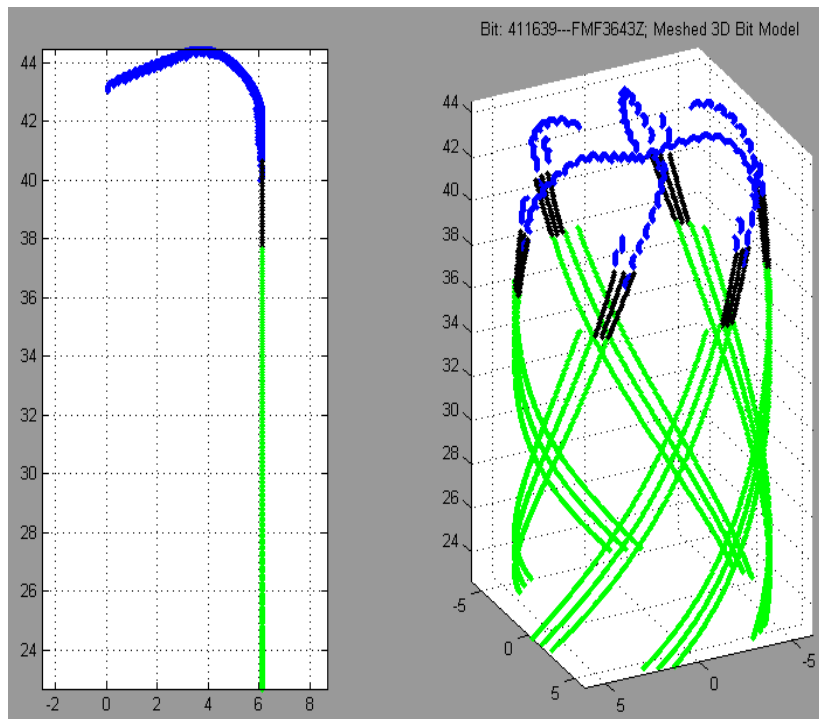
Input Data	
Bit type	438320 - FMF3643Z
Drill mode	Kickoff
BHA type	GP w/o SLH
ROP [ft/hr]	55
RPM	140
Tilt Length ["]	18,7153
Hole size ["]	12,25
Rock Strenght [psi]	15000
Dip angle [deg]	0
Gage pad length ["]	3
Undergage 1/ ["]	NO
Sleeve blades	4
Sleeve blades angle	12
Sleeve gage length ["]	12
Undergage 1/ ["]	32
Tapered angle [deg]	0
Comment	Passive gage



Material #438320

Design B-FMF3643Z (411639)

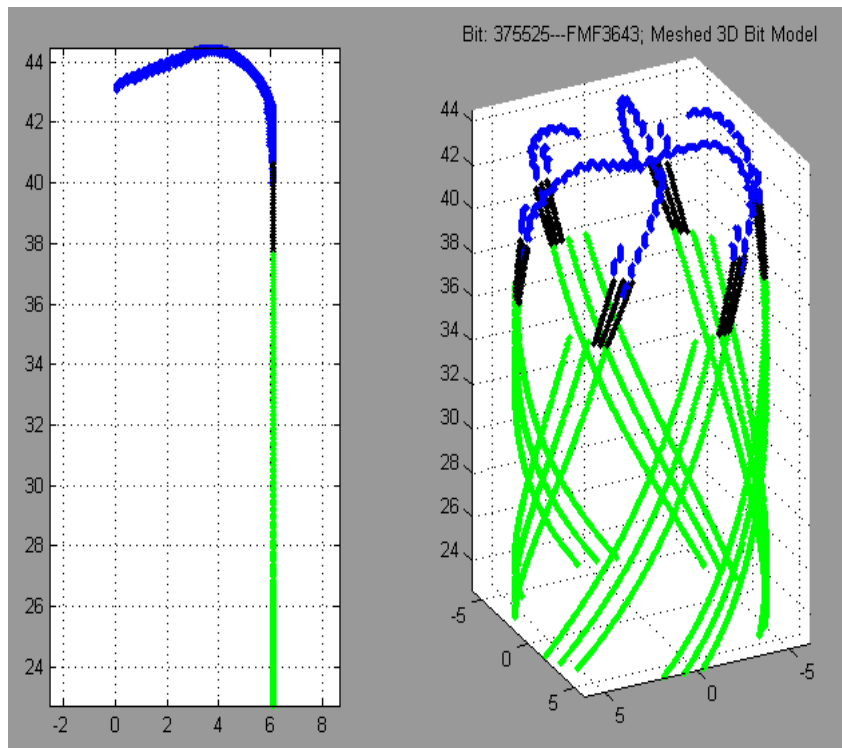
Input Data	
Bit type	411639 - FMF3643Z
Drill mode	Kickoff
BHA type	GP w/o SLH
ROP [ft/hr]	55
RPM	140
Tilt Length ["]	21,7153
Hole size ["]	12,25
Rock Strenght [psi]	15000
Dip angle [deg]	0
Gage pad length ["]	3
Undergage 1/ ["]	NO
Sleeve blades	6
Sleeve blade angle	5
Sleeve gage length ["]	15
Sleeve width ["]	2
Undergage 1/ ["]	32
Tapered angle [deg]	0
Comment	Passive gage



Material #411639

Design C-FMF3643 (375525)

Input Data	
Bit type	375525 - FMF3643
Drill mode	Kickoff
BHA type	GP w/o SLH
ROP [ft/hr]	55
RPM	140
Tilt Length ["]	21,7153
Hole size ["]	12,25
Rock Strenght [psi]	15000
Dip angle [deg]	0
Gage pad length ["]	3
Undergage 1/ ["]	NO
Sleeve blades	6
Sleeve blade angle	5
Sleeve gage length ["]	15
Sleeve width ["]	2
Undergage 1/ ["]	32
Tapered angle [deg]	0
Comment	Passive gage



Material #375525

d) Results and comparison

As can be seen from Figure 141, for the building analysis:

- Field and simulation tendencies correlate. This is verified by comparing the slopes and the maximum DLS achieved. Design (438320) had the best performance.
- Between Design (B) and (C) the simulation does not show a clear difference. However, from field data design (411639) has a slope 21% higher than (375525). Anyway, both designs (411639) and (375528) reach almost the same DLS of 3.4 deg/30m.

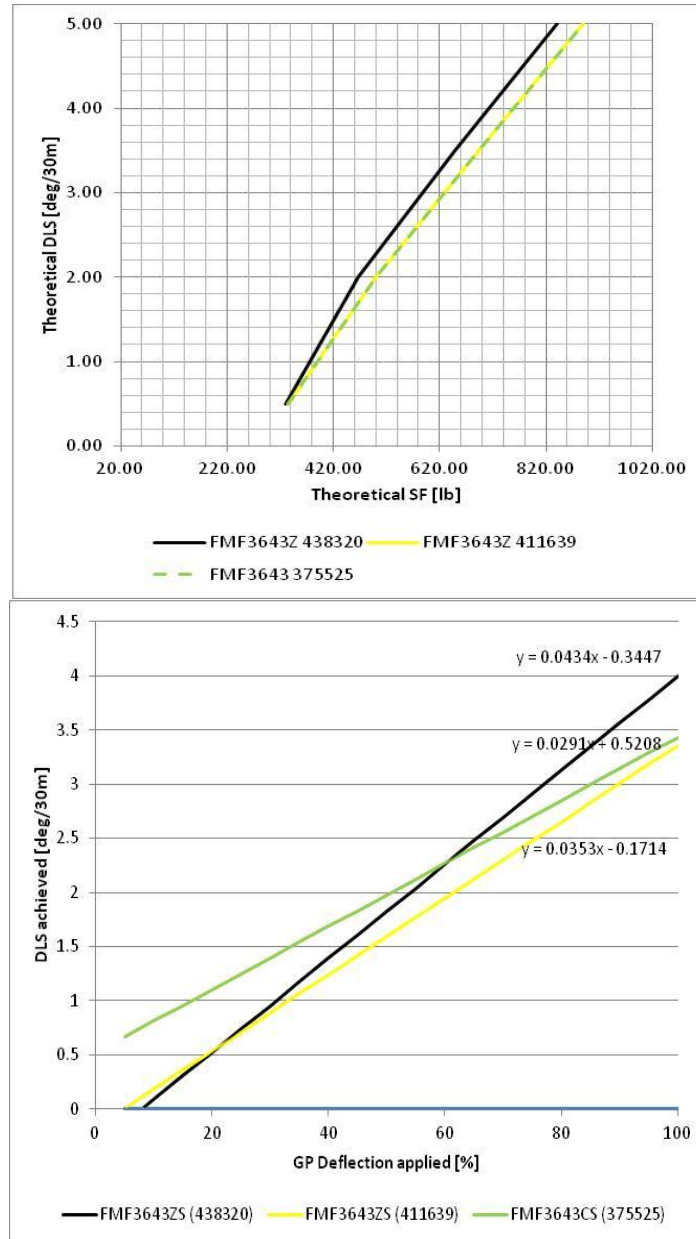


**Figure 141 Building @ range E
Model (top) vs. Field data (bottom) tendencies**

4.3.6 Case F – 12 ¼ section, with reamer to 13 ½”

For this case, 4 bit designs bits were available. In order to support the decision of considering the building behavior, an initial correlation of “DLS achieved vs GP deflection applied” is plotted for each design Figures 142 - 145. These correlations consider all the behaviors and all ROPs and RPMs.

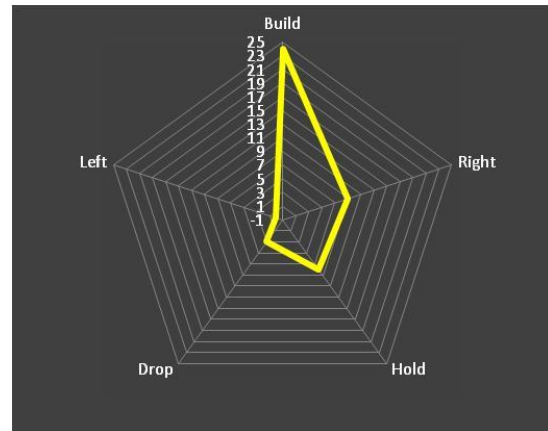
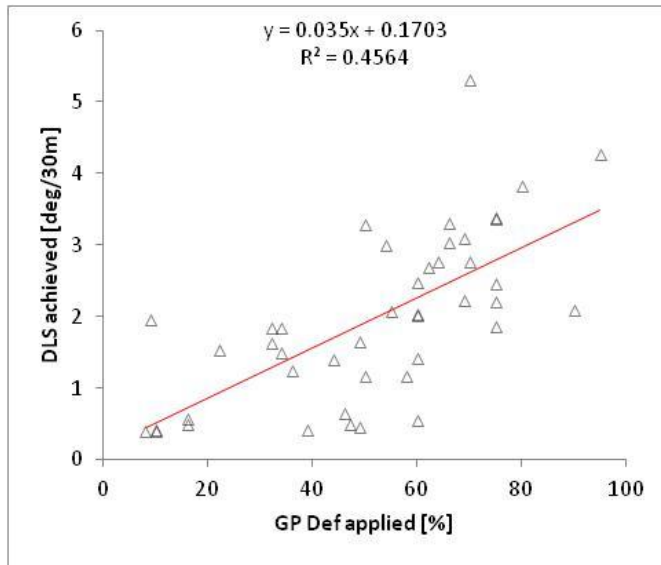


Figure 142, Design (605284) steering response all behaviors

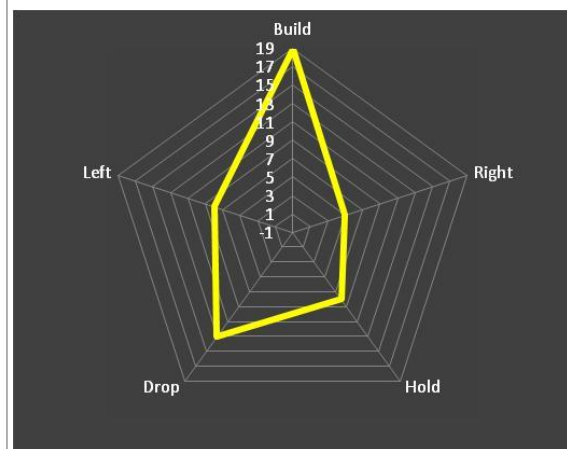
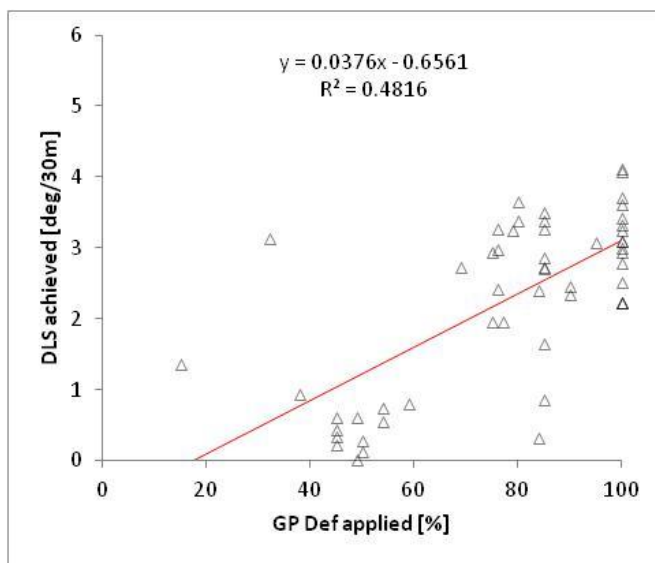


Figure 143, Design (585609) steering response all behaviors

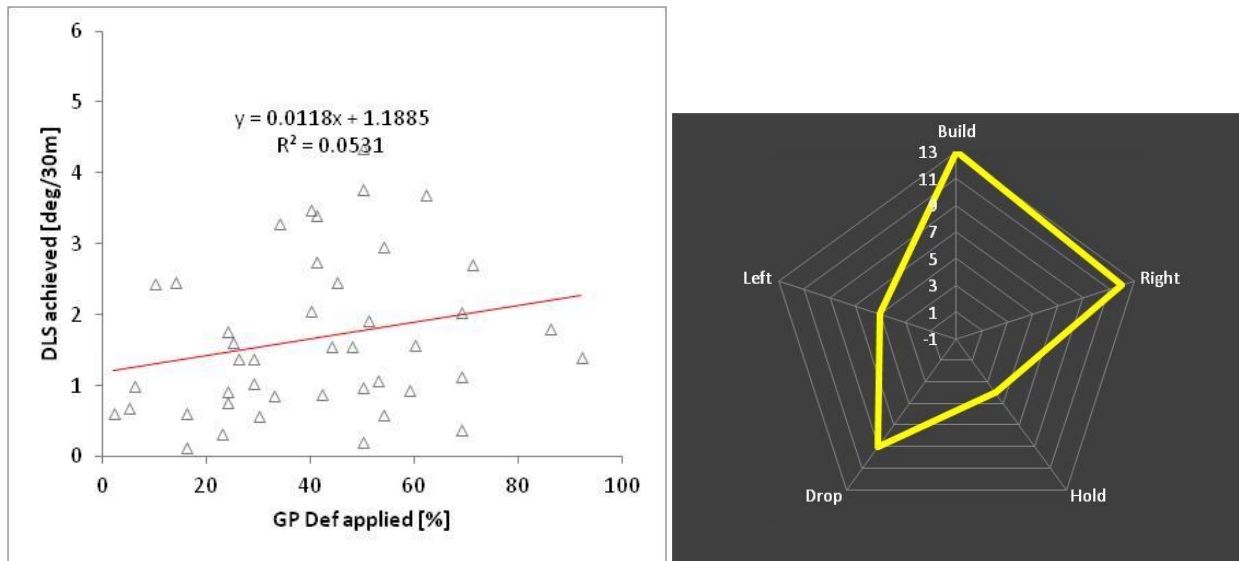


Figure 144, Design (478186) steering response all behaviors

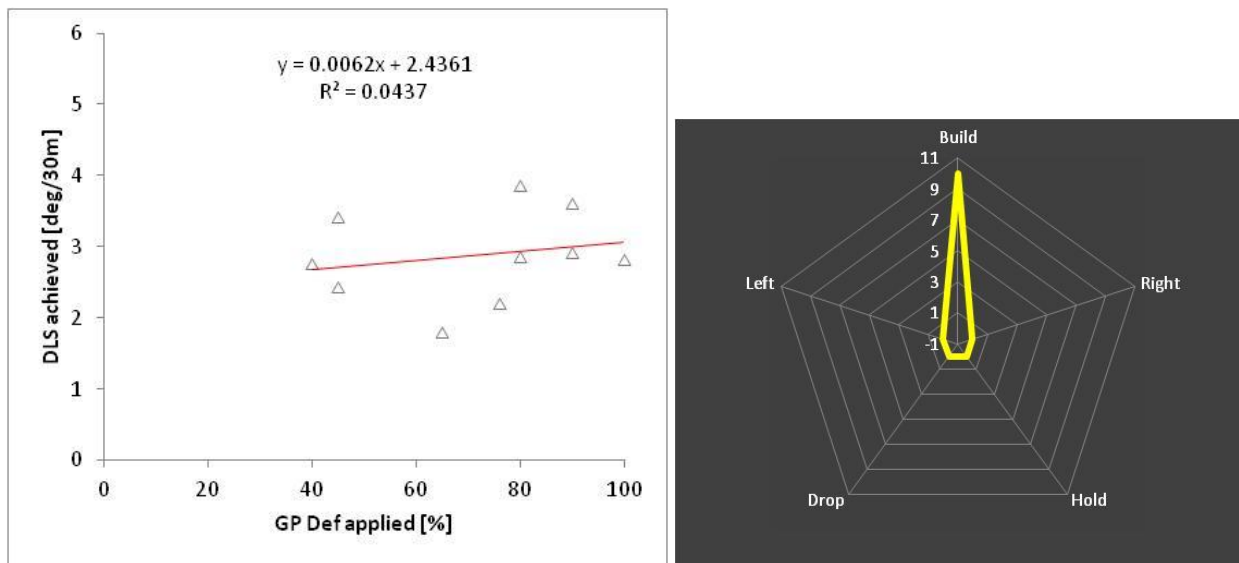


Figure 145, Design (422785) steering response all behaviors

As can be seen from the Figures 142 – 145 (behaviors), the main behavior displayed is building. Then, the analysis will be performed for building.

Table 16 summarizes the data of the three designs. As can be seen from the table, the ROP is very spread from 10,4 to 85,4 ft/hr and RPM is between 78 and 160. Then a statistical review is provided to select the most appropriate ranges.

Table 16, Case F - 12 ¼ reamed to 13 ½ bit designs

605284	Av	Min	Max
ROP	46,40	10,389	83,499
RPM	140,21	77,836	150,55
Count	44		

585609	Av	Min	Max
ROP	63,48	26,196	85,388
RPM	133,47	101,47	150,31
Count	53		

478186	Av	Min	Max
ROP	44,44	26,731	60,23
RPM	142,11	109,37	150,44
Count	43		

422785	Av	Min	Max
ROP	40,89	17,867	60,493
RPM	156,18	139,82	160,29
Count	10		

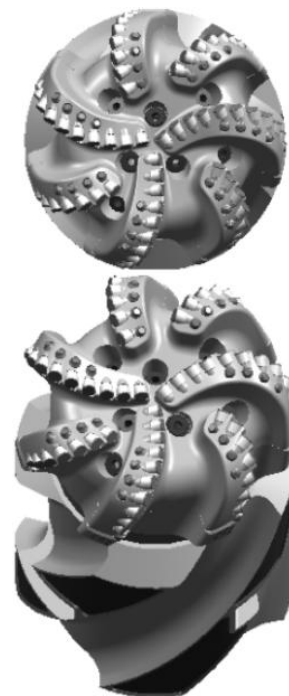
More details about these three designs can be found in Figures 146 - 149. The specification sheets show the cutting structure materials, gage design, sleeve design and special features of the bits.

PRODUCT SPECIFICATIONS

Cutter Type	X1 - Conventional Drilling	
IADC Code	M322	
Body Type	MATRIX	
Total Cutter Count	67	
Cutter Distribution	<u>13mm</u>	<u>16mm</u>
Face	0	53
Gauge	7	7
Number of Large Nozzles	7	
Number of Medium Nozzles	0	
Number of Small Nozzles	0	
Number of Micro Nozzles	0	
Number of Ports	0	
Junk Slot Area (sq in)	33.55	
Normalized Face Volume	43.84%	
API Connection	6-5/8 REG. BOX	
Recommended Make-Up Torque*	58.885 Ft*lbs.	
Nominal Dimensions**		
Make-Up Face to Nose	21.77 in - 553 mm	
Gauge Length	1 in - 25 mm	
Sleeve Length	12 in - 305 mm	
Shank Diameter	8.75 in - 222 mm	
Break Out Plate (Mat.#/Legacy#)	181978/44757	
Approximate Shipping Weight	704Lbs. - 319Kg.	

SPECIAL FEATURES

Secondary Cutting Element - "R" Feature, 1/32" Relieved Gage.
 (MEG) Modified Extended Gage Sleeve - 4 Blade, 1/16" Undergage Sleeve



Material #605284

Figure 146, Design 605284

PRODUCT SPECIFICATIONS

Cutter Type	X1 - Conventional Drilling	
IADC Code	M322	
Body Type	MATRIX	
Total Cutter Count	70	
Cutter Distribution	<u>13mm</u>	<u>16mm</u>
Face	6	47
Gauge	7	10
Number of Large Nozzles	7	
Number of Medium Nozzles	0	
Number of Small Nozzles	0	
Number of Micro Nozzles	0	
Number of Ports	0	
Junk Slot Area (sq in)	30.84	
Normalized Face Volume	44.3%	
API Connection	6-5/8 REG. BOX	
Recommended Make-Up Torque*	58,885 Ft*lbs.	
Nominal Dimensions**		
Make-Up Face to Nose	18.92 in - 481 mm	
Gauge Length	1 in - 25 mm	
Sleeve Length	12 in - 305 mm	
Shank Diameter	8.75 in - 222 mm	
Break Out Plate (Mat.#/Legacy#)	181978/44757	
Approximate Shipping Weight	880Lbs. - 399Kg.	

SPECIAL FEATURES

13mm IN CTR, FullDrift Design, 1/32" Under Gauge Bit, Sleeve 1/16" Under Gauge, P100, R1 Backup



Material #585609

Figure 147, Design 585609

Case F wells were drilled with very similar BHA templates. As can be seen from the tally Figures 148 - 151, these wells were reamed to 13,5". The addition of this component has an important impact on S-WOB and S-Torque, as well as hydraulics. However, these parameters are considered and balanced so the directional tool can perform as expected with equivalent necessary drilling parameters down-hole at the bit.

Another important feature that validates the comparison is that all the BHAs have the same directional components behind the bit, the Geo-Pilot™ 9600 series with GABI, a stabilizer and a GP flex in all the cases.

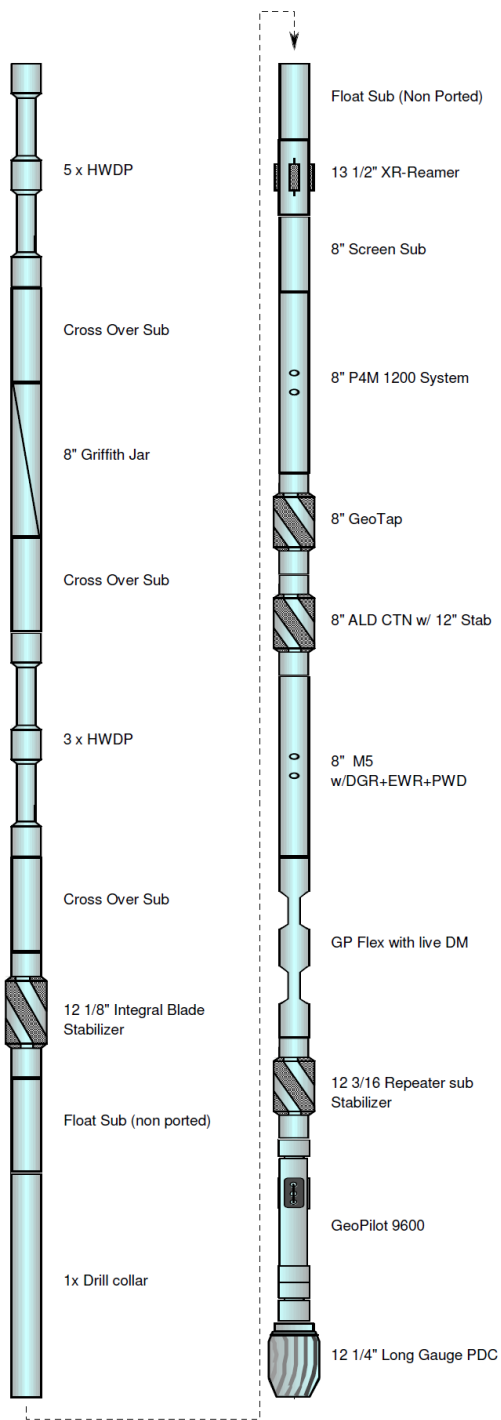


Figure 148, BHA type of design (605284)

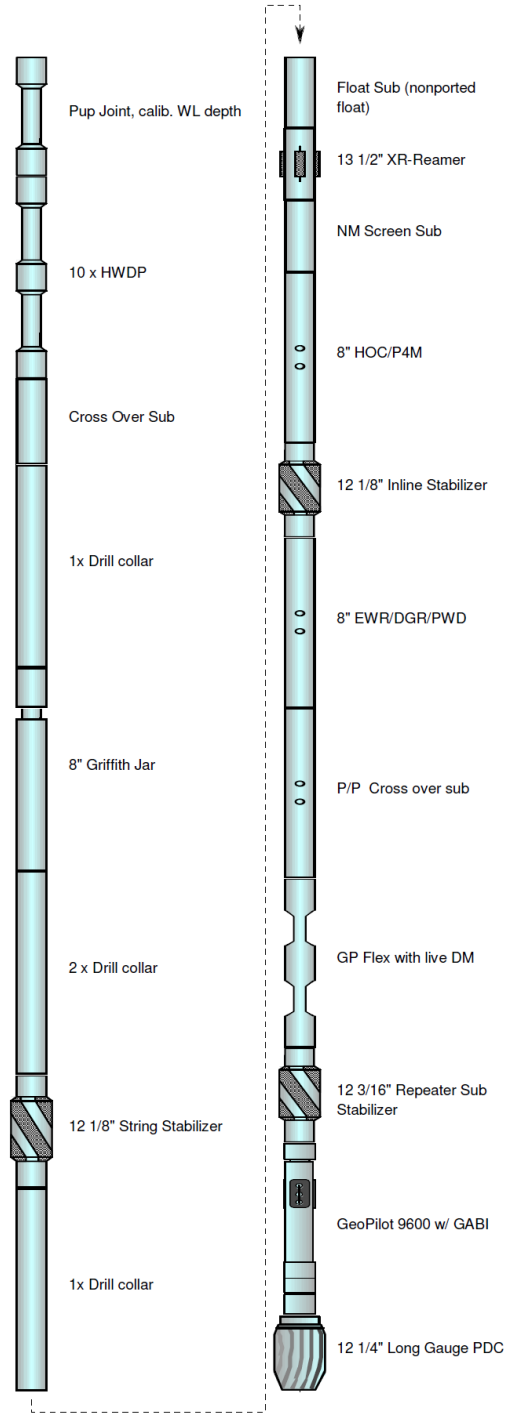


Figure 149, BHA type of design (585609)

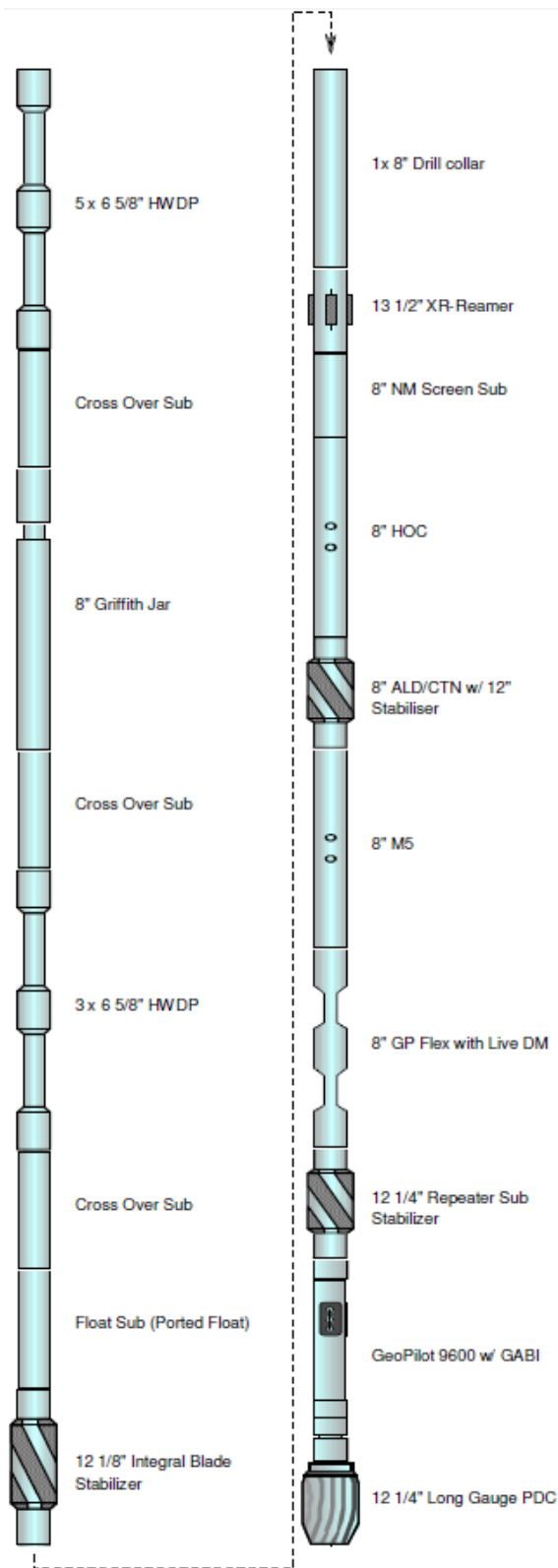


Figure 150, BHA type of design (478186)

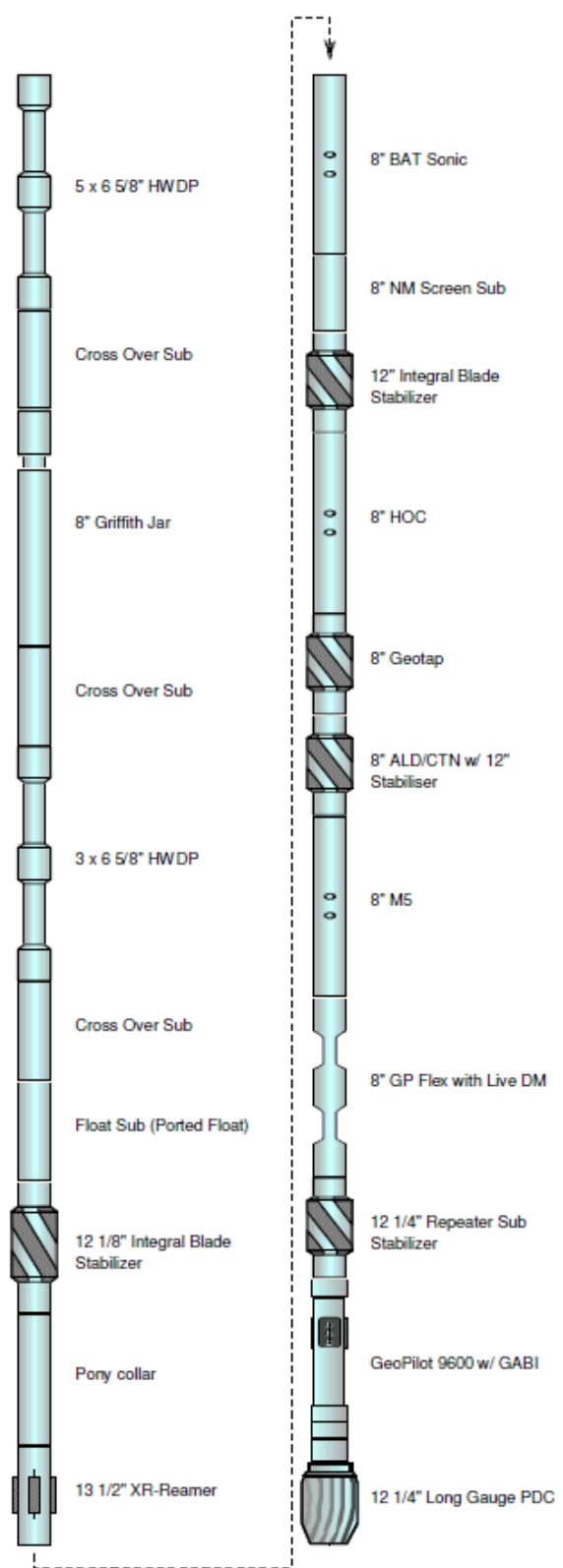


Figure 151, BHA type of design (422785)

a) Statistical analysis

Once selected building as the behavior that will be analyzed, all the data-points in the main matrix were plotted in distributions for ROP and RPM. Figures 152 – 155 show the results.

As seen in the same Figures, there is one range identified for ROP and one for RPM. Those ranges define data considered for this case study.

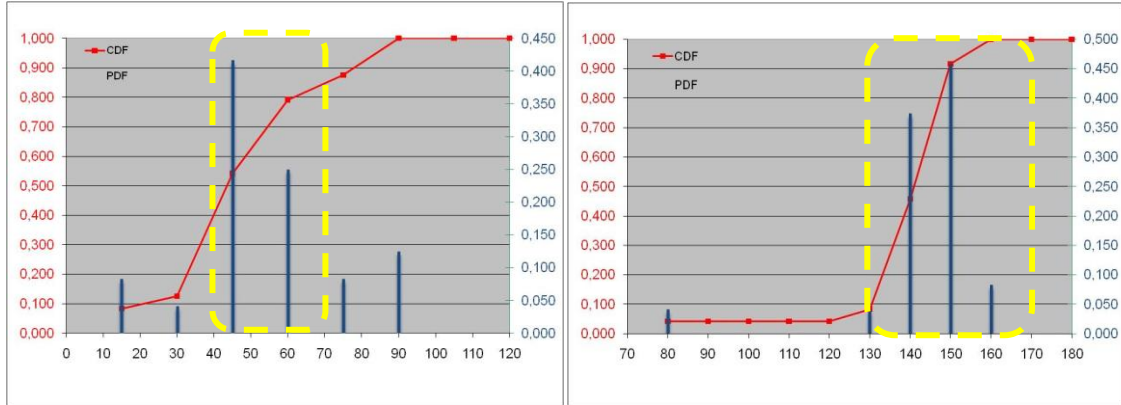


Figure 152, 605284 Building ROP (left) and RPM (right) stats

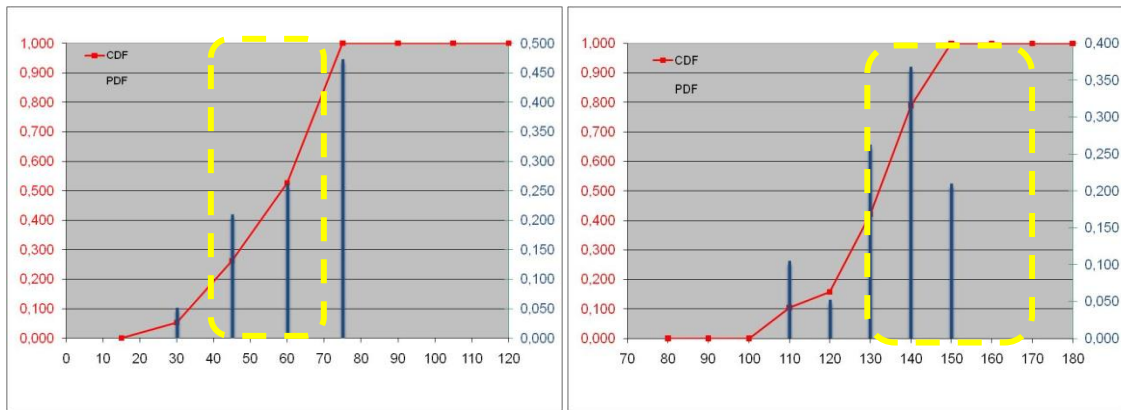


Figure 153, 585609 Building stats ROP (left) and RPM (right) stats

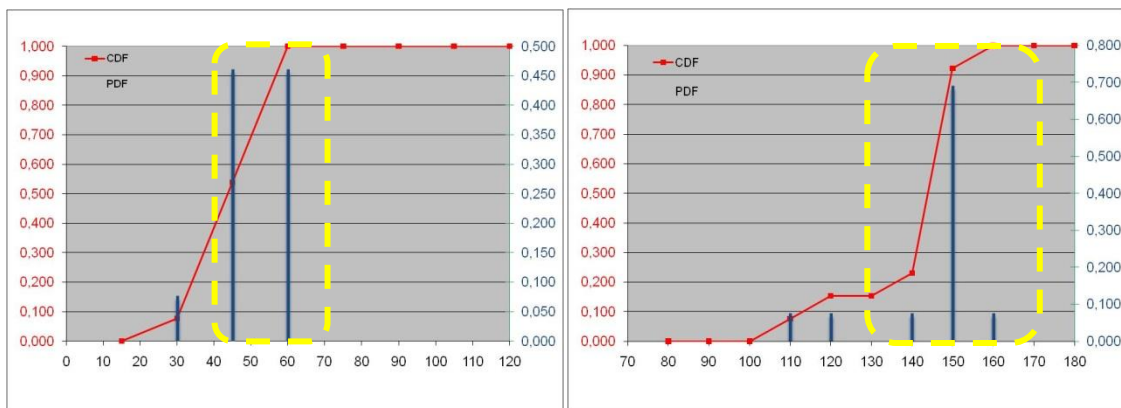


Figure 154, 478186 Building stats ROP (left) and RPM (right) stats

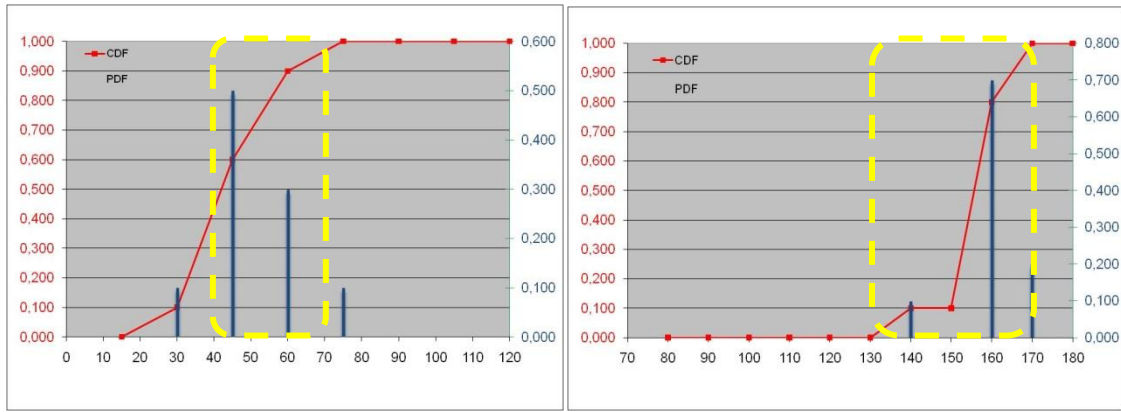


Figure 155, 422785 Building stats ROP (left) and RPM (right) stats

From that analysis, the following ROP and RPM ranges are selected to compare the building behavior for the three designs. Table 17 displays the ranges that contain more data-points regarding the building behavior.

Table 17, Case F, Ranges

Case F	Min	Max	Av
ROP	40	70	55
RPM	130	170	150

b) Field tendencies

The following figures 156 – 159, display the correlations found within the operational parameters of ROP [40-70] ft/hr and between 130 and 170 RPM.

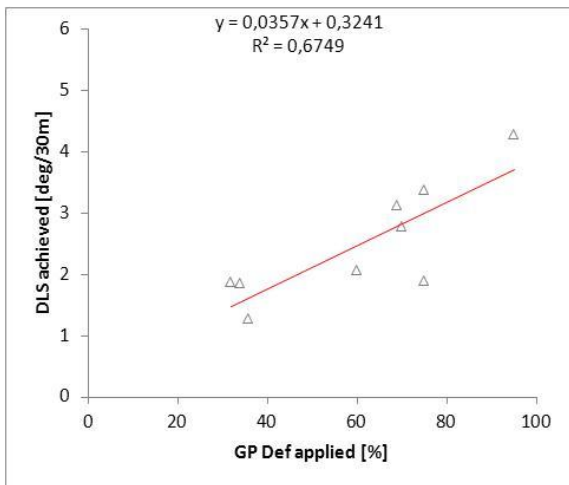


Figure 156, Design (605284) @ range F

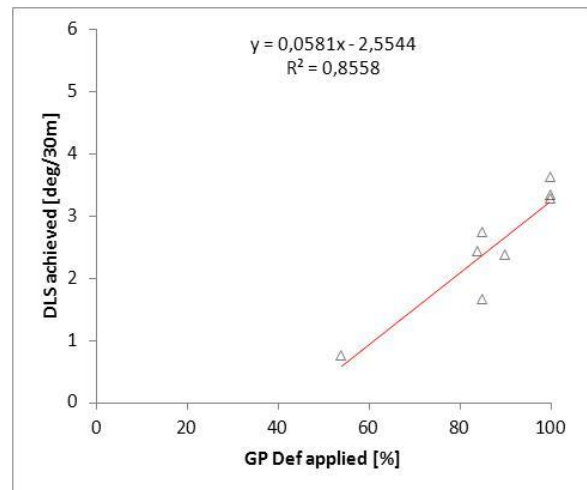


Figure 157, Design (585609) @ range F

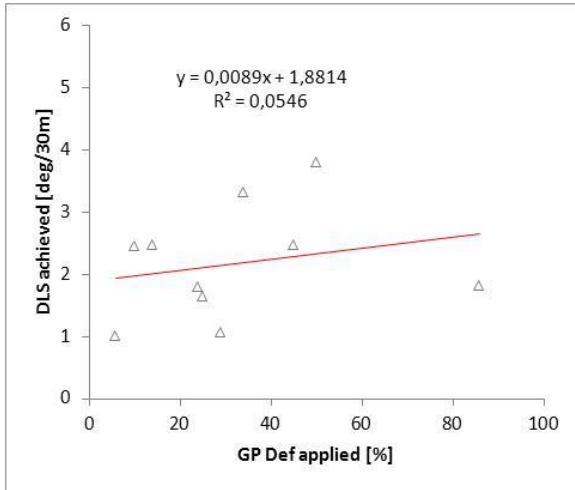


Figure 158, Design (478186) @ range F

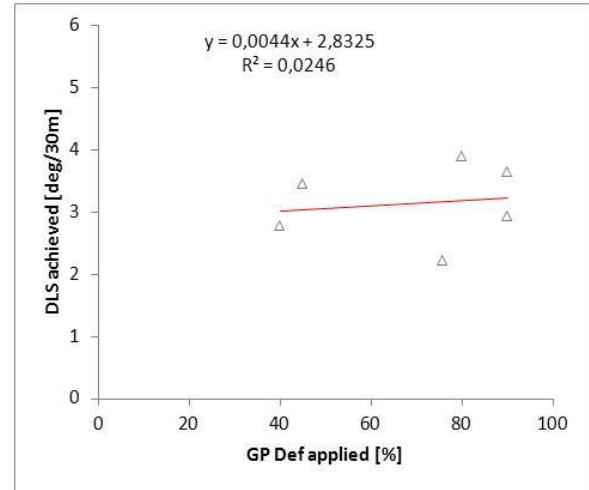


Figure 159, Design (422785) @ range F

Figure 160 puts together the responses for the three designs. These are the final field tendencies for this case.

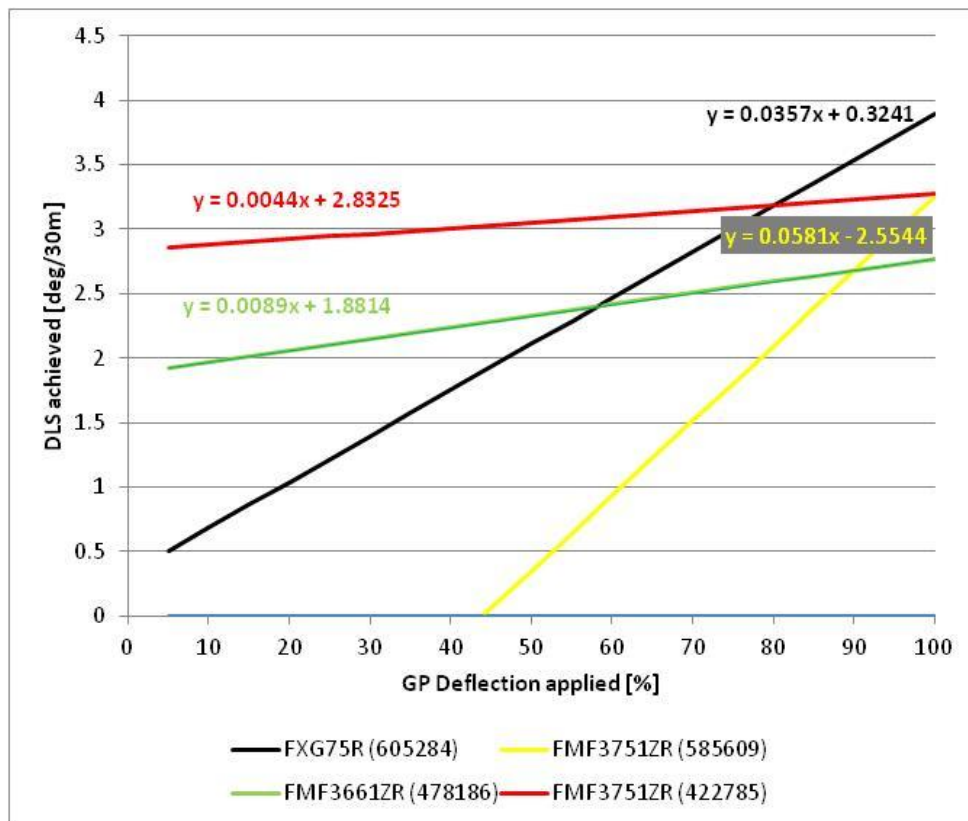


Figure 160 Field tendencies Case F M [130-170]

From Figure 160 the study can point out the following observations regarding the field tendencies:

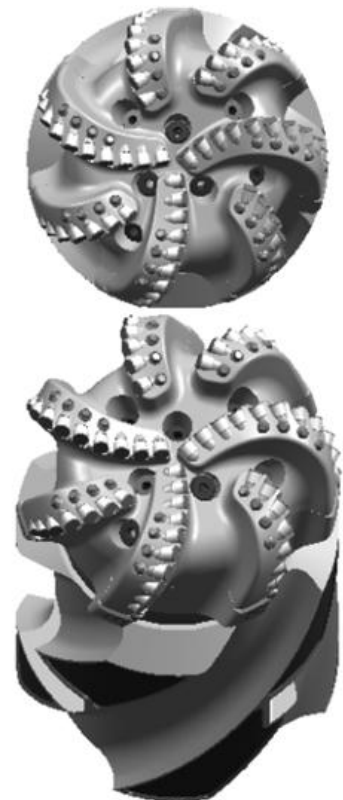
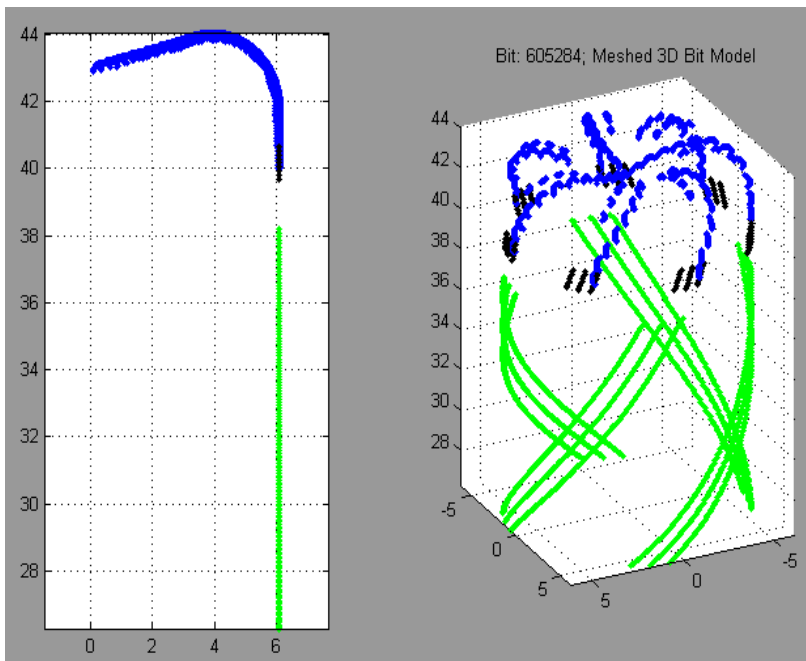
- Considering high values of slopes. Design (585609) has a slope 63 % higher than (605284), however the (605284) reaches the highest DLS of 3.9 deg/30m.
- In the other group with very low slopes. Design (478186) has a slope 100% higher than (422785), however, a higher DLS is achieved by (422785).

c) Simulation and Model Tendencies

The simulation is performed as described in 3.5. The input parameters used in the simulation are the average of the ranges on Table 17.

Design A-FXG75R (605284)

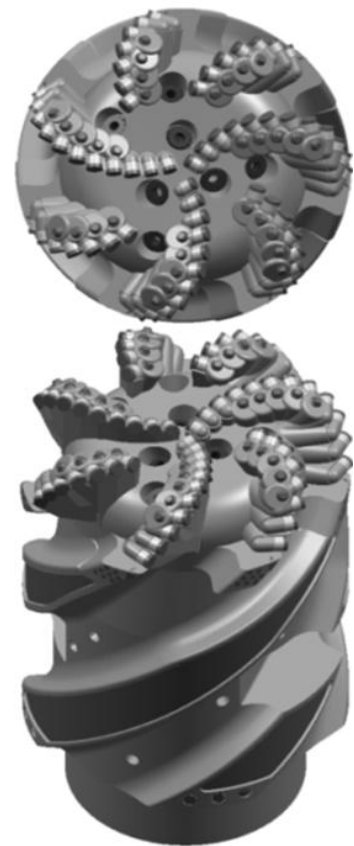
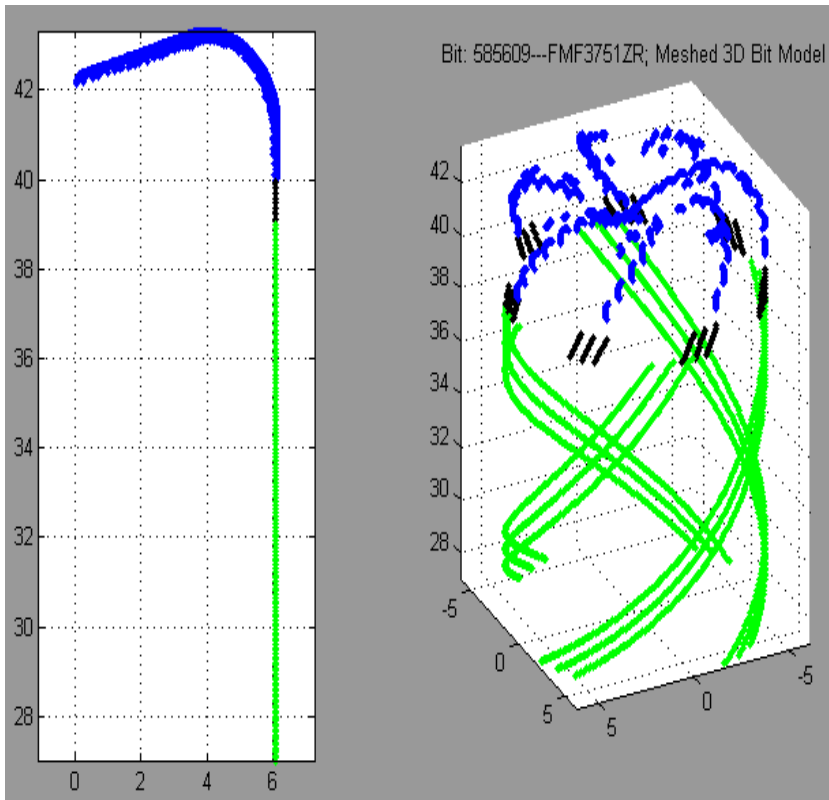
Input Data	
Bit type	605284 – FXG75R
Drill mode	Kickoff
BHA type	GP w/o SLH
ROP [ft/hr]	55
RPM	150
Tilt Length ["]	17,7451
Hole size ["]	12,25
Rock Strenght [psi]	15000
Dip angle [deg]	0
Gage pad length ["]	1
Undergage 1/ ["]	32
Sleeve blades	4
Sleeve blades angle	8
Sleeve gage length ["]	12
Undergage 1/ ["]	16
Tapered angle [deg]	0
Comment	R1 cutting element Passive gage MEG 1,5"



Material #605284

Design B-FMF3751ZR (585609)

Input Data	
Bit type	585609-FMF3751ZR
Drill mode	Kickoff
BHA type	GP w/o SLH
ROP [ft/hr]	55
RPM	150
Tilt Length ["]	16.2862
Hole size ["]	12,25
Rock Strength [psi]	15000
Dip angle [deg]	0
Gage pad length ["]	1
Undergage 1/ ["]	32
Sleeve blades	4
Sleeve blade angle	12
Sleeve gage length ["]	12
Sleeve width ["]	2
Undergage 1/ ["]	16
Tapered angle [deg]	0
Comment	Passive gage R1 back up cutters



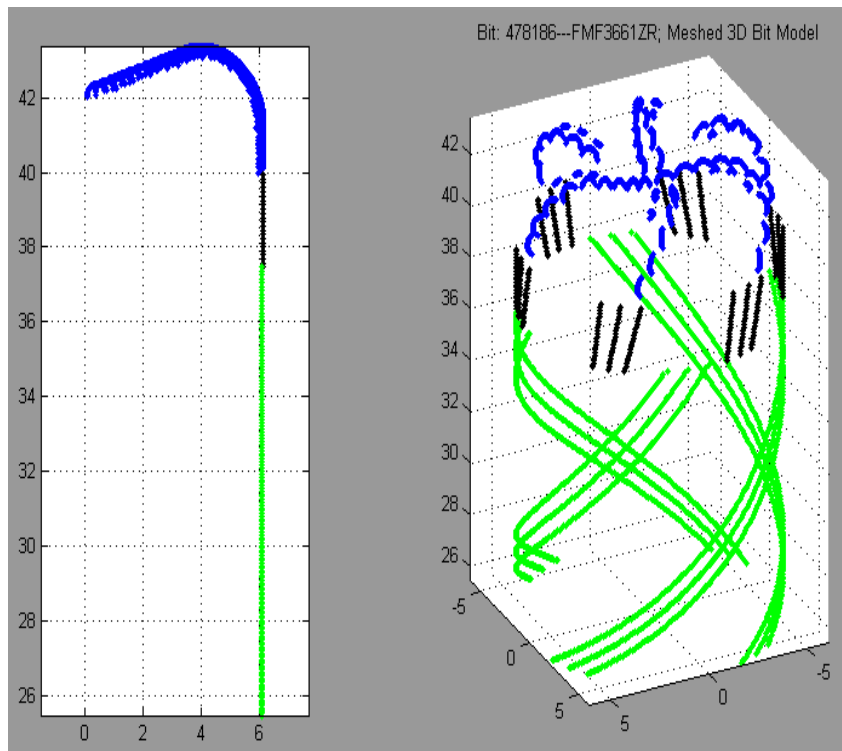
Material #585609

Design C-FMF3661ZR (478186)

Input Data	
Bit type	478186-FMF3661ZR
Drill mode	Kickoff
BHA type	GP w/o SLH
ROP [ft/hr]	55
RPM	150
Tilt Length ["]	17,7224
Hole size ["]	12,25
Rock Strenght [psi]	15000
Dip angle [deg]	0
Gage pad length ["]	2,5
Undergage 1/ ["]	NO
Sleeve blades	4
Sleeve blade angle	12
Sleeve gage length ["]	12
Sleeve width ["]	2
Undergage 1/ ["]	16
Tapered angle [deg]	0
Comment	Passive gage R1 backup cutters

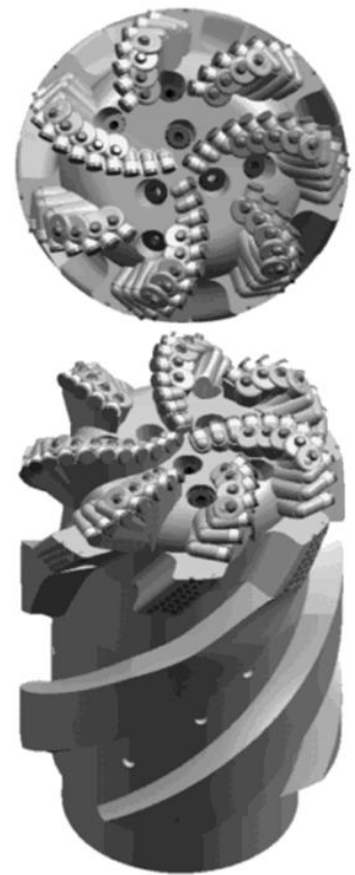
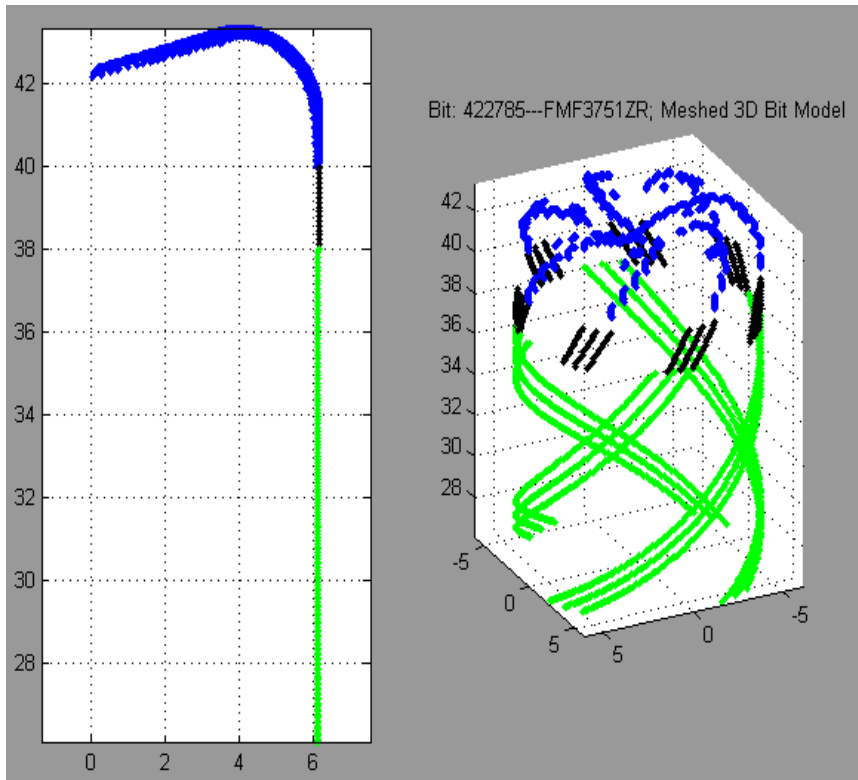


Material #478186



Design D-FMF3751ZR (422785)

Input Data	
Bit type	422785-FMF3751ZR
Drill mode	Kickoff
BHA type	GP w/o SLH
ROP [ft/hr]	55
RPM	150
Tilt Length ["]	17,2862
Hole size ["]	12,25
Rock Strength [psi]	15000
Dip angle [deg]	0
Gage pad length ["]	2,0
Undergage 1/ ["]	NO
Sleeve blades	4
Sleeve blade angle	12
Sleeve gage length ["]	12
Sleeve width ["]	2
Undergage 1/ ["]	0
Tapered angle [deg]	0,1492
Comment	Tapered gage to 1/16 R1 backup cutters



Material #422785

d) Simulation results and comparison

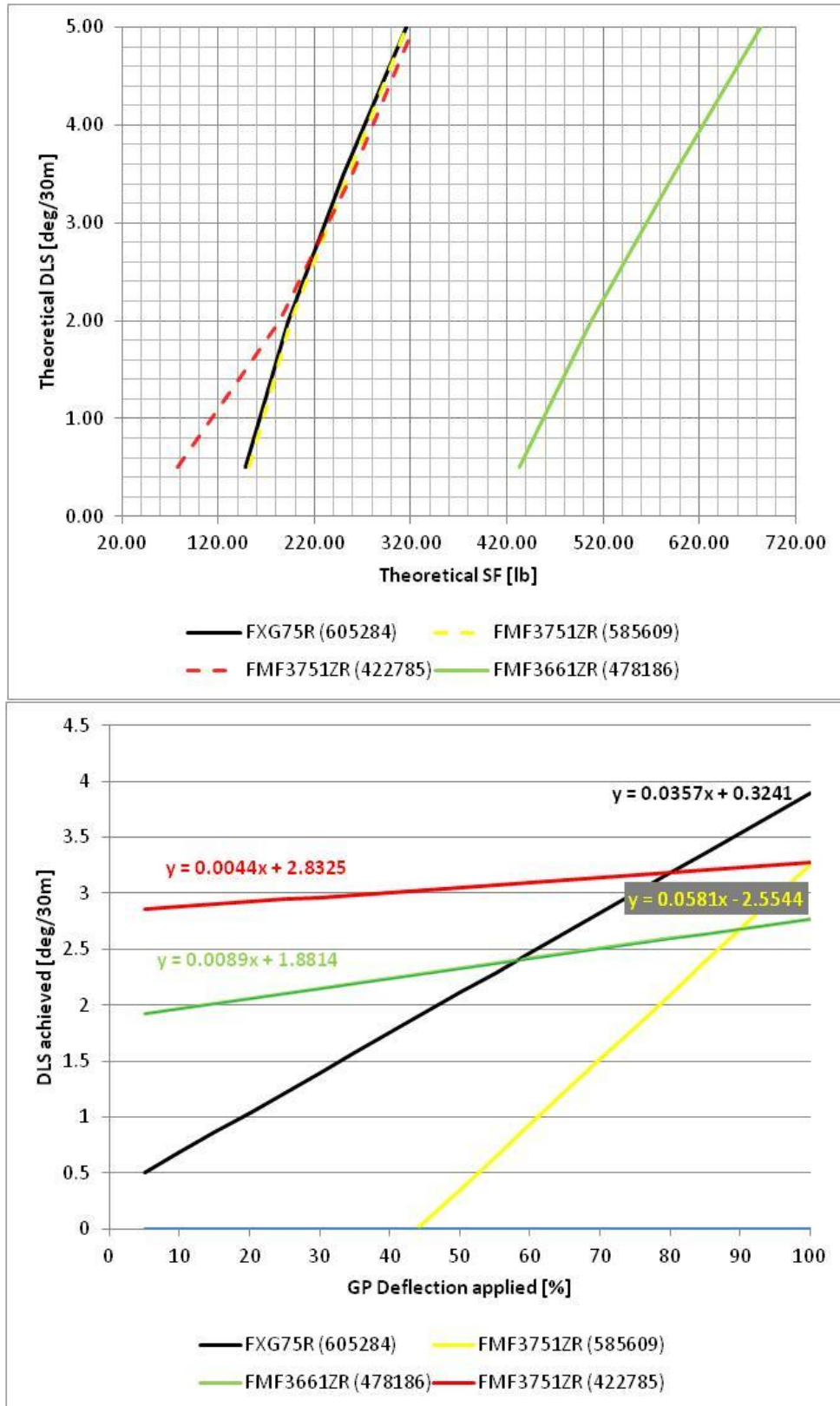


**Figure 161 Model (top) vs. field (bottom) tendencies
Case F Building**

As can be seen from Figure 161, for building analysis:

-
- Field and simulation tendencies correlated partly. Design (478186) has the poorest response. Then design (422785). The best two performances are not conclusive from simulation where both have almost the same response. However, from field data, design (585609) has the best performance.
 - When considering the maximum DLS achieved, model and field data confirm that the most steerable design is (605284) reaching a 3.9 deg/30m at maximum deflection.

5 Summary and major findings

Table 18 shows the summary of the case studies and final results.

Table 18, Summary table

	8 1/2 section			12 1/4 section		
	Case A	Case B	Case C	Case D	Case E	Case F
Description of case	-Bits with more available data. -To display and show the relevancy of identifying the different steering behaviors.	-Low ROP range considered. -Focus on a single feature change MEG.	-Medium ROP range considered. -Data allowed to analyse different behaviors.	-High ROP range considered. -Data allowed to analyse different behaviors.	-Mainly building section. -No reamer used hole 12 1/4.	-Mainly building section. -Section reamed to 13 1/2.
Bit designs considered	FMF3651Z (487256) FMF3653Z (405148)	FMF3651Z (487256) FMF3653Z (551396)	FMF3651Z (487256) FMF3653Z (551396) FMF33653Z (405148) FMF3741Z (475040)	FMF3741Z (475040) FMF3731C (384968) FMF3651Z (562259)	FMF3643ZS (438320) FMF3643ZS (411639) FMF3643CS (375525)	FXG75 (605284) FMF3751 (585609) FMF3661ZR (478186) FMF3751ZR (422785)
Analysis done	-Comparison behavior by behavior. -Turning behavior qualified for comparison Field vs. Model.	-Range of ROP identified from statistics. -Same RPM for cases B, C and D. -Turning left behavior qualified for comparison Field vs. Model.	-Range of medium ROP identified from statistics. -Same RPM for cases B, C and D. -Building, Turning left and Turning right behaviors qualified for comparison Field vs. Model.	-Range of HIGH ROP identified from statistics. -Same RPM for cases B, C and D. -Building, and Turning right behaviors qualified for comparison Field vs. Model.	-Ranges of ROP and RPM identified from statistics. -Building behavior qualified for comparison Field vs. Model.	-Ranges of ROP and RPM identified from statistics. -Building behavior qualified for comparison Field vs. Model.
ROP range [ft/hr]	61 - 76	40 - 55	55 - 70	70 - 85	40 - 70	40 - 70
RPM range	132 - 162	140 - 170	140 - 170	140 - 170	130 - 170	130 - 170
Results	-Verification of the relevance of the analysis of behaviors. -Design 487256 performed better than 405148. -Model matched field data -Improvement with active gage and flat profile.	-Verification of relevance of the analysis behavior by behavior. -Design 551396 performed better than 487256. -Model partly match field data. -Improvement seen by the addition of MEG.	-Verification of relevance of the analysis behavior by behavior. -In building: design 487256 performed better than 475040. Model matched field data. -In turning left: design 487256 performed better than 475040. Model matched field data. -Improvement seen by the addition of the active gage, change from 6 to 7 blades cutting structure, and 16 mm better than 13mm cutters. -In turning right: (405148) performed better than (475040). Improvement seen with tapered gage to 1/16.	-Verification of relevance of the analysis behavior by behavior. -In building: design 384968 performed better than 562259. Model did not matched field data. -In turning right: design (562259) performed better than (384968). Improvement seen in active gage (under gage), over (smaller cutters and tapered sleeve.	-Verification of relevance of the analysis behavior by behavior. -Design 438320 performed better than 411639 and 375525. -Model match field data. -Improvement seen by the change from 6 blades to 4 blades sleeve and also from reduction of sleeve length.	-Verification of the relevance of the analysis behavior by behavior. -Design 605284 performed better than 585609, 422785 and 478186. -Model matched field data partly. -Improvements: by the change from 6 to 7 blades. when adding MEG changing cutting structure to only one cutter size of 16mm. when reducing the cutters from 19mm to 16mm. when reducing gage pad length from 2,5" to 2".

5.1 Regarding the bit designs

- Bit design is a complex process where there are many parameters that need to be balanced in order to prioritize a specific application on the field. The literature review covered and the many designs analyzed in the thesis work provided valuable insight about the impact of the modification of these design parameters.
- After the data analysis was performed it is clear that can be improved by considering other important scenarios such as hole cleaning capacity or washouts. As the results showed that the modification in the bit design adding a MEG (Modified Extended Gage) and/or the change from 6 to 4 blades in the sleeve generates a positive impact. The simulator considers these modifications in a geometrical/mechanical way, however as no fluid dynamics analysis is added to the model the true impact of this features is totally modeled.
- The positive impact for steerability of several design features presented in the literature review were confirmed by the data analysis. These include the impact of a cutting structure with flat profile, the addition of active gage, the increase of JSA (Junk Slot Area), reducing the gage of the gage pad (1/32") and sleeve (1/16") showed the best overall results when compared with the tapered designs to (1/16) or the full gage designs. In addition, the tapered feature showed better than the full gage designs.
- The reduction in gage and tilt length potentially improve steerability, however the behavior of the bit will be less stable. Then, the expected hole conditions should be assessed and the drilling parameters optimize to balance the requirement of steerability but without leaving behind the stability of the drilling string and the quality of the hole.

5.2 Regarding the Directional tool

- In holding behavior, has been verified that it is not enough to set the GP deflection to 0% or neutral. In most of the wells it was required to set the tool around 40 % at the high side of the hole to maintain angle. As a result of that behavior, when dropping, the operational procedure will be to reduce deflection first to 0% and then if an increased rate of dropping is required the next step will be to set the tool face to the lower side of the hole and increase deflection gradually.
- In cases where building is difficult and DLS planned is not achieved. Some DD reports suggest using a LSH (Lower Stab Housing) in the GP. That addition is believed to increase the response of the tool.

5.3 Regarding the methodology developed

- The behaviors identification algorithm was set to a sensitivity that allows the study to see clear differences within the responses at building turning or dropping in the conditions defined by the study. That sensitivity might need to be change if the analysis is done in other geological settings or different directional tool.
- The delay on the setting of the tool to a specific tool face and the response seen in the field can introduce certain error. That was accounted in the study by analyzing the GP deflection manually around the depth of certain survey point in each run. That analysis can be more strictly done by improving the code in the look up table.

-
- The statistical approach of selecting ranges of ROP and RPM to collect the most relevant data proved to be effective when reducing the spread of the data-points and enable a more accurate analysis.
 - The relevancy of the method can also be verified by comparing the correlations of different behaviors. Important discrepancies are seen mainly when comparing turning left with turning right. This difference can be observed when comparing the slopes of the responses where one behavior has a negative response and the other behavior a positive one.
 - The tendencies displayed in the simulator in most of the cases matched qualitatively those of the field data. The steering response in the field is close to the one generated by the simulator in most of the cases.

6. Suggestions

- Another way of assessing the steerability can be developed by combining the method developed to identify behaviors and ranges of drilling parameters, with the approach related to the measurement and further calculation of cumulative tilt angle covering the data-points of any given run. And plot this as ΔB (change in angle) vs Δt (time) [2],
- As the simulator does not consider all the heterogeneities of the rock a good approach will be the possibility of including a CCS profile and dip profile so the real behavior can be modeled.
- Perform an integral analysis considering not only the bit but also all the components of the BHA. That will provide a higher degree of understanding with respect to the directional response of the system.
- It will be interesting to perform a study within other sections of a well. The issue of vertical conservation in shallow sections or an analysis considering the radius of curvature as another filtering process, making a distinction between long, medium and short radius well profiles.
- Make a variation of the study considering the impact of flow dynamics. Assessing the importance of good cleaning and cuttings removal for directional control.
- The tendencies generated from field data: *GP Deflection applied vs DLS achieved*, in several runs show that they do not strictly correlate to a straight line. The method applied fulfills the objective of sorting the data in a more relevant way, increasing the correlation. However, a more complex study can be done using another nonlinear correlation model to describe the variables as seen in the scatter figures.

7 References

- [1] Ho, H.S., "Method and System of Trajectory Prediction and Control using PDC Bits", Unated States Patent 5456141 Oct. 10, 1995.
- [2] dB/dt, "Rate of increasing angle", Presentation on Direction by Design. Halliburton.
- [3] <http://homepage.usask.ca/~mjr347/prog/geoe118/geoe118.033.html>, Department of Civil and Geological Engineering, University of Saskatchewan, , Saskatoon, SK, Canada, S7N 5A9.
- [4] Sparta Rock Strength workflow, Halliburton.
- [5] Abbas Khaksar, Baker RDS, "Determination of Rock Strength from Core Logs – Where We Are and Ways to Go". FESAus (Formation Evaluation Society of Australia).
- [6] Horsrud, P. 2001 //Estimating mechanical properties of shale from empirical correlations//, SPE Drilling & Completion, 16, 68-73.
- [7] Halliburton, Hallworld intranet, Sperry Drilling Geo-Pilot™ Marketing sheets.
- [8] S. Chen, G.J. Collins, M.B. Thomas, «Reexamination of PDC Bit Walk in Directional and Horizontal Wells», SPE-112641.
- [9] Insite™, Data Manager, Logging Dataset, Halliburton Sperry Drilling Services.
- [10] www.halliburton.com
- [11] Halliburton, Hallworld intranet, Sperry Drilling Services L/MWD Marketing sheets.
- [12] Fred E. Duprlest, Steven F. Sowers, "Maintaining Steerability While Extending Gauge Length to Manage Whirl", SPE-119625.
- [13] S. Menand, H. Sellami, "Classification of PDC bits According to their Steerability", SPE-79795.
- [14] Bit school presentation material, Halliburton.
- [15] Chase Hanna, Encana Oil and Gas (USA) Inc., Charles Douglas, Hany Asr, Bala Durairajan Martin Gerlero, Levi Mueller, Bhushan Pendse, Chris Travers, Smith Bits, a Schlumberger Company, "Application Specific Steel Body PDC Bit Technology Reduces Drilling Costs in Unconventional North America Shale Plays", SPE-144456.
- [16] S. Barton, Reed-Hycalog Schlumberger, "Development of Stable PDC Bits for Specific Use on Rotary Steerable Systems", SPE 62779.
- [17] S. Menand, H. Sellami, Armines/Ecole des Mines de Paris; C. Simon, DrillScan, "PDC Bit Classification According to Steerability", SPE-87837.
- [18] Menand S., Simon C., Gaombalet J., Macresy L., DrillScan, Gerbaud L., Ben Hamida M., Mines ParisTech, Amghar Y., Total, Denoix H., Schlumberger, Cuiller B., Sinardet H., Varel, "PDC Bit Steerability Modeling and Testing for Push-the-bit and Point-the-bit RSS", SPE-151283.

-
- [19] Stephen Ernst, Paul Pastusek, and Paul Lutes, Hughes Christensen, "Effects of RPM and ROP on PDC Bit Steerability", SPE-105594.
- [20] Tom Gaynor and David C-K Chen, Halliburton Sperry Sun "Making steerable bits: separating side-force from side-cutting", SPE-88446, at the SPE Asia Pacific Oil and Gas Conference and Exhibition held in Perth, Australia, 18–20 October 2004
- [21] Direction by Design (D x D) User's Manual, Halliburton Drill Bits & Services, Nov., 17, 2009
- [22] Sigmud Sognesand, Norsk Hydro, "Evaluation of Oseberg Horizontal Wells after four years production", SPE-36864.
- [23] G. Mensa-Wilmot, SPE, and B. James, Smith Bits; L. Aggarwal and H. Van Luu, Schlumberger; and F. Rueda, BP, "Gage Design-Effects of Gage Pad Length, Geometry and Activity (Side Cutting) on PDC Bit Stability, Steerability, and Borehole Quality in Rotary Steerable Drilling Applications" SPE 98931, SPE Conference Paper.
- [24] Halliburton, DBS database.
- [25] Halliburton, Logging database.
- [26] Directional Drilling End of Well reports Oseberg field.
- [27] MWD end of well reports Oseberg field.
- [28] SDL end of well reports Oseberg field.

Appendix A: Formulas and Excel Macros

Algorithm to tag behaviors

IF(Q20>\$H\$2;IF(R20>\$H\$2;"Build R";IF(R20<-\$H\$2;"Build L";"Build"));IF(Q20<-\$H\$2;IF(R20>\$H\$2;"Drop R";IF(R20<-\$H\$2;"Drop L";"Drop"));IF(R20>\$H\$2;"Turn R";IF(R20<-\$H\$2;"Turn L";"Hold"))))

Where:

'Q20: Build rate

'R20: Turn rate

'H2: Sensitivity

Macro to plot figures in customary axes

```
Sub New_fig()
'
' New_fig Macro
' New_col of data
'
' Keyboard Shortcut: Ctrl+Shift+F
'
  x1 = Range("H8").Value ' GP deflection (7), DLS (15)
  Y1 = Cells(9, 8) 'col(8) = H 'Y axis

  X2 = Cells(10, 8)
  Y2a = Cells(11, 8)
  Y2b = Cells(12, 8)
  'Mag = MsgBox(Nxy2, vbOKOnly, "checking content of var")

  ActiveSheet.ChartObjects("Chart 3").Activate
  ActiveChart.SeriesCollection(1).Name = Cells(19, Y1)
  ActiveChart.SeriesCollection(1).Values = Range(Cells(20, Y1), Cells(1500, Y1))
  ActiveChart.SeriesCollection(1).XValues = Range(Cells(20, x1), Cells(1500, x1))
  'to set new axis titles
  ActiveChart.Axes(xlValue).HasTitle = 1
  ActiveChart.Axes(xlValue).AxisTitle.Caption = Cells(19, Y1).Value
  ActiveChart.Axes(xlCategory).HasTitle = 1
  ActiveChart.Axes(xlCategory).AxisTitle.Caption = Cells(19, x1).Value

  ActiveSheet.ChartObjects("Chart 4").Activate
  ActiveChart.SeriesCollection(1).Name = Cells(19, Y2a)
  ActiveChart.SeriesCollection(1).Values = Range(Cells(20, Y2a), Cells(1500, Y2a))
  ActiveChart.SeriesCollection(1).XValues = Range(Cells(20, X2), Cells(1500, X2))

  ActiveChart.SeriesCollection(2).Name = Cells(19, Y2b)
  ActiveChart.SeriesCollection(2).Values = Range(Cells(20, Y2b), Cells(1500, Y2b))
  ActiveChart.SeriesCollection(2).XValues = Range(Cells(20, X2), Cells(1500, X2))

  'to set new axis titles
  ActiveChart.Axes(xlValue).HasTitle = 1
  ActiveChart.Axes(xlValue).AxisTitle.Caption = Cells(19, Y2a).Value
  ActiveChart.Axes(xlValue, xlSecondary).HasTitle = 1
  ActiveChart.Axes(xlValue, xlSecondary).AxisTitle.Caption = Cells(19, Y2b).Value

  ActiveChart.Axes(xlCategory).HasTitle = 1
  ActiveChart.Axes(xlCategory).AxisTitle.Caption = Cells(19, X2).Value

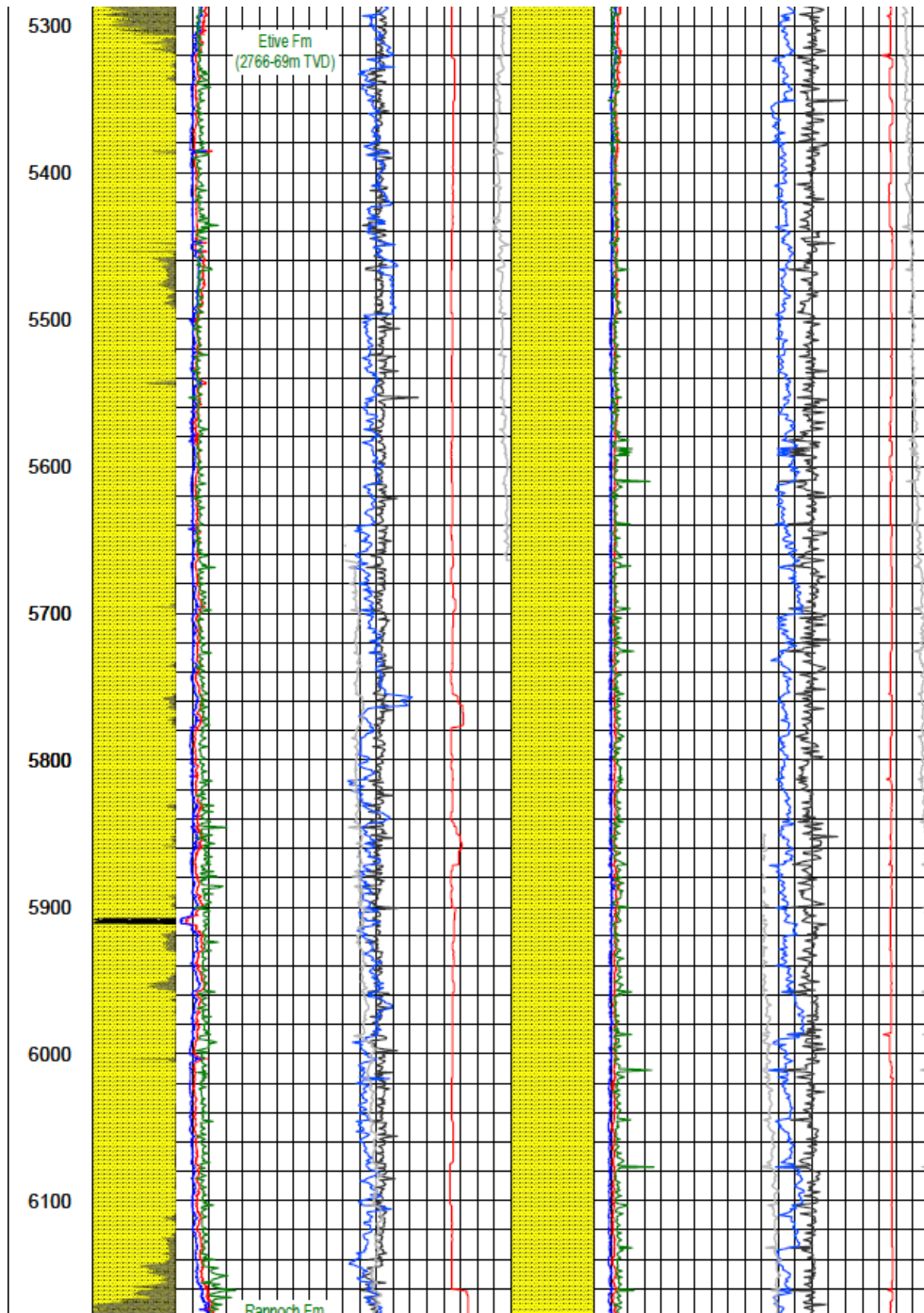
End Sub
```

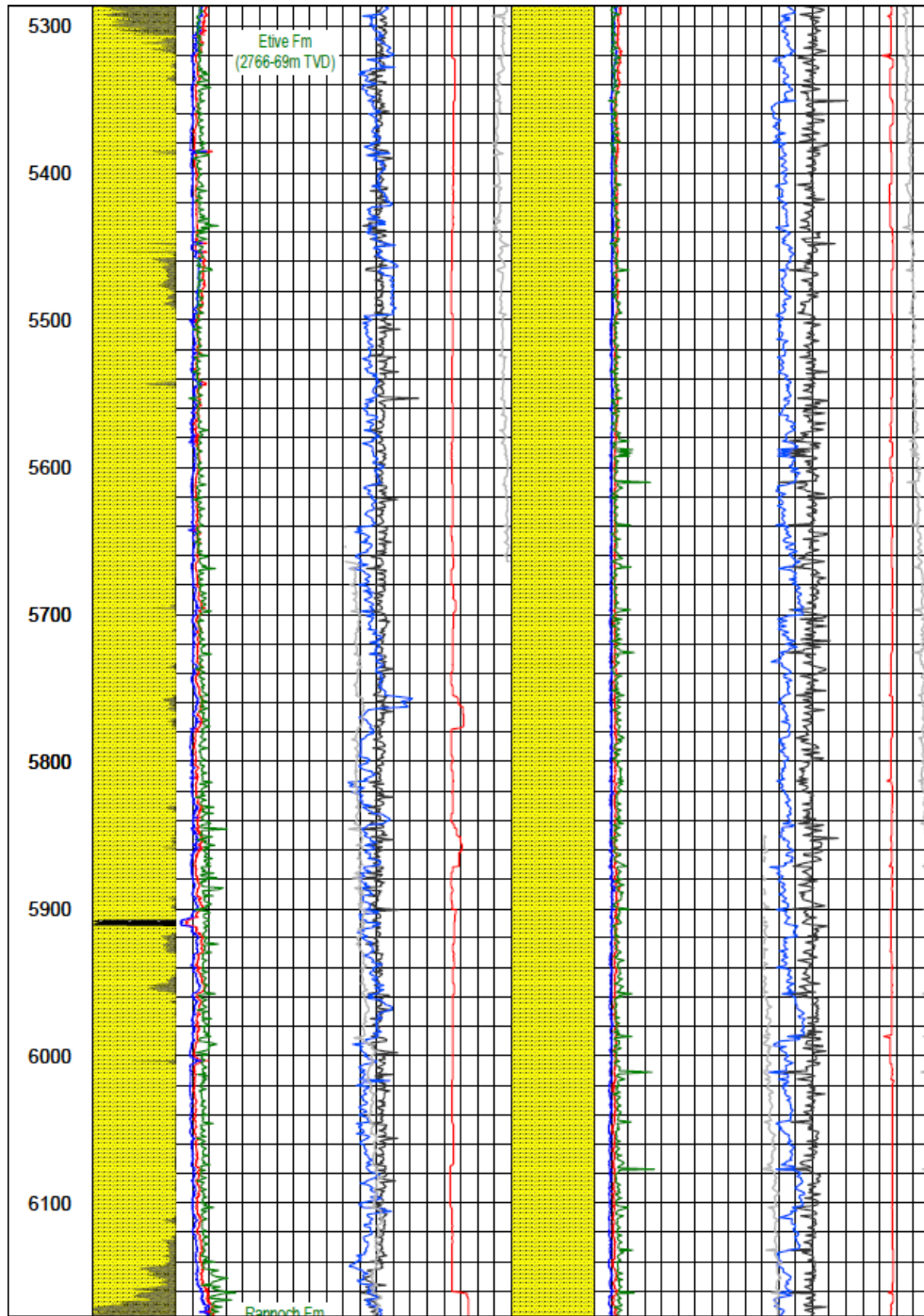
Look up table macro

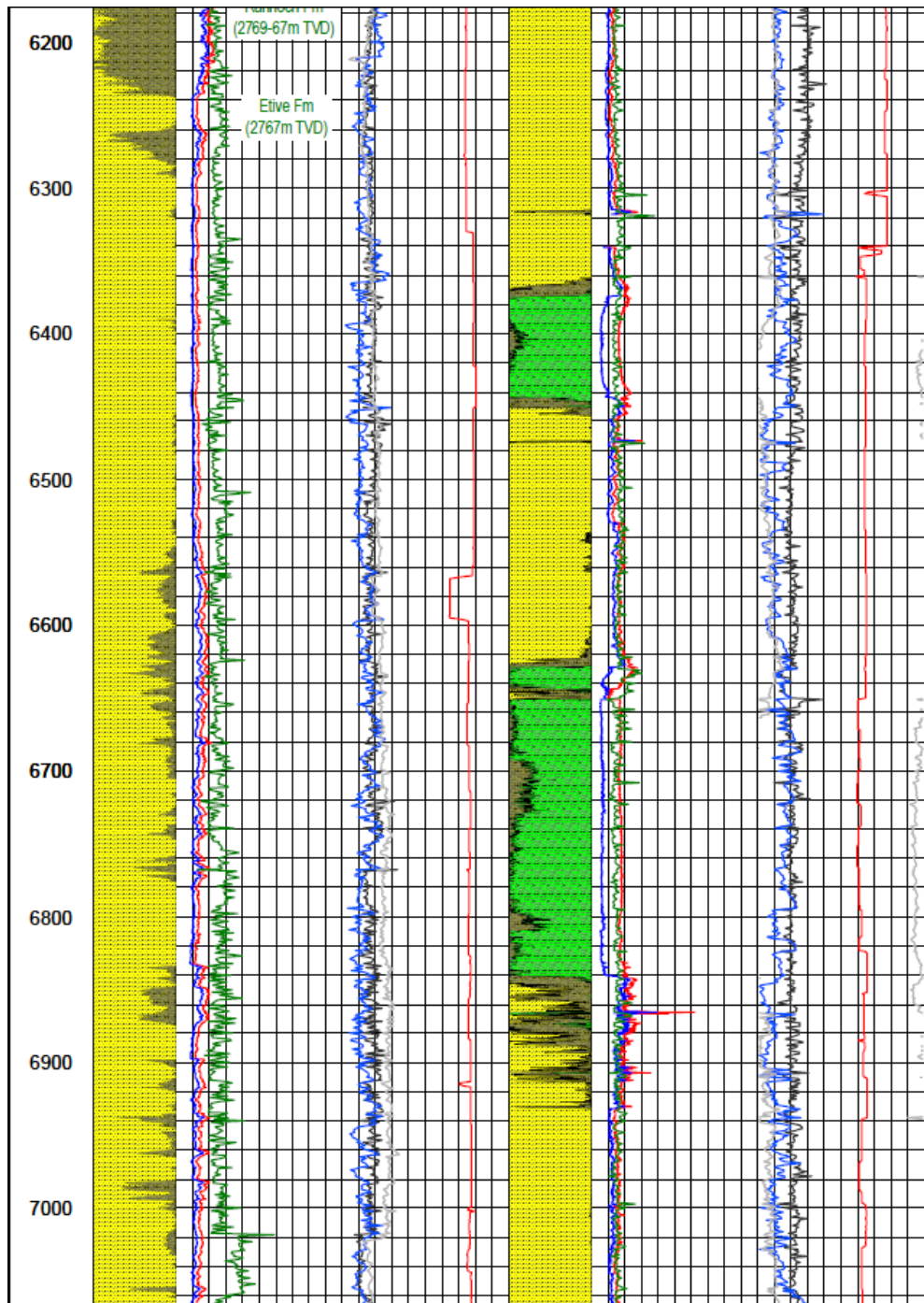
```
Sub tabla()  
  '' tabla Macro  
  '' Keyboard Shortcut: Ctrl+Shift+t  
  Dim CoRow As Variant 'array that will content the info at each depth  
  Sno = Range("B2").Value 'Source number of data  
  Rno = Range("B3").Value 'Reference table number of data  
  Col1 = Range("B4").Value 'First col to be filtered  
  Coln = Range("B5").Value 'Last col  
  
  For j = 7 To (Rno + 7) 'Range of reference table  
    m = Range("AA" & j).Value 'The first value of MD m ref table  
  
    CC = 0 'index step search to make it faster  
  
    C = 0 'index counter  
    For i = 7 To (Sno + 7) 'search lenght, for now must be the range of source table  
      p = m - Range("A" & (C + i + 1)).Value  
  
      If p <= 0 Then  
        Q = Range("A" & (C + i)).Value - m  
        If Abs(Q) < Abs(p) Then  
          n = Range("A" & (C + i)).Value  
          Range("AC" & j).Value = n  
          f = C + i 'index of source row  
          Range("AD" & j).Value = f  
  
          For m = 3 To Coln  
            Cells(j, m + 28).Value = Cells(f, m).Value  
          Next  
        Exit For  
      Else  
        n = Range("A" & (C + i + 1)).Value  
        Range("AC" & j).Value = n  
        f = C + i + 1 'index of source row  
        Range("AD" & j).Value = f  
  
        For m = 3 To Coln  
          Cells(j, m + 28).Value = Cells(f, m).Value  
        Next  
  
      Exit For  
    End If  
    C = C + 1  
  End If  
Next  
Cells.Select  
Selection.Columns.AutoFit  
End Sub
```

Appendix B: Example of the Main Data Matrix

Rig/Field	Bit SN	Bit size	Hole	Bit type	Material #	Wellpath	GP Def applied [%]	MD [m]	Incl [deg]	Azim [deg]	TVD [m]	+W/-S [m]	+W [m]	VS [m]	DLS achieved [deg/30m]	Build	Turn	Behaviour	ROP [ft/hr]	WOB [klb]	RPM
OSEBERG C	11055150	8 1/2"	8 1/2"	FSF3653Z	526377	30/6-C-08A	80	1176.30	48.75	194.75	1073.98	-333.33	-72.57	345.59	0.759	0.754	-0.111	Build	93.5141	5.4501	141.0845
OSEBERG C	11055150	8 1/2"	8 1/2"	FSF3653Z	526377	30/6-C-08A	100	1205.40	51.62	194.26	1092.61	-354.97	-78.16	367.9	2.984	2.959	-0.505	Build L	98.8522	5.8788	150.2868
OSEBERG C	11055150	8 1/2"	8 1/2"	FSF3653Z	526377	30/6-C-08A	89	1234.20	54.67	194.15	1109.89	-377.31	-83.82	390.91	3.178	3.177	-0.115	Build	100.4959	3.9195	150.8599
OSEBERG C	11055150	8 1/2"	8 1/2"	FSF3653Z	526377	30/6-C-08A	100	1261.40	57.75	193.79	1125.01	-399.24	-89.27	413.49	3.413	3.397	-0.397	Build	90.5746	3.2264	150.8732
OSEBERG C	11055150	8 1/2"	8 1/2"	FSF3653Z	526377	30/6-C-08A	100	1292.30	61.5	193.45	1140.63	-425.15	-95.55	440.12	3.652	3.641	-0.33	Build	120.719	3.9219	150.5734
OSEBERG C	11055150	8 1/2"	8 1/2"	FSF3653Z	526377	30/6-C-08A	100	1321.50	64.74	192.36	1153.84	-450.53	-101.36	466.14	3.475	3.329	-1.12	Build L	121.7878	9.0291	147.4731
OSEBERG C	11055150	8 1/2"	8 1/2"	FSF3653Z	526377	30/6-C-08A	100	1350.80	68.31	191.32	1165.51	-476.83	-106.87	493.01	3.783	3.655	-1.065	Build L	106.134	11.7122	147.4455
OSEBERG C	11055150	8 1/2"	8 1/2"	FSF3653Z	526377	30/6-C-08A	61	1379.70	71.29	188.53	1175.37	-501.58	-111.54	520.16	4.523	3.612	-2.896	Build L	101.3068	14.3572	150.3722
OSEBERG C	11055150	8 1/2"	8 1/2"	FSF3653Z	526377	30/6-C-08A	38	1409.20	72.9	188.33	1184.48	-531.34	-115.65	548.19	0.473	0.417	-0.234	Hold	94.1127	17.1233	149.6962
OSEBERG C	11055150	8 1/2"	8 1/2"	FSF3653Z	526377	30/6-C-08A	39	1439.20	72	188.47	1193.71	-559.58	-119.81	576.7	0.257	-0.2	0.17	Hold	83.5266	15.2732	150.305
OSEBERG C	11055150	8 1/2"	8 1/2"	FSF3653Z	526377	30/6-C-08A	6	1467.90	71.59	188.02	1202.67	-586.56	-123.72	603.93	0.619	-0.429	-0.47	Hold	104.5993	9.2117	150.2975
OSEBERG C	11055150	8 1/2"	8 1/2"	FSF3653Z	526377	30/6-C-08A	39	1496.70	71.98	188.26	1211.67	-613.64	-127.6	631.25	0.471	0.406	0.25	Hold	102.9649	14.7558	152.6239
OSEBERG C	11055150	8 1/2"	8 1/2"	FSF3653Z	526377	30/6-C-08A	14	1525.70	71.6	188.36	1220.74	-640.9	-131.58	658.77	0.405	-0.393	0.103	Hold	180.6707	7.5866	150.3538
OSEBERG C	11055150	8 1/2"	8 1/2"	FSF3653Z	526377	30/6-C-08A	39	1554.90	70.15	188.41	1230.30	-668.19	-135.6	686.32	1.491	-1.49	0.051	Drop	111.2656	2.1857	125.6693
OSEBERG C	11055150	8 1/2"	8 1/2"	FSF3653Z	526377	30/6-C-08A	100	1584.30	67.84	188.61	1240.84	-695.34	-139.66	713.74	2.365	-2.357	0.204	Drop	31.6891	15.6816	123.2099
OSEBERG C	11055150	8 1/2"	8 1/2"	FSF3653Z	526377	30/6-C-08A	14	1613.30	63.85	189.63	1252.71	-721.46	-143.85	740.18	4.238	-4.128	1.055	Drop R	19.9546	16.6085	112.2534
OSEBERG C	11055150	8 1/2"	8 1/2"	FSF3653Z	526377	30/6-C-08A	50	1642.30	61.63	188.94	1265.99	-746.9	-148.01	765.94	2.383	-2.297	-0.714	Drop L	20.69	17.1626	89.5824
OSEBERG C	11055150	8 1/2"	8 1/2"	FSF3653Z	526377	30/6-C-08A	51	1671.20	59.36	188.58	1280.22	-771.75	-151.84	791.07	2.379	-2.356	-0.374	Drop	55.7127	3.9511	159.8856
OSEBERG C	11055150	8 1/2"	8 1/2"	FSF3653Z	526377	30/6-C-08A	39	1700.90	57.03	188.67	1295.87	-796.71	-155.63	816.28	2.355	-2.354	0.091	Drop	37.6144	18.3534	159.7372
OSEBERG C	11055150	8 1/2"	8 1/2"	FSF3653Z	526377	30/6-C-08A	95	1730.90	55.86	188.17	1312.45	-821.44	-159.29	841.26	1.242	-1.17	-0.5	Drop	24.9958	17.5044	139.8244
OSEBERG C	11055150	8 1/2"	8 1/2"	FSF3653Z	526377	30/6-C-08A	59	1758.90	52.54	188.14	1328.83	-843.91	-162.51	863.93	3.557	-3.557	-0.032	Drop	160.5524	1.5432	151.7477
OSEBERG C	11055150	8 1/2"	8 1/2"	FSF3653Z	526377	30/6-C-08A	51	1788.20	49.28	188.59	1347.30	-866.41	-165.81	886.64	3.357	-3.338	0.461	Drop	47.2863	7.2919	150.0305
OSEBERG C	11055150	8 1/2"	8 1/2"	FSF3653Z	526377	30/6-C-08A	59	1817.30	48.81	188.71	1366.76	-887.8	-169.07	908.26	2.548	-2.546	0.124	Drop	12.9096	7.426	146.1855
OSEBERG C	11055150	8 1/2"	8 1/2"	FSF3653Z	526377	30/6-C-08A	20	1846.40	42.55	190.32	1387.44	-907.98	-172.74	948.09	3.351	-3.274	-1.095	Drop R	40.1952	18.8653	140.118
OSEBERG C	11055150	8 1/2"	8 1/2"	FSF3653Z	526377	30/6-C-08A	100	1876.00	39.32	189.22	1409.80	-927.09	-175.73	948.09	4.006	-3.962	-1.045	Drop L	117.4573	12.3966	150.2357
OSEBERG C	11055150	8 1/2"	8 1/2"	FSF3653Z	526377	30/6-C-08A	100	1905.00	36.5	190.08	1432.68	-944.65	-178.71	965.9	2.968	-2.917	0.89	Drop R	111.5436	7.8085	150.2247
OSEBERG C	11055150	8 1/2"	8 1/2"	FSF3653Z	526377	30/6-C-08A	1	1933.70	32.71	189.08	1456.30	-960.72	-181.43	982.19	3.145	-3.048	-0.949	Turn L	110.0845	1.5856	150.3658
OSEBERG C	11055150	8 1/2"	8 1/2"	FSF3653Z	526377	30/6-C-08A	90	1963.10	32.24	188.15	1481.10	-976.33	-183.8	997.96	0.7	-0.48	-0.949	Turn L	117.4573	14.5856	150.2357
OSEBERG C	11055150	8 1/2"	8 1/2"	FSF3653Z	526377	30/6-C-08A	80	1992.10	28.87	187.46	1506.07	-990.93	-185.8	1012.68	3.505	-3.486	-0.714	Drop L	111.1675	4.2757	147.7321
OSEBERG C	11055150	8 1/2"	8 1/2"	FSF3653Z	526377	30/6-C-08A	100	2021.20	25.84	188.24	1531.91	-1004.18	-187.62	1026.03	3.145	-3.124	0.804	Drop R	61.978	7.922	151.6533
OSEBERG C	11055150	8 1/2"	8 1/2"	FSF3653Z	526377	30/6-C-08A	90	2050.10	22.08	187.98	1558.32	-1015.79	-189.28	1037.75	3.905	-3.903	-0.27	Drop	53.7277	0.6614	150.2775
OSEBERG C	11055150	8 1/2"	8 1/2"	FSF3653Z	526377	30/6-C-08A	90	2055.80	21.44	188	1563.61	-1017.89	-189.57	1039.86	3.369	-3.368	0.105	Drop	76.1628	0.9996	150.266
OSEBERG C	10745126	8 1/2"	8 1/2"	FMF3653Z	405148	30/6-C-08A	0	2826.2	56.08	324.18	2107.94	-1418.31	-754.2	1605.6	0.561	0.403	-0.472	Hold	56.87	12.7	82
OSEBERG C	10745126	8 1/2"	8 1/2"	FMF3653Z	405148	30/6-C-08A	33	2854.7	56.41	324.09	2123.78	-1437.51	-768.09	1629.23	0.356	0.347	-0.095	Hold	66.66	11.4	140
OSEBERG C	10745126	8 1/2"	8 1/2"	FMF3653Z	405148	30/6-C-08A	40	2882.7	56.48	323.3	2139.26	-1456.32	-781.9	1659.49	0.709	0.075	-0.846	Turn L	68.48	12.1	139
OSEBERG C	10745126	8 1/2"	8 1/2"	FMF3653Z	405148	30/6-C-08A	25	2911.2	56.61	321.49	2154.97	-1475.15	-796.41	1676.15	1.595	0.137	-1.905	Turn L	45.87	12.7	142
OSEBERG C	10745126	8 1/2"	8 1/2"	FMF3653Z	405148	30/6-C-08A	1	2939.8	57.07	320.21	2170.61	-1493.72	-811.53	1699.89	1.223	0.483	-1.343	Turn L	68.61	11.1	141
OSEBERG C	10745126	8 1/2"	8 1/2"	FMF3653Z	405148	30/6-C-08A	32	2968.4	56.6	320.94	2186.26	-1512.21	-826.73	1723.61	0.809	-0.493	0.766	Turn R	82.56	7.9	140
OSEBERG C	10745126	8 1/2"	8 1/2"	FMF3653Z	405148	30/6-C-08A	52	2997.1	56.28	319.69	2202.12	-1530.62	-842	1747.3	1.139	-0.334	-1.307	Turn L	92.75	6.2	143
OSEBERG C	10745126	8 1/2"	8 1/2"	FMF3653Z	405148	30/6-C-08A	43	3025.7	56.95	319.4	2217.86	-1548.79	-857.5	1770.91	0.747	0.703	-0.304	Build	75.29	7.4	139
OSEBERG C	10745126	8 1/2"	8 1/2"	FMF3653Z	405148	30/6-C-08A	23	3054.4	56.99	319.26	2233.51	-1567.04	-873.18	1794.68	0.13	0.042	-0.146	Hold	71.45	8.3	142
OSEBERG C	10745126	8 1/2"	8 1/2"	FMF3653Z	405148	30/6-C-08A	40	3083.1	56.64	319.54	2249.21	-1585.27	-888.81	1818.41	0.44	-0.366	0.293	Hold	83.8	11.9	141
OSEBERG C	10745126	8 1/2"	8 1/2"	FMF3653Z	405148	30/6-C-08A	42	3112	57.2	321.4	2264.99	-1603.95	-904.22	1842.4	1.719	0.581	1.931	Build R	101.83	7.4	144
OSEBERG C	10745126	8 1/2"	8 1/2"	FMF3653Z	405148	30/6-C-08A	2	3140.8	56.69	322.3	2280.7	-1623.93	-919.13	1866.39	0.948	-0.531	0.937	Drop R	78.11	9.1	141
OSEBERG C	10745126	8 1/2"	8 1/2"	FMF3653Z	405148	30/6-C-08A	34	3168.1	56.93	322.91	2295.64	-1644.08	-933.01	1889.12	0.62	0.264	0.67	Turn R	85.94	8.6	142
OSEBERG C	10745126	8 1/2"	8 1/2"	FMF3653Z	405148	30/6-C-08A	40	3197.6	56.85	323.55	2311.76	-1660.88	-947.8	1913.74	0.551	-0.081	0.651	Turn R	93.23	2.6	144
OSEBERG C	10745126	8 1/2"	8 1/2"	FMF3653Z	405148	30/6-C-08A	40	3226.2	57.42	323.19	2327.28	-1680.16	-962.13	1937.67	0.677	0.598	-0.378	Build	114.89	11.7	142
OSEBERG C	10745126	8 1/2"	8 1/2"	FMF3653Z	405148	30/6-C-08A	25	3254.7	57.08	322.71	2342.69	-1699.29	-976.57	1961.54	0.556	-0.358	-0.505	Turn L	84.18	6.6	143
OSEBERG C	10745126	8 1/2"	8 1/2"	FMF3653Z	405148	30/6-C-08A	24	3283.7	56.91	322.79	2358.49	-1718.64	-991.29	2005.75	0.189	-0.176	0.083	Hold	51.5	5.7	140
OSEBERG C	10745126	8 1/2"	8 1/2"	FMF3653Z	405148	30/6-C-08A	33	3312.4	56.75	321.95	2374.19	-1737.67	-1005.96	2089.65	0.754	-0.167	-0.878	Turn L	45.74	5.9	151
OSEBERG C	10745126	8 1/2"	8 1/2"	FMF3653Z	405148	30/6-C-08A	24	3340.8	57	322.59	2389.71	-1756.68	-1020.51	2093.3	0.625	0.264	0.676	Turn R			







Appendix C: BHAs 8 1/2 section

